A Well-to-Wake Emissions Projection Framework for Canadian Domestic Air Cargo: Assessing Sustainable Aviation Fuel, Alternative Propulsion, and Modal Shift Pathways

by

Hao Thi Lam

A thesis

presented to the University of Waterloo

in fulfillment of the

thesis requirement for the degree of

Master of Applied Science

in

Civil Engineering

Waterloo, Ontario, Canada, 2026

© Hao Thi Lam 2026

Author's Declaration

I hereby declare that I am the sole author of this thesis. This is a true copy of the thesis, including any required final revisions, as accepted by my examiners.

I understand that my thesis may be made electronically available to the public.

Abstract

Domestic air cargo plays an important role in supporting freight movements and connecting communities across Canada. However, continued growth in air cargo demand may increase greenhouse gas emissions and make long-term climate targets harder to achieve. This thesis develops a Canada-focused, freight-oriented modelling framework to project domestic air-cargo activity and evaluate potential decarbonization pathways to 2050.

Origin-destination air-cargo demand is forecast using gravity models based on IATA CargoIS commodity- and service-level data and projected economic growth. The resulting forecasts are integrated with a well-to-wake emissions-accounting framework to assess sustainable aviation fuel, alternative aircraft propulsion technologies, selective modal shift to truck and rail, surface-freight decarbonization, and combined mitigation scenarios. Scenario outcomes are also compared/evaluated with national and global climate targets.

The findings indicate that domestic air-cargo emissions are likely to increase significantly without additional mitigation. Sustainable aviation fuel provides the largest network-level reduction among the individual strategies examined, with 2050 emissions reductions ranging from approximately 30.8% to 86.4%. Alternative propulsion produces smaller network-wide reductions of approximately 3.6%-7.1% by 2050 but offers meaningful benefits on eligible shorter-distance corridors. Modal shift can also achieve substantial corridor-level reductions where cargo flows can be transferred to lower-emission truck or rail alternatives. Combined mitigation portfolios achieve substantially greater reductions than any individual strategy.

Overall, the study demonstrates that deep decarbonization of Canadian domestic air cargo will require coordinated implementation of multiple measures. It also provides a transparent, replicable, and extensible framework that can be updated as improved data and technology information become available.

Acknowledgements

I would like to express my sincere gratitude to my supervisors, Dr. Chris Bachmann and Dr. Clarence Woudsma, for their guidance, support, and encouragement throughout my master's research. Their expertise, thoughtful feedback, and patience have been invaluable in shaping this thesis and helping me develop as a researcher.

I am especially grateful for the time they dedicated to reviewing my work, discussing research ideas, and providing direction at each stage of the project. Their mentorship has helped me improve not only the technical quality of this research but also my critical thinking, communication, and confidence in addressing complex transportation and sustainability challenges.

I would also like to thank my parents and my younger brother for their unconditional love, encouragement, and support throughout my academic journey. Their patience, support, and belief in me have given me the strength to continue through the challenges of graduate studies. I am deeply grateful for everything they have done for me.

Finally, I would like to thank my colleagues, friends, and everyone who supported me during this process. Their encouragement, conversations, and kindness helped make this journey more meaningful and manageable.

Thank you all for being part of this important chapter of my life.

Table of Contents

Author's Declaration ii

Abstract iii

Acknowledgements iv

List of Figures xi

List of Tables xiv

List of Abbreviations xvi

Chapter 1 : Introduction 1

1.1 Background 1

1.2 Policy Context 3

1.3 Problem Statement 5

1.4 Research Objectives 5

1.5 Research Scope 6

1.6 Structure of Thesis 8

Chapter 2 : Literature Review 10

2.1 Air cargo demand modelling and forecasting 11

2.1.1 Gravity Trade Model 11

2.1.1.1 Gravity model overview & theory 11

2.1.1.2 Gravity model applications to air cargo: estimation and forecasting 13

2.1.2 Time Series Models 20

2.1.3 Machine Learning Models 23

2.1.4 Hybrid Models 27

2.2 Aviation decarbonization levers for freight 30

2.2.1 Sustainable aviation fuels 31

2.2.1.1 Certification and blending constraints 32
2.2.1.2 Deployment and market constraints 34
2.2.1.3 Applications of SAFs and their GHG reduction potential 36
2.2.2 Alternative aircraft propulsion technologies 40
2.3 Freight mode choice, selective mode shift, and surface freight decarbonization 46
2.3.1 Freight mode choice and Modal Shift concepts 47
2.3.2 Evidence on modal shift benefits and constraints 48
2.4 Roadmap and scenario-based decarbonization studies 53
Chapter 3 : Methodology 58
3.1 Scope and system boundaries 58
3.1.1 Spatial coverage 58
3.1.2 Temporal coverage 59
3.1.3 Modes considered 59
3.1.4 Life-cycle boundary for emissions 60
3.2 Data and Variables 61
3.2.1 Air Cargo Data 61
3.2.2 Regional and city-level GDP and Population 64
3.2.2.1 Population Data 64
3.2.2.2 Gross Domestic Product (GDP) 65
3.2.3 GDP Growth Rate 66
3.2.3.1 Constructing 2023 nominal GDP (needed for the 2019-2023 gravity estimation) 66
3.2.3.2 Projecting 2024-2050 GDP “mass” using real GDP growth 67
3.2.4 Air Distances 68
3.2.5 Truck Distances 70

3.2.6 Rail Distances 71
3.2.7 Emission Factors 71
3.2.7.1 Electricity generation and hydrogen production assumptions: 72
3.2.7.2 Upstream fuel and energy pathway assumptions 73
3.2.7.3 Aviation emission factors assumptions 74
3.2.7.4 Surface transportation emission factors assumptions: 74
3.2.8 Climate Target Ranges 75
3.3 Gravity Trade Model Formulation and Forecasting 76
3.3.1 CargoIS OD-Year Panel and Handling of Zero Flows 76
3.3.2 Variable Selection and Model Controls 77
3.3.3 Gravity Model Specification 78
3.3.4 Gravity-Based Forecasting Based on GDP Growth 79
3.4 Emissions Measurement Methodology 79
3.4.1 Airport Mapping and Realized Route Distance Estimation 80
3.4.2 Network-based emissions equation (applied to OD-level flows) 80
3.5 Scenario design and implementation 81
3.5.1 Baseline (no modal shift, conventional technology) 82
3.5.2 Modal shift scenarios (air to rail/truck) 83
3.5.3 Surface freight technology scenarios 86
3.5.3.1 Truck decarbonization (fleet turnover under ZEV sales targets) 86
3.5.3.2 Rail decarbonization (Rail Pathway Initiative adoption trajectory) 89
3.5.3.2.1 Scenario structure (four rail technology cases): 90
3.5.3.2.2 Alternative fuels and blending constraints 91
3.5.3.2.3 Alternative propulsion options: 91

3.5.3.2.4 Translating the roadmap into an implementable emissions pathway 91
3.5.3.2.5 Scenario implementation and interpolation: 92
3.5.4 Aviation technology scenarios 93
3.5.4.1 SAF scenarios: 93
3.5.4.1.1 SAF blending trajectories 94
3.5.4.1.2 SAF pathway portfolios 95
3.5.4.1.3 SAF scenario matrix (12 sub-scenarios) 97
3.5.4.2 Alternative propulsion scenarios (electric / hydrogen / hybrid), 2030-2050 98
3.5.4.2.1 Commercialization timeline (technology availability windows) 99
3.5.4.2.2 Distance-Based Alternative-Propulsion Eligibility Framework 99
3.5.4.2.3 Adoption dynamics 102
3.5.4.2.4 Hybrid-to-Battery and Hybrid-to-Hydrogen Transition Assumptions: 103
3.5.4.2.5 Timing uncertainty: lagged variants and Scenario implementation tables 104
3.5.5 Scenario sequencing 105
Chapter 4 : Baseline Forecast and Gravity Model Results 109
4.1 Segmented gravity model results 109
4.1.1 Commodity-level PPML gravity-model results 109
4.1.2 Service-level PPML gravity-model results 110
4.2 Baseline cargo forecast by commodity and service type 112
4.3 Baseline WTWa emissions projection 117
Chapter 5 : Emissions Scenario Results 120
5.1 Sustainable aviation fuel-only scenario results 120
5.2 Alternative propulsion systems-only scenario results 125
5.2.1 Network-level emissions results 126

5.2.2 Disaggregate OD-level results 129
5.3 Modal shift scenario results 131
5.3.1 Modal shift-only results 131
5.3.2 Modal shift with surface transportation decarbonization results 137
5.3.3 Illustrative OD-level comparison 142
5.4 Combined mitigation scenario results 144
5.5 Summary of key findings 147
Chapter 6 : Conclusions, Limitations, and Future Research 148
6.1 Conclusion 148
6.2 Study limitations and future research 149
References 152
Appendix A : Gravity Trade Model Estimation 191
Appendix B : Time-Series Forecasting Models 194
Appendix C : Machine-Learning Forecasting Models 200
Appendix D : Sustainable Aviation Fuel Production Pathways 204
Appendix E : Alternative Aircraft Propulsion Technologies 209
Appendix F : Surface Freight Decarbonization Pathways 216
Appendix G : Population Data for CMA and CA Cities 222
Appendix H : Supplementary City-Level Population Data for the Origin-Destination Dataset 225
Appendix I : Provincial GDP Inputs Used for City-Level GDP Estimation 228
Appendix J : City-Level GDP Estimates 230
Appendix K : Provincial and Territorial GDP Growth Rates and Projection Sources, 2023-2050 237
Appendix L : Python Workflow for Extracting FlightAware Air-Route Distances 239
Appendix M : Representative Sample of FlightAware-Derived OD Flight Distances 250

Appendix N : Python Workflow for Extracting Road Distances Using OpenStreetMap 252

Appendix O : Representative Sample of OSM-Derived Truck-Route Distances 263

Appendix P : Representative Sample Rail Distances 265

Appendix Q : Summary of Reference Emission Factors 267

Appendix R : Annual Alternative-Propulsion Eligibility and Penetration Schedules for the Waypoint-Based and Delayed-Deployment Scenarios 269

Appendix S : Full Commodity-Level PPML Gravity-Model Estimation Results 280

Appendix T : Full Service-Level PPML Gravity-Model Estimation Results 289

Appendix U : Supplementary Modal-Shift Results with Surface Transportation Decarbonization ... 296

Appendix V : Supplementary Results for Alternative Combinations of SAF, Alternative Propulsion, Modal Shift, and Surface-Freight Decarbonization 309

List of Figures

Figure 2-1. Overview of alternative fuel routes for aviation (Bauen et al., 2020) 31
Figure 3-1. Well-to-Wake and Well-to-Wheel Emissions Boundaries Applied in This Study 60
Figure 3-2. Example FlightAware Flight Finder Results for a Selected Origin-Destination Pair 69
Figure 3-3. Flowchart of Air-Cargo Decarbonization Scenario Sequencing and Combinations 108
Figure 4-1. Domestic air-cargo demand by commodity category, 2023-2050 113
Figure 4-2. Total commodity-based baseline cargo forecast demand, 2023-2050 114
Figure 4-3. Domestic air-cargo demand by service category, 2023-2050 116
Figure 4-4. Baseline WTWa emissions projection for domestic air cargo, 2023-2050 118
Figure 5-1. GHG Emissions under SAF scenarios (2023 - 2050) 121
Figure 5-2. SAF scenarios compared with Canada IPCC 1.5 climate target 123
Figure 5-3. SAF scenarios compared with Canada net-zero climate target 124
Figure 5-4. AP scenarios and the remaining gap to IPCC 1.5 climate target 127
Figure 5-5. AP scenarios and the remaining gap to Canada's net-zero climate target 128
Figure 5-6. Selected OD corridor emissions: Baseline vs AP scenarios in 2050 130
Figure 5-7. Modal shift-only scenarios and remaining gap to the IPCC 1.5°C target range: commodity-based shifts. 133
Figure 5-8. Modal shift-only scenarios and remaining gap to the IPCC 1.5°C target range: service-tag shifts. 134
Figure 5-9. Modal shift-only scenarios and remaining gap to the Canada net-zero target range: commodity-based shifts. 135
Figure 5-10. Modal shift-only scenarios and remaining gap to the Canada net-zero target range: service-tag shifts. 136
Figure 5-11. Modal Shift with Surface Decarbonization Scenarios and Remaining Gap to IPCC 1.5°C target range: commodity-based shifts 138
Figure 5-12. Modal Shift with Surface Decarbonization Scenarios and Remaining Gap to Canada Net Zero target range: commodity-based shifts. 139
Figure 5-13. Modal Shift with Surface Decarbonization Scenarios and Remaining Gap to IPCC 1.5°C target range: service-tag shifts 140
Figure 5-14. Modal Shift with Surface Decarbonization Scenarios and Remaining Gap to Canada Net Zero target range: service-tag shifts 141

Figure 5-15. OD-Level Emissions Reduction from Modal Shift Scenarios 143
Figure 5-16. Combined Mitigation Scenarios Compared with the IPCC 1.5°C-Aligned and Canada Net-Zero Benchmark Ranges, 2023-2050 145
Figure C.1. Structure of an Artificial Neural Network with Input, Hidden, and Output Layers (Weiss et al., 2022) 202
Figure D.1. HEFA-SPK Production Process Flow Diagram (Rosales Calderon et al., 2024) 204
Figure D.2. Fischer-Tropsch (FT) Process Flow Diagram (Wei et al., 2019) 205
Figure D.3. Alcohol-to-Jet Production Process Flow Diagram (Wei et al., 2019) 206
Figure D.4. Hydroprocessing of Fermented Sugars to Jet Fuel Process Flow Diagram (Ng et al., 2021) 207
Figure D.5. Catalytic Hydrothermolysis Synthetic Paraffinic Kerosene Process Flow Diagram (Lau et al., 2024) 207
Figure D.6. Power-to-Liquid Route with FT-SPK Process Flow Diagram (Lau et al., 2024) 208
Figure E.1. Parallel Hybrid-Electric Configuration (Sahoo et al., 2020) 210
Figure E.2. Series Hybrid-Electric Configuration (Sahoo et al., 2020) 211
Figure E.3. Series-Parallel Hybrid Configuration (Sahoo et al., 2020) 211
Figure E.4. Full-Electric Configuration (Sahoo et al., 2020) 212
Figure U.1. Commodity-Based Modal-Shift Emissions under Rail Technology Scenario 1 Relative to the IPCC 1.5°C Target Range 297
Figure U.2. Commodity-Based Modal-Shift Emissions under Rail Technology Scenario 1 Relative to Canada's Net-Zero Targets 298
Figure U.3. Service-Tag Modal-Shift Emissions under Rail Technology Scenario 1 Relative to the IPCC 1.5°C Target Range 299
Figure U.4. Service-Tag Modal-Shift Emissions under Rail Technology Scenario 1 Relative to Canada's Net-Zero Targets 300
Figure U.5. Commodity-Based Modal-Shift Emissions under Rail Technology Scenario 2 Relative to the IPCC 1.5°C Target Range 301
Figure U.6. Commodity-Based Modal-Shift Emissions under Rail Technology Scenario 2 Relative to Canada's Net-Zero Targets 302
Figure U.7. Service-Tag Modal-Shift Emissions under Rail Technology Scenario 2 Relative to the IPCC 1.5°C Target Range 303
Figure U.8. Service-Tag Modal-Shift Emissions under Rail Technology Scenario 2 Relative to Canada's Net-Zero Targets 304
Figure U.9. Commodity-Based Modal-Shift Emissions under Rail Technology Scenario 3 Relative to the IPCC 1.5°C Target Range 305

Figure U.10. Commodity-Based Modal-Shift Emissions under Rail Technology Scenario 3 Relative to Canada's Net-Zero Targets 306
Figure U.11. Service-Tag Modal-Shift Emissions under Rail Technology Scenario 3 Relative to the IPCC 1.5°C Target Range 307
Figure U.12. Service-Tag Modal-Shift Emissions under Rail Technology Scenario 3 Relative to Canada's Net-Zero Targets 308
Figure V.1. Category 4 (AP + SAF): Minimum- and Maximum-Emission Cases 310
Figure V.2. Category 6 (MS + SAF): Minimum- and Maximum-Emission Cases 311
Figure V.3. Category 7 (MS + AP): Minimum- and Maximum-Emission Cases 312
Figure V.4. Category 8 (MS + AP + SAF): Minimum- and Maximum-Emission Cases 313
Figure V.5. Category 10 (MS + SAF + SD): Minimum- and Maximum-Emission Cases 314
Figure V.6. Category 11 (MS + AP + SD): Minimum- and Maximum-Emission Cases 315

List of Tables

Table 2-1. Summary of gravity-model applications in air-cargo research: determinant and forecasting studies 15
Table 2-2. Case studies on time-series applications in air-cargo forecasting 21
Table 2-3. Case studies on machine learning applications in air-cargo forecasting 25
Table 2-4. Case studies on hybrid models applications in air-cargo forecasting 28
Table 2-5. Overview of SAF Conversion Pathways and Certification Characteristics (*Alternative Fuels Data Center*, n.d.; ICAO, n.d.) 32
Table 2-6. Minimum jet fuel selling price for different jet fuel production pathways 35
Table 2-7. Summary of Case Studies on SAF Pathways and Their GHG Reduction Potential 37
Table 2-8. Summary of case studies on alternative propulsion systems and their GHG reduction potential 41
Table 2-9. Summary of Modal-Shift Case Studies, Emissions Impacts, and Implementation Constraints 49
Table 2-10. Summary of Major Aviation Decarbonization Roadmaps, Pathways 54
Table 3-1. CargoIS mid-level commodities (International Air Transport Association, n.d.-b, n.d.-c) 63
Table 3-2. CargoIS mid-level services (International Air Transport Association, n.d.-b, n.d.-c) 64
Table 3-3. Correlation between city-level GDP and population, 2019 - 2023 77
Table 3-4. Milestone Rail Propulsion and Fuel Shares by Technology Scenario, 2023-2050 92
Table 3-5. SAF sub-scenarios defined by blending case and pathway portfolio 98
Table 3-6. Adoption of SAF, Electric, and Hydrogen Propulsion Technologies by Aircraft Market Segment, 2020-2050 (ATAG, 2021) 100
Table 3-7. Typical Flight Speeds and Representative Aircraft by Aircraft Category 101
Table 3-8. Estimated Flight-Range Assumptions by Aircraft Category 102
Table 4-1. Summary of commodity-level PPML gravity-model results 109
Table 4-2. Summary of service-level PPML gravity-model results 111
Table G.1. Annual Population for CMA and CA Cities in the Origin-Destination Dataset 222
Table H.1. Supplementary Population Estimates and Data Sources for Cities and Years Not Covered by Statistics Canada 225
Table I.1. Provincial and Territorial GDP Used for City-Level GDP Estimation, 2019-2023 228
Table J.1. Annual Origin- and Destination-City GDP Estimates Used in the Gravity Model, 2019-2023 230

Table K.1. Annual Real GDP Growth Rates (%) by Province and Territory, 2024-2036 237
Table K.2. Annual Real GDP Growth Rates (%) by Province and Territory, 2037-2050 238
Table M.1. Representative Sample of Flight Distances from FlightAware 250
Table O.1. Representative Sample of OpenStreetMap Truck Distances by Origin-Destination Pair 263
Table P.1. Representative Sample of GIS-Derived Rail Distances by Origin-Destination Pair 265
Table Q.1. Summary of 2023 Reference Emission Factors by Mode and Technology 267
Table R.1. Alternative-Propulsion Eligibility and Annual Penetration Rates under the Waypoint-Based Timeline (Scenario AP1) 270
Table R.2. Alternative-Propulsion Eligibility and Annual Penetration Rates under the Three-Year Deployment Delay 272
Table R.3. Alternative-Propulsion Eligibility and Annual Penetration Rates under the Six-Year Deployment Delay 274
Table R.4. Alternative-Propulsion Eligibility and Annual Penetration Rates under the Nine-Year Deployment Delay 276
Table R.5. Alternative-Propulsion Eligibility and Annual Penetration Rates under the Twelve-Year Deployment Delay 278
Table S.1. Biological Commodity - PPML Gravity-Model Estimates 280
Table S.2. General Cargo - PPML Gravity-Model Estimates 281
Table S.3. Perishables - PPML Gravity-Model Estimates 282
Table S.4. High-Value Cargo - PPML Gravity-Model Estimates 283
Table S.5. Pharmaceuticals - PPML Gravity-Model Estimates 284
Table S.6. Dangerous Goods - PPML Gravity-Model Estimates 285
Table S.7. Live Animals - PPML Gravity-Model Estimates 286
Table S.8. Other Special Cargo - PPML Gravity-Model Estimates 287
Table S.9. Commodity Information Pending - PPML Gravity-Model Estimates 288
Table T.1. Commodity Information Pending - PPML Gravity-Model Estimates 289
Table T.2. Express and Time-Sensitive Cargo - PPML Gravity-Model Estimates 290
Table T.3. General Cargo - PPML Gravity-Model Estimates 291
Table T.4. Other Special Cargo (No Service) - PPML Gravity-Model Estimates 292
Table T.5. Oversize and Heavy-Weight Cargo - PPML Gravity-Model Estimates 293
Table T.6. Temperature-Sensitive Cargo - PPML Gravity-Model Estimates 294
Table T.7. Vulnerable Cargo - PPML Gravity-Model Estimates 295

List of Abbreviations

Acronym	Full Term
ANN	Artificial Neural Network
ANSP	Air Navigation Service Provider
AR	Autoregressive Model
ARFIMA	Autoregressive Fractionally Integrated Moving-Average
ARIMA	Autoregressive Integrated Moving-Average
ARIMAX	Autoregressive Integrated Moving-Average with Exogenous Variables
ARMA	Autoregressive Moving-Average
ASTM	American Society for Testing and Materials
ATAG	Air Transport Action Group
ATJ	Alcohol-to-Jet
ATJ-SKA	Alcohol-to-Jet Synthetic Kerosene with Aromatics
ATJ-SPK	Alcohol-to-Jet Synthetic Paraffinic Kerosene
AWB	Air Waybill
BAU	Business-As-Usual
BEV	Battery Electric Vehicle
BPN	Back-Propagation Neural Network
BSTS	Bayesian Structural Time Series
CASS	Cargo Accounts Settlement System
CDD	CargoIS Direct Data
CH-SK	Catalytic Hydrothermolysis Synthetic Paraffinic Kerosene
CI	Carbon Intensity
CITES	Convention on International Trade in Endangered Species
CMA	Census Metropolitan Area
CO_2	Carbon Dioxide
CO_2e	Carbon Dioxide Equivalent
CORSIA	Carbon Offsetting and Reduction Scheme for International Aviation
C-SAF	Canadian Sustainable Aviation Fuel
EIS	Entry Into Service

Acronym	Full Term
FCEV	Fuel Cell Electric Vehicle
FT	Fischer-Tropsch
FT-SKA	Fischer-Tropsch Synthetic Kerosene with Aromatics
FT-SPK	Fischer-Tropsch Synthetic Paraffinic Kerosene
GDP	Gross Domestic Product
GHG	Greenhouse Gas
GIS	Geographic Information System
GREET	Greenhouse gases, Regulated Emissions, and Energy use in Technologies
HC-HEFA-SPK	Hydrocarbon Hydroprocessed Esters and Fatty Acids Synthetic Paraffinic Kerosene
HDRD	Hydrotreated Renewable Diesel
HEFA	Hydroprocessed Esters and Fatty Acids
HEFA-SPK	Hydroprocessed Esters and Fatty Acids Synthetic Paraffinic Kerosene
HFS-SIP	Hydroprocessed Fermented Sugars Synthetic Isoparaffin
HSR	High-Speed Rail
HTL	Hydrothermal Liquefaction
IATA	International Air Transport Association
ICAO	International Civil Aviation Organization
ICE	Internal Combustion Engine
ILUC	Induced Land-Use Change
IMHZEV	Incentives for Medium and Heavy Duty Zero-Emission Vehicles Program
IPCC	Intergovernmental Panel on Climate Change
IV	Instrumental Variable
LCA	Life Cycle Assessment
LCFS	Low Carbon Fuel Standard
LCI	Life Cycle Inventory
LSTM	Long Short-Term Memory
LTAG	Long-Term Aspirational Goal
MA	Moving-Average Model
MHDV	Medium- and Heavy-Duty Vehicle

Acronym	Full Term
MJFP	Minimum Jet Fuel Price
MLP	Multi-Layer Perceptron
OD	Origin-Destination
OLS	Ordinary Least Squares
OSM	OpenStreetMap
PBO	Parliamentary Budget Officer
PHEV	Plug-in Hybrid Electric Vehicle
PPML	Poisson Pseudo-Maximum Likelihood
PtL	Power-to-Liquid
RAC	Railway Association of Canada
RF	Random Forest
RTK	Revenue Tonne-Kilometre
SAF	Sustainable Aviation Fuel
SARIMA	Seasonal Autoregressive Integrated Moving-Average
SARIMAX	Seasonal Autoregressive Integrated Moving-Average with Exogenous Variables
SIP	Synthetic Isoparaffin
SVR	Support Vector Regression
TC	Transport Canada
TEA	Techno-Economic Analysis
TSLS	Two-Stage Least Squares
TTW	Tank-to-Wheel
TTWa	Tank-to-Wake
VAR	Vector Autoregression
VARMA	Vector Autoregressive-Moving Average
WTT	Well-to-Tank
WTW	Well-to-Wheel
WTWa	Well-to-Wake
ZE	Zero-Emission
ZEV	Zero-Emission Vehicle

Chapter 1: Introduction

1.1 Background

Canada's freight and passenger transportation system is shaped by its vast geography and scattered population. With 42 million people spread across roughly 9 million square kilometers, many communities and economic centers are separated by long distances and, in some regions/areas, limited surface connectivity (Government of Canada, 2011, 2025c; Loprespub, 2025; Transport Canada, 2025b). As a result, aviation serves a dual national function: (i) it enables high-volume passenger and freight flows between major urban regions, and (ii) it provides essential year-round access to remote communities where alternative modes can be slow, seasonal, or unavailable.

The scale of aviation activity indicates its central role in Canada's domestic mobility and logistics system. In 2024, Canadian airports handled 156.7 million passengers, including enplaned and deplaned passengers. Domestic travel accounted for 85.9 million passengers, exceeding both transborder travel at 39.0 million passengers and international travel at 31.8 million passengers (Government of Canada, 2025a). This demonstrates the importance of aviation for travel within Canada. Air freight activity also shows a similar pattern. Total air cargo reached approximately 1.58 million tonnes in 2024, up 5.1% from 2023. Domestic cargo accounted for 802,000 tonnes, making it the largest component compared with international cargo at 534,000 tonnes and transborder cargo at 243,000 tonnes (Statistics Canada, 2025). These figures demonstrate that intra-Canada movements account for a major share of national air freight activity.

Beyond its role in connectivity, aviation is also economically significant. The International Air Transport Association (IATA) estimates that air transport in Canada yields approximately US$82.2 billion in gross value added, equivalent to about 3.8% of national GDP, and supports around 809,000 jobs, including 265,400 jobs directly employed in the aviation sector (International Air Transport Association, 2019).

Despite its importance to Canada's mobility, logistics, and economy, aviation is widely recognized as a hard-to-abate transport sector and poses growing environmental challenges. Domestic cargo-related aviation emissions are estimated to have increased by approximately 43% between 2013 and 2023, reaching roughly 3 Mt CO_2e in 2023, even after a temporary decline during the COVID-19 period (Transport Canada & Sustainable Aviation Task Force, 2025). At the same time, the Canadian air freight market is expected to continue growing. Its market size is projected to reach USD 11.52

billion by 2033, expanding at a compound annual growth rate of 6.07% between 2025 and 2033 (IMARC, n.d.). This projected growth of air cargo volumes and activities may increase aviation fuel demand and further expand the sector's environmental footprint unless lower-carbon alternatives and mitigation measures are adopted.

Both academic research and industry roadmaps generally emphasize that aviation decarbonization will require a portfolio of measures rather than reliance on a single solution (ATAG, 2021; EUROCONTROL Air Transport Association, 2022; Royal Netherlands Aerospace Centre & SEO Amsterdam Economics, 2021; Zheng et al., 2025). Technology-specific studies often focus on individual pathways, such as sustainable aviation fuels (SAF), hydrogen propulsion, or battery-electric aircraft, to quantify their emissions-reduction potential under clearly defined assumptions. In contrast, system-level roadmaps take a broader view and typically combine multiple levers.

Key aviation decarbonization pathways include: (i) the development and adoption of green aerospace technologies, such as electric, hybrid-electric, and hydrogen propulsion, over the longer term; (ii) improvements in operational efficiency, infrastructure, and air-traffic management; (iii) the increased adoption of SAF as lower-carbon alternatives to fossil-based jet fuel; and (iv) the use of out-of-sector reductions or offset mechanisms to address residual emissions where necessary (ATAG, 2021; EUROCONTROL Air Transport Association, 2022; Royal Netherlands Aerospace Centre & SEO Amsterdam Economics, 2021; Zheng et al., 2025). Together, the research and policy literature identify SAF deployment, advanced propulsion technologies, and operational efficiency improvements as primary in-sector strategies. However, the pace and scale of adoption will depend on technology readiness, supply-chain constraints, fuel availability, and enabling infrastructure.

A complementary but less emphasized strategy, particularly in aviation-focused roadmaps, is selective modal shift, in which some air-cargo shipments are diverted to lower-carbon surface modes such as truck, rail, or marine. Modal shift is frequently discussed in broader freight-decarbonization literature, especially in the context of road-to-rail and road-to-marine substitutions. It has also been examined in the passenger context by replacing short-haul flights with high-speed rail. However, comparatively less attention has been given to diverting air cargo to road and rail. This may be because air freight is often assumed to serve time-critical and reliability-sensitive markets, where surface alternatives may involve longer transit times or service trade-offs.

Nevertheless, not all air-cargo movements necessarily require next-day delivery, and some flows may have sufficient time flexibility to be served by surface modes. Shippers and firms that purchase freight transportation services play an important role in enabling modal shifts because their service requirements, consolidation practices, and procurement decisions largely determine whether road, rail, or marine options can meet delivery-time and reliability needs (SLOCAT, 2024). With effective policy support and careful consideration of service constraints, selective air-to-surface modal shift could represent a meaningful strategy for reducing greenhouse gas (GHG) emissions while making the associated transit-time trade-offs explicit.

1.2 Policy Context

The policy context for domestic air-cargo decarbonization in Canada sits within a broader climate-policy framework. Although the Intergovernmental Panel on Climate Change (IPCC) pathways and Canada's national net-zero climate targets are not specific to domestic aviation or air cargo, they provide broader emissions-reduction benchmarks against which sectoral pathways can be assessed. The IPCC indicates that limiting warming to 1.5°C requires rapid, deep, and sustained GHG emissions reductions across sectors, with global carbon dioxide emissions reaching net zero around mid-century (IPCC, 2023). However, sectoral reductions are not expected to occur uniformly, and hard-to-abate sectors such as transport may retain residual emissions for longer, requiring a combination of in-sector mitigation and out-of-sector reductions or removals (IPCC, 2023). The IPCC-aligned pathway used in this thesis is therefore treated as an illustrative sectoral benchmark rather than a binding aviation-specific target.

Canada's national climate commitments provide a second benchmark. Under the Canadian net-Zero Emissions Accountability Act, Canada has committed to achieving net-zero GHG emissions by 2050, with interim targets of 40-45% below 2005 levels by 2030 and 45-50% by 2035 (Government of Canada, 2024a; Service Canada, 2024). When applied in this thesis to domestic air-cargo emissions, these targets serve as proportional alignment benchmarks to evaluate how closely air-cargo mitigation scenarios align with Canada's broader emissions-reduction trajectory.

Within aviation, Canada's Aviation Climate Action Plan provides the sector-specific policy framework, setting out a vision for net-zero GHG emissions from Canadian aviation by 2050 (Transport Canada, 2022). The plan identifies a portfolio of mitigation pathways, including SAF,

operational improvements, longer-term green aerospace technologies, and out of sector reductions (Transport Canada, 2022).

A major near- to medium-term pathway identified in both the Aviation Climate Action Plan and the C-SAF Roadmap is the scale-up of SAF (Bentley et al., 2023; Transport Canada, 2022). SAF is policy-relevant because it can reduce life-cycle emissions using existing aircraft and fuel infrastructure (Transport Canada, 2022). Both documents identify an aspirational goal of 10% SAF use by 2030. This is intended to send a market signal rather than operate as a binding blending mandate (Bentley et al., 2023; Transport Canada, 2022). This differs from the European Union's ReFuelEU aviation regulation, which establishes mandatory minimum SAF shares at EU airports through 2050 (European Union, 2023).

The federal clean-fuel policy in Canada also has limited effects on SAF adoption. The clean fuel regulations establish life-cycle carbon-intensity reduction requirements for gasoline and diesel fuel pools, but do not currently impose a similar requirement for jet fuel (Government of Canada, 2024b). As a result, clean-fuel regulations may support broader low-carbon fuel markets and allow some aviation fuels to generate credits, but do not directly require suppliers or operators to meet specific SAF blending levels. British Columbia is an exception. Under its Low Carbon Fuels Act, the province has introduced carbon-intensity requirements for jet fuel and mandates for SAF blending (Government of British Columbia, 2022).

International aviation climate policy in Canada is shaped through ICAO's Carbon Offsetting and Reduction Scheme for International Aviation (CORSIA), which Canada has incorporated into its regulatory framework (Government of Canada, 2026a; Transport Canada, 2025a). However, CORSIA applies to international flights, not to domestic flights within Canada, meaning it does not directly address the decarbonization of domestic operations (Transport Canada, 2025a).

Economic measures for domestic aviation have also been uneven. Canada's Aviation Climate Action Plan notes that while carbon pricing could apply to some aviation emissions sources, coverage of inter-provincial aviation was not fully established (Transport Canada, 2022). Since the federal fuel charge was ceased effective April 1, 2025, any future carbon-pricing measure applying to aviation would require careful design to ensure consistent coverage of domestic operations (Department of Finance Canada, 2025)

Overall, Canada's aviation policy context supports long-term decarbonization but remains incomplete for domestic air freight. Existing frameworks identify important mitigation pathways, but several measures remain aspirational, enabling, or focused on broader aviation rather than domestic operations. Current policies also provide limited evidence on how different decarbonization strategies would perform under Canada-specific domestic air-cargo conditions, where route distance, shipment type, service requirements, and the availability of surface-mode alternatives can strongly affect implementation. This motivates the need for a Canada-specific, freight-oriented assessment of domestic aviation decarbonization pathways.

1.3 Problem Statement

Although Canada has established national climate objectives and developed an aviation-specific climate action plan, domestic air-cargo emissions remain a growing concern. Cargo-related aviation emissions and activities have increased over the last decade, and continued market growth is projected to further expand the sector's environmental footprint. Yet domestic air cargo remains underexamined relative to passenger aviation in both research and policy.

Most existing studies focus on single decarbonization pathways, conducting well-to-wake or cradle-to-grave assessments of specific options such as SAF, hydrogen, or battery-electric aircraft under narrowly defined assumptions. Broader industry roadmaps synthesize portfolios of measures across SAF, operational improvements, and propulsion transitions, but these analyses are generally global, regional, or passenger-oriented in scope (ATAG, 2021; EUROCONTROL Air Transport Association, 2022; Royal Netherlands Aerospace Centre & SEO Amsterdam Economics, 2021; Zheng et al., 2025). Neither approach fully addresses Canada-specific domestic air-cargo conditions. Therefore, there is a need for Canada-specific, freight-oriented evidence that evaluates decarbonization pathways using consistent methods and comparable metrics. This thesis addresses that gap by developing a well-to-wake emissions framework for domestic air cargo in Canada. The following section outlines the specific research objectives.

1.4 Research Objectives

This thesis develops and applies a Canada-focused, freight-oriented modelling framework to evaluate domestic air-cargo decarbonization pathways to 2050. The specific objectives are to:

- Quantify current domestic air-cargo activity and project baseline freight demand to 2050.
- Quantify the well-to-wake emissions associated with projected domestic air-cargo activity.
- Evaluate the emissions-reduction potential of SAF adoption and alternative aircraft propulsion technologies.
- Evaluate the emissions-reduction potential of selectively shifting suitable air-cargo flows to truck and rail.
- Assess the relative contributions of individual and combined decarbonization pathways to reducing domestic air-cargo emissions.
- Determine how the resulting emissions trajectories compare with climate-aligned benchmarks and quantify the remaining emissions-reduction gap.

1.5 Research Scope

This thesis examines domestic Canadian air-freight shipments that both originate and end within Canada, represented at the OD city-pair level using IATA CargoIS data. The empirical dataset covers 2019-2023, and baseline air-cargo activity is forecast to 2050 using a gravity model driven by projected economic growth.

Modes and representation of modal shift

The analysis focuses on intercity domestic air cargo movements between origin-destination city pairs. Air transportation represents the baseline mode, while truck and rail are introduced in the modal-shift scenarios as potential substitutes for the same intercity movement. The analysis does not include first-mile pickup, last-mile delivery, terminal handling, or transfer processes due to data limitations. As a result, the comparison focuses on corridor-level differences in distance, emissions, and travel time among air, truck, and rail.

Emission Boundary:

Emissions are assessed using a fuel-cycle boundary: well-to-wake for aircraft and well-to-wheel for surface modes. This includes well-to-tank processes, such as fuel or feedstock extraction, processing, production, transportation, and distribution, as well as tank-to-wake aircraft operation and tank-to-

wheel vehicle operation. Infrastructure construction and maintenance, vehicle and aircraft manufacturing, end-of-life processes, and aviation non-CO_2 effects are excluded.

The study accounts for upstream fuel and energy emissions through the emission-factor assumptions described in the methodology, including electricity-generation and hydrogen-production assumptions. However, it does not explicitly model the physical availability, production capacity, infrastructure build-out, or supply-chain constraints required to achieve the adoption levels tested in the scenarios. The scenarios, therefore, evaluate potential emissions impacts under the assumed adoption pathways rather than the feasibility of large-scale deployment. A detailed Canada-specific assessment of feedstock and energy supply, infrastructure build-out, and associated constraints is identified as an important direction for future research.

Scenario assumptions are developed from policy targets, industry roadmaps, and published technology assumptions where available. For aviation decarbonization pathways, both conservative and more aggressive adoption cases are included, and some scenarios account for delayed deployment. These scenarios are intended to test a range of plausible and upper-bound outcomes rather than predict a single most likely future.

Scope exclusions: cost and endogenous demand response:

This study evaluates emissions outcomes and does not model costs, including fuel prices, capital costs, operating costs, infrastructure costs, or freight-rate impacts. It also does not model endogenous demand responses, such as changes in air-cargo demand caused by technology adoption, policy implementation, fuel-price changes, or service changes. Baseline activity is projected using macroeconomic drivers, and technology pathways are evaluated by applying changes in emissions intensity to projected activity rather than as market-equilibrium outcomes.

Data limitations and reporting of results:

CargoIS has limitations in coverage and underestimates total domestic air-cargo activity relative to aggregate statistics reported by Statistics Canada. Nevertheless, CargoIS is used because it provides disaggregated origin-destination city-pair detail that is not available in Statistics Canada's air-cargo tables, which report system-level totals rather than OD flows. To reduce sensitivity to uncertainty in reporting levels, results are reported primarily as relative percentage changes in emissions across

pathways and portfolios. Absolute emissions estimates are also presented but should be interpreted more cautiously.

1.6 Structure of Thesis

The structure of the thesis is as follows:

Chapter 1 introduces the study by presenting the research background, policy context, problem statement, research objectives, study scope, and thesis structure.

Chapter 2 presents the literature review. It first reviews air-cargo demand modelling and forecasting approaches. It then examines aviation decarbonization levers relevant to freight, including sustainable aviation fuels and alternative aircraft propulsion technologies. The chapter also reviews freight mode choice, selective modal shift, and surface freight decarbonization pathways. Finally, it discusses roadmap and scenario-based decarbonization studies that are similar in purpose to this thesis but differ in scale, scope, or geographic focus.

Chapter 3 presents the methodology. It first defines the study boundaries and modelling framework. It then describes the data sources and variables used in the analysis. The chapter presents the gravity trade model formulation and forecasting approach, followed by the emissions accounting methodology and scenario design for the baseline, modal-shift, aviation technology, surface freight technology, and combined mitigation scenarios.

Chapter 4 presents the gravity-model results and baseline domestic air-cargo projections. It reports the commodity- and service-level PPML gravity-model results, baseline cargo forecasts to 2050, and the resulting WTWa emissions projection. These results establish the reference case and demand inputs used for the emissions scenario analysis in Chapter 5.

Chapter 5 presents the emissions scenario results. It evaluates sustainable aviation fuel, alternative aircraft propulsion, selective modal shift with and without surface freight decarbonization, and combined mitigation scenarios. Scenario outcomes are evaluated relative to the baseline and compared with climate-aligned benchmarks. Where relevant, the chapter also presents network-level results and selected OD-level outcomes.

Chapter 6 concludes the thesis. It summarizes the main findings, highlights the research's contributions, discusses the policy and industry implications of domestic air-cargo decarbonization, identifies key limitations, and outlines directions for future research.

Chapter 2: Literature Review

This literature review has four main aims:

1. To review the main approaches used to model and forecast air-freight demand
2. To review aviation decarbonization levers relevant to freight, with a focus on sustainable aviation fuels (SAFs) and alternative propulsion technologies (battery-electric, hybrid-electric, and hydrogen), and to assess their associated GHG reduction potential.
3. To review freight mode-choice theory and modal-shift studies and provide supporting background on truck and rail decarbonization pathways.
4. To synthesize findings from roadmap reports, scenario studies, and technical literature that assess and compare different aviation decarbonization pathways

A comprehensive literature review is necessary to establish the methodological context for assessing air freight decarbonization pathways in Canada. Since air-cargo emissions are influenced by both demand growth and the carbon intensity of transport operations, the review considers both forecasting methods and decarbonization pathways. It also examines the role of freight mode choice and surface-mode decarbonization, because shifting selected air-cargo movements to truck or rail depends not only on emissions differences, but on service characteristics. Finally, roadmap reports and scenario studies are reviewed to identify how different decarbonization levers have been combined in previous long-term assessments and to position the contribution of this thesis within the broader literature. Together, these areas provide the foundation for developing realistic long-term scenarios and evaluating their WTWa emissions implications for Canadian domestic air cargo.

The scope of this review includes academic and technical literature gathered through indexing databases such as SCOPUS, Google Scholar, ResearchGate, and ScienceDirect. In addition, technical documentation and methodological papers for emissions models, along with roadmaps and government/industry reports, were obtained directly from model developers, government agencies, and the relevant organizations.

The remainder of this chapter is organized into four subsections:

- Air cargo demand modelling and forecasting

- Aviation decarbonization levers for freight
- Freight mode choice, selective mode shift, and surface freight decarbonization
- Roadmaps, scenario studies, and technical reports on decarbonization pathways

2.1 Air cargo demand modelling and forecasting

Forecasting is critical in air transport because it provides the foundation for airline scheduling, network design, and ground operations across both passenger and freight markets. Accurate forecasts are essential for reducing passenger and freight loading delays, which can negatively affect airports, airlines, and customers by lowering profitability, weakening operational performance, and reducing service quality (Verma, 2023). In air-cargo operations specifically, uncertainty between booked and realized shipments creates additional risk by increasing overbooking losses, spoilage, and inefficient capacity utilization, further emphasizing the importance of robust and accurate demand-forecasting models (Sirikhorn et al., 2014). Beyond operations, air-cargo forecasting also provides the baseline for aviation GHG-reduction pathway and roadmap studies (ATAG, 2021; EUROCONTROL Air Transport Association, 2022), as it establishes the reference demand trajectory against which decarbonization measures are assessed.

Although air-cargo demand forecasting is important, the body of research remains relatively limited compared with the much larger literature on air-passenger demand forecasting (Baier et al., 2022). Nevertheless, recent studies report several forecasting approaches, with the most common in the past decade including the gravity model, time series models, machine learning, and hybrid models (Baier et al., 2022; British Columbia, Ministry of Finance, 2025; Q. H. Nguyen, 2024). Accordingly, this subsection provides a brief overview of each of these models.

2.1.1 Gravity Trade Model

2.1.1.1 Gravity model overview & theory

The gravity trade model was initially conceived as an analogy to Newton's law of universal gravitation, in which the interaction between two places increases with their "mass" and decreases with separation. In economics and transport, early gravity-style formulations are linked to Reilly (1931) (Elshehawy et al., 2014), while formal applications to international trade are commonly

attributed to Tinbergen (1962) and Pöyhönen (1963). Over time, the gravity model evolved from the intuitive empirical form into a more rigorous theoretical framework. A major advance was provided by Anderson & van Wincoop (2003), who developed the structural gravity model and showed that bilateral trade depends not only on direct trade costs between two partners but also on their multilateral resistance relative to all other trading relationships.

As an intuitive starting point, bilateral trade from the origin i to destination j can be expressed as:

$$T_{ij} = \alpha_0 \frac{Y_i^{\alpha_1} Y_j^{\alpha_2}}{D_{ij}^{\alpha_3}} \tag{2.1}$$

- T_{ij}: trade (or freight flow) from i to j
- Y_i, Y_j: "economic mass" (often GDP, sometimes population)
- D_{ij}: distance or a trade-cost proxy
- $\alpha_0, \alpha_1, \alpha_2, \alpha_3$: parameters

However, while intuitive, this traditional form is incomplete, lacks multilateral structure, and has major inconsistencies because it treats bilateral changes as isolated and assumes a uniform decline in trade costs across all routes (Shepherd, 2013). For this reason, a large literature has developed a range of theoretical or structural gravity models derived from different trade frameworks (Kerr & Gaisford, 2007; Piermartini & Teh, 2005; Shepherd, 2013). Among these contributions, Anderson & van Wincoop (2003) stands out for introducing multilateral resistance terms that capture outward and inward trade resistance, ensuring that trade flows are determined by relative trade costs rather than bilateral costs alone.

The Anderson & van Wincoop (2003) gravity model is given by:

$$x_{ij} = \frac{y_i y_j}{y_w} \left(\frac{t_{ij}}{\Pi_i P_j} \right)^{1-\sigma} \tag{2.2}$$

Where:

- x_{ij}: exports (or shipments) from i to j
- y_i, y_j: economic size of i and j (e.g., income/output)

- y_w: world total income/output
- t_{ij}: bilateral trade costs between i and j
- Π_i: outward multilateral resistance of origin i
- P_j: inward multilateral resistance of the destination j
- σ: elasticity of substitution across varieties

In empirical applications, the multilateral resistance terms Π_i and P_j are typically not computed by explicitly solving the Anderson-van Wincoop system. Instead, they are commonly absorbed using exporter and importer fixed effects, and exporter-time and importer-time fixed effects in panel settings (Kerr & Gaisford, 2007; Piermartini & Teh, 2005; Yotov et al., 2016). This approach captures unobserved country-specific factors and multilateral resistance. Still, it also means that country-specific variables (e.g., GDP, GDP per capita, population) are typically not separately identified. At the same time, exporter/importer fixed effects are included, leaving identification primarily to bilateral variables (distance, adjacency, policy dummies, etc.). In addition, a detailed review of gravity-model estimation methods is provided in Appendix A.

2.1.1.2 Gravity model applications to air cargo: estimation and forecasting

Gravity models have been applied in air-cargo research in several ways, ranging from explaining observed spatial patterns of flow to supporting short-, medium-, and long-term forecasting. In some studies, gravity models are used within broader analyses of the air transport system, where cargo is examined alongside passenger services. Other work applies gravity specifically to air-cargo markets, modelling freight flows independently of passenger demand and focusing on cargo-relevant drivers. A further stream uses gravity as a forecasting framework for air traffic and/or air freight over time, either as a stand-alone model or as part of scenario-based projections. Then, gravity-based methods are also used to compare air with alternative modes and to quantify how trade and transport costs shape observed routing, modal substitution, and the distribution of flows across corridors.

This subsection focuses on two groups of studies: (i) determinant-oriented applications, which use gravity models to explain/analyze the drivers of observed air-cargo flows, and (ii) forecasting-oriented applications, which use gravity models to project future air-cargo demand/flows. Table 2.1

summarizes a few representative studies across these two strands, including each study's objective, spatial unit, forecast horizon (or study period), dependent variable, and estimation approach.

Table 2-1. Summary of gravity-model applications in air-cargo research: determinant and forecasting studies

Study	Geography / Scope	Unit of Analysis	Study Objective	Forecast Horizon or Study Period	Dependent Variable	Explanatory Variables	Estimation	Outcome
Forecasting Studies								
(Turner, 2002)	International exports from YVR (Vancouver)	YVR-to-countries (aggregate; disaggregate by commodity)	To build a gravity model and generate air-cargo export forecasts	Short-term out-of-sample (1998, 1999 forecasts)	Export air-cargo volume (tonnes)	GDP per capita, distance, CPI, tariffs, population	OLS	Forecast accuracy was limited; aggregate performed better than disaggregate, but both were not highly accurate
(Alexander & Merkert, 2021)	US international air freight markets	Country-pairs	To evaluate the gravity model's robustness and generate forecasts after the Global Financial Crisis	2005-2018 dataset; pre-GFC 2005-2007, GFC 2008-2009, post-GFC 2010-2018	Air freight volume (tonnes); air freight values (US dollars)	Consumer spending, transport cost, and sea freight competition	Not reported (OLS and PPML were discussed in the literature).	Comparative forecastability across GFC phases; no headline RMSE/MAE table reported; aggregate forecasts stronger than disaggregate
(Baier et al., 2022)	Global air-cargo network	Airport-pairs	To build a global gravity model and generate country-/airport-level air-cargo forecasts	Estimation: 2010-2019; forward forecasts to 2047 (case example shown for FRA)	Air-freight flow in ton-kilometers	GDP per capita, distance, contiguity, common language, colonial ties, time FE, fuel proxy	PPML	Back-forecast fit (2010-2019) plus scenario-style forward projections; results broadly aligned with Boeing long-run trend, with slight long-run decrease globally; FRA case suggests strong Asia growth
(Kaya et al., 2023)	Turkey international	Country-pairs	To compare gravity-model forecast	2012-2019 estimation period; 2020 out-	Total cargo carried (tonnes)	GDP per capita, distance, and population	OLS (log-linear), OLS with small	PPML performs best overall for total cargo, with variation by city

	air-cargo market		performance across estimators	of-sample forecast test			constant for zeros, and PPML	
Determinant / Explanatory studies								
(Matsumoto & Domae, 2019)	Europe & Asia	City-pairs	To explain/assess competitive hub status and shifting urban hierarchy (rise of second-ranked cities)	2000-2012	International air passenger flows and international air cargo flows	GDP per capita. population, global network connectivity, and distance	OLS	Business connectivity is a significant driver of network position, with established global hubs maintaining dominance while several secondary hubs gained importance over time. Model validation indicates statistically significant key variables, but a lower adjusted R^2 in 2012 than 2000
(Aydın & Ülengin, 2022)	Turkey domestic air-cargo market	City-pairs	To explain determinants of domestic air-cargo flows; compare estimators	2012-2020	Cargo carried between city pairs	Population, GDP per capita, and distance	OLS and PPML	Population, GDP per capita, and distance are significant positive determinants of Turkey's domestic air cargo market. It also shows PPML is preferable to OLS.
(Gong et al., 2014)	Mainland China domestic network & China's international air-trade partners	(i) Domestic airport network; (ii) Country-level China-partner trade links (top 100	To analyze China's air-freight network structure and identify drivers of international air cargo trade	2002-2012: Trend analysis of cargo traffic; 2011: Cross-sectional data used for the Gravity Model estimations and	(i) Model 1: Total trade by air, air cargo export, and air cargo import values between China and trading partners. (ii) Model 2: Air cargo flow, between a	GDP, population, distance, common border/culture, tertiary industry share, liberalization	OLS	China's air-cargo system remained structurally immature for dedicated cargo operations and economic structure/quality mattered more than GDP size in explaining air-cargo trade. It also finds that US liberalization increased volumes but much of the gain accrued to foreign integrators, with clear regional heterogeneity

		partners, 2011)		detailed network analysis	specific Chinese economic zone and a trading country			
(Alexander & Merkert, 2017)	Australia domestic air freight market	City-pairs	(i) To investigate the challenges of the Australian domestic air freight market. (ii) To compare the provision of road vs. air freight services (time and cost) and identify key determinants of air freight demand using gravity modelling	2014-2015	Domestic air freight volume	Gross Regional Product, distance, industry activity (e.g., unemployment, technicians/trades workers, laborers, machinery operators, and sales workers), trade resistance, aircraft dummy, and freighter dummy	OLS	The augmented model provided the best fit compared to the basic and the Anderson van Wincoop models. The economic activity of the origin was more significant than that of the destination, indicating air freight is demand-pulled by production capabilities. Distance remains a significant barrier, and air freight is generally not cost-competitive on short-haul routes; however, it retains a clear advantage in geographically isolated markets where surface alternatives are limited
(Hwang & Shiao, 2011)	Taiwan's international air-trade partners	Airport-pairs	(i) To develop a panel gravity model that incorporates a wider array of factors beyond standard geo-economic variables to explain international air cargo flows (ii) To analyze the impact of service qualities and unique	2004-2007	Total air cargo volumes	GDP per capita, population, distance, flight frequency, freight rate, open skies agreement dummy variables	OLS	GDP per capita showed an unexpected negative coefficient and was removed from the model. The authors attributed this to the "hub" nature of cities like Hong Kong and Luxembourg, where cargo volumes are high despite varying local GDP levels. Population has a significant positive effect on air-cargo volumes, while freight rate has a significant negative effect, although the estimated elasticity is relatively small, likely reflecting the low-price sensitivity of

			political/historical factors on Taiwan's air cargo demand					Taiwan's high-value electronics exports. In addition, institutional and historical linkages, Chinese Circle connectivity, colonial ties with Japan, and Open Skies agreements, are all associated with significantly higher cargo flows.
(Hong Tsui et al., 2025)	New Zealand's international air-trade market	Airport-to-Country pairs	To investigate the determinants and drivers of New Zealand's airfreight exports	2015 - 2018	Gross weight of airfreight exports & gross value of airfreight exports	GDP, population, distance, capacity, transport costs, exchange rate, trade agreement and culture/language dummy variables	2SLS	GDP per capita and population were confirmed as significant positive drivers for both export weight and value. Scheduled air cargo capacity had a limited positive effect, suggesting that air cargo is largely a derived demand. Flying distance showed a positive relationship with export *value*, contrary to standard gravity theory. The authors attribute this to the fact that high-value, perishable goods require air transport for long-haul routes regardless of distance

The studies summarized in Table 2.1 demonstrate that gravity models have been applied to air cargo at several spatial scales, including airport pairs, city pairs, country pairs, and airport-to-country relationships. Across these applications, economic mass variables such as GDP, GDP per capita, and population are among the most commonly included explanatory variables, while distance is generally used to represent geographic separation or transport resistance. Several studies also extend the conventional gravity specification by including air-service characteristics, such as flight frequency, freight rates, cargo capacity, aircraft type, trade agreements, and institutional or historical relationships (Alexander & Merkert, 2017; Gong et al., 2014; Hong Tsui et al., 2025; Hwang & Shiao, 2011).

The determinant-oriented studies show that the effects of gravity-model variables vary across air-cargo markets. Economic activity and population are generally associated with higher flows, but their relative importance depends on market characteristics. Alexander & Merkert (2017), for example, found that origin-side economic activity was especially important in Australia, while Aydın & Ülengin (2022) identified population, GDP per capita, and distance as significant determinants in Turkey. Also, distance does not always have the expected negative effect. Hong Tsui et al. (2025) found a positive relationship between distance and the value of New Zealand's airfreight exports, reflecting the importance of air transport for long-distance movements of high-value and perishable goods. Overall, the effects of gravity variables appear to depend on commodity composition, geography, and service characteristics.

Air-cargo forecasting studies are more limited. Turner (2002) found that aggregate forecasts performed better than commodity-level forecasts, although accuracy remained limited. More recent studies have examined alternative estimators and longer forecasting horizons. Kaya et al. (2023) found that PPML generally outperformed log-linear OLS when forecasting Turkish air cargo, particularly in the presence of zero flows. Baier et al. (2022) used PPML to produce global airport-pair forecasts to 2047, while Alexander & Merkert (2021) showed that forecast performance can vary across economic periods and levels of aggregation.

Overall, the literature supports the use of gravity models to explain and forecast air-cargo flows. However, most existing studies focus on international markets, countries outside Canada, or global air-cargo networks. Limited research has examined the Canadian domestic air-cargo market.

2.1.2 Time Series Models

Time-series modelling offers an alternative approach for forecasting air-transport demand by focusing on temporal dynamics observed in historical data, such as trend, seasonality, cyclical movements, growth patterns, and irregular fluctuations (Verma, 2023). Unlike the gravity model, which explains flows primarily through relationships between origins and destinations and their economic characteristics, time-series models focus on how demand evolves over time. These models are generally classified as either univariate or multivariate, as discussed in detail in Appendix B (Verma, 2023).

Time-series models are commonly used in air cargo forecasting because they can exploit historical patterns, such as trends, seasonality, and persistence, directly from the cargo series itself (Verma, 2023). Existing studies suggest that a wide range of time-series models, including ARIMA, BSTS, automatic ARIMA, and exponential smoothing, have been applied to aviation demand forecasting. Table 2.2 below summarizes selected studies on time-series forecasting of air cargo demand, including the models employed, the application context, and key findings.

Table 2-2. Case studies on time-series applications in air-cargo forecasting

Study	Geography / Scope	Context/data	Models used	Main findings
(M. Wu et al., 2024)	China; national air-cargo volume	Annual time-series data from 2000-2023; 5-year-ahead forecast	ARIMA and Holt-Winters (non-seasonal smoothing)	ARIMA(1,1,0) outperformed Holt-Winters on RMSE, MAE, and MAPE. ARIMA forecast cargo volume rising from 6.90 million tons in 2024 to 7.89 million tons in 2028.
(Madhavan et al., 2023)	India; domestic and international passenger and air-cargo sectors	10 years of data (2009-2018) from DGCA India	ARIMA and BSTS	The study found that, alongside ARIMA, BSTS was also suitable for short-term forecasting of all four sectors, including domestic and international air cargo, highlighting the usefulness of uncertainty-aware methods.
(Hussain & Alidrisi, 2025)	Saudia Cargo; regional markets including American, European, African, Saudi Arabia, Middle East and North Africa, Indian Sub-Continent, and Far East Regions.	Monthly air-cargo demand in chargeable weight; forecast for 2024 and beyond; post-pandemic and disruption context	Time-series decomposition, ARIMA	Model performance differed by region: ARIMA performed best in AME, EUR, AFR, and KSA; decomposition performed best in FES; The study recommends region-specific model selection.
(H. K. Kim & Lee, 2019)	South Korea; Incheon International Airport	Monthly cargo throughput data, January 2009-December 2016; service delays and costs due to severe weather	SARIMA	The study developed a SARIMA model to forecast delay times and costs associated with air-cargo service disruptions under low-visibility conditions, demonstrating that seasonal time-series methods can

				support cargo planning in operational disruption contexts.
(Gudmundsson et al., 2021)	Global and macro-regional aviation markets	Global and macro-regional aviation markets	ARIMAX with GDP and oil-price assumptions, plus shock-recovery simulation	For freight, the study estimated average global recovery in about 2.2 years, with recovery typically between 2022 and 2023, and used ARIMAX to forecast aviation output under GDP, oil-price, and COVID-shock assumptions.
(Rodríguez & Olariaga, 2024)	Colombia; airport-system demand	Medium- to long-term (10-year) demand forecast for passengers and air cargo	BSTS	The study developed a BSTS model to forecast passenger and air-cargo demand in Colombia, primarily to support airport planning and infrastructure investment.
(Alsayed & Cameletti, 2026)	Italy; national air passenger and freight demand forecasting	Monthly Italian passenger and freight demand data from Assaeroporti, January 2000 to December 2023; forecasts generated to 2035 at monthly and yearly resolution; economic variables and population included as regressors, with separate forecasts developed for those regressors	SARIMAX and structural time-series model	Both models were applied to forecast passenger and freight demand while accounting for seasonality, trend, and economic drivers. The structural time-series approach additionally allowed decomposition of the series and estimation of cyclical components using the Kalman filter. The forecasts were presented as useful for infrastructure planning and strategic investment in sustainable aviation technologies.

Overall, the studies demonstrate that the ARIMA model remains an important benchmark in air-cargo forecasting. For example, Wu et al. (2024) found that ARIMA outperformed non-seasonal Holt-Winters smoothing for annual air-cargo volume in China, while Madhavan et al. (2023) found both ARIMA and BSTS suitable for short-term passenger and cargo forecasting in India. However, the results also show the value of matching the model to the forecasting context. Hussain & Alidrisi (2025), for instance, found that the best-performing method differed across Saudia Cargo's regional markets, with ARIMA, LSTM, and decomposition models each performing best in different regions. More recent applications have also incorporated explanatory variables and structural components, as illustrated by SARIMAX and structural time-series models for forecasting Italian passenger and freight demand (Alsayed & Cameletti, 2026).

The selected studies, therefore, do not identify a universally best-performing forecasting model. Model performance depends on factors such as data frequency, seasonality, volatility, forecast horizon, geographic scale, and the availability of explanatory variables. The literature also shows increasing use of flexible statistical and machine-learning approaches alongside traditional time-series benchmarks. Machine-learning methods, including ANN and LSTM models, are discussed further in Section 2.1.3.

2.1.3 Machine Learning Models

Machine-learning models are increasingly used for forecasting air-transport demand, especially when the data relationships are nonlinear or difficult to represent with conventional statistical models. Although many machine-learning models can be applied to time-series data, they are treated in this review as a distinct category from classical time-series models such as ARIMA, SARIMA, and BSTS. These models are generally classified as either supervised or unsupervised. Supervised learning approaches use labelled data, such as historical demand observations and explanatory variables, to learn predictive relationships, whereas unsupervised learning methods identify patterns or structures in unlabelled data (Verma, 2023).

Supervised learning methods are more commonly applied in air-transport demand forecasting because the objective is generally to predict a known outcome using historical demand and related explanatory variables (Verma, 2023). Accordingly, Appendix C provides a detailed review of commonly used supervised machine learning models in the aviation demand forecasting literature, including support vector regression, artificial neural networks, random forests, and gradient boosting.

These models are particularly relevant to air-cargo forecasting because they can capture nonlinear relationships and complex interactions among explanatory variables that traditional statistical models may not adequately represent. Existing studies have applied approaches such as backpropagation neural networks, support vector regression, random forests, and gradient-boosting methods in a range of air-cargo forecasting contexts. Table 2.3 summarizes selected case studies on the application of machine learning models to air cargo forecasting.

Table 2-3. Case studies on machine learning applications in air-cargo forecasting

Study	Geography / Scope	Context/data	Models used	Main findings
(S.-C. Chen et al., 2012)	Japan-Taiwan air passenger and air cargo demand	Forecasting demand while evaluating input variables affecting both passenger and cargo demand	Back-propagation neural network (BPN)	The BPN approach improved forecasting accuracy, with reported MAPEs of 0.34% for passenger demand and 7.74% for air cargo demand.
(Liu et al., 2020)	China; daily air-cargo volume forecasting using data from InfoSky Technology Limited, whose cargo service coverage is described as broadly reflecting air-cargo variation across China	365 standardized daily observations from Jan-Dec 2018; 265 training and 100 testing samples; 1-, 5-, and 10-step forecasting; static and dynamic strategies	Multiple linear regression (MLRR), ARIMA, Support vector regression (SVR), Neural network (NN), Gradient boosting regression tree (GBRT)	SVR performed best overall on RMSE, MAE, and MAPE, especially for longer horizons; ARIMA was competitive and stronger for short-term forecasting; dynamic forecasting improved performance; statistical and ML approaches were found to be complementary.
(Glenn & Panarat, 2018)	Australia's export air-cargo market	Annual export air-cargo demand, 1993-2016	ANN / multi-layer perception (MLP) with feed-forward back-propagation	Using variables such as world merchandise exports, fuel prices, cargo yields, outbound flights, and exchange rate, the ANN achieved a highest R-value of 0.97844, suggesting ANN is an efficient tool for predicting Australia's annual export air-cargo demand.
(Hussain & Alidrisi, 2025)	Saudia Cargo; regional markets including American, European, African, Saudi Arabia, Middle East and North	Monthly air-cargo demand in chargeable weight; forecast for 2024 and beyond; post-pandemic and disruption context	LSTM, ANN	LSTM performed best in MNT and ISC; ANN did not outperform the other models in any region. The study recommends region-specific model selection.

	Africa, Indian Sub-Continent, and Far East Regions.			
(Çatuk, 2025)	Turkey; national air-cargo tonnage forecasting	Monthly Turkish air-cargo tonnage data for 2012-2023; explanatory variables included GDP, USD exchange rate, and crude oil prices; forecasts evaluated at 1-, 5-, and 10-month ahead horizons	SARIMA, Autoregressive Integrated Moving Average with Exogenous Variables (ARIMAX), SVR, RF, and Gradient Boosting Regression (GBR)	Machine-learning models generally outperformed the statistical models. Random Forest performed best for 1- and 10-month forecasts, while GBR performed best for the 5-month period ahead. The study concluded that ML methods were more effective overall for forecasting Turkey's air-cargo tonnage, though SARIMA remained competitive in some short-term settings.
(Yang et al., 2022)	Global; 10 major international airports	Monthly airport freight-volume data from August 2014 to December 2019 for 10 major international airports; training set from August 2014 to December 2018, and test set from January to December. 2019.	Fuzzy-based support vector regression (FSVR), compared with Holt-Winters, ETS, ARIMA, SARIMA, and SVR.	FSVR performed best overall; its mean RMSE was 0.304, compared with 1.681 for the next-best model (SVR), and it outperformed the comparison models across the airports studied.

Machine-learning models generally show strong forecast performance in air-cargo applications and often outperform traditional statistical models. For example, Chen et al. (2012) and Glenn & Panarat (2018) reported favorable results for neural-network approaches, while Liu et al. (2020) found that SVR performed best overall for daily air-cargo forecasting in China, particularly for longer forecasting horizons. Similarly, Yang et al. (2022) showed that fuzzy-based SVR outperformed several benchmark models, including ARIMA, SARIMA, and standard SVR, for monthly freight-volume forecasting across major international airports. However, the literature also suggests that model performance is highly context-specific, depending on factors such as geography, forecasting horizon, data frequency, and the structure of the forecasting problem. For instance, Çatuk (2025) found that Random Forest performed best for 1- and 10-month-ahead forecasts in Turkey, whereas GBR performed best for the 5-month-ahead horizon. Likewise, Hussain & Alidrisi (2025) showed that the best-performing model varied across regional markets, with LSTM outperforming ANN in some cases.

2.1.4 Hybrid Models

Hybrid models combine two or more forecasting approaches to improve predictive accuracy by capturing different features of the data that may not be fully represented by a single model. In aviation applications, hybrid models often integrate classical statistical methods with machine learning techniques, enabling them to exploit both structured temporal patterns and more complex nonlinear relationships. Table 2.4 below summarizes selected studies on the application of hybrid models in air-cargo forecasting.

Table 2-4. Case studies on hybrid models applications in air-cargo forecasting

Study	Geography / Scope	Context/data	Models used	Main findings
(Li et al., 2020)	China; air-cargo forecasting using data from Beijing, Shenzhen, and Shanghai airports	Daily air-cargo data collected from January 1, 2006, to September 9, 2018. The study mainly compares the performance of alternative hybrid models and does not clearly specify the forecasting horizon.	Secondary decomposition-ensemble approach with cuckoo search optimization (SDE-ARIMA-PSR-CSA-ENN)	The study compared the proposed model against a range of benchmark and hybrid alternatives, including a classical ARIMA model, simpler neural-network-based hybrids, decomposition-based hybrids, and several optimization-based model combinations. The results showed that the full proposed hybrid model, SDE-ARIMA-PSR-CSA-ENN, achieved the best overall forecasting performance.
(Sulistyowati et al., 2018)	Indonesia; air passenger and air cargo at the three largest international airports	Monthly passenger and cargo data from January 2001 to August 2017 for Soekarno Hatta, I Gusti Ngurah Rai, and Juanda airports in Indonesia, and generated forecasts for September 2017 to December 2018.	Time series regression (TSR)-neural network (NN), TSR-SVR, ARIMAX-NN, ARIMAX-SVR	The study found that hybrid models generally improved accuracy over the base linear models. Among the hybrids, ARIMAX-NN and TSR-NN were reported as the stronger performers overall, suggesting that combining linear time-series structure with neural-network correction can better capture nonlinear patterns.
(Xu et al., 2019)	China; national aviation-industry indicators, including domestic and international passenger and cargo-related time series	Monthly data from February 2005 to February 2018 (157 observations), from the Civil Aviation Administration of China, and evaluated forecasts over a 24-month horizon.	SARIMA-SVR hybrid models, SARIMA	The study compared several SARIMA-SVR variants and found one hybrid specification (SARIMA_SVR3) performed best for forecasting the aviation indicators
(Nguyen, 2024)	Singapore; international air freight in ten major markets (e.g., Malaysia,	Monthly air-cargo volumes, January 1991 to December 2022. Forecast horizon is not clearly specified and the	SARIMAX-EGARCH	This study combines a mean model with exogenous variables and a volatility model. It reports that the combined SARIMAX-EGARCH specification fit the

	Indonesia, Thailand, Vietnam, Mainland China, Hong Kong SAR, Japan, UK, France, and Germany)	study appears to focus mainly on modelling and forecasting volatility		data well and was reliable for explaining and forecasting volatility in international air-freight flows.
(Nguyen et al., 2025)	Vietnam; national air cargo traffic (domestic and international)	Quarterly data from 1999 to 2022 with forecasts to 2030	SARIMA-X / EGARCH	The study uses a combined hybrid structure linking SARIMA-type dynamics, exogenous drivers, and volatility modelling. It models and forecasts Vietnam's air cargo traffic, finding that international trade plays a more important positive role than GDP in explaining volatility; forecasts are developed under different scenarios to 2030.
(Emami Javanmard et al., 2024)	Canada; national air transportation demand for passenger and freight	Two datasets were used: a 2000-2019 dataset for correlation analysis and SVM sensitivity analysis, and a 1970-2019 dataset for forecasting passenger and freight demand; data were collected from the World Data Bank and Statistics Canada	Hybrid machine-learning framework integrating pairwise ML algorithms, SVM-based sensitivity analysis, and optimization	The paper develops a hybrid framework integrating machine-learning algorithms and reports higher prediction accuracy than single algorithms, with improvements of 24.5% for passenger demand and 25.85% for freight demand. It then uses the demand forecasts to assess energy and emissions impacts.

Overall, the selected studies suggest that hybrid models can improve air-cargo forecasting by combining methods that capture different features of the data. Statistical models such as ARIMA, SARIMA, and ARIMAX are commonly used to represent linear, seasonal, and explanatory relationships, while machine-learning, decomposition, optimization, or volatility models are added to capture nonlinear patterns and changing variability. Although hybrid models often outperform individual models, their performance depends on the data, forecast horizon, and model configuration. They may also be more complex and difficult to interpret.

2.2 Aviation decarbonization levers for freight

This section reviews the main aviation decarbonization technologies with a specific focus on SAFs and advanced propulsion technologies, including full-electric, hybrid-electric, and hydrogen aircraft. While operational measures and infrastructure improvements are also recognized as important contributors to aviation decarbonization (ATAG, 2021; EUROCONTROL Air Transport Association, 2022; Transport Canada, 2022), they are not explicitly modelled in this study. Their exclusion reflects both data limitations and the scope of this thesis. This thesis uses scenario-based calculations to estimate emissions reductions associated with changes in fuel carbon intensity and aircraft technology performance, which can be represented more consistently within the modelling framework.

In contrast, operational and infrastructure improvements tend to be highly context-dependent, may overlap with existing efficiency trends, and are often more difficult to quantify consistently in a long-term modelling framework. Moreover, they generally offer more limited reduction potential than SAFs or major propulsion shifts, with their long-term contribution often estimated at only about 4-9% by 2050, depending on the scenario design, modelling assumptions, and analytical context (ATAG, 2021; EUROCONTROL Air Transport Association, 2022; Transport Canada, 2022). Figure 2.1 provides a broad overview of aviation energy pathways from feedstock to propulsion system, including drop-in jet fuels, hydrogen, and electricity-based propulsion options (Bauen et al., 2020).

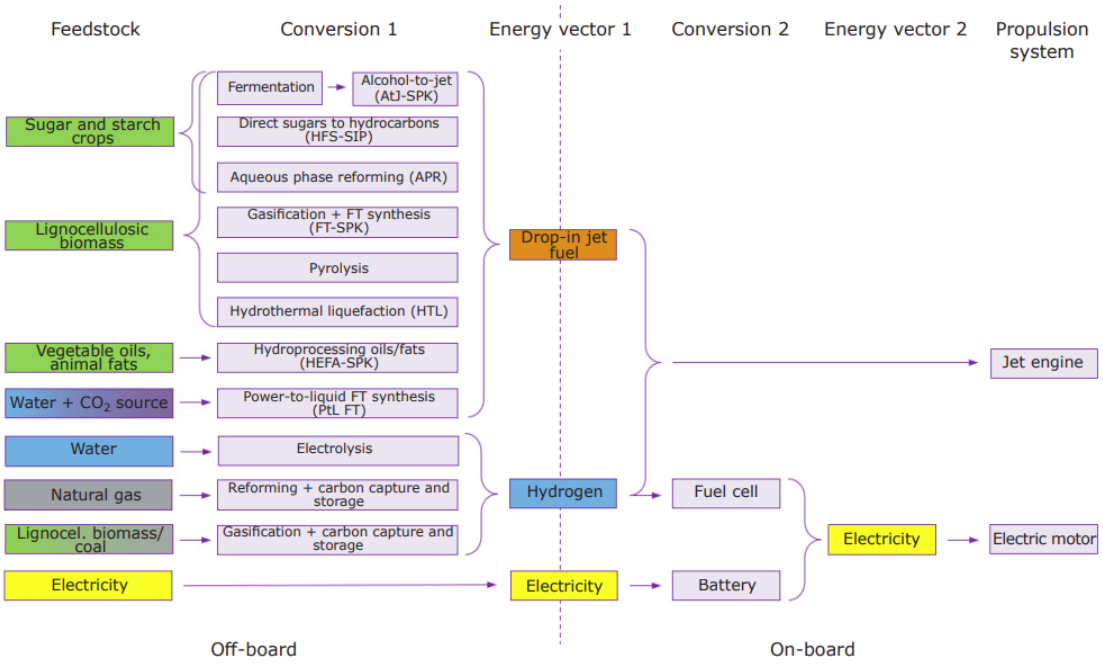


Figure 2-1. Overview of alternative fuel routes for aviation (Bauen et al., 2020)

The following subsections review SAFs and advanced aircraft propulsion technologies relevant to aviation decarbonization. The SAF section discusses certification and blending requirements, deployment and market constraints, and selected case studies illustrating the lifecycle GHG-reduction potential of different pathways and feedstocks. The alternative propulsion section examines the potential emissions benefits and operational limitations of full-electric, hybrid-electric, and hydrogen-powered aircraft, drawing on findings from selected aircraft design and life-cycle assessment studies. Detailed technical reviews of major SAF production pathways and alternative propulsion configurations are provided in Appendices D and E, respectively.

2.2.1 Sustainable aviation fuels

Sustainable aviation fuels are produced from renewable resources or waste-based feedstocks and serve as more sustainable alternatives to conventional petroleum-based jet fuel (Alternative Fuels Data Center, n.d.; Kurzawska-Pietrowicz, 2023). They can provide significant lifecycle greenhouse gas emission reductions (Hu et al., 2022; Kurzawska-Pietrowicz, 2023) and are generally classified as “drop-in” fuels because they can be used with existing aircraft engines and fueling infrastructure

without substantial modification (Smith et al., 2017; Wang et al., 2024). SAFs are therefore widely viewed as a near- to medium-term pathway for aviation decarbonization because they can reduce emissions without requiring immediate changes to aircraft design or airport infrastructure (Transport Canada, 2022). However, their large-scale deployment remains constrained by limited production capacity, higher costs relative to conventional jet fuel, feedstock availability, and technical restrictions on approved blending ratios (Wandelt et al., 2025).

2.2.1.1 Certification and blending constraints

Several pathways can be used to produce SAF. Before a fuel can be used in commercial aviation, however, it must satisfy internationally recognized technical, fuel-quality, and safety requirements (Klimczyk et al., 2025). In particular, ASTM D7566 defines the specifications for synthetic aviation fuels and identifies approved production pathways and associated blending limits (Klimczyk et al., 2025). ICAO separately establishes sustainability and lifecycle-emissions criteria for eligible aviation fuels (Klimczyk et al., 2025).

As of July 2023, 11 conversion pathways for SAF production were approved, with an additional 11 pathways under evaluation (ICAO, n.d.). Table 2-5 presents the approved SAF production pathways, their current maximum approved blending rates, and the potential feedstocks associated with each pathway.

Table 2-5. Overview of SAF Conversion Pathways and Certification Characteristics (*Alternative Fuels Data Center*, n.d.; ICAO, n.d.)

Pathway/Conversion process	Approved Name	ASTM reference	Possible Feedstocks	Maximum Blend Ratio
Hydroprocessed Esters and Fatty Acids	HEFA-SPK	ASTM D7566 Annex A2	Oil-based feedstocks (e.g., jatropha, algae, camelina, canola and yellow grease)	50%
Fischer-Tropsch hydroprocessed synthesized paraffinic kerosene	FT-SPK	ASTM D7566 Annex A1	Municipal solid waste, coal, natural gas, agricultural and forest wastes	50%
Alcohol-to-Jet Synthetic Paraffinic Kerosene	ATJ-SPK	ASTM D7566 Annex A5	Cellulosic biomass, ethanol, isobutanol	50%

Hydrocarbon-Hydroprocessed Esters and Fatty Acids	HC-HEFA-SPK		Algal oil	10%
Catalytic Hydrothermolysis Synthesized Kerosene	CH-SK or CHJ	ASTM D7566 Annex A6	Fatty acids or fatty acid esters or lipids from fat oil greases	50%
Synthesized iso-paraffins from hydroprocessed fermented sugars	SIP	ASTM D7566 Annex A3	Biomass used for sugar production	10%
Synthesized kerosene with aromatics derived by alkylation of light aromatics from non-petroleum sources	FT-SKA	ASTM D7566 Annex A4	Coal, natural gas, biomass	50%
Co-hydroprocessing of esters and fatty acids in a conventional petroleum refinery		ASTM D1655 Annex A1	Vegetable oils, animal fats, used cooking oils from biomass processed with petroleum	5%
Co-hydroprocessing of Fischer-Tropsch hydrocarbons in a conventional petroleum refinery		ASTM D1655 Annex A1	Fischer-Tropsch hydrocarbons co-processed with petroleum	5%
Co-Processing of HEFA		ASTM D1655 Annex A1	Hydroprocessed esters/fatty acids from biomass	10%
Synthetic Paraffinic Kerosene with Aromatics	ATJ-SKA	ASTM D7566 Annex A8	C2-C5 alcohols from biomass	50%

A key limitation under current certification standards is that many approved SAF pathways are qualified only as blending components with conventional Jet A, rather than as fully standalone fuels (ICAO, n.d.). This reflects that synthesized fuel components are not necessarily interchangeable with conventional jet fuel when used alone (Kramer et al., 2022). Some approved SAF pathways, particularly synthetic paraffinic kerosene routes such as HEFA-SPK, FT-SPK, and ATJ-SPK, may lack key chemical constituents, such as aromatics. Aromatic compounds are especially important for fuel-system seal swelling and material compatibility in some older aircraft and engines (Kramer et al., 2022). As a result, these fuels are currently subject to maximum approved blending ratios that commonly range from 10% to 50%, depending on the pathway (ICAO, n.d.).

In contrast, some SAF pathways are designed to include aromatic compounds in the final fuel product, such as FT-SPK/A and ATJ-SKA, which generally follow similar production routes to their

paraffinic counterparts with additional steps or modifications to introduce aromatics (the descriptions of these production processes are provided in Appendix D.). This improves compatibility with conventional jet fuel properties and may support higher blending levels or the future development of fully synthetic drop-in fuels (Kramer et al., 2022). In addition, modern engines increasingly use improved seal materials, such as fluorocarbon and fluorosilicone, rather than nitrile. Therefore, a fuel without aromatics that meets all other Jet A specifications could potentially be used in compatible aircraft (Kramer et al., 2022).

2.2.1.2 Deployment and market constraints

Beyond certification constraints, SAF deployment is further limited by economic and supply-side barriers (Wandelt et al., 2025). Global SAF production remains only a small fraction of total aviation fuel demand, approximately 0.3% as of 2024, while SAF production costs remain higher than conventional jet fuel (IATA, 2024; Wandelt et al., 2025). These higher costs are driven by feedstock prices and energy-intensive conversion processes (Grimme, 2023; Shahriar & Khanal, 2022). Cost reductions are expected to depend on improvements in feedstock availability, conversion efficiency, pathway diversification, and technology maturity (Wandelt et al., 2025). Since many SAF technologies remain at relatively early stages of commercial development, further research, demonstration, and scale-up are needed to reduce production costs (Gary Grim et al., 2022; Grimme, 2023).

Wei et al. (2019) provide a summary of economic evaluations for different SAF production pathways and feedstocks by compiling reported minimum jet fuel prices (MJFPs) from previous literature and techno-economic studies. However, these values should not be interpreted as a direct apple-to-apple comparison because the underlying studies differ in cost year, currency conversion, plant scale, feedstock price assumptions, technology maturity, co-product treatment, and system boundaries. Nevertheless, the compiled MJFP values are useful for indicating the approximate order of magnitude of SAF cost premiums relative to conventional jet fuel and for identifying which pathways tend to have lower or higher production costs under reported assumptions. Table 2.6 below summarizes the reported MJFP values compiled by Wei et al. (2019) for selected SAF pathways and feedstocks.

Table 2-6. Minimum jet fuel selling price for different jet fuel production pathways

Pathway	Feedstocks	MJFP (US dollars/gallon)
HEFA	Camelina oil	1.63-4.62
	Soybean oil	3.82-4.39
	Jatropha	5.42-5.74
	Waste oil and animal fat	2.36-4.73
	Microalgae	31.98
CH	Camelina oils	2.48-3.23
	Lignocellulose	3.66-5.06
HDCJ	Lignocellulose	5.23-7.15
FT	Lignocellulose	6.23-7.57
ATJ	Sugar cane (Biochemistry)	3.65-8.08
	Corn grain (Biochemistry)	3.84-6.63
	Lignocellulose (Biochemistry)	4.32-10.91
	Lignocellulose (Thermochemistry)	7.30-7.82
DSHC	Sugar cane	7.17
	Lignocellulose	18.14-24.42
APR	Lignocellulose	4.66-4.75

The average price of jet fuel is 2.07 USD·gallon^{-1} in 2018

Feedstock availability is consistently identified as a key constraint in SAF literature, with more than 30 studies/journal articles emphasizing its importance (Wandelt et al., 2025). Existing research indicates that feedstock supply is sensitive to market dynamics, policy frameworks, and competing demands from sectors such as food production, renewable diesel, and other bio-based industries. In

addition, as SAF demand increases, competition for eligible feedstocks from other biofuel sectors, food production, and bio-based industries may further increase prices and reduce available supply (Wandelt et al., 2025). Addressing these challenges requires improved forecasting of feedstock availability, diversified sourcing strategies, and continued development of alternative feedstocks, such as algae and lignocellulosic biomass (Cabrera & Sousa, 2022; Wandelt et al., 2025; Wei et al., 2019). In the Canadian context, evidence on SAF feedstock availability remains relatively limited. Existing sources mainly include industry reports and a small number of Canada-specific academic studies. The C-SAF Roadmap proposes a Canadian SAF portfolio to 2030 and identifies representative value chains, defined as regional clusters linking feedstock supply, pre-processing, refining, and end use (Bentley et al., 2023). Antony et al. (2024) examine canola-based SAF and estimate potential SAF production based on available Canadian canola feedstock. These sources suggest that Canada has potential SAF feedstock opportunities; however, further research is needed to assess long-term feedstock availability, competing uses, regional logistics, and scalability.

2.2.1.3 Applications of SAFs and their GHG reduction potential

To better understand the potential of different SAF pathways, several recent studies have evaluated their GHG-reduction performance under varying assumptions, feedstocks, and system boundaries. These studies include a mix of technical/policy reports, LCA, and techno-economic analyses (TEA), providing insights into both environmental and economic aspects of SAF production and deployment. Table 2.7 below summarizes selected case studies on SAF pathways.

Table 2-7. Summary of Case Studies on SAF Pathways and Their GHG Reduction Potential

Study	Geography / Scope	Context/data	Pathways/Feedstocks	Method/boundary	Main findings
(Gladstein & Associates, 2020)	Bay Area airports, especially SFO, OAK, and SJC; California / regional airport application report	Report using airport fuel use, GHG inventory data, California air resource board (CARB) low carbon fuel standard (LCFS) carbon intensity values, and Bay Area SAF deployment scenarios	**HEFA** (animal tallow)	Well-to-wheel GHG scenario analysis	Neat HEFA SAF reduces full-fuel-cycle GHG emissions by about 60% relative to CJF; LCFS-certified HEFA pathways discussed show about 52-73% reductions; airport-wide use of SAF blends at SFO, OAK, and SJC could reduce annual GHG emissions by about 0.47 million metric tons CO_2e (SAF5) to 4.7 million metric tons CO_2e (SAF50).
(Oehmichen et al., 2022)	Germany/Europe; based on the DEMO-SPK project (2016-2020) at Leipzig/Halle Airport; real-world multiblend supply chain tested under operational conditions	Umberto LCA software; ecoinvent v3.3; ReCiPe (H) v1.13 midpoint method; mass and energy flows from actual SAF producer data and literature	**ATJ** (isobutanol), **HEFA** (tallow oil), and **SIP** (sugarcane)	Attributional LCA; ISO 14040/14044; cradle-to-grave (biomass production to airport use)	HEFA showed the lowest environmental and GHG impacts due to its waste-based feedstock, while ATJ and SIP had higher impacts from cultivation and fossil energy use. SAF multiblends reduced GHG emissions by up to 35%, with results strongly influenced by feedstock type and energy source.
(Rogachuk & Okolie, 2024)	United States (Oklahoma)	Aspen Plus v11 process simulation; Aspen Economic Analyzer + literature for costing; OpenLCA v2.0 with Ecoinvent and BioEnergieDat for LCA; base year 2022; 25,000 kg/h waste tire feedstock	**Pyrolysis** (waste tires) and **FT** (waste tires)	Combined TEA+ LCA; well-to-tank (WtT) LCA boundary	Pyrolysis had a lower GWP (34.3 kg CO_2-eq/kg SAF) than FT (58.6 kg CO_2-eq/kg SAF), but it showed higher impacts in several other environmental categories, including indicators of toxicity and photochemical pollution. In contrast, FT had a lower minimum fuel selling price (0.66 USD/L) than pyrolysis (0.78 USD/L), while pyrolysis exhibited a slightly higher energy conversion efficiency (88.7%) than gasification (87%).
(Zhang et al., 2023)	China; Luodian County (Guizhou) for Jatropha and Hailun County (Heilongjiang) for soybean-corn rotation	GREET 2021 for baseline LCA; CENTURY soil carbon model with historical climate data (CRU 1901-2021) and future projections from 6 CMIP6	**HEFA** (jatropha, soybean)	Attributional LCA; cradle-to-combustion, CENTURY model used to simulate soil organic carbon, dynamics, and add soil carbon	When soil carbon sequestration is included, Jatropha-based aviation kerosene shows very strong emissions-reduction potential and can become net negative. Life cycle GHG emissions for the two Jatropha pathways were −36.1 and −59.4 g CO_2e/MJ, while soybean-based aviation kerosene was 2.9 g CO_2e/MJ with

		models across 7 SSP scenarios (2022-2060); CORSIA ILUC default values		sequestration credit on top of consequential LCA and interactive land use change; BP neural network used to project China civil aviation CO_2 to 2060	straw return and 66.1 g CO_2e/MJ without straw return. Jatropha showed the strongest carbon-reduction potential.
(P. H. Chen et al., 2024)	United States	GREET 2022 model; pilot-scale process data from Applied Research Associates (developer and pilot-scale operator of the CH technology); benchmarked against 89 g CO_2e/MJ petroleum jet fuel (WTWa)	**CH** (soybean, carinata, camelina, canola, corn oil, yellow grease, brown grease)	Well-to-wake analysis	The study found CH reduced carbon intensity by about 48-82% relative to conventional jet fuel, with waste feedstocks such as yellow grease and brown grease performing best. Crop-based feedstocks emit more, while green hydrogen has great long-term potential. In addition, the authors estimated that CH could support large-scale U.S. biofuel production and highlighted brown grease as a particularly promising feedstock that may provide CH with a distinct advantage over HEFA.
(Tzanetis et al., 2017)	Sweden, European context	Aspen Plus v11 process simulation for mass/energy balances; SimaPro with Ecoinvent v2.2 for LCA; economic data in 2014 euros; base year 2014/2015 prices; RENJET project (EIT Climate-KIC); partners include Utrecht University, Imperial College, SkyNRG, KLM, Schiphol Airport	**HTL** (forestry residues)	Combined TEA + attributional LCA; cradle-to-grave, ILUC excluded	The study found that HTL-based SAF produced from forestry residues could reduce life cycle GHG emissions by about 85% compared to conventional jet fuel. Nevertheless, the estimated production cost remained high at about 25.1 €/GJ, indicating that although the pathway offers substantial environmental benefits, it is not yet economically competitive in the near term.
(Deuber et al., 2023)	Brazil	Virtual Biorefinery (VB) platform + CanaSoft for agricultural costs; Aspen Plus mass/energy balances; ecoinvent v3.4 for background LCI; RenovaBio carbon credit (Cbios) framework; base	**HTL** (straw, sugarcane stalks	Combined TEA and LCA, Well-to-wake analysis	SAF from HTL showed strong climate-mitigation potential, with 73-82% reductions in GHG emissions relative to fossil jet fuel. The best integrated scenario reached a minimum fuel selling price of 15.4 USD/GJ, suggesting potential competitiveness with fossil

		year December 2019; Monte Carlo uncertainty analysis (10,000 runs)			jet fuel, while stand-alone cases were not economically viable even with high projected carbon prices.
(Peters et al., 2015)	Spain	Aspen Plus process simulation for foreground data; ecoinvent background inventory; SimaPro 7.3 for impact calculations; Spanish electricity mix, fossil fuel origin, and heat supply mix used throughout	**Pyrolysis** (hybrid polar)	Attributional LCA; cradle-to-end-use	Co-combustion of bio-oil in coal power plants showed the highest GHG reduction and overall environmental benefits, followed by cogeneration. Biorefinery pathways (fuel production) showed lower environmental benefits due to higher energy and electricity requirements. Overall, pyrolysis-based biofuels can achieve significant GHG reductions (~60-85%) compared to fossil fuels.
(Pipitone et al., 2023)	Europe	Mass/energy balances in Microsoft Excel; equipment costs via module costing technique; GaBi with CML 2001 baseline (v2016) for LCA; European grid mix (2019); sensitivity analysis + Monte Carlo (10,000 runs) for both TEA and LCA	**HEFA is integrated with the APR of glycerol** (vegetable oils and glycerol by-product)	Combined TEA and LCA, cradle to gate analysis	APR-based hydrogen supply reduced direct manufacturing costs by 22% and lowered MFSP to 1.84 $/kg compared with 2.20 $/kg for the conventional case. The advanced APR scenario had a carbon footprint of about 12 g CO_2/MJ SAF, which was about 54% lower than that of the conventional configuration.

Overall, the case studies show that SAF can achieve significant GHG reductions, but results vary widely depending on feedstocks, production pathways, energy sources, and life-cycle assumptions. Waste- and residue-based feedstocks generally perform well. For example, Chen et al. (2024) reported GHG reductions of approximately 48-82% for CH fuels, with yellow and brown grease producing the lowest carbon intensities. Similarly, Tzanetis et al. (2017) estimated an approximately 85% reduction for HTL fuel produced from forestry residues, although its production cost remained relatively high.

The results are also highly sensitive to methodological choices. Oehmichen et al. (2022) found that a blend containing multiple SAF pathways reduced GHG emissions by up to 35%, with HEFA from waste tallow outperforming crop-based ATJ and SIP pathways. Zhang et al. (2023) reported that jatropha-based HEFA could become net negative when soil-carbon sequestration credits were included, illustrating how land-use and soil-carbon assumptions can significantly affect estimated emissions. Therefore, SAF pathways should be compared using consistent system boundaries and assumptions.

2.2.2 Alternative aircraft propulsion technologies

While SAF is often viewed as a short- to medium-term solution for reducing aviation GHG emissions because it can be applied within existing aircraft and fuel infrastructure, alternative propulsion systems represent longer-term pathways for deeper aviation decarbonization. These technologies include battery-electric, hybrid-electric, and hydrogen-powered aircraft, which have the potential to reduce or eliminate direct in-flight CO_2 emissions, depending on the energy source, grid carbon intensity, and system design.

The potential of alternative propulsion systems to reduce aviation GHG emissions has been widely examined in recent literature through a combination of aircraft-level design studies and LCA analyses. These studies evaluate battery-electric, hybrid-electric, and hydrogen-powered aircraft across different aircraft classes, mission ranges, and technology assumptions. Table 2-8 summarizes key findings from representative studies, highlighting their scope, methodological approaches, and reported GHG or environmental reduction outcomes.

Table 2-8. Summary of case studies on alternative propulsion systems and their GHG reduction potential

Study	Aircraft Type / Scope	Configuration	Method / Assumptions	Key Findings	GHG Reduction
(Nasoulis et al., 2023)	19-seat commuter aircraft; 400 nm mission + 100 nm reserve	Parallel and series hybrid-electric	Aircraft sizing, direct operating cost, and life-cycle assessment for 2027, 2030, and 2040 entry-into-service (EIS) scenarios	Hybrid-electric aircraft can significantly reduce fuel use and emissions, particularly in future scenarios (2030-2040), with series configurations showing the greatest potential. However, benefits depend on battery improvements, system weight, and the carbon intensity of electricity, and early-stage designs may not yet be viable.	The study includes several scenarios, but LCA/GHG reduction results are reported only for the 2030 EIS variants. For this scenario, the parallel-hybrid configuration reduced environmental impact by 19.5% using the EU electricity mix and by 22.8% using renewable electricity. The series-hybrid configuration showed larger reductions, decreasing environmental impact by 52.1% with the EU electricity mix and by 59.7% with renewable electricity
(D. D. Nguyen et al., 2020)	Small 4-seat aircraft, based on a Cessna 172N-type aircraft	Hybrid-electric, and full-electric aircraft	Total life-cycle cost and emissions method, including aircraft, infrastructure, operation, electricity mix, and battery production	Full-electric aircraft can reduce emissions only if range is greatly reduced; hybrid aircraft provide smaller total GHG reductions but can reduce local airport-region emissions	Hybrid-electric configurations achieved relatively modest emission reductions, in the range of approximately 5-15%. In contrast, full-electric aircraft demonstrated a higher emission-reduction potential, with total life-cycle reductions of approximately 20-27%. However, these benefits are associated with significant performance trade-offs, particularly reductions in flight range. For example, full-electric configurations showed range reductions of up to approximately 60-72% compared to conventional aircraft, primarily due to the lower energy density of current battery technologies.
(Ribeiro et al., 2020)	Multiple aircraft categories with different sizes and range classes (SR22T, E190 AR, A320neo, B777-300ER);	Hybrid-electric propulsion using Li-S and Li-air battery assumptions	Consequential LCA combined with conceptual aircraft design and multidisciplinary design optimization, with sensitivity analysis for	Hybrid-electric propulsion shows great potential for small and regional aircraft, while larger aircraft (narrow- and wide-body) face significant limitations in range and payload capacity. Fuel savings vary widely depending on aircraft type and battery performance, with moderate reductions achievable in the near term	Results vary by aircraft type and scenario. Hybrid-electric configurations achieve moderate fuel and emission reductions (e.g., ~11-16% for small/regional aircraft in 2030 and up to ~50-60% in 2050 scenarios), but life-cycle results show that battery charging dominates emissions, meaning overall GHG reductions depend strongly on the electricity mix and may be limited under carbon-intensive grids.

	conceptual hybrid-electric aircraft		future electricity grid mixes from 2030 to 2050.	and larger reductions possible under future (2050) technology assumptions.	
(Thonemann et al., 2024)	50-passenger regional aircraft; 200 nmi typical mission and 600 nmi design mission; Europe; 2030, 2040, 2050	Conventional gas turbine, battery hybrid-electric, and hydrogen fuel-cell hybrid-electric configurations	Prospective cradle-to-grave LCA using IMPACT World+; includes aircraft, airport, fuel/electricity/hydrogen systems, manufacturing, operation, and end-of-life	Battery-hybrid-electric aircraft may serve as a short-term transition option, while hydrogen-fuel-cell aircraft show stronger long-term potential. However, impacts shift from flight emissions toward airport operations, aircraft manufacturing, electricity, and hydrogen production.	Hybrid-electric aircraft reduce climate-change impacts, but overall benefits are mixed because water use, land use, and human-health impacts can increase. Hybridization reduced climate-change damages by about **15%** in the short term and up to **83%** for long-term hydrogen aircraft.
(Scholz et al., 2022)	Single-aisle transport aircraft; A320-class; 1000 nmi mission	Battery hybrid-electric aircraft with discrete parallel powertrain	Conceptual aircraft design, environmental LCA, and direct operating cost analysis	Hybrid-electric aircraft are not inherently more environmentally or economically efficient than conventional aircraft. In the baseline scenario, the hybrid-electric configuration results in higher aircraft weight, increased energy demand, and higher operating costs due to battery and electric powertrain requirements. However, the study shows that hybrid-electric aircraft can become environmentally beneficial under future conditions, particularly with low-carbon electricity, improved battery performance, and stronger environmental policies.	In the baseline scenario, the hybrid-electric aircraft exhibited a 15.1% increase in total life-cycle environmental impact compared to the conventional aircraft. Under a future scenario with renewable electricity and improved technology assumptions, the hybrid-electric aircraft achieved a reduction in environmental impact of approximately 7.0% relative to the conventional aircraft.
(Arvidsson et al., 2024)	Two-seater aircraft (pilot training / general aviation); 1-hour flight functional unit	Fully electric	Attributional cradle-to-grave LCA; includes airframe, battery, manufacturing, use phase, and end-of-life; scenarios	The study finds that all-electric aircraft can have lower global warming impacts than comparable fossil-fuel aircraft, but only when the aircraft has a sufficiently long operating lifetime and uses low-carbon electricity. The main	Under short-lifetime assumptions, the airframe impact is high because it is spread over fewer flight hours, making the electric aircraft worse than the fossil-fuel aircraft. With a longer lifetime, the electric aircraft performs better: using EU electricity provides an estimated 10-20% reduction in global

			for lifetime (500-4000 h) and electricity mix	environmental hotspots are the airframe, lithium-ion battery, and use-phase electricity. However, the study also shows an important trade-off: although all-electric aircraft can reduce climate impacts, they have higher mineral resource impacts because of battery materials such as lithium, nickel, cobalt, and copper	warming impact, while using low-carbon electricity reduces global warming impact by approximately 50-60%.
(Mukhopadhaya & Graver, 2022)	Regional electric aircraft; 9-seat, 19-seat, and 90-seat concepts; short-range passenger aviation	Fully electric aircraft	Performance and emissions analysis using electric range equation, battery specific energy scenarios, route coverage, and WTW GHG analysis including electricity generation and battery replacement	Electric aircraft are most suitable for short-range commuter and regional routes. They are 2.1-3.2 times more energy efficient than comparable fossil-fuel aircraft, but market coverage is limited by battery energy density and reserve requirements.	The study finds that electric aircraft can significantly reduce life cycle GHG emissions compared with fossil-fuel aircraft, particularly when powered by low-carbon electricity. Even under "current policy" electricity scenarios, electric aircraft can reduce carbon intensity by approximately 49-57%, while renewable electricity can increase reductions to 82-88%. However, these benefits are mainly limited to short-range commuters and regional aircraft because of current battery energy-density and range constraints.
(Schäfer et al., 2019)	Projected 180-seat all-electric aircraft; short-haul mission ~400 nmi or 741 km	Fully electric aircraft	First-order energy, economic, and environmental assessment; compares electric aircraft with A320neo-type jet aircraft under different electricity carbon intensities	The study finds that all-electric aircraft could eliminate direct in-flight CO_2 emissions, air pollutants, and non-CO_2 warming effects, but their overall climate benefit depends strongly on the electricity mix and battery technology.	For a 400 nmi mission, the electric aircraft produced about 91 g CO_2/RPK using the 2015 U.S. grid, which is about 20% higher than the A320neo reference aircraft at 75 g CO_2/RPK. However, when non-CO_2 impacts are included, the total warming impact is reduced by about 30% because electric aircraft eliminate direct combustion-related non-CO_2 effects. Battery production could add another 2-10 g CO_2e/RPK.

(Evon et al., 2026)	Hypothetical 70-seat regional aircraft; 3.12 MW fuel-cell system	Hydrogen fuel-cell aircraft	Python-based LCA tool integrated with fuel-cell system sizing; includes fuel-cell production and upstream hydrogen production/use	The study finds that hydrogen fuel-cell aircraft can substantially reduce climate-change impacts compared with both conventional kerosene aircraft and SAF. However, the main disturbance comes from hydrogen production, even when hydrogen is produced using renewable wind electricity. Fuel-cell system production has a smaller contribution overall, but the platinum catalyst and bipolar plates are important hotspots. The study also found that fuel-cell efficiency is the most important parameter for further reducing climate impacts	The fuel-cell aircraft achieved up to 92% climate-change impact reduction compared to conventional kerosene aircraft and up to 77% reduction compared to SAF (PtL) powered aircraft on a passenger-kilometer basis. It also performed better than fossil kerosene in 10 of 16 midpoint impact categories, including climate change, eutrophication, and human toxicity.
(Kossarev et al., 2023)	Long-range wide-body aircraft; A330-200 class; EIS 2040	Hydrogen combustion aircraft	Environmental LCA + direct operating cost analysis; comparing current and future renewable-energy fuel production scenarios	The study finds that under current fuel production methods, both hydrogen- and biofuel-powered long-range aircraft can have higher overall environmental impacts than conventional kerosene aircraft due to the energy-intensive production processes. However, under future scenarios using renewable electricity and cleaner production pathways, both hydrogen and biofuel aircraft show significant environmental improvements and become more sustainable alternatives.	Under current production pathways, liquid hydrogen increased total environmental impact by 14.8%, mainly because hydrogen production remained energy intensive. The algae-based biofuels performed worse, with impacts increasing by 238-548%, due to the high energy demand of biofuel production. Under a future renewable-energy scenario, the results improved substantially: liquid hydrogen reduced environmental impact by 59.5%, while SAF pathways reduced impacts by 35.8-112%.
(Lai & Björklund, 2025)	Future Swedish aviation pathways; long-distance air travel	Hydrogen combustion aircraft	Prospective life-cycle assessment of six future aviation pathways	Hydrogen-powered aviation can reduce global warming impacts compared with fossil kerosene, but can increase other impacts such as toxicity, land use, and infrastructure-related	Hydrogen-powered aviation could achieve 20-70% lower climate change impacts than fossil kerosene. The study also finds that LH_2 pathways could have up to 60% lower climate change impacts than e-kerosene pathways. However, hydrogen

				burdens. Results depend strongly on energy supply, fuel production, and airport operations.	pathways may increase other environmental impacts, so the benefit is mainly strongest for GHG/climate change.
(Stine et al., 2020)	Boeing 787-8-based long-range aircraft	Hydrogen fuel-cell aircraft	Life-cycle assessment using openLCA, Ecoinvent, Piano-X, and ReCiPe midpoint method	Hydrogen-electric aircraft significantly reduce life-cycle emissions compared to conventional kerosene aircraft, particularly when low-carbon hydrogen is used. However, impacts remain due to electricity use in hydrogen production.	Hydrogen-electric aircraft reduce life cycle GHG emissions by roughly 58% compared to conventional kerosene aircraft.

Overall, the case studies show that the GHG benefits of alternative aircraft propulsion depend strongly on aircraft size, flight distances, battery performance, and the carbon intensity of electricity or hydrogen production. Hybrid-electric aircraft generally provide moderate reductions. For example, Nasoulis et al. (2023) reported reductions of about 20-23% for a parallel-hybrid configuration and 52-60% for a series-hybrid configuration. Fully electric aircraft can achieve larger reductions on short routes, with Mukhopadhaya and Graver (2022) estimating reductions of 49-57% under current-policy electricity scenarios and 82-88% with renewable electricity. However, their use remains limited by battery weight and range.

Hydrogen aircraft also show substantial long-term potential, but results depend strongly on hydrogen production. Kossarev et al. (2023) found that liquid hydrogen increased environmental impacts under current production conditions but reduced them by about 60% under a future renewable-energy scenario. Therefore, alternative propulsion technologies are most effective when combined with low-carbon energy sources and applied to aircraft and routes suited to their technical limitations.

2.3 Freight mode choice, selective mode shift, and surface freight decarbonization

In freight transport, much of the existing literature focuses on road-to-rail or road-to-water substitution, while relatively less attention has been given to shifting freight away from air transport. A similar concept is also discussed in passenger aviation, where short-haul flights may be replaced by lower-emission alternatives, such as high-speed rail. Given the limited availability of air-freight-specific modal-shift studies, this section draws on broader freight and passenger transport literature to provide relevant insights into modal substitution, emissions impacts, and operational constraints, while focusing as closely as possible on evidence relevant to air freight.

This section first explains the concepts of freight mode choice and modal shift and reviews the key determinants influencing freight mode choice decisions. It then examines selected studies covering different modal-shift contexts, implementation approaches, reported environmental benefits, and practical constraints. Additional background on truck and rail decarbonization pathways that inform the future surface-mode emissions assumptions used in this thesis is provided in Appendix F.

2.3.1 Freight mode choice and Modal Shift concepts

Freight mode choice refers to the decision about which mode, such as road, rail, water, air, or intermodal combinations, is used to move goods between an origin and destination. This decision is usually made by shippers or logistics managers and reflects trade-offs among different service, economic, and operational requirements (H. C. Kim, 2014; X. Xu et al., 2024). Modal shift, in contrast, refers to the reallocation of transport activity from one mode to another, typically from more carbon-intensive modes to lower-emission alternatives (Björk et al., 2023; KLRI, 2018; Rodrigue, 2017). These concepts are closely related because modal shift occurs only when the factors that determine mode choice change, or when another mode becomes attractive enough to replace the current one (Rodrigue, 2017). In other words, shifting freight from one mode to another requires understanding why the original mode was chosen in the first place. Therefore, before evaluating modal shift, it is necessary to review the key determinants of freight mode choice.

Across literature, several determinants are consistently identified as important in freight mode choice. Transport cost is often considered one of the most important criteria because it directly affects the economic competitiveness of freight movement (Beil et al., 2025; Grue & Ludvigsen, 2006; Kreutzberger, 2003). Alongside cost, transit time and reliability are also repeatedly identified as dominant mode-choice factors, although their relative ranking varies across studies (Tavasszy et al., 2020). The transit time value depends on customer requirements and product characteristics (Blauwens et al., 2006; Fries, 2009; Mary et al., 2012; Massiani et al., 2007); for example, time-sensitive or perishable goods may place greater importance on faster delivery. On the other hand, reliability depends on logistics practices, transport distance, and the type of goods being shipped (De Jong et al., 2014; Fries, 2009; Tavasszy et al., 2020). Perceived reliability varies across transport modes. Konstantinus & Mark (2018) finds that road transport was perceived as the most reliable mode for on-time arrival, followed closely by air and maritime transport, while rail was perceived as less reliable.

Other service-related factors, such as service frequency, flexibility, and damage and loss, are also commonly identified as freight mode-choice criteria (Beil et al., 2025; Tavasszy et al., 2020). Frequency refers to how often a transport service is available, which affects scheduling flexibility and the ability to accommodate frequent or smaller shipments (Tavasszy et al., 2020). Flexibility reflects

the ability of a mode or carrier to respond to changing shipment needs or unplanned transport requirements without excessive delay (Day, 1994). Damage and loss refer to the risk that goods may lose value due to damage, theft, or accidents during transport (Witlox & Vandaele, 2005). Environmental performance, particularly CO_2 emissions, has been considered in relatively few freight mode-choice studies and is often ranked lower than traditional criteria such as cost, time, and reliability (Tavasszy et al., 2020); however, it is becoming increasingly relevant due to climate-change concerns and policy interest in lower-emission freight systems (S. Anderson et al., 2005; Centobelli et al., 2017)

2.3.2 Evidence on modal shift benefits and constraints

The literature on freight modal shift shows that shifting freight from higher-emission modes to lower-emission alternatives can reduce emissions, but the feasibility of such shifts depends strongly on corridor characteristics, service requirements, infrastructure availability, and shipper behavior. As discussed above, studies directly related to modal shift applications in aviation freight are limited. Therefore, this section reviews both air-freight modal-shift studies and broader freight modal-shift studies involving road, rail, and sea shipping. The purpose is to identify the potential benefits of modal shifts as a decarbonization strategy, assess their emissions-reduction potential, and highlight the operational constraints that may limit real-world implementation.

The studies summarized in Table 2.9 show that modal shift can be evaluated in several ways. Some studies estimate direct reductions in emissions or energy savings from shifting freight from trucks or air to rail-based alternatives. Others focus on behavioral mode-choice modelling, shipper acceptance, policy effectiveness, or implementation barriers. Together, these studies provide useful evidence that a modal shift can be an effective freight decarbonization strategy, with the potential to reduce or offset part of the CO_2 emissions from higher-emission modes. However, the literature also shows that this potential is constrained by logistics-service requirements, including cost, transit time, reliability, service frequency, capacity, infrastructure availability, and coordination among transport stakeholders.

Table 2-9. Summary of Modal-Shift Case Studies, Emissions Impacts, and Implementation Constraints

Study	Mode Shift Type	Geography / Context	Objective / Purpose	Key Findings/GHG Reduction	Key Constraint
(Li, 2025)	Air & road to high-speed rail (HSR) (express freight)	China; Beijing-Shanghai corridor; 5 cities (Beijing, Tianjin, Jinan, N anjing, Shanghai)	Evaluate whether a carbon tax can shift express freight from higher-emission modes to HSR while limiting impacts on shippers	Carbon tax induces modal shift from air and road to HSR, particularly on medium- and long-distance routes where HSR competes with air. Under a 3% increase in total freight demand, emissions rise from 1,131.9 t CO_2 to 1,181.7 t CO_2 without policy. A carbon tax of 367.03 CNY/tCO_2 maintains emissions at the baseline level through modal shift, with air freight decreasing by 5.02%, HSR increasing by 3.34%, and road increasing slightly by 0.36%.	Effectiveness is limited by HSR capacity and policy constraints. At higher demand growth, modal shift alone cannot fully offset emissions. Results are context-specific and depend on corridor characteristics and assumed demand growth (the 3% demand growth assumption is scenario-based rather than derived from a forecast)
(Yao et al., 2023)	Air freight to air-HSR intermodal express freight network	China; nationwide network; hub location and route planning across major Chinese cities using real national freight flow data from Southwest Jiaotong University's National Engineering Laboratory	Develops a freight network design model for air-HSR express freight planning. The model considers node centrality, carbon emissions, and time efficiency to balance service speed and emission reduction.	The planned air-HSR express network could provide nationwide express service within 24 hours. Compared with the original airline network, the proposed network reduced carbon emissions by 2.08 million tonnes, equal to a 57.35% reduction, and saved the transport sector 498.7 million RMB.	The study relies on simplified theoretical assumptions and assumes full implementation of the proposed air-HSR network. Actual outcomes would depend on stakeholder coordination, intermodal hub investment, and whether HSR can meet the 24-hour delivery requirement on each corridor. The model is also static and sensitive to the freight-flow data source, so it shows potential rather than guaranteed real-world reductions.
(Bruno et al., 2025)	Passenger air to HSR	Short-haul flight routes; policy context for short-haul flight bans	Evaluates the impacts of replacing short-haul flights with train travel under different policy designs, focusing on CO_2e	The study estimates that replacing short-haul flights with rail could reduce CO_2e emissions by about 1-12%, depending on the policy design and route-selection criteria. More restrictive short-haul flight bans produce	The study assumes that passengers on banned short-haul flights fully shift to rail, which may overestimate achievable emission reductions because some travellers may instead drive, cancel trips, or choose connecting flights. The results also depend on whether the rail system has enough capacity

			emissions, passenger travel time, and rail capacity	larger emissions savings but also create greater impacts on passenger travel time and rail-capacity requirements. The study assumes full air-to-rail substitution, so these reductions represent potential savings rather than guaranteed real-world outcomes.	to absorb additional passengers without overcrowding or major new investment. In addition, air-to-rail substitution can increase total travel time, especially where rail services are slower, less frequent, or require transfers, so the feasibility of replacement depends strongly on corridor-level rail connectivity and service quality.
(Eng-Larsson & Kohn, 2012)	Road freight to intermodal road-rail transport	Europe; six case companies shipping non-bulk, fast-moving goods across industries such as fashion, food/beverages, automotive, and industrial products	Examines modal shift from the shipper's perspective, focusing on what contextual factors and operational changes allow firms to shift from road to intermodal road-rail without reducing logistics performance	No single GHG estimate is provided for all cases. IndustryCo reported a 6% emissions reduction, and the paper cites prior European evidence showing 20-50% CO_2 reductions from truck-to-road-rail shifts. Environmental benefits were often secondary; cost/service considerations drove most cases, while AutoCo was the clearest or only environmentally driven case.	Key constraints include longer transit times, lower delivery time precision, lower flexibility, and possible goods-damage risk compared with road-only transport. Shippers may need operational adjustments such as increased inventory, wider delivery windows, better planning, improved lashing/handling, stronger carrier coordination, and centralized system control to maintain service performance.
(Zhou et al., 2017)	Truck freight to rail freight	United States; national freight flows using FHWA Freight Analysis Framework (FAF), EIA Annual Energy Outlook, Argonne NEAT, and GREET	Evaluates the potential energy-use and GHG-emissions impacts of shifting suitable long-distance truck freight to rail, considering commodity type, OD-level flows, distance, tonnage, and rail level of service	Under the baseline scenario, truck-to-rail modal shift produced a 4.3% net energy saving and 4.4% GHG reduction by 2040 at the national freight-sector level. Cumulative energy savings reached 6,350 trillion Btu by 2040. Sensitivity analysis showed that annual energy/GHG savings could range from about 1.1% to 7.8% in 2040, depending mainly on rail level of service and commodity shiftability.	Results are constrained by commodity suitability, rail service quality, OD-level rail availability, shipment distance, and minimum freight volume. The study excludes many low-volume, time-sensitive, and delicate commodities, considers only truck trips over 300 miles, and requires OD flows of at least 10,000 tons. It also assumes rail has enough capacity to absorb shifted freight.

(Kowalska & Bonk, 2021)	Road freight to rail, inland shipping, and short-sea shipping	Poland; international import/export freight flows from 2005, 2010, 2015, and 2019	Evaluates whether EU and Polish modal-shift policies successfully shifted international freight away from road transport toward lower-impact modes	Modal shift targets were not achieved. Road transport's share increased from 26.7% to 30.2% in imports and from 27.6% to 47.6% in exports between 2005-2019. Rail's share fell from 23.8% to 11.4% in exports and remained roughly flat in imports (~19%). Inland shipping nearly disappeared (from 1.8% to 0.07% in exports). Air freight remained negligible throughout, never exceeding 0.3% by weight in any year, confirming air is a marginal mode by volume in this context. No GHG reduction was achieved; the trend moved in the opposite direction. The authors conclude Poland cannot meet the 2030 White Paper target of 30% shift from road to alternatives	The study suggests that modal shift in Poland is constrained by the strong competitiveness of road transport, especially due to relatively low trucking costs and high flexibility compared with rail. High rail infrastructure access costs, weaker rail punctuality, and lower service flexibility discourage shippers from switching. The growth of smaller private firms and the shift from bulk commodity exports toward manufactured goods also increased demand for flexible road-based logistics. In addition, policy instruments appear too broad because many initiatives focused on infrastructure and carriers rather than directly targeting cargo shippers, who often make the mode-choice decision. Air freight is included in the modal split data, but its share by weight is very small, so changes in air freight would have little effect on aggregate modal-shift outcomes.
(Park et al., 2007)	Truck freight to rail	Southern California ports region; Ports of Los Angeles/Long Beach and the Alameda Corridor	Evaluates the air-quality impacts of shifting port-related freight traffic from heavy-duty trucks to rail using on-road vehicle emissions modelling and locomotive emissions estimates	A 20% shift of port-related heavy-duty truck traffic to rail reduced NOx by 71.9 kg/hour, PM by 1.3 kg/hour, CO by 82.2 kg/hour, and HC by 5.7 kg/hour. This equals about 0.86 tons/day of NOx and 15.6 kg/day of PM reduction. The study finds rail produces about 3.3 times lower NOx emissions than trucks for shifted freight.	Large-scale diversion is unlikely without policy intervention. Rail is often viewed as operationally suitable mainly for longer distances, while short-haul rail faces terminal handling and drayage costs that reduce competitiveness. Implementation depends on underused rail capacity, port/terminal integration, incentives such as peak-hour fees, and broader air-quality policies.
(Kurtuluş & Çetin, 2020)	Road freight to intermodal rail	Turkey; short-distance inland container corridor	Uses a stated-choice experiment to evaluate modal-shift potential from	The base intermodal rail share was estimated at 10.6%. The most effective policy was to double train frequency and reduce intermodal	Road remains strongly preferred due to better speed and flexibility. Modal shift depends on improving rail frequency, reducing transit time and delays, lowering rail cost, and

		between Denizli and the seaports of Izmir	road to intermodal rail based on cost, transit time, delay, frequency, and free time	transit time by 50%, increasing rail share to 29.7%. A 10% road-cost increase increased rail share to 18.3%, while a 10% intermodal rail-cost reduction increased to 15.5%. The study does not directly estimate GHG reductions.	overcoming infrastructure/capacity limits on a short-distance corridor. Results are corridor-specific and based on stated-choice responses, so actual behavior may differ.
(Gupta & Dhar, 2022)	Road freight to rail / lower-carbon freight alternatives	Freight sector transition analysis; India context	Examines how modal shifts in freight transport affects emissions, energy demand, and the economy	The CO_2 emissions reductions range from about 34% by 2030 under the road-focused transition to up to 96% by 2050 under the harmonized multimodal scenario, relative to current policy. Benefits also include reduced fossil-fuel imports, up to 87.6% by 2050, lower logistics costs, from 14% to 11% of GDP, and cumulative foreign-exchange savings of up to USD 3.8 trillion.	Benefits depend on major investment in multimodal logistics, rail capacity, clean electricity, EVs, charging infrastructure, and digital systems. The HMML pathway requires about 451 billion USD more investment from 2016-2030 compared to the current policy. Rail service also faces barriers such as capacity saturation, poor time reliability, unscheduled freight movements, limited frequency, and weak last-mile connectivity. The study focuses mostly on road and rail, with less detail on coastal shipping and inland waterways.

Overall, the reviewed studies show that modal shift can provide meaningful emissions benefits, but the scale of reduction varies widely depending on the mode being replaced, the substitute mode, and the assumptions used in the analysis. The largest reductions are reported in studies that shift air or road freight to high-speed rail or integrated multimodal systems. For example, Yao et al. (2023) report a large reduction from an air-HSR express freight network, while Gupta and Dhar (2022) show that multimodal freight strategies can produce substantial long-term emissions reductions when combined with electrification and clean energy. Road-to-rail studies such as Zhou et al. (2017) and Park et al. (2007) also show positive emissions or air-quality benefits from shifting suitable truck freight to rail.

However, the literature also shows that the potential for modal shift is not automatic or guaranteed. The Poland case study by Kowalska and Bonk (2021) shows that road freight can continue to increase even when policies are in place to shift freight toward rail and waterborne modes. This suggests that policy targets alone are not enough; modal shift depends on whether alternative modes are competitive in terms of cost, reliability, flexibility, and service quality.

2.4 Roadmap and scenario-based decarbonization studies

Net-zero aviation emissions by 2050 have become a major goal guiding aviation decarbonization plans across both industry and government. At the international level, the aviation industry, through the Air Transport Action Group (ATAG), adopted a net-zero carbon target for civil aviation in 2021 (ATAG, 2021). This was followed in 2022 by the International Civil Aviation Organization (ICAO), which adopted a Long-Term Aspirational Goal (LTAG) aligned with the Paris Agreement (ICAO, 2022). These commitments have led to an increasing number of roadmap and scenario-based studies exploring possible pathways to reduce aviation emissions to net-zero by 2050. Rather than relying on a single technology or scenario, these studies use multiple scenarios and combine multiple strategies/technologies to reflect uncertainty in future demand growth, technology readiness, SAF availability, infrastructure development, and policy ambition. Table 2.10 summarizes selected roadmap and scenario-based studies on aviation decarbonization

Table 2-10. Summary of Major Aviation Decarbonization Roadmaps, Pathways

Study / Roadmap	Scope	Main Pathways	Key Findings	Limitations / Relevance to This Study
ATAG Waypoint 2050	Global aviation	SAFs, innovative aircraft technologies, infrastructure and operational improvements, and out-of-sector carbon reductions	This report finds that net-zero aviation by 2050 will require a portfolio of measures, including SAFs, new aircraft technologies, operational improvements, and offsets. SAF is expected to be the dominant near- to medium-term pathway because it can be used with existing aircraft and infrastructure, while electric and hydrogen aircraft are mainly expected to contribute to shorter-range routes.	Global and climate-target-focused roadmap; does not provide Canadian domestic air-cargo corridor analysis.
EUROCONTROL Outlook 2050	European aviation	SAFs, fleet renewal and conventional aircraft efficiency improvements, air traffic management (ATM) and operational improvements, revolutionary aircraft technologies such as electric and hydrogen aircraft, and out-of-sector carbon reductions.	This report finds that reaching net-zero aviation by 2050 requires a combination of measures, with SAFs providing the largest emissions-reduction contribution in the base scenario. Operational and air traffic management improvements also contribute but are treated as relatively low-hanging fruit compared with deeper technology and fuel transitions. Electric and hydrogen aircraft are expected to have a much smaller system-wide impact by 2050, while market-based measures and carbon capture remain important for closing the remaining gap to net-zero.	Europe-focused roadmap; not specific to Canadian domestic air cargo
Destination 2050	European aviation	SAFs, aircraft and engine technology improvements, ATM and aircraft operational improvements, hydrogen aircraft technology, and economic and market-based measures	This report finds that reaching net-zero aviation emissions by 2050 requires a combination of measures. SAFs and alternative fuels provide the largest emissions-reduction contribution, supported by aircraft and engine technology improvements, ATM and operational improvements, hydrogen aircraft, and economic measures such as EU ETS and CORSIA. The report also highlights that strong near-term action from both industry and policymakers is needed to stay on track for the 2050 net-zero pathway.	Europe-focused roadmap; not specific to Canadian domestic air cargo
ICCT Vision 2050	Global aviation	SAFs, aircraft and operational improvements, carbon pricing and economic measures, modal shift and alternative propulsion systems	The report finds that aligning aviation with the Paris Agreement requires strong and immediate action, including aircraft efficiency improvements, SAF scale-up, zero-emission aircraft, carbon pricing, demand effects, and carbon removals. The report is more critical than many industry roadmaps	Global and climate-target-focused roadmap; does not provide Canadian domestic air-cargo corridor analysis.

			because it shows that technology and fuels alone may not be enough, especially if aviation demand continues to grow rapidly.	
UK Sustainable Aviation Net Zero Carbon Road-Map	UK aviation	SAFs, aircraft technology improvements, and economic and market-based measures	The report finds that UK aviation can reach net-zero carbon emissions by 2050 through a portfolio approach. SAFs and carbon removals play major roles, supported by aircraft efficiency, operational improvements, and future zero-carbon aircraft technologies.	UK-focused report; does not provide Canadian domestic air-cargo corridor analysis.
Canada's Aviation Climate Action Plan 2022 - 2030	Canada	SAFs, alternative propulsion systems, aircraft and operational improvements, and out-of-sector reductions	The report finds that the plan sets Canada's vision for net-zero aviation emissions by 2050 and identifies SAF as the largest in-sector emissions-reduction pathway, supported by operational improvements and emerging aircraft technologies. It also recognizes that out-of-sector reductions will still be needed to close the remaining gap to net-zero.	Canada-specific and useful for policy context and technology pathways, but primarily strategic and high-level with limited domestic air-cargo-specific analysis

Across the studies summarized in Table 2.10, SAF is consistently identified as the most important near- to medium-term emissions-reduction pathway because it can be used in existing aircraft and fuel-distribution systems with relatively limited operational changes. All of the reviewed roadmaps conclude that substantial SAF deployment will be necessary to achieve deep reductions in aviation emissions. However, they also recognize that SAF alone is unlikely to achieve net-zero emissions. Improvements in conventional aircraft and engine efficiency, fleet renewal, air traffic management, airport and flight operations, and the introduction of electric- and hydrogen-powered aircraft are therefore included as complementary measures. Because these strategies are unlikely to eliminate all emissions, particularly from long-haul aviation, most roadmaps also include market-based measures, carbon capture, or other out-of-sector reductions to address residual emissions.

The relative contribution assigned to each pathway differs across the reviewed studies. For example, ATAG's Waypoint 2050 places greater emphasis on the role of SAF, technological innovation, and carbon removals in supporting continued growth in aviation activity. In contrast, ICCT's Vision 2050 presents a more conservative assessment of whether technology and fuels alone can align aviation with the Paris Agreement, emphasizing that rapid demand growth could offset some of the reductions achieved through aircraft efficiency, SAF, and alternative propulsion. Despite these differences, the studies broadly agree that immediate action is required because aircraft fleet turnover, fuel-production expansion, infrastructure development, and the commercialization of new propulsion technologies require long implementation periods.

Within the Canadian context, Canada's Aviation Climate Action Plan 2022-2030 provides the most directly relevant national roadmap. Developed by the Government of Canada in collaboration with aviation-sector stakeholders, the plan establishes a shared vision for achieving net-zero aviation emissions by 2050 and identifies priority actions to 2030. These include improving aircraft and operational efficiency, supporting the development and adoption of SAF, advancing emerging aircraft technologies, improving airport and air navigation operations, and addressing emissions that cannot be eliminated through in-sector measures. The plan, therefore, follows the same portfolio-based approach as the international roadmaps, applying it to Canada's aviation policy and operating context.

The plan identifies SAF as the largest potential source of in-sector emissions reductions because few other technologies are expected to substantially reduce emissions from medium- and long-distance flights within the required timeframe. However, the benefits of SAF depend on both blending levels and the lifecycle carbon intensity of the selected fuel pathways. The plan therefore emphasizes expanding domestic SAF production, strengthening feedstock supply chains, encouraging investment,

and reducing the cost gap between SAF and conventional jet fuel. It also identifies fleet renewal, efficiency improvements, operational measures, and alternative propulsion as supporting strategies. Electric-, hybrid-electric-, and hydrogen-powered aircraft may provide larger reductions on suitable routes but are expected to remain concentrated mainly on shorter-distance operations. The plan also recognizes that carbon removals or other out-of-sector reductions may still be required to achieve net-zero emissions by 2050. This conclusion is consistent with ATAG, EUROCONTROL, Destination 2050, and the UK roadmap, which also include market-based measures or carbon removals in their net-zero pathways.

Although the Canadian plan provides important policy direction, it remains strategic and highly aggregated. It does not clearly separate passenger and freight operations, forecast air-cargo demand by origin-destination pair, or assess how mitigation potential varies by route distance, commodity, service requirements, or access to road and rail alternatives. SAF, alternative propulsion, and operational improvements are therefore presented as broad sector-level pathways rather than being modelled for specific domestic air-cargo corridors. This limitation creates a need for a Canada-specific, freight-focused, and corridor-level assessment of aviation decarbonization pathways.

Chapter 3: Methodology

The literature review shows that, although numerous studies have examined aviation decarbonization pathways, most focus on a single pathway or a specific technology within it (e.g., the HEFA SAF pathway). Studies that attempt to compare the decarbonization potential of multiple pathways (e.g., SAFs, electric and hydrogen aircraft, efficiency improvements, or infrastructure measures) do so at a global/regional scale and often lack the level of detail and transparency needed to explain the assumptions supporting their results. Moreover, the review revealed little to no Canada-specific, freight-oriented Well-to-Wake (WTWa) assessments that comprehensively evaluate the potential of emerging aviation technologies to meaningfully inform policymakers and industry decision-makers. To bridge this gap, this chapter develops a Canada-focused, freight-oriented WTWa emissions-projection framework. The framework is designed to:

1. Assess the decarbonization potential of aviation technologies, including SAFs and alternative propulsion (battery-electric, hybrid-electric, hydrogen), and
2. Evaluate opportunities for mode shift from air to surface freight (truck and rail), including the adoption of lower-carbon technologies in surface freight (e.g., battery-electric or hydrogen trucks and electric rail) to further reduce overall emissions.

The chapter proceeds as follows. First, it defines the spatial and temporal scope, modes considered, and emissions accounting boundary. Next, it describes the data sources and construction of core variables (cargo flows, GDP/population, and distances by mode). Then, it presents the gravity-model formulation used to estimate and forecast baseline domestic air-cargo activity. After that, it details the emissions measurement approach, which is anchored to the IATA RP 1678 structure but extended to a WTWa boundary. Finally, it outlines scenario design and sequencing consistent with the scope and system boundary.

3.1 Scope and system boundaries

3.1.1 Spatial coverage

The analysis focuses on domestic Canadian air-freight movements, defined as shipments that both originate and terminate at airports within Canada. The primary spatial unit is the origin-destination (OD) city pair, consistent with the CargoIS dataset's reporting structure.

Because CargoIS is reported at the city-city level (rather than specific airports), the study assumes that all freight associated with a given city is routed through a single primary cargo-handling airport

for that city. This assumption is justified by the fact that the distance between multiple airports in the same city is relatively insignificant compared to long-haul domestic flight distances.

For mode-shift scenarios, truck and rail movements are assumed to replace the line-haul air segment between the same OD endpoints. Accordingly, the truck and rail origins/destinations are treated as co-located with each city's representative airport. This avoids adding uncertain assumptions about freight consolidation across multiple terminals (railyards, trucking depots) when shipment-level distribution data are unavailable. Because any local drayage distance between terminals and airports is small relative to intercity line-haul distances, these differences are treated as negligible within the scope of this thesis. Mode-specific distances are defined for each OD pair.

International and transboundary flows are excluded as modelling them would require detailed representation of foreign energy systems, policies, and infrastructure, whereas the thesis is explicitly Canada-focused and centered on domestic decarbonization levers.

3.1.2 Temporal coverage

The empirical analysis window is 2019-2023, aligning with the available IATA CargoIS domestic Canadian data. Within this period, 2019 is considered the last year before COVID-19, 2020 reflects the major pandemic-related drop in demand, and 2021 to 2023 show the return to more normal conditions.

From this historical baseline, activity is forecast to 2050, consistent with Canada's net-zero timeline. Milestone years 2030, 2035, 2040, and 2050 are used for scenario comparison against national and international decarbonization targets.

For model estimation, 2023 is used as the reference year for year-fixed effects, and as baseline for forecasting. Using 2023 as the reference year does not affect the estimated elasticities; it only defines the interpretation of estimated year effects relative to 2023 and provides a consistent anchor year for forward projections.

3.1.3 Modes considered

In this study, three main line-haul modes are considered: (i) air freight, (ii) truck and (iii) rail. Waterborne freight is excluded because most city-to-city movements in Canada lack direct marine

connectivity and cannot be substituted for airline-haul on a one-to-one basis. The analysis is restricted to the line-haul ("middle-mile") segment of the supply chain. First- and last-mile road movements are excluded because pickup and delivery legs are typically truck-based across all modal options and would require shipment-specific information on terminal choice and warehouse/distribution locations, which are not available at the OD level. Excluding these access/egress segments avoids introducing uncertain terminal-handling assumptions and keeps the modal comparison focused on the portion of the journey where mode choice and energy technology differences drive the largest changes in tonne-kilometre emissions.

3.1.4 Life-cycle boundary for emissions

The emissions are assessed using a WTWa boundary for aviation and a WTW boundary for surface freight fuels and energy carriers:

- **Well-to-Tank (WTT):** extraction or production of feedstocks, processing and refining, fuel or energy production, and transport and distribution to the aircraft, truck, or locomotive.
- **Tank-to-Wake/Tank-to-Wheel (TTWa/TTW):** combustion or use of fuel or energy during aircraft, truck, or locomotive operation.

Figure 3-1 illustrates the emissions-accounting boundaries applied to aviation and surface-freight operations in this study.

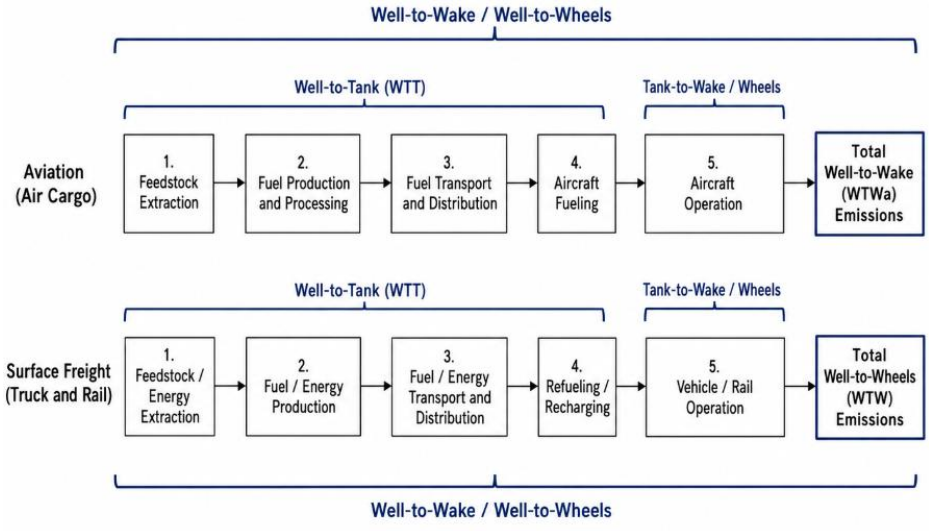


Figure 3-1. Well-to-Wake and Well-to-Wheel Emissions Boundaries Applied in This Study

The functional unit is 1 tonne-kilometre (t-km) of freight moved between an origin-destination (OD) pair. Emission factors are reported as CO_2e intensity in grams of CO_2e per tonne-kilometre (g CO_2e/t-km), while total CO_2e emissions are aggregated across OD pairs and years.

Within these WTWa/WTW boundaries, the analysis excludes emissions associated with infrastructure construction and maintenance, including airports, runways, rail lines, and highways, as well as the manufacturing and end-of-life stages of aircraft, trucks, and locomotives. Non-CO_2 aviation climate impacts, such as contrails and NO_x-related effects, are also not quantified. These elements are excluded to keep the study focused on operational energy use and fuel-cycle emissions, which are directly affected by modal shift, SAF adoption, and alternative propulsion technologies. A more detailed discussion of emission-factor data sources and specific assumptions is provided in Section 3.2.7.

3.2 Data and Variables

This study combines several data sources to construct a coherent dataset for freight demand modelling and WTWa emissions analysis.

3.2.1 Air Cargo Data

The primary dataset for modeling Canadian domestic air cargo activity is sourced from IATA CargoIS (International Air Transport Association, n.d.-b). Reported as a leading market intelligence tool and commonly used by a wide range of air cargo stakeholders, CargoIS provides disaggregated, city-to-city transactional data, which offers a more precise and reliable alternative to the aggregate numbers/figures typically found in standard public databases (International Air Transport Association, n.d.-c). The CargoIS dataset is a robust integration of two distinct, complementary data streams:

- **CASS (Cargo Accounts Settlement System):** This constitutes the financial core of the platform, providing audited records of actual transactions between airlines and over 30,000 freight forwarders (International Air Transport Association, n.d.-c). It encompasses over 21 million air waybills (AWBs) settled annually through IATA, capturing approximately US$32 billion in air freight charges globally. CASS data is validated by both airline carriers and forwarders, ensuring a high level of precision in weight and billing reporting (International

Air Transport Association, n.d.-c). These statistics refer to the entire global CASS system, whereas this study uses only the Canadian domestic subset of the CargoIS data.

- **CDD (CargoIS Direct Data):** This consists of data contributed directly and voluntarily by airlines from their internal operational systems (International Air Transport Association, n.d.-c). CDD enriches the dataset by capturing "non-CASS" transactions, such as direct airline-to-shipper business that bypassed IATA's forwarder settlement process (International Air Transport Association, n.d.-c).

Coverage limitation and rationale for use

A key limitation is that CargoIS represents only a partial sample of total domestic air-cargo activity. When benchmarked against aggregate domestic air-cargo totals reported by Statistics Canada (Statistics Canada, 2025), the CargoIS totals used in this thesis account for approximately 5-6% of the national total over 2019-2023. One important source of this difference is the exclusion of cargo movements that are directly billed to aircraft operators and therefore do not generate a master air waybill captured through CASS. For example, an earlier assessment of the CargoIS data identified Cargojet's operations for Amazon under crew, maintenance, and insurance (CMI) or aircraft, crew, maintenance, and insurance (ACMI) arrangements as activity that may not be represented because these transactions are directly billed and do not require an MAWB. Other transactions conducted outside CASS and not voluntarily submitted by airlines through CDD may similarly be absent. Coverage may therefore vary across carriers, freight forwarders, shipment channels, and years. Accordingly, the CargoIS data should be interpreted as a detailed sample of the Canadian domestic air-cargo market rather than a complete census of national activity.

Despite this limitation, CargoIS is used because it provides the OD-level spatial distribution required for this research. Statistics Canada's domestic air-cargo statistics are reported as aggregate annual totals, which are insufficient to model corridor-level heterogeneity or to evaluate how modal shift and technology adoption affect emissions across different city pairs.

To avoid imposing a strong assumption that CargoIS coverage is uniform across cities and corridors, this thesis does not scale OD-level flows upward to match aggregate totals. Scaling would be problematic because many OD pairs are zero or unobserved in CargoIS, potentially reflecting

incomplete reporting rather than true absence of shipments; applying a uniform expansion factor would disproportionately inflate observed corridors and bias the spatial distribution of activity. Instead, results are reported primarily as percentage changes in emissions relative to the baseline using the same CargoIS sample. Absolute emissions totals should therefore be interpreted as CargoIS-sample-based rather than national totals, while percent reductions represent the primary outcomes used to compare scenarios.

Data Application in Modeling and Analysis:

For the purposes of this study, the integrated CASS and CDD data streams serve as the dependent variable (cargo tonnage) in the gravity model, providing a comprehensive view of domestic demand.

In addition, every Air Waybill (AWB) includes a special handling code that specifies logistical requirements or shipment attributes. Within CargoIS, these codes are categorized into mid-level commodities (Table 3.1) and mid-level services (Table 3.2) (International Air Transport Association, n.d.-b, n.d.-c). This thesis uses these categories to estimate gravity models by segment and to apply scenario assumptions at the commodity/service level.

Table 3-1. CargoIS mid-level commodities (International Air Transport Association, n.d.-b, n.d.-c)

Mid-level Commodity	Definition/Examples
Biological Commodity	Examples: living Human Organs/Blood, Diagnostic Specimen, CITES (Convention on International Trade in Endangered Species) required, Human Remains in Coffin
Dangerous Goods	Articles or substances that can pose a significant risk to health, safety, or property when transported by air. Some dangerous goods may require cargo-only aircraft. Examples: Lithium batteries
General Cargo	Defined by IATA as cargo that does not require any extra precautions or special handling. Examples: retail and consumer goods, dry goods, hardware, and textiles.
High Value Goods	Cargo with importance due to monetary value, rarity, or sensitive nature. Examples: Undeveloped/unexposed film, electronics
Live Animals	Examples: Laboratory animals, livestock, aquatic life
Perishable	Examples: Flowers, fruits and vegetables, meat, fish, hatching eggs
Pharmaceuticals	Examples: Vaccines, insulin, emergency medication

Commodity Information Pending	CASS cargo without the standard mapping handling code
Other Special Cargo	Cargo that requires service, but is not a commodity

Table 3-2. CargoIS mid-level services (International Air Transport Association, n.d.-b, n.d.-c)

Mid-level Services	Definition
Express and Time-Sensitive	Cargo that requires efficient deliveries, meeting the urgent logistical demands of various industries Examples: General perishables, integrator shipment, save human life
General Cargo	Defined by IATA as cargo that does not require any extra precautions or special handling.
Oversized and Heavy	Items exceeding standard dimensions or weight limits, by 150kg or over per piece.
Special (no service)	Goods that are special commodities, but require no services
Temperature Sensitive	Cargo that requires temperature-controlled system, frozen goods, dry ice. Examples: Living human organs/blood, diagnostic specimen
Vulnerable	Goods that are sensitive to various risks Examples: high-value electronics, artwork, seafood
Commodity Information Pending	CASS cargo without the standard mapping handling code

3.2.2 Regional and city-level GDP and Population

To represent the "mass" of the origin and destination cities, a prerequisite for gravity modelling, this study utilizes population and gross domestic product (GDP) as primary indicators of demographic scale and economic activity.

3.2.2.1 Population Data

- Provincial population estimates were obtained from Statistics Canada as quarterly series (Government of Canada, 2025c); therefore, annual population values were calculated by averaging the four quarterly estimates for each calendar year
- **City-level population data**
    - **Primary Source:** City-level population data are predominantly retrieved from Statistics Canada (Census of Population) at the Census Metropolitan Area (CMA) and Census

Agglomeration (CA) levels (Government of Canada, 2026b). A comprehensive list of the city populations sourced from Statistics Canada is provided in Appendix G.

- **Supplementary Source:** To maintain the spatial and temporal integrity of the dataset, particularly for geographic areas or years not included in the relevant Statistics Canada tables, population figures are supplemented using official provincial/municipal records and City Population (citypopulation.de) (City Population, n.d.-b). City Population is compiled from official census results, government estimates, and validated interpolation methods (City Population, n.d.-a). The additional data used to complete OD coverage and fill temporal gaps is detailed in Appendix H.

To ensure consistency, Statistics Canada data were treated as the primary data source; official provincial/municipal estimates were used as the secondary source, and City Population (citypopulation.de) were used only as the tertiary (last resort) source when official data were unavailable.

When specific annual figures were missing, linear interpolation was used to bridge temporal gaps. To best preserve local trends, interpolation was based on the data source with the densest time coverage (i.e., the greatest number of observed years) for each location.

3.2.2.2 Gross Domestic Product (GDP)

The economic activity of cities is quantified using GDP at basic prices, sourced from Statistics Canada Table 36-10-0468-01 (annual), which reports CMA-level GDP values (Government of Canada, 2025b). As the CMA dataset does not include all municipalities identified in the air cargo OD pairs, a proportional downscaling method is used for non-CMA locations. Specifically, provincial GDP is allocated to cities based on their share of provincial population:

$$GDP_{city} = GDP_{prov} \times \frac{Pop_{city}}{Pop_{prov}} \tag{3.1}$$

Where:

- GDP_{city} is the Gross Domestic Product for the target city ($).
- GDP_{prov} is the Gross Domestic Product for the target province ($).

- Pop_{city} is the population of the specific city or region (persons).
- Pop_{prov} is the total population of the respective province (persons).

The formula above assumes that GDP per capita is uniform across cities within a province (each city's average output per person equals the provincial average). Accordingly, these estimates should be interpreted as a population-weighted proxy for economic mass rather than a precise measure of local GDP, as they do not capture variation in productivity, industrial structure, or economic concentration across municipalities.

Provincial GDPs are available from Statistics Canada Table 36-10-0711-02 (Government of Canada, 2025d). A complete list of the provincial GDP inputs (2019 - 2023) is provided in Appendix I, and the resulting city-level GDP values (2019 - 2023) used in the analysis are provided in Appendix J. All GDP values in Appendices I and J are expressed in current dollars (nominal).

3.2.3 GDP Growth Rate

GDP growth projections are not consistently available for all cities/municipalities in the OD dataset, either in the short- to medium-term or over the long term. Therefore, this study uses projected provincial GDP growth rates as a proxy for local economic growth. City-level GDP is projected by assuming that each city's GDP follows the corresponding province/territory's GDP growth trajectory. This approach enables a transparent, internally consistent extension of city-level economic "mass" variables across the 2023-2050 analysis horizon when city-specific forecasts are unavailable.

3.2.3.1 Constructing 2023 nominal GDP (needed for the 2019-2023 gravity estimation)

The gravity trade model is estimated over 2019-2023 using nominal GDP (current dollars), whereas the most recent complete Statistics Canada GDP level data are available only through 2022. Therefore, 2023 nominal GDP levels are constructed by applying an estimated 2023 nominal growth rate to the 2022 GDP base.

Nominal growth is approximated using the Fisher equation, combining the published real GDP growth rate and CPI inflation for 2023 (Government of Canada, 2024c):

$$g^N_{p,2023} = \left(1 + g^R_{p,2023}\right)(1 + \pi_{2023}) - 1 \tag{3.2}$$

$$GDP^N_{p,2023} = GDP^N_{p,2022}\left(1 + g^N_{p,2023}\right) \tag{3.3}$$

If city GDP is required in nominal terms for 2023, the same provincial nominal growth rate is applied as stated above:

$$GDP^{N}_{i,2023} = GDP^{N}_{i,2022}\left(1 + g^{N}_{p,2023}\right) \quad (3.4)$$

Where:

- $g^{N}_{p,2023}$= estimated nominal GDP growth in 2023 for province/territory p (%)
- $g^{R}_{p,2023}$= real GDP growth in 2023 for province/territory p (%)
- π_{2023}= CPI inflation rate in 2023 (%)
- GDP^{N}= nominal GDP level (current dollars) ($)
- i = the city/municipality
- p = the province/territory

3.2.3.2 Projecting 2024-2050 GDP "mass" using real GDP growth

From 2024 onward, the analysis applies provincial/territorial real GDP growth rates to project GDP "mass" variables for each origin and destination. Using real GDP growth supports forecasting of underlying economic activity relevant to physical trade volumes while avoiding additional uncertainty associated with long-run inflation assumptions. Accordingly, projected GDP levels for 2024-2050 are interpreted as constant-dollar values expressed in $2023 (2023 prices), with 2023 serving as the baseline year for forward projections. In estimation (2019-2023), GDP enters in nominal terms and year fixed effects absorb common economy-wide shocks (including price-level changes); in forecasting, future year effects are set to zero and the model is re-evaluated using the constant-dollar GDP trajectories.

The city-level projection is implemented recursively as:

$$GDP^{R}_{i,t} = GDP^{R}_{i,t-1}\left(1 + g^{R}_{p,t}\right), t = 2024, \ldots, 2050 \quad (3.5)$$

where

- $GDP_{i,t}^{R}$= projected real GDP "mass" for city i in year t (\$)
- $g_{p,t}^{R}$= real GDP growth rate for province/territory $p$in year t (%)

Real GDP growth for 2024 is obtained from Statistics Canada; short-to-medium term projections (typically 2025-2030) are taken from provincial fiscal plans/budget documents (British Columbia. Ministry of Finance, 2025; Government of Alberta, 2025; Government of Saskatchewan, 2025; Government of the Northwest Territories (NWT Finance), 2025; New Brunswick. Department of Finance and Treasury Board, 2025; Nova Scotia. Department of Finance and Treasury Board, 2025; Ontario. Ministry of Finance, 2025; Québec. Ministère des Finances, 2025) and, where required, supplemented with major-bank forecasts (TD Economics, 2025); long-run provincial/territorial real GDP growth paths are sourced from the Office of the Parliamentary Budget Officer (PBO) Fiscal Sustainability Report 2024 baseline projection (Barkova et al., 2024), which is grounded in potential GDP determined by trends in labor input (total hours worked) and labor productivity (GDP per hour worked). Appendix K summarizes the provincial/territorial GDP growth rates applied over 2023-2050.

These projected GDP series are inserted into the estimated gravity model to generate future cargo forecasts (see Section 3.3).

3.2.4 Air Distances

Air-route distances for each OD pair were derived from historically operated flights rather than great-circle distances. This approach better reflects operational routing, since actual flown paths can deviate from the shortest path due to airway structure, air traffic control constraints, weather avoidance, and terminal procedures. Using realized distances improves the accuracy for both gravity trade model estimation and WTWa emission analysis. Flight distance information was obtained from FlightAware using the Flight Finder interface, which provides flight records for specific airport pairs and reports a distance value for each operated flight (*Flight Finder*, n.d.).

FlightAware is a flight-tracking data aggregator that compiles and fuses aircraft movement information from multiple surveillance and operational data sources. These include (i) air navigation service provider (ANSP) feeds, such as ATC radar positions and flight plan information (including real-time departure/arrival/delay and flow-management messages), with transoceanic position updates

available via HF and/or satellite communications in major oceanic regions; (ii) a global network of terrestrial ADS-B receivers hosted by contributors, providing frequent position updates over land and surface movement at airports, with the ability to track some non-ADS-B aircraft using multilateration (MLAT); (iii) position reports and flight information (FLIFO) obtained through agreements with VHF and satellite datalink providers; (iv) airline operational feeds, including out/off/on/in and other FLIFO messages (e.g., flight plans, departure/arrival times, and cancellations); and (v) space-based ADS-B data from the Aireon satellite constellation, which FlightAware integrates to support global coverage with regular position updates (*Data Sources - FlightAware*, n.d.). For most OD pairs, Flight Finder returns multiple flights operated by different airlines and aircraft types as shown in Figure 3.2.

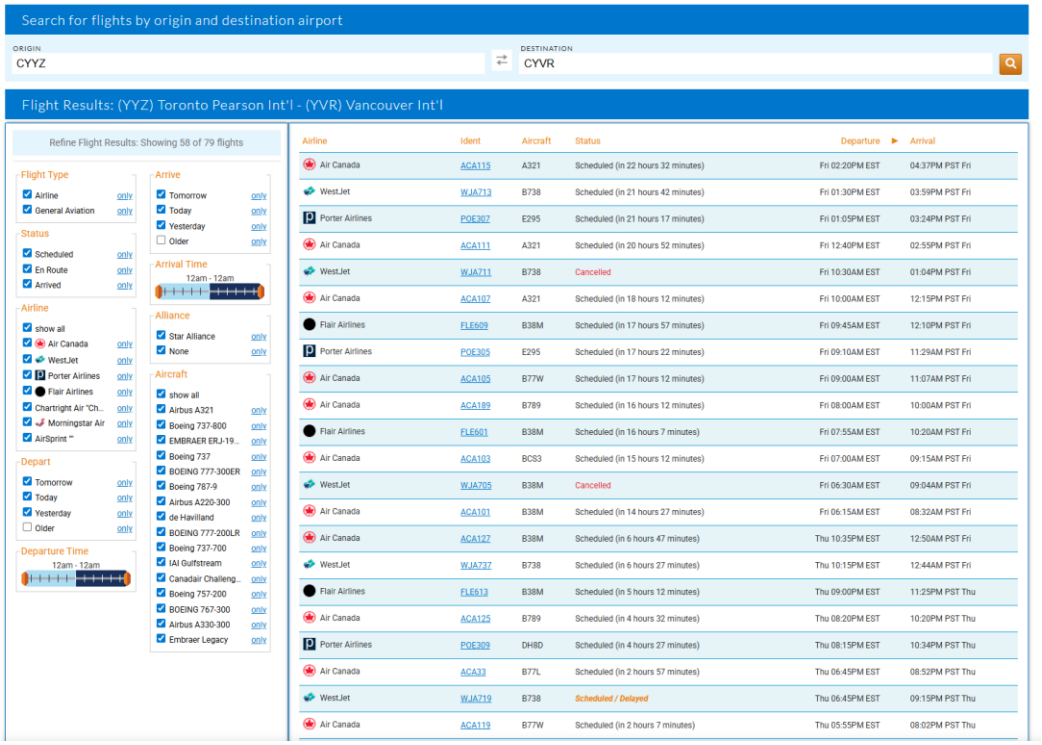


Figure 3-2. Example FlightAware Flight Finder Results for a Selected Origin-Destination Pair

To ensure consistency across routes, a non-stop (direct) flight was selected as the representative observation for each OD pair, and its reported distance was assigned as the OD-level air distance. This is justified because distance differences across airlines/aircraft for the same direct city-pair are typically small and do not materially affect the representative route distance (e.g., Toronto-Calgary

shows reported distances of 1,673 mi (Air Canada AC159), 1,704 mi (WestJet WS659), and 1,708 mi (Flair), a range of 35 mi (~2.1%)). Appendix L documents the Python automation workflow used to extract FlightAware distances for all OD pairs. As the complete dataset contains 5,760 OD records, presenting the full dataset in the appendix would be impractical and would substantially increase the length of the thesis. Therefore, Appendix M presents a representative sample containing the origin, destination, and FlightAware-derived flight distance

3.2.5 Truck Distances

Truck-route distances for each OD pair were derived using the OpenStreetMap (OSM) road network through the GraphHopper routing service. This approach reflects feasible road routing along the mapped highway network, rather than straight-line distances, and is therefore more appropriate for mode comparison and WTWa emissions calculations (OpenStreetMap, n.d.-b). OSM is an open-source, community-maintained geospatial database built and continuously updated by many contributors worldwide (OpenStreetMap, n.d.-a). For Canada, it also incorporates openly licensed datasets from national sources, including GeoBase/GeoGratis and CanVec (Natural Resources Canada) and Statistics Canada (Geography Division) (OpenStreetMap, n.d.-a).

A Python automation script queried the OSM directions interface (GraphHopper engine) for each OD pair and extracted the reported driving distance (and travel time where available). GraphHopper is an open-source routing engine that computes shortest-path routes on road networks and provides routing results (*GraphHopper Directions API*, n.d.); here, it was used with OSM as the underlying road network dataset to ensure consistent, repeatable distance estimation across all OD pairs. In addition, truck-specific access, weight, height, and dimensional restrictions were not explicitly incorporated into the routing procedure. Therefore, the resulting distances represent generalized road-route distances rather than operational routes for a specific truck configuration.

Appendix N documents the Python automation workflow used to extract truck distances. As noted above, the complete dataset contains 5,760 OD records. Therefore, Appendix O presents a representative sample of the resulting truck-distance data using the same OD pairs shown in Appendix M, allowing direct comparison between the air- and truck-route distances. For each OD pair, the table reports the origin, destination, and estimated driving distance.

3.2.6 Rail Distances

Rail-route distances for each OD pair were derived using a GIS network-based approach. Rail line network data and rail terminal/hub layers were obtained from the University of Waterloo Geospatial Centre data library (University of Waterloo, n.d.). Using ArcGIS Network Analyst, a shortest-path analysis was performed along the rail network to compute the route distance between the relevant rail hubs associated with each OD pair.

For consistency with the long-haul focus of this study, the distance between airports and the nearest rail terminals (i.e., first-/last-mile transfer segments) is not explicitly modelled, as it is assumed to be small relative to the intercity rail-haul distance and does not materially affect the total rail distance for most OD pairs. For each city, the primary airport is used as the representative origin/destination node for the OD pair, and rail distances are computed between the corresponding rail hubs serving those city-level endpoints. Consistent with the presentation of air and road distances, Appendix P provides a representative sample of the rail distances calculated for selected OD pairs

3.2.7 Emission Factors

This section documents the emission factors used to convert freight activity, measured in tonne-kilometres, into CO_2e emissions. The emission factors are specified by transport mode, fuel, and technology pathway, including conventional Jet-A aircraft, SAF pathways, alternative aircraft propulsion systems, heavy-duty trucks, and rail technologies. The analysis applies a well-to-wake boundary for aviation and a well-to-wheel boundary for surface transportation, so that upstream fuel or energy production, processing, distribution, and vehicle operation are included in the emissions calculation.

Several tools and databases were explored for quantifying WTW and WTWa emission factors, including SimaPro, openLCA, MOVES, EMFAC, and GHGenius. However, GREET is used as the primary source of emission factors in this study. Unlike general-purpose LCA tools such as SimaPro and openLCA, GREET is specifically designed for transportation fuel and vehicle pathway analysis. It provides pathway assumptions that are directly relevant to the modes, fuels, and technologies examined in this study, including conventional Jet-A, sustainable aviation fuels across multiple

pathways and feedstocks, electricity- and hydrogen-based technologies, heavy-duty trucks, and alternative rail fuels.

Although GHGenius is also a transportation-focused lifecycle model and is particularly relevant in the Canadian context, GREET was selected because it provides broader coverage of the SAF pathways, alternative fuels, hydrogen pathways, electricity-related technologies, truck technologies, and rail technologies required for this study. MOVES and EMFAC are primarily road-vehicle emissions inventory models. While they are useful for estimating vehicle emissions under different operating conditions, fleet characteristics, and regional contexts, they are less suitable for this study because the analysis requires upstream fuel and energy production emissions within a consistent WTW/WTWa framework across aviation, truck, rail, SAF, electricity, and hydrogen pathways.

Most emission factors used in this study are therefore obtained from GREET, including those for conventional Jet-A, SAF pathways and feedstocks, diesel and electric heavy-duty trucks, diesel rail, biodiesel rail, renewable diesel rail, electric rail, hydrogen rail, and hydrogen production pathways. The main exception is the alternative aircraft propulsion scenarios. For electric, hybrid-electric, and hydrogen aircraft, emission factors are derived using literature-based reduction assumptions relative to conventional Jet-A aircraft because mature aircraft-specific WTWa emission factors are not available for all future alternative propulsion technologies considered in this study. Appendix Q summarizes the 2023 reference emission factors used for each transportation mode, fuel, and technology pathway.

3.2.7.1 Electricity generation and hydrogen production assumptions:

Canada's Energy Future 2023 is used to update the projected electricity generation mix over time. However, the lifecycle carbon intensity associated with each electricity-generation source is retained from GREET default assumptions. This approach is used because Canada's Energy Future provides projected generation shares by fuel source but does not provide a complete year-by-year lifecycle carbon intensity dataset for each generation technology. Retaining GREET's source-specific carbon intensity values maintains consistency within the GREET WTW framework while allowing the electricity mix to reflect Canada's projected grid evolution.

Hydrogen production assumptions are also aligned with Canada's Energy Future 2023. Similar to the electricity-grid assumptions, the projected hydrogen production mix is used to update the hydrogen pathway shares in GREET where possible. The hydrogen production pathways considered include natural gas-based hydrogen production with and without carbon capture and storage, biomass-based hydrogen production, and electrolysis. Other process-level assumptions within each pathway, including hydrogen production design, co-product treatment, feedstock options, compression or liquefaction requirements, delivery assumptions, and CO_2 sequestration settings, follow GREET default assumptions unless otherwise specified.

It should also be noted that the assumptions for electricity and hydrogen differ by scenario type. For the baseline or "do-nothing" case, electricity generation and hydrogen production assumptions follow those of the Current Measures scenario in Canada's Energy Future 2023. For scenarios that include decarbonization technologies and fuels, the electricity and hydrogen production mixes align with those in Canada's Energy Future 2023 for the Canada Net-Zero scenario. In addition, Canada's Energy Future 2023 includes a Global Net-Zero Scenario that assumes more rapid, coordinated worldwide climate action. However, this scenario was not used in the present study because the analysis focuses specifically on Canadian domestic air-cargo decarbonization

3.2.7.2 Upstream fuel and energy pathway assumptions

For upstream fuel and energy production stages, this study relies on the corresponding GREET default assumptions unless otherwise specified. This includes assumptions related to feedstock extraction or cultivation, feedstock and fuel transportation and distribution, fuel refining or conversion, process energy use, co-product treatment, carbon capture or sequestration settings, induced land-use change impacts, and other plant-design assumptions. GREET allows pathway-specific options, such as induced land-use change emissions, co-product allocation, plant design, electricity or steam co-production, and CO_2 capture. In this thesis, these detailed process-level settings generally follow GREET defaults unless they are explicitly modified as part of the scenario design. For example, land-use change emissions are not included when the selected GREET pathway setting excludes them, and CO_2 capture is included only when it is specified in the selected pathway assumptions. Energy consumption, water consumption, and process emissions associated with fuel production and refining are also taken from GREET default values rather than modeled separately.

This approach allows the analysis to maintain consistent WTW/WTWa emission-factor assumptions across fuels, modes, and technologies while modifying only key scenario inputs, such as SAF pathway shares, SAF blending rates, the electricity generation mix, and the hydrogen production mix.

3.2.7.3 Aviation emission factors assumptions

Aviation emission factors are used to estimate emissions from baseline air-cargo activity and aviation-related mitigation scenarios. Three aviation technology groups are considered: conventional Jet-A aircraft, sustainable aviation fuel pathways, and alternative propulsion aircraft. Conventional Jet-A and SAF emission factors are obtained from GREET, while alternative propulsion technologies are evaluated using emission-reduction estimates from literature.

The GREET-based aviation emission factors are derived using the single-aisle aircraft category as the representative aircraft type. This category is used because it reflects a common narrowbody aircraft type for domestic operations. The operational assumptions used to convert aircraft fuel use into tonne-kilometer-based emission factors follow GREET defaults. These include average payload per operation, average trip great-circle distance, average petroleum jet fuel consumption per operation, fuel consumption during the landing and takeoff cycle, and load factor assumptions.

Alternative propulsion aircraft are handled separately because mature aircraft-specific WTWa emission factors for electric, hybrid-electric, and hydrogen aircraft are not directly available in GREET or the other lifecycle tools reviewed for this study. Accordingly, literature-based percentage reductions are applied to the GREET-derived Jet-A WTWa emission factor used in this thesis rather than adopting absolute emission values directly from the literature. This approach maintains consistency with the GREET-based emission-factor framework while allowing alternative propulsion technologies to be included in the scenario analysis.

3.2.7.4 Surface transportation emission factors assumptions:

Surface transportation emission factors are used for air-cargo flows that are shifted to truck or rail under the modal shift scenarios. These emission factors are obtained from GREET and are interpreted within a well-to-wheel boundary. For the modal shift-only scenarios, shifted freight is assumed to move by conventional diesel truck or diesel rail. For surface transportation decarbonization scenarios,

lower-emission truck and rail technologies are introduced in accordance with the adoption assumptions described in Section 3.5.3.

For truck transportation, the GREET combination long-haul truck category is used as the representative vehicle type. This category is selected because the truck modal shift scenarios represent intercity freight movements between OD pairs, rather than local or within-city delivery. It is therefore used as a proxy for Class 8 tractor-trailer freight movements. Diesel is used as the baseline truck fuel. In the truck decarbonization scenarios, diesel truck emissions are progressively replaced by battery-electric truck emission factors as the fleet turns over toward zero-emission vehicles. The fleet turnover and ZEV adoption assumptions are discussed in further detail in Section 3.5.3.

For rail transportation, the GREET freight rail category is used as the representative rail mode. Diesel rail is used as the baseline rail technology. Rail decarbonization scenarios are represented using GREET-based emission factors for biodiesel rail, renewable diesel rail, electric rail, and hydrogen rail. The adoption of these rail technologies follows the roadmap-based assumptions described in Section 3.5.3.

Like the aviation emission factors, the operational characteristics used to develop the truck and rail emission factors follow GREET default assumptions unless otherwise specified. These include assumptions related to vehicle energy use, fuel consumption, payload, and fuel or energy pathway characteristics. Electricity- and hydrogen-related upstream emissions follow the cross-cutting assumptions described in Section 3.2.7.1. Therefore, electric truck and electric rail technologies are treated as zero tailpipe-emission technologies, but not as zero well-to-wheel-emission technologies, because upstream electricity generation is still included. Similarly, hydrogen rail emissions depend on the assumed hydrogen production mix and GREET hydrogen pathway assumptions.

3.2.8 Climate Target Ranges

The emissions pathways examined in this thesis are evaluated against two illustrative climate-alignment benchmarks: an IPCC 1.5°C-aligned range and a Canada net-zero-aligned pathway (Government of Canada, 2024a; IPCC, 2023). Neither benchmark represents an emissions target specifically allocated to Canadian air cargo. Instead, the published percentage reductions are applied proportionally to the modelled domestic air-cargo emissions to provide consistent reference pathways for scenario comparison. The IPCC 1.5°C-aligned range is based on the upper and lower bounds of

the transport-sector relative emissions pathways presented in Figure 4.1 of the IPCC AR6 Synthesis Report, which are expressed relative to 2015 emissions (IPCC, 2023). The Canada net-zero-aligned pathway is similarly constructed using Canada's economy-wide targets of 40%-45% below 2005 levels by 2030, 45%-50% below 2005 levels by 2035, and net-zero emissions by 2050 (Government of Canada, 2024a; Service Canada, 2024). The 2005 and 2015 domestic air-cargo reference emissions are estimated by scaling the modelled 2019 emissions according to the proportional changes in total Canadian aviation emissions between 2005, 2015, and 2019 (Canada, 2026).

3.3 Gravity Trade Model Formulation and Forecasting

This section presents the gravity trade model for estimating and forecasting domestic Canadian air-cargo flows between given OD city pairs using the CargoIS data set. The gravity model is suited for freight-demand analysis because it links transport flows to economic activity at the origin and destination while accounting for separation costs, proxied by distance (ADB, 2011; Kerr & Gaisford, 2007; Shepherd, 2013). The estimated elasticities are then used to generate baseline demand projections that feed into the WTWa emissions assessment framework. Given the occurrence of zero flows in air-cargo data, the gravity model is estimated using Poisson Pseudo-Maximum Likelihood (PPML) (Head & Mayer, 2014; Shepherd, 2013).

3.3.1 CargoIS OD-Year Panel and Handling of Zero Flows

The CargoIS dataset provides annual observations of domestic Canadian air-cargo flows by OD city pair for the period 2019-2023. Each observation corresponds to a unique origin city (i), destination city (j), and year (t), forming an OD-year panel used for gravity-model estimation. As noted above, CargoIS significantly underestimates the total domestic air-cargo activity relative to aggregate Statistics Canada totals (Statistics Canada, 2025), reflecting coverage and reporting limitations. Accordingly, zero entries in the OD matrices are interpreted with caution: they may reflect (i) a positive flow that occurred but was not captured in CargoIS, or (ii) a true absence of trade between the OD pair in that year. Because the gravity model is estimated using PPML, zero-valued outcomes in the dependent variable are accommodated naturally, without log-transformation or ad hoc adjustments. PPML estimates the model in levels while preserving the standard multiplicative gravity structure, making it well-suited to air-cargo data where zero or very small flows can occur.

3.3.2 Variable Selection and Model Controls

Based on the literature review, core explanatory variables include: (i) economic "mass" at the origin and destination (commonly GDP and/or population), and (ii) separation costs (distance and/or transport-cost proxies). In a domestic Canadian setting, international frictions typically included in gravity-based trade models, such as free trade agreements, common language, or common border, are not applicable. In addition, the short annual time span (2019-2023) limits the ability to separately identify detailed cost drivers (e.g., fuel-price dynamics) using explicit cost variables.

To account for time-specific shocks affecting all OD pairs simultaneously, including the COVID-19 disruptions (in macroeconomic conditions) and system-wide generalized cost shocks (e.g., fuel prices, inflation), the model includes year fixed effects. To capture time-invariant geographic and regulatory differences across Canadian regions that may influence air-cargo activity (e.g., remoteness, infrastructure, and provincial economic structure), the model includes origin-province and destination-province fixed effects.

Population is often used as an alternative mass proxy, but it is highly correlated with GDP in the study dataset (correlation > 0.9) (Table 3.3). Thus, to reduce multicollinearity and maintain a clear economic interpretation for forecasting, GDP is used as the primary mass variable, and population is excluded from the baseline specification. Additionally, GDP is measured in nominal (current dollar) terms for model estimation (2019-2023).

Table 3-3. Correlation between city-level GDP and population, 2019 - 2023

	Air Distance	Population Origin	Population Destination	GDP Origin	GDP Destination
Air Distance	**1**				
Population Origin	**-0.034**	**1**			
Population Destination	**-0.041**	**-0.0123**	**1**		
GDP Origin	**-0.034**	**0.993**	**-0.013**	**1**	

GDP Destination	**-0.039**	**-0.013**	**0.993**	**-0.013**	**1**

Finally, gravity models are estimated separately by commodity type and by service type. This segmentation supports the scenario analysis (Section 3.5.2), where modal-shift assumptions are applied at the commodity/service level rather than at the aggregate cargo level. Estimating segment-specific models allows the GDP and distance elasticities to differ across shipment types and ensures that the forecasted total flow is obtained by summing the predicted flows across segments, rather than imposing a single aggregate response that may mask heterogeneity.

3.3.3 Gravity Model Specification

Let $F_{ij,t}$ denote the annual air-cargo flow (e.g., tonnes or chargeable weight) from origin city i to destination city j in year t. The baseline PPML gravity model is specified as:

$$\mathrm{E}\left[F_{ij,t} \mid X \right] = \exp\left(\beta_1 \ln\left(GDP_{i,t}\right) + \beta_2 \ln\left(GDP_{j,t}\right) + \beta_3 \ln\left(D_{ij}\right) + \gamma_t + \delta_{p(i)} + \phi_{p(j)}\right) \qquad (3.6)$$

where:

- X represents all the explanatory variables in the model.
- $GDP_{i,t}$ and $GDP_{j,t}$ denote the gross domestic product of the origin and destination cities (or their corresponding economic regions) in year t ($).
- D_{ij} is the distance between origin and destination cities (km), serving as a proxy for separation and transport costs.
- γ_t represents year fixed effects capturing common time-specific shocks (2023 is treated as the baseline/reference year).
- $\delta_{p(i)}$ and $\phi_{p(j)}$ denote origin-province and destination-province fixed effects, respectively (Alberta is treated as baseline/reference province).

Because the model is log-log in economic mass and distance, the estimated coefficients β_1, β_2, and β_3 can be interpreted as elasticities of air-cargo flows with respect to origin GDP, destination GDP,

and distance. These elasticities form the basis for forecasting baseline air-cargo demand under alternative GDP growth scenarios, which are subsequently combined with technology and fuel-mix assumptions in the WTWa emissions analysis.

3.3.4 Gravity-Based Forecasting Based on GDP Growth

Forecasting of domestic Canadian air-cargo demand is conducted by applying the estimated gravity model for each future year using projected GDP levels at the origin and destination. In estimation, GDP is measured in nominal terms (current dollars), while year-fixed effects absorb economy-wide time shocks, including common price-level changes or inflation. However, because year-fixed effects are not projected forward, GDP trajectories used for forecasting are constructed from exogenous annual real GDP growth rates (constant dollars) to better reflect growth in underlying economic activity and associated freight volumes, without requiring assumptions about future inflation. The resulting GDP trajectories are inserted into the estimated gravity equation to generate OD-pair flow predictions for each forecast year, while holding time-invariant corridor characteristics (distance) and provincial fixed effects constant.

Formally, letting $GDP_{i,t} = GDP_{i,t-1}(1 + g_{i,t})$ and $GDP_{j,t} = GDP_{j,t-1}(1 + g_{j,t})$, where $g_{i,t}$ and $g_{j,t}$ are annual real GDP growth rates, predicted flows are computed as:

$$\hat{F}_{ij,t} = \exp\left(\hat{\beta}_1 \ln(GDP_{i,t}) + \hat{\beta}_2 \ln(GDP_{j,t}) + \hat{\beta}_3 \ln(D_{ij}) + \hat{\delta}_{p(i)} + \hat{\phi}_{p(j)}\right) \quad (3.7)$$

where $\hat{\beta}_1$ and $\hat{\beta}_2$ are the estimated GDP elasticities. Year fixed effects are used in the estimation to absorb common historical shocks (e.g., COVID-19), but they are not projected into the future. In the forecast scenarios, future-year effects are set to zero, assuming no additional system-wide shocks beyond those reflected in GDP growth.

3.4 Emissions Measurement Methodology

The air cargo shipment emissions are anchored to the structure of IATA RP 1678, which defines a three-step process (International Air Transport Association, n.d.-a):

1. Identify all route segments (legs) composing the service;
2. Estimate CO_2 emissions for each leg; and

3. Sum the emissions across all legs (International Air Transport Association, n.d.-a).

In Step 2, RP 1678 provides two alternative approaches for estimating shipment-level emissions: the leg-based and network-based approaches. The leg-based approach relies on route-specific operational inputs (e.g., average fuel burn and payload by leg), whereas the network-based approach applies to a network-average emission factor intended to reflect the average performance of the carrier/network (International Air Transport Association, n.d.-a).

Given the scope of this thesis and the availability of data, the analysis adopts a network-based approach. Consistent route-specific fuel burn and payload data at the required resolution are not available for all domestic OD pairs and years; therefore, using a network-average factor enables transparent, repeatable estimation across the full OD set.

3.4.1 Airport Mapping and Realized Route Distance Estimation

Although RP 1678 is framed around shipment legs (airport-to-airport), the air-cargo activity data in this thesis is reported at the OD city-pair level using CargoIS. For distance assignment, each city is mapped to a representative primary cargo handling airport (as defined above in section 3.2.4). The distance for each OD pair is then calculated as the airport-to-airport distance between the two representative airports

Under the RP 1678 network-based method, distance is represented using great-circle distance (International Air Transport Association, n.d.-a). This thesis instead uses a realized route distance derived from FlightAware operated flight records for each mapped airport pair. Using realized distance improves accuracy for domestic Canadian routings, since flown paths can deviate from the shortest path due to airway structure, air traffic control constraints, weather avoidance, and terminal procedures.

3.4.2 Network-based emissions equation (applied to OD-level flows)

Using the network-based approach, air-cargo emissions are calculated as the product of cargo weight, route distance, and a network average emissions factor (International Air Transport Association, n.d.-a):

$$E_{CO2e} = W \times D_{ij} \times EF_{Network} \quad (3.8)$$

Where

- E_{CO2e} = total CO_2-equivalent emissions associated with transporting the cargo flow (kg CO_2e).
- $W_{Shipment}$ = cargo weight (kg). In this thesis, W is taken from CargoIS as the annual OD-level cargo flow.
- D_{ij} = realized route distance (km) between origin i and destination j, derived from FlightAware for the mapped primary-airport pair.
- $EF_{network}$ = the network-average CO_2 emission factor (kg CO_2/kg·km).

In implementation, the equation is applied to each OD pair (and where applicable, to each OD pair within each commodity/service segment), producing OD-level emissions that are then aggregated to obtain annual totals and scenario results. RP 1678 is designed for operational reporting and typically reflects TTW emissions only (emissions from fuel use during flight) (International Air Transport Association, n.d.-a). To enable comparison of conventional Jet-A operations with alternative fuels and propulsion systems, this thesis extends the RP 1678 network-based structure to a WTWa boundary by using WTWa emission factors.

3.5 Scenario design and implementation

This section presents the scenario framework used in this thesis. It includes: (i) the set of decarbonization scenarios evaluated, (ii) the main assumptions used to define each scenario, and (iii) the sequencing procedure used to combine individual strategies into mixed (integrated) pathways. The scenarios are based mainly on available policy targets and current adoption trends for emerging technologies in aviation (SAF and alternative propulsion), trucking (ZEV adoption), and rail (transition to alternative fuels and alternative propulsion). The framework also considers realistic opportunities for mode shift from air to surface freight.

To make results comparable, all scenarios are applied to the same underlying air-cargo activity forecast (the business-as-usual OD-level forecast). This means scenarios differ only in two ways:

1. How much freight is moved by air versus truck/rail (mode shift), and/or

2. How emissions per tonne-km change over time as cleaner technologies are adopted (changes in WTWa emission factors)

The scenarios do not re-forecast cargo demand under different technologies or cost conditions. This choice is intentional. In reality, new technologies and policies could affect air-cargo demand by altering costs, service availability, infrastructure readiness, and operational constraints. However, modelling these demand responses would require a detailed shipper-choice/logistics model and long-term projections of key inputs (e.g., technology costs, fuel prices, carbon prices, SAF supply limits, and infrastructure rollout). These inputs are highly uncertain and are not available at the resolution needed for Canadian domestic air cargo. Therefore, the business-as-usual (BAU) activity forecast is kept constant, and each scenario is implemented as a clear overlay. This approach isolates the emissions impacts of the assumed pathways and allows consistent "mix-and-match" comparisons using the same sequencing procedure.

3.5.1 Baseline (no modal shift, conventional technology)

The baseline scenario represents business-as-usual (BAU) domestic air cargo, with no additional decarbonization strategies beyond those already reflected in today's system. It also assumes the "current measures" electricity pathway from Canada's Energy Future 2023 (CER), which reflects only existing policies and therefore implies limited additional future action beyond those measures.

Baseline assumptions:

- **No modal shift**: all forecasted OD activity remains in aviation:

$$s_{ij,c,t}^{MS} = 0 \implies A_{ij,c,t}^{Air} = A_{ij,c,t}^{Air\ base} \tag{3.9}$$

Where:

- i= origin city (where the shipment starts)
- j= destination city (where the shipment ends)
- c= cargo segment (e.g., sub-commodity or service category from CargoIS)
- t= year (e.g., 2023, 2024, …, 2050)
- $s_{ij,c,t}^{MS}$= mode-shift share (unitless, between 0 and 1)

- The fraction of the baseline air-cargo activity on OD-segment (i, j, c)in year t is shifted from air to surface modes (truck or rail) (e.g., s=0.30 means 30% is shifted away from air).

- $A_{ijc,t}^{air}$= air-cargo activity by air after applying the scenario (unit = tonne-km by air) for OD-segment (i, j, c) in year t.
- $A_{ijc,t}^{air,base}$= baseline (BAU) air-cargo activity by air before any scenario changes (same units as A^{air}).

- **Conventional aviation fuel**: all aircraft energy use is supplied by Jet-A (conventional jet fuel) over 2023-2050.
- **No SAF mandate and no alternative propulsion adoption:** the baseline does not impose SAF blending or electric/hydrogen/hybrid aircraft uptake (beyond anything already implicitly included in the default emission factor assumptions).
- **Electricity decarbonization follows "current measures" only**: this mainly affects electrified modes/technologies in other scenarios; the direct impact on the baseline is small because aviation remains Jet-A dominated.

Purpose:

The baseline provides the reference emissions pathway against which all strategy scenarios (mode shift and/or technology adoption) are compared.

3.5.2 Modal shift scenarios (air to rail/truck)

Modal shift scenarios reallocate a share of baseline domestic air-cargo activity from air to surface freight (truck or rail). In this thesis, mode shift is implemented at the OD-segment level, where a "segment" refers to the service type and/or commodity type identified in the CargoIS dataset (Section 3.2.1). Segment-level treatment is used because the practical potential to shift away from air is not necessarily the same for all cargo types.

The literature review above identifies key factors that generally influence freight mode choice across air, truck, and rail, including cost, transit time, reliability, distance, product types, shipment value, handling/service requirements, and external and policy factors. However, the exact mode-selection process is not directly observable in this study and may differ across shippers and freight forwarders (e.g., due to internal logistics systems, customer contracts, network constraints, and operational practices). In addition, there is limited Canada-specific evidence and insufficient survey or revealed-preference data to quantify how much each segment (commodity/service type) would shift in response to future technology, policy, or cost changes. For example, express/time-sensitive shipments and temperature-controlled goods are generally expected to be less likely to shift than standard/general cargo because they place greater value on speed, reliability, and specialized handling; however, this research lacks sufficient data to estimate segment-specific switching behavior.

For these reasons, mode shift is treated as an exogenous scenario assumption rather than an endogenously modelled outcome. Mode shifts are implemented as a set of transparent sensitivity scenarios. Each scenario targets a selected OD segment and assumes a gradual shift from air to surface freight over time, while other segments remain unchanged. This design avoids imposing a single "one-size-fits-all" shiftability rule and allows results to be compared consistently across cargo segments and corridors. Future research could improve this component by collecting shipper/forwarder survey data (or using revealed preference shipment datasets) to estimate a formal mode-choice model for Canadian domestic air cargo.

Mode assignment (truck vs rail):

Shifted freight is assigned to truck or rail using a distance-based rule informed by the "break-even distance" concept in modal competition. Rodrigue (2017) notes that the first break-even point where rail becomes more cost-effective than road in a simplified cost-distance framework is generally located between 500 and 750 km from the departure point. Consistent with this guidance, this thesis adopts 750 km as a conservative cutoff:

- Truck for corridors with air-route distance $d_{ij}^{air} < 750\text{km}$
- Rail for corridors with air-route distance $d_{ij}^{air} \geq 750\text{km}$

To avoid understating surface emissions, shifted truck activity is represented using heavy-duty, line-haul freight truck. Although Canadian fleet statistics show a large share of light-duty trucks, these vehicles are largely used for urban/local pickup-and-delivery, service operations, and last-mile logistics. In contrast, the mode-shift scenarios in this thesis represent intercity city-pair movements (line-haul corridor transport between cities), which are typically served by heavy-duty trucks rather than light-duty vehicles. Therefore, for simplicity and to better match the operating context of intercity freight corridors, shifted truck tonne-kilometres are modelled using heavy-duty truck emission factors.

Shift trajectory (gradual adoption):

For a targeted OD-segment $(\boldsymbol{i}, \boldsymbol{j}, \boldsymbol{c})$, mode shift is represented using a time-varying mode-shift share $s_{ijc,t}^{MS} \in [0,1]$in each year t. The parameter $s_{ijc,t}^{MS}$ indicates the fraction of baseline air-cargo activity that is shifted from air to surface freight (truck or rail) for that OD-segment in year t. Baseline air activity is denoted $A_{ijc,t}^{air,base}$, measured in tonne-kilometres. After applying mode shift, the remaining air activity and the shifted surface activity are computed as:

- Remaining air activity:

$$A_{ijc,t}^{air} = \left(1 - s_{ijc,t}^{MS}\right) A_{ijc,t}^{air,base} \tag{3.10}$$

- Shifted surface activity:

$$A_{ijc,t}^{surf} = s_{ijc,t}^{MS}\, A_{ijc,t}^{air,base} \tag{3.11}$$

In scenarios that assume a complete shift of the targeted segment by 2050, $s_{ijc,t}^{MS}$is modelled as a linear ramp from 0 in the start year t_0 to 1.0 in 2050:

$$s_{ijc,t}^{MS} = \begin{cases} 0, & t < t_0 \\ \dfrac{t - t_0}{2050 - t_0}, & t_0 \le t \le 2050 \end{cases} \tag{3.12}$$

A linear ramp is used because this research lacks sufficient evidence to justify a faster or slower segment-specific shift pattern. Although baseline activity $A_{ijc,t}^{air,base}$may increase over time, the ramp

is applied as a share to each year's baseline activity; total activity is therefore preserved, while the mode split changes gradually over time.

3.5.3 Surface freight technology scenarios

Surface freight technology scenarios do not determine how much air cargo shifts to surface modes. Instead, they describe how the emissions per tonne-kilometre of truck and rail change over time as the emerging technologies for truck and rail are adopted. In this thesis, surface technology assumptions are applied to the truck/rail tonne-kilometres created by the modal shift scenarios in Section 3.5.2. Because this study forecasts only air-cargo activity, surface technology scenarios mainly affect results when combined with modal shift, since modal shift is what generates surface freight activity in the model.

The surface technology pathways are based on Canadian policy and roadmap initiatives. Truck decarbonization follows Canada's Zero-Emission Vehicle (ZEV) sales targets published by Transport Canada (Transport Canada, 2024). Rail decarbonization follows the Rail Pathways Initiative, a joint project between Transport Canada (TC) and the Railway Association of Canada (RAC), which supports a pathway toward net-zero rail emissions by 2050 (The Delphi Group & Pollution Probe, 2022).

3.5.3.1 Truck decarbonization (fleet turnover under ZEV sales targets)

Truck decarbonization is modelled through fleet turnover: zero-emission trucks enter the fleet through new sales and gradually replace retiring internal-combustion engine (ICE) trucks. This approach is consistent with how policy is defined in Canada, as Transport Canada specifies ZEV targets for new vehicle sales rather than for the composition of the operating fleet (Transport Canada, 2024). In this thesis, "ZEV" follows the Transport Canada definition (battery-electric (BEV), plug-in hybrid electric (PHEV), and fuel-cell electric vehicles (FCEV)). However, because long-run projections of the future BEV/PHEV/FCEV mix for Canadian medium- and heavy-duty trucks are not available at the required resolution, the analysis uses battery-electric trucks as a proxy for the ZEV category.

The adoption pathway is implemented using a three-step stock update method that converts sales targets into a time-varying ZEV share of the operating fleet.

Step 1 - Estimate annual fleet turnover.

A replacement rate is first estimated to represent how quickly the operating truck fleet is renewed each year. This rate is derived from observed fleet statistics (e.g., sales-to-stock relationships) and represents a fraction of the fleet that is replaced annually. Historical stock and sales data are derived from annual registration statistics. Annual retirements are not directly reported and are therefore inferred from the stock-flow identity:

$$R_t = K_{t-1} + S_t - K_t \tag{3.13}$$

where K_t is total truck stock in year t, S_t is total new truck sales (entries), and R_t is total retirements (exits). Using these quantities, the annual replacement (retirement) rate and annual sales (entry) rate are defined as:

$$\rho_t = \frac{R_t}{K_{t-1}};\ \tau_t = \frac{S_t}{K_{t-1}} \tag{3.14}$$

with $\rho_t$and τ_t expressed either as fractions or percentages.

Net stock growth is defined as:

$$g_t = \frac{K_t - K_{t-1}}{K_{t-1}} \tag{3.15}$$

which implies:

$$\tau_t = \rho_t + g_t \tag{3.16}$$

This relationship ensures internal accounting consistency between entries, exits, and net fleet change. For projection years, ρ_t and τ_t are parameterized from historical trends and then used to update fleet stock before applying the technology shares in the following steps. Based on data from Natural Resources Canada, for 2000-2021, the historical sales-to-stock rate (τ_t) ranges from approximately 4% - 10% per year and is most frequently concentrated between 5% - 8% (Natural Resources Canada, 2026). Over the same period, the retirement rate (ρ_t) ranges from approximately 1% to 8% per year, with most concentrations between 3% and 6%. Thus, this study assumes a central turnover case of $\tau_t = 7\%$ and $\rho_t = 4\%$ per year (Natural Resources Canada, 2026).

Step 2 - Apply ZEV sales targets and update the operating fleet composition.

In each year t, the ZEV share of new sales, z_t, is applied to the trucks entering the fleet through replacement. The ZEV sales share is assumed to align with Canada's medium- and heavy-duty ZEV targets (35% of new sales by 2030 and 100% by 2040). Since the most recent Statistics Canada vehicle-registration data shows the heavy-duty truck segments (vehicles weighing 11,794 kilograms) as diesel-dominated in 2024 (Statistics Canada, 2022), the policy ramp is assumed to be implemented starting in 2025. After 2040, the sale shares are held at 100% through 2050. Accordingly, the ZEV sales shares for each year during the analysis period (2023-2050) are estimated as follows:

$$z_t = \begin{cases} 0 & t \leq 2024 \\ \left(\frac{0.35}{2030-2025}\right)(t-2025) & 2025 \leq t \leq 2030 \\ 0.35 + \left(\frac{1.00-0.35}{2040-2030}\right)(t-2030) & 2030 < t \leq 2040 \\ 1.00 & t > 2040 \end{cases} \quad (3.17)$$

Where:

- z_t= the ZEV share of new sales in year t (%)
- t= calendar year

ZEV and ICE sales are then computed as:

$$S_t^{ZEV} = z_t S_t;\ S_t^{ICE} = (1-z_t)S_t \quad (3.18)$$

where $0 \leq z_t \leq 1$.

Step 3 - Update ZEV and ICE operating stock over time:

Technology-specific stock is updated annually to convert sales targets into in-use fleet composition.

Total stock:

$$K_t = K_{t-1} + S_t - R_t \quad (3.19)$$

ZEV stock:

$$K_t^{ZEV} = K_{t-1}^{ZEV} + S_t^{ZEV} - R_t^{ZEV} \quad (3.20)$$

ICE stock:

$$K_t^{ICE} = K_t - K_t^{ZEV} \text{ or}$$
$$K_t^{ICE} = K_{t-1}^{ICE} + S_t^{ICE} - R_t^{ICE} \quad (3.21)$$

To represent delayed retirement of ZEV cohorts, this study assumes a fixed ZEV service life $L = 15$ years. If first non-zero ZEV sales occur in 2025, then:

$$R_t^{ZEV} = \begin{cases} 0, & t < 2025 + L \\ S_{t-L}^{ZEV}, & t \geq 2025 + L \end{cases} \tag{3.22}$$

Hence, ZEV retirements begin in 2040 under this assumption. ICE retirements are obtained residually:

$$R_t^{ICE} = R_t - R_t^{ZEV} \tag{3.23}$$

The in-use ZEV share is:

$$\phi_t^{ZEV} = \frac{K_t^{ZEV}}{K_t} \tag{3.24}$$

Once the in-use ZEV share is computed/estimated from the steps above, the time-varying WTWa emission factor for truck freight in year t is then computed as a weighted average:

$$EF_t^{truck} = \phi_t^{ZEV}\, EF_t^{ZEV} + (1-\phi_t^{ZEV}) EF_t^{ICE} \tag{3.25}$$

where EF_t^{ZEV} and EF_t^{ICE} are WTWa emission factors for ZEV (proxied as battery-electric) and conventional ICE trucks, respectively. Electricity-related emissions for ZEV trucks follow the electricity pathway assumptions described in Section 3.27 above.

3.5.3.2 Rail decarbonization (Rail Pathway Initiative adoption trajectory)

Rail technology adoption in this thesis is guided by the Rail Pathways Initiative, a joint effort between Transport Canada (TC) and the Railway Association of Canada (RAC) established under a Memorandum of Understanding to support a national rail decarbonization roadmap aligned with net-zero emissions by 2050 (The Delphi Group & Pollution Probe, 2022). The Initiative does not publish a single quantitative scenario (i.e., it does not provide year-by-year adoption shares for specific technologies). Instead, it outlines a high-level transition logic and milestone timing, informed by stakeholder consultation and an assessment framework that considers technology cost, decarbonization potential, and implementation challenges (The Delphi Group & Pollution Probe, 2022).

Phase 1 compiles an inventory of ongoing rail decarbonization actions, policies, and research. Phase 2 builds on this inventory to evaluate emerging technology options and describes rail decarbonization as unfolding in three overlapping "waves" (The Delphi Group & Pollution Probe, 2022):

- **Wave 1 (near-term):** efficiency improvements in locomotives and operations to reduce fuel use per tonne-km.
- **Wave 2 (medium-term, toward 2030):** increased uptake of drop-in alternative fuels that can be used with existing infrastructure.
- **Wave 3 (long-term, after 2030):** transition away from diesel traction toward alternative propulsion, with three options discussed: battery-electric, catenary electric, and hydrogen fuel cell. The Initiative highlights a decision period in the 2030s when the sector must converge on a platform to replace diesel locomotives to remain on a net-zero pathway.

The Rail Pathways Initiative report also presents a milestone-based pathway that provides a more detailed timing interpretation than the three-wave summary. This milestone pathway is used in this thesis as a qualitative reference to guide scenario design (and to define modelling milestones used for interpolation) (The Delphi Group & Pollution Probe, 2022).

3.5.3.2.1 Scenario structure (four rail technology cases):

Because the Rail Pathways Initiative is milestone-based rather than fully quantified, this thesis translates the roadmap into scenarios using two design choices:
(a) which drop-in alternative fuel is assumed for the remaining diesel rail operations (renewable diesel/HDRD or biodiesel), and
(b) which zero-emission (ZE) propulsion pathway is assumed as rail transitions away from diesel (electric or hydrogen).

This results in four rail technology scenarios: (1) biodiesel to electric; (2) biodiesel to hydrogen; (3) renewable diesel/HDRD to electric; and (4) renewable diesel/HDRD to hydrogen. This structure avoids unsupported assumptions about future technology shares. In practice, Canada's rail system may adopt a portfolio of renewable diesel and biodiesel, along with a mix of electric and hydrogen propulsion, with proportions varying by corridor, operator, and locomotive class. However, available evidence does not support credible long-term market shares for these options at a national scale.

Therefore, the thesis evaluates transparent bookend combinations that can be implemented consistently in the emissions model.

3.5.3.2.2 Alternative fuels and blending constraints

Two drop-in alternative-fuel options are considered:

1. **Renewable diesel / HDRD blending (RD pathway):** Locomotive OEM certification and warranty constraints typically limit HDRD blends to approximately 20-30%, and higher blends can create warranty and operational risks. Limited disclosure of renewable content in supplied fuels adds additional uncertainty in verifying blend rates. For these reasons, the renewable diesel pathway is capped at RD30, defined as a maximum 30% renewable diesel share within the diesel-fuel portion of operations, until ZE propulsion dominates rail activity.
2. **Biodiesel blending (BD pathway):** Biodiesel is mature and is already blended into diesel in Canada at low mandated levels. For locomotive applications, blends up to B20 are feasible for many existing diesel locomotives, while higher blends may require component upgrades for some fleets, particularly older units. This thesis therefore caps biodiesel at B20 as a conservative core assumption. Neat biodiesel (B100) is not assumed in the core scenarios and, if discussed, is treated only as an upper-bound sensitivity.

3.5.3.2.3 Alternative propulsion options:

The propulsion options modelled in this thesis follow the technology assessment presented in the Rail Pathways Initiative report and include:

- **Electric rail** (battery-electric and/or catenary electric), and
- **Hydrogen fuel-cell rail**.

The propulsion split is implemented using two separate cases (all-electric vs all-hydrogen) to avoid assuming future electric/hydrogen market shares that are not quantitatively specified in the Rail Pathways materials.

3.5.3.2.4 Translating the roadmap into an implementable emissions pathway

Because the Rail Pathways Initiative does not specify quantitative year-by-year adoption shares, this thesis operationalizes the roadmap by defining two time-varying parameters and mapping them to milestone years:

- $\phi_t \in [0,1]$: share of diesel rail energy supplied by a low-carbon drop-in fuel (RD or BD),
- $\beta_t^{ZE} \in [0,1]$: share of rail tonne-km operated using ZE propulsion (electric or hydrogen).

The rail WTWa emission factor in year t is computed as:

$$EF_t^{rail} = (1 - \beta_t^{ZE})\left[\phi_t \, EF_t^{rail,altfuel} + (1 - \phi_t) \, EF_t^{rail,diesel}\right] + \beta_t^{ZE} \, EF_t^{rail,ZE} \qquad (3.26)$$

where $EF_t^{rail,diesel}$ is the WTWa emission factor for diesel rail, $EF_t^{rail,altfuel}$ is the WTWa emission factor for the selected drop-in fuel pathway (RD or BD), and $EF_t^{rail,ZE}$ is the WTWa emission factor for ZE propulsion rail.

3.5.3.2.5 Scenario implementation and interpolation:

Table 3.4 reports the milestone shares for each rail technology scenario. Values for intermediate years are obtained by linear interpolation between milestones. Once zero-emission (ZE) propulsion is introduced, the RD/BD blending rate applies only to the remaining diesel-operated share, not to total rail activity. For example, "66.7% diesel traction with B20 + 33.3% electric" indicates that 33.3% of rail tonne-kilometres are served by electric propulsion, while the remaining 66.7% are served by diesel locomotives operating with a B20 fuel blend.

Table 3-4. Milestone Rail Propulsion and Fuel Shares by Technology Scenario, 2023-2050

	Rail Tech 1: BD → Electric	**Rail Tech 2: BD → Hydrogen**	**Rail Tech 3: RD(HDRD) → Electric**	**Rail Tech 4: RD(HDRD) → Hydrogen**
2023	98% diesel + 2% biodiesel	98% diesel + 2% biodiesel	98% diesel + 2% renewable diesel	98% diesel + 2% renewable diesel
2030	80% diesel + 20% biodiesel;	80% diesel + 20% biodiesel;	70% diesel + 30% renewable diesel;	70% diesel + 30% renewable diesel;

	electric mainline testing	hydrogen mainline testing	electric mainline testing	electric mainline testing
2035	80% diesel + 20% biodiesel + 0% electric	80% diesel + 20% biodiesel + 0% hydrogen	70% diesel + 30% renewable diesel + 0% electric	70% diesel + 30% renewable diesel + 0% hydrogen
2040	66.7% B20 + 33.3% electric	66.7% B20 + 33.3% hydrogen	66.7% HDRD30 + 33.3% electric	66.7% HDRD30 + 33.3% hydrogen
2050	100% ZE (Electric)	100% ZE (H_2)	100% ZE (Electric)	100% ZE (H_2)

3.5.4 Aviation technology scenarios

Aviation technology scenarios modify the WTWa emissions intensity of the remaining air-cargo activity after any mode shift (Section 3.5.2 and 3.5.3). In other words, these scenarios do not change how much cargo is flown; they change how clean air freight becomes over time through:

- **Sustainable Aviation Fuel (SAF) adoption**, represented as blending SAF with conventional jet fuel, and/or
- **Alternative propulsion**, represented as the gradual introduction of hybrid-electric, battery-electric, and hydrogen aircraft within the feasible range categories.

3.5.4.1 SAF scenarios:

In the SAF scenarios, aviation emissions intensity is determined by two factors:

- **SAF blending rate** in year t (i.e., the share of aviation fuel demand met by SAF rather than conventional jet fuel), and
- **SAF production pathway**, which determines the WTWa emission factor of the SAF itself.

Pathway-specific WTWa emission factors also depend on upstream assumptions, including the electricity-grid pathway, the hydrogen production pathway and carbon intensity (where relevant), land-use change effects for biomass-based feedstocks, and feedstock/product transport distance and

mode. These upstream assumptions are specified in Section 3.2.7 and are applied consistently across all scenarios to ensure comparability.

Accordingly, the air-mode emission factor in year t is computed as a weighted average of conventional jet fuel and SAF:

$$EF_t^{air} = (1 - b_t^{SAF})\, EF_t^{JetA} + b_t^{SAF} \sum_k w_{k,t}\; EF_{k,t}^{SAF} \tag{3.27}$$

where

- $b_t^{SAF} \in [0,1]$is the SAF blend share,
- $EF_t^{JetA}$is the WTWa emission factor for conventional jet fuel, and
- $w_{k,t}$: share of SAF that comes from pathway $k$in year t (HEFA, FT, ATJ, PtL, …), where

$$\sum_k w_{k,t} = 1$$

- $EF_{k,t}^{SAF}$ is the WTWa emission factor for SAF produced via pathway k in year t.

Because Canada-specific sources do not currently provide a single, fully specified SAF scenario that jointly defines (i) year-by-year blending rates and (ii) year-by-year pathway shares to 2050 for domestic aviation, this thesis operationalizes SAF deployment using two explicit scenario inputs:

1. a blending trajectory b_t^{SAF}, and
2. a pathway portfolio $\{w_{k,t}\}$ that allocates SAF supply across pathways k.

The combination of three blending trajectories and four pathway portfolios yields 12 SAF sub-scenarios.

3.5.4.1.1 SAF blending trajectories

Three blending trajectories are used to span a conservative, central, and aggressive range. The policy-style (“reasonable”) trajectory is benchmarked to the ReFuelEU Aviation mandate adopted by the European Commission (European Union, 2023). An upper-bound trajectory explores the implications of reaching full SAF substitution by 2050. A conservative capped trajectory limits blending to 50% by 2050, reflecting the current blending-rate cap for many approved drop-in SAF pathways. For each

case, blending shares are specified at milestone years and linearly interpolated between milestones to obtain annual values of b_t^{SAF} over 2025-2050:

- **Case B1 (Policy-style / "ReFuelEU-like")**:
  2025: 2%, 2030: 6%, 2035: 20%, 2040: 34%, 2045: 42%, 2050: 70%.
- **Case B2 (Aggressive/full substitution by 2050)**:
  2025: 5%, 2030: 9%, 2035: 29%, 2040: 49%, 2045: 60%, 2050: 100%.
- **Case B3 (Conservative/capped blending)**:
  2025: 1%, 2030: 4%, 2035: 14%, 2040: 24%, 2045: 30%, 2050: 50%.

It should be noted that the ReFuelEU Aviation mandate is used as the central trajectory because it provides an established set of policy-based milestone years and blending percentages. The conservative and aggressive trajectories are then constructed by proportionally scaling the intermediate ReFuelEU milestone shares to reflect their respective 2050 endpoints of 50% and 100%.

3.5.4.1.2 SAF pathway portfolios

Four portfolios are defined to represent different assumptions about how SAF supply may be distributed across pathways over time. Portfolios range from single-pathway, single feedstock cases to multi-pathway cases that reflect broader roadmap narratives.

Portfolio P1: HEFA-only (single pathway, single feedstock - canola)

This portfolio represents a near-term commercial baseline where SAF deployment relies on the most mature and currently commercial pathway. For all years t,

$$w_{\text{HEFA},t} = 1, w_{k,t} = 0 \text{ for } k \neq \text{HEFA}.$$

Within HEFA, the representative feedstock is canola, reflecting Canadian availability and relevance.

Portfolio P2: HEFA-only (single pathway, multiple feedstocks)

This portfolio keeps the SAF conversion pathway fixed as HEFA but represents a diversified lipid feedstock supply. SAF is produced entirely via HEFA in all years, while the HEFA feedstock mix is assumed constant over time. Specifically, for all years t,

$$w_{\text{HEFA},t} = 1, w_{k,t} = 0 \text{ for } k \neq \text{HEFA},$$

and within HEFA the feedstock shares are:

$$w_{\text{Canola|HEFA},t} = 0.34, w_{\text{Soybean|HEFA},t} = 0.33, w_{\text{CornOil|HEFA},t} = 0.33, \forall t.$$

The within-HEFA feedstock shares are set to an approximately equal split as a deliberately neutral assumption. This choice avoids imposing an unverified feedstock dominance pattern in the absence of Canada-specific evidence on how HEFA feedstock sourcing will be distributed over time. WTWa emission factors for HEFA SAF under this portfolio are computed as the feedstock-weighted average consistent with the upstream assumptions in Section 3.2.7.

Portfolio P3: Fixed multi-pathway portfolio (C-SAF roadmap-based, held constant to 2050)
This portfolio adopts a published SAF "portfolio" concept and extends it through the full horizon by holding pathway shares constant after the milestone year provided in the source (the composition does not change over time). The pathway shares used in this thesis are:

This portfolio is adapted from the pathway mix presented in the "C-SAF roadmap" report. The roadmap was developed by the Canadian Council for Sustainable Aviation Fuels in collaboration with the Transition Accelerator, Energy Futures Lab, and stakeholders across the Canadian aviation-fuel supply chain. It identifies the development of multiple domestic SAF production pathways as an important component of scaling Canadian SAF supply rather than relying exclusively on a single conversion technology or feedstock (Bentley et al., 2023). The pathway shares used in this thesis are:

$$w_{\text{HEFA},t} = 0.571, w_{\text{FTgas},t} = 0.286, w_{\text{PtL},t} = 0.095, w_{\text{ATJ},t} = 0.048, \forall t.$$

The representative feedstocks/processes are:

- **HEFA (57.1%)**: canola
- **FT biomass gasification (28.6%)**: forestry waste and municipal solid waste
- **PtL / FT e-SAF (9.5%)**: industrial CO_2 + low-CI blue hydrogen
- **ATJ (4.8%)**: corn

The C-SAF Roadmap provides a strategic pathway composition rather than a complete annual pathway-share trajectory extending to 2050. Therefore, this thesis assumes that the roadmap-based shares remain constant throughout the modeling period. The portfolio should consequently be

interpreted as a fixed scenario adapted from the C-SAF pathway mix, rather than as a prediction that Canada's actual SAF production composition will remain unchanged to 2050. This transparent assumption allows the emissions implications of a diversified Canadian SAF portfolio to be evaluated without introducing additional assumptions regarding the future timing of pathway deployment or substitution among technologies.

Portfolio P4: Dynamic transition portfolio (ATAG Waypoint 2050 based, milestone-based)

This portfolio represents a time-varying SAF pathway mix based on the Waypoint 2050 roadmap published by the ATAG (ATAG, 2021). It reflects the long-term transition narrative in that report: early SAF deployment is HEFA-dominated, followed by greater contributions from FT pathways, and an increasing reliance on PtL/e-SAF in later decades as renewable electricity expands and sustainable biogenic feedstocks face stronger competition and constraints.

Pathway shares are specified at milestone years and linearly interpolated between milestones to obtain annual $w_{k,t}$. The milestone shares used are:

- **2023-2030**: HEFA-dominated

$$w_{\mathrm{HEFA}} = 1.0, w_{\mathrm{FTgas}} = 0, w_{\mathrm{ATJ}} = 0, w_{\mathrm{PtL}} = 0.$$

- **By 2035**: Growth shifts toward advanced feedstocks

$$w_{\mathrm{HEFA}} = 0.50, w_{\mathrm{FTgas}} = 0.40, w_{\mathrm{ATJ}} = 0.10, w_{\mathrm{PtL}} = 0.$$

- **By 2040**: PtL expansion

$$w_{\mathrm{HEFA}} = 0.10, w_{\mathrm{FTgas}} = 0.50, w_{\mathrm{ATJ}} = 0.10, w_{\mathrm{PtL}} = 0.30.$$

- **By 2050**: Transition to PtL pathway using captured CO_2 and green hydrogen

$$w_{\mathrm{HEFA}} = 0.10, w_{\mathrm{FTgas}} = 0.30, w_{\mathrm{ATJ}} = 0.10, w_{\mathrm{PtL}} = 0.55.$$

This structure provides a more "dynamic" representation than Portfolio P3 because it allows different pathways to dominate at different stages of the transition, while remaining implementable with a small set of transparent parameters.

3.5.4.1.3 SAF scenario matrix (12 sub-scenarios)

The SAF scenarios are defined by the combination of three blending trajectories (Cases B1-B3) and four pathway portfolios (Portfolios P1-P4). This produces 12 SAF sub-scenarios, summarized in Table 3.5 below.

Table 3-5. SAF sub-scenarios defined by blending case and pathway portfolio

Pathway portfolio ×Blending case	**B1 Policy-style (ReFuelEU-like)**	**B2 Aggressive (100% by 2050)**	**B3 Conservative (50% cap by 2050)**
P1: HEFA-only (Canola)	**SAF-1** (P1×B1)	**SAF-2** (P1×B2)	**SAF-3** (P1×B3)
P2: HEFA-only (multi-feedstocks)	**SAF-4** (P2×B1)	**SAF-5** (P2×B2)	**SAF-6** (P2×B3)
P3: Fixed multi-pathway portfolio (constant shares)	**SAF-7** (P3×B1)	**SAF-8** (P3×B2)	**SAF-9** (P3×B3)
P4: Dynamic transition portfolio (ATAG Waypoint 2050-based)	**SAF-10** (P4×B1)	**SAF-11** (P4×B2)	**SAF-12** (P4×B3)

For each sub-scenario, the annual SAF blend b_t^{SAF} follows the selected blending case (linearly interpolated between milestones), and the annual pathway shares $w_{k,t}$ follow the selected portfolio definition (constant for P1-P3 and milestone/interpolated for P4).

3.5.4.2 Alternative propulsion scenarios (electric / hydrogen / hybrid), 2030-2050

This thesis evaluates alternative propulsion scenarios as a technology pathway that can reduce the WTWa emissions intensity of the remaining air-cargo activity after mode shift. In these scenarios, a subset of domestic OD corridors is assumed to be served by hybrid-electric, battery-electric, or hydrogen powered aircraft, thereby lowering per-tonne-kilometre WTWa emissions relative to conventional jet operations. Because alternative propulsion technologies are not expected to become technically and commercially feasible for all aircraft classes and stage lengths at the same time, alternative propulsion adoption is modelled using two components:

- an assumed commercialization timeline, and
- a distance-based eligibility rule that determines which OD pairs can plausibly adopt each technology in each year.

3.5.4.2.1 Commercialization timeline (technology availability windows)

The alternative propulsion deployment timeline is based on Waypoint 2050, which describes a staged entry of radical propulsion technologies by aircraft segment (ATAG, 2021). The key implications used in this thesis are:

- **Near term (2025-2030): commuter aircraft**
    - Hybrid-electric and small battery-electric aircraft are expected to enter service first in the smallest segments (commuter operations).
- **Mid-term (2030-2035): regional scaling + first hydrogen**
    - Battery-electric and hybrid-electric are expected to expand into regional aircraft classes, while hydrogen aircraft are expected to enter service around the mid-2030s, targeted primarily at short-haul flights.
- **Long term (2040-2050): limited extension to larger segments**
    - Hybrid-electric aircraft may become feasible for larger aircraft later (post-2040).
    - Hydrogen-powered aircraft are expected to be more feasible for short-haul and medium haul operation but are not expected to become the dominant solution for long range by 2050
    - Full battery-electric aircraft above approximately 100 seats remain highly uncertain within this timeframe.

Consistent with these statements, and to avoid imposing speculative assumptions, this thesis adopts the central feasibility constraint that:

- Battery-electric adoption is limited to commuter and regional stage lengths.
- Hydrogen adoption is limited to short-haul and medium-haul stage lengths (with no hydrogen adoption assumed for long-haul air-cargo operations through 2050).

3.5.4.2.2 Distance-Based Alternative-Propulsion Eligibility Framework

Distance-based eligibility rule (OD corridors that can adopt alternative propulsion)

Because the OD cargo dataset is corridor-based, adoption feasibility is approximated using estimated flight distances. The OD dataset is classified into distance bins, and only OD pairs whose flight distance fall within a feasible range are considered eligible for adoption each year. In other words, the model filters OD corridors by distance to determine which routes can plausibly be served by hybrid-electric, battery-electric, or hydrogen fuel-cell aircraft as commercialization progresses.

How distance eligibility is computed from Waypoint 2050:

Table 3.6 taken from Waypoint 2050 reports technology relevance by aircraft class and flight-time window (e.g., commuter <60 minutes, regional 30-90 minutes) (ATAG, 2021).

Table 3-6. Adoption of SAF, Electric, and Hydrogen Propulsion Technologies by Aircraft Market Segment, 2020-2050 (ATAG, 2021)

	2020	2025	2030	2035	2040	2045	2050
Commuter » 9-19 seats » < 60 minute flights » <1% of industry CO_2	SAF	Electric or Hydrogen fuel cell and/or SAF	Electric or Hydrogen fuel cell and/or SAF	Electric or Hydrogen fuel cell and/or SAF	Electric or Hydrogen fuel cell and/or SAF	Electric or Hydrogen fuel cell and/or SAF	Electric or Hydrogen fuel cell and/or SAF
Regional » 50-100 seats » 30-90 minute flights » ~3% of industry CO_2	SAF	SAF	Electric or Hydrogen fuel cell and/or SAF	Electric or Hydrogen fuel cell and/or SAF	Electric or Hydrogen fuel cell and/or SAF	Electric or Hydrogen fuel cell and/or SAF	Electric or Hydrogen fuel cell and/or SAF
Short haul » 100-150 seats » 45-120 minute flights » ~24% of industry CO_2	SAF	SAF	SAF	SAF potentially some Hydrogen	Hydrogen and/or SAF	Hydrogen and/or SAF	Hydrogen and/or SAF
Medium haul » 100-250 seats » 60-150 minute flights » ~43% of industry CO_2	SAF	SAF	SAF	SAF	SAF potentially some Hydrogen	SAF potentially some Hydrogen	SAF potentially some Hydrogen
Long haul » 250+ seats » 150 minute + flights » ~30% of industry CO_2	SAF	SAF	SAF	SAF	SAF	SAF	SAF

To apply this guidance to OD-pair corridors, this thesis converts flight-time windows into stage-length eligibility thresholds using representative cruise-speed ranges for aircraft commonly used in Canada within each class (Table 3.7).

Table 3-7. Typical Flight Speeds and Representative Aircraft by Aircraft Category

	Average Flight Speed (km/h)	**Examples**	**Sources**
Commuter (9 to 19 seats)	~340 - 480km/h	Cessna 172; De Havilland Canada Dash 8	(Air Inuit, 2026; Cessna, 2011)
Regional (50 to 100 seats)	~490 - 871 km/h	Bombardier CRJ Series (The CRJ100/200), ATR 42/72	(Airliners, n.d.; Bombardier, n.d.)
Short haul (100-150 seats)	~829 - 890 km/h	Airbus A320P2F, Boeing 737-800, Airbus A321P2F	(Airlines Inform, n.d.; PCJ, n.d.)
Medium haul (100 - 250 seats)	~850 - 920 km/h	Boeing 767-300F/BCF; Airbus A330-300P2F	(Air Charter Service, n.d.; Airbus Aircraft, 2024)
Long haul	~900-1100 km/h	Boeing 777F; Boeing 747-8F	(AXON Aviation Group, n.d.; Flugzeuginfo, n.d.)

Let c index aircraft class and t index year. For each class c, define representative cruise-speed bounds $v_c^{\min}$and $v_c^{\max}$, and Waypoint-based feasible flight-time bounds $\tau_{c,t}^{\min}$and $\tau_{c,t}^{\max}$(hours). The implied eligible stage-length interval is computed as:

$$d_{c,t}^{\min} = v_c^{\min}\,\tau_{c,t}^{\min} \tag{3.28}$$

$$d_{c,t}^{\max} = v_c^{\max}\,\tau_{c,t}^{\max} \tag{3.29}$$

Table 3.8 then summarizes the resulting estimated flight distance ranges by aircraft class (computed from the representative speed bounds and the indicative flight-time windows). These distance ranges are subsequently used to bin OD pairs by stage length and determine which corridors are eligible to adopt hybrid-electric, battery-electric, or hydrogen aircraft in each scenario year.

Table 3-8. Estimated Flight-Range Assumptions by Aircraft Category

	Flight Range (km)
Commuter (9 to 19 seats)	340 - 480km
Regional (50 to 100 seats)	245 - 1306.5 km
Short haul (100-150 seats)	621.8 - 1780 km
Medium haul (100 - 250 seats)	850 - 2300 km
Long haul	More than 2300 km

Although the flight-distance categories overlap, this thesis uses the upper distance threshold calculated for each category as the boundary between consecutive aircraft classes. Accordingly, routes of up to 480 km are assigned to the commuter category; routes longer than 480 km and up to 1,306.5 km are assigned to the regional category; routes longer than 1,306.5 km and up to 1,780 km are assigned to the short-haul category; routes longer than 1,780 km and up to 2,300 km are assigned to the medium-haul category; and routes exceeding 2,300 km are assigned to the long-haul category. This sequential classification creates mutually exclusive distance bands, ensures that each OD pair is assigned to only one aircraft category, and provides a consistent basis for applying alternative-propulsion eligibility assumptions.

3.5.4.2.3 Adoption dynamics

Commercial availability does not imply instantaneous fleet turnover. Therefore, once a technology becomes available for a given distance bin, its adoption share is assumed to ramp linearly to full penetration over seven years, reflecting gradual aircraft replacement, certification, infrastructure build-out, and operational learning (ATAG, 2021).

It should be noted that the seven-year adoption period is not interpreted as complete replacement of the national aircraft fleet. Rather, it represents the assumed penetration of the new technology within the portion of OD activity that satisfies the distance-based eligibility threshold. In practice, adoption may take longer because aircraft retirement, production capacity, certification, infrastructure deployment, and operator investment decisions may constrain fleet turnover. However, aircraft age, remaining service life, fleet composition, and corridor-specific deployment data were not available

for the operations represented in this study. The seven-year assumption from Waypoint 2050 is therefore retained as a modelling assumption but should be interpreted cautiously. Future research should replace this simplified adoption trajectory when sufficiently detailed aircraft and operational data become available.

For a technology that becomes available in year t_0 for distance bin b, the penetration share applied to eligible OD activity is:

$$p_b(t) = \min\left(1, \max\left(0, \frac{t - t_0 + 1}{7}\right)\right) \tag{3.30}$$

This formulation yields $p_b(t_0) = 1/7$ in the first year of entry and $p_b(t_0 + 6) = 1$, matching the scenario tables used in the analysis.

Additionally, because the model does not identify which specific OD corridors adopt first within a bin, adoption is applied proportionally to activity. In any year t and eligibility bin b, the model allocates a share $p_b(t)$of the total RTK flown within that bin to the new technology. For example, if battery-electric becomes available for the 0-480 km bin in 2025 and $p_b(2025) = 1/7 \approx 14\%$, then 14% of total RTK flown on OD pairs with stage length in 0-480 km is assigned to battery-electric operations in 2025. This proportional allocation preserves aggregate RTK by distance class while representing early-stage diffusion in the absence of corridor-specific adoption evidence.

3.5.4.2.4 Hybrid-to-Battery and Hybrid-to-Hydrogen Transition Assumptions:

Consistent with the Waypoint-based timing assumptions adopted in this study, alternative propulsion technologies are assumed to be introduced gradually as they become technically feasible, commercially mature, and incorporated into the fleet. Hybrid-electric aircraft are therefore treated as an initial bridge technology that enters service before fully battery-electric and hydrogen-powered aircraft. This sequencing is broadly informed by ATAG, which identifies hybridization as a necessary intermediate step for larger aircraft toward fully electric propulsion (ATAG, 2021).

In the commuter and regional distance bins, hybrid-electric aircraft provide an early deployment pathway before being progressively replaced by battery-electric aircraft. In the short- and medium-haul bins, hybrid-electric aircraft similarly serve as a transitional technology before being gradually replaced by hydrogen-powered aircraft. The transition from hybrid-electric to hydrogen propulsion

represents a modelling assumption informed by the indicative technology timelines, rather than an explicit ATAG prediction.

In practice, hybrid-electric aircraft may not be completely phased out, as operators may retain them where they remain economically competitive or operationally advantageous. The complete replacement assumed in this study should therefore be interpreted as an upper-bound scenario used to estimate the maximum potential emissions reductions from alternative propulsion systems, rather than as a prediction of future fleet composition.

In addition, it should also be noted that ATAG's high-level technology timeline indicates that hybrid propulsion could become technically possible for both regional and short-haul aircraft from around 2030 (ATAG, 2021). Accordingly, this study applies the same assumed hybrid-electric introduction year to the regional and short-haul distance bins.

Accordingly, for each eligible distance bin b, the model defines a penetrated share $p_b(t)$ representing the total share of operations that have transitioned away from conventional jet aircraft. The penetrated share is initially dominated by hybrid-electric aircraft, then progressively shifts toward the segment-specific successor technology: battery-electric for commuter and regional routes, and hydrogen for short- and medium-haul routes. The penetration rate represents total alternative-propulsion adoption within each distance bin, while the technology mix determines how that adopted share is divided among propulsion types.

3.5.4.2.5 Timing uncertainty: lagged variants and Scenario implementation tables

To account for uncertainty in certification, infrastructure readiness, and market uptake, and to recognize that this thesis is developed in 2025-2026, whereas the Waypoint 2050 roadmap was published in 2021, the analysis also evaluates delayed-deployment variants in which all technology entry years t_0 are shifted uniformly by +3, +6, +9 and +12 years relative to the Waypoint-based timeline. These lagged cases represent plausible delays between indicative roadmap timelines and realized commercial deployment. In each lagged variant, the distance-bin eligibility structure and the seven-year linear penetration ramp are held constant; only the assumed start years are delayed.

To ensure transparent implementation at the OD-pair level, Appendix R reports the annual alternative-propulsion eligibility and penetration tables for the Waypoint-based timeline and each delayed-deployment variant. For each scenario variant, the appendix provides:

1. **Distance-bin eligibility by technology and year** (i.e., which stage-length bins are eligible for hybrid-electric/battery-electric and hydrogen in year t); and
2. **Annual penetration rate** $p_b(t)$ within each eligible bin, based on the seven-year linear ramp.

These scenarios in Appendix R enable reproducible mapping from the narrative Waypoint timeline to corridor-level adoption by applying the following steps in each year t:
(i) classify each OD pair into a distance bin,
(ii) identify which technologies are eligible for that bin in year t, and
(iii) allocate the penetrated share $p_b(t)$ of total RTK in that bin to the corresponding technology (split between hybrid-electric and battery-electric where applicable).

3.5.5 Scenario sequencing

The scenario structure is designed to evaluate, in a transparent and internally consistent manner, the individual and combined effects of demand reallocation (mode shift), aviation fuel substitution (SAFs), aircraft propulsion technology change (alternative propulsion), and surface-freight decarbonization, while avoiding double counting of emissions reductions. Because future technology uptake and policy implementation are uncertain (it is unclear which strategies will emerge first, scale fastest, or be adopted at all) the analysis evaluates a structured set of scenario combinations spanning these changes. This enables systematic comparison of outcomes and identification of which individual measures or pathway bundles are most capable of moving the system toward Canada's climate targets and milestone years.

Mode shift is treated as a first-order decision that reallocates freight activity across transport modes and therefore reduces the volume of air-cargo revenue tonne-kilometres (RTK) before any aviation-specific decarbonization measures are applied. This reflects the fact that freight that no longer travels by air cannot simultaneously benefit from aviation fuel or propulsion technologies. Under mode-shift scenarios, baseline air-cargo RTK is reduced by an assumed mode shift share, and the displaced

activity is assigned to truck and/or rail, with emissions calculated using mode-specific well-to-use emission factors (aviation: WTWa; surface modes: WTW)

Following mode shift, aviation decarbonization is represented through two distinct but complementary mechanisms: sustainable aviation fuel (SAF) adoption and alternative aircraft propulsion systems. These mechanisms are modelled separately because they differ fundamentally in their technological, operational, and deployment characteristics, and therefore require different implementation structures in the scenario framework.

SAFs are treated as a direct fuel substitution within the existing fleet of fuel-burning aircraft. Because SAFs are certified as drop-in replacements for conventional Jet-A and require no major changes to aircraft design, airport infrastructure, or operational practices, SAF adoption is modelled through a blending approach applied uniformly to the remaining air-cargo RTK (i.e., the same underlying activity derived from CargoIS after any mode shift). Increasing SAF penetration therefore reduces WTWa emissions intensity without altering fleet composition or route feasibility.

In contrast, alternative propulsion technologies, including electric, hybrid-electric, and hydrogen aircraft, represent a structural fleet transition rather than a simple fuel substitution. Their adoption depends on aircraft size and range limitations, certification timelines, and the availability of enabling infrastructure such as charging or hydrogen supply. Consequently, alternative propulsion is modelled through gradual market penetration, beginning with shorter-range and smaller aircraft segments and expanding to longer distances over time, consistent with the technology-entry and penetration-ramp assumptions defined in the scenario tables. Where SAF and alternative propulsion are combined, SAF blending is applied only to the fuel-burning share of the remaining fleet (conventional and, where applicable, hybrid aircraft), while electric and hydrogen aircraft are treated as non-SAF-eligible.

Surface freight decarbonization is applied only to cargo that has shifted from air to truck or rail, ensuring that emissions reductions from low-carbon surface technologies are not attributed to freight that remains airborne. By systematically combining these levers across scenarios, the framework enables transparent attribution of emissions reductions to individual pathways and their interactions, providing a robust basis for comparative evaluation of freight decarbonization strategies under uncertainty.

Figure 3-3 summarizes the complete set of scenario combinations evaluated in this study and serves as the reference framework for all scenario results reported in the subsequent analysis chapters (the yes/no branches indicate that the corresponding pathway is activated in the scenario). Together, these scenarios span the principal decarbonization levers available to the freight and aviation system, enabling direct comparison of how different strategy bundles contribute to emissions reduction relative to Canada's climate targets and milestone years.

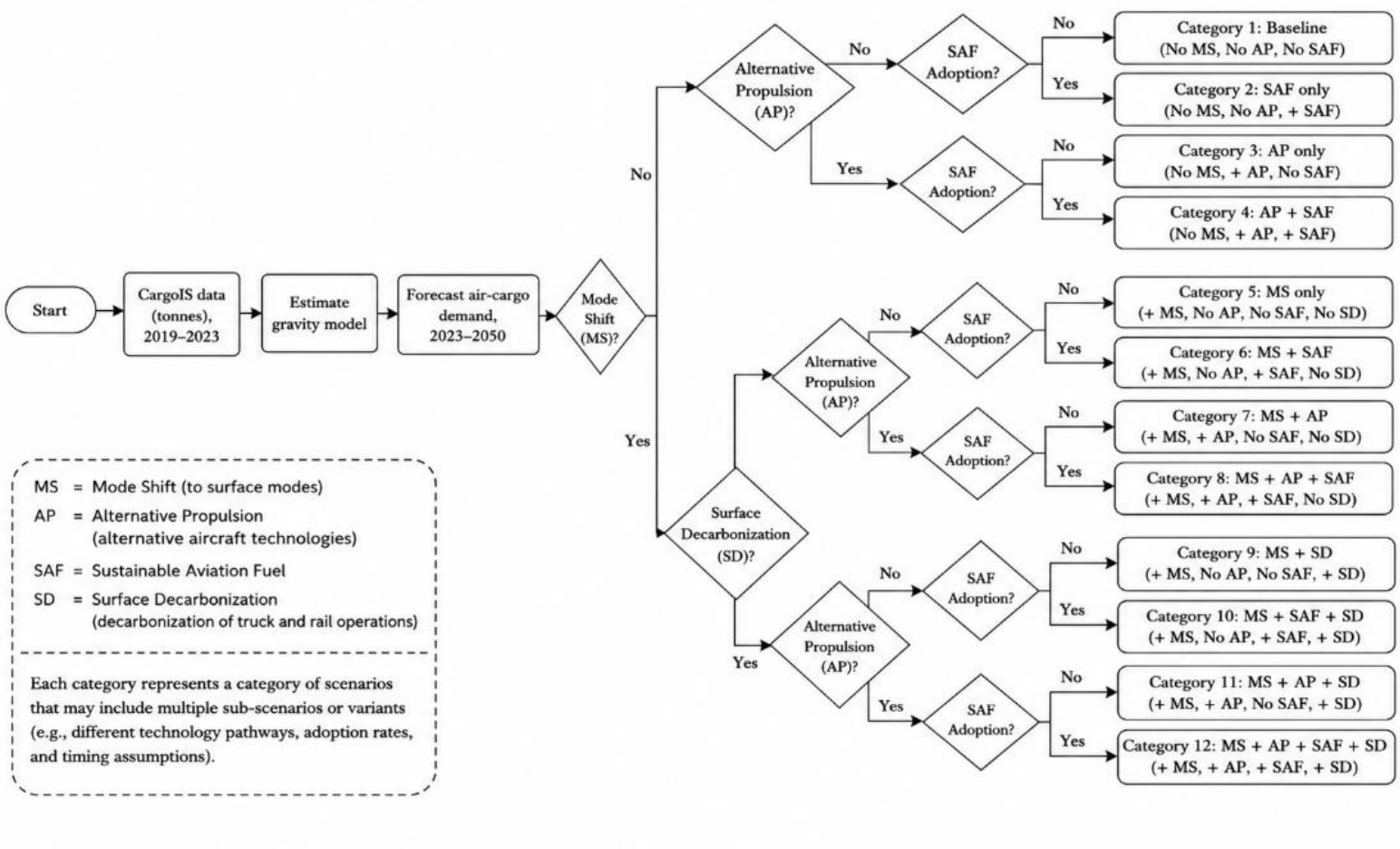


Figure 3-3. Flowchart of Air-Cargo Decarbonization Scenario Sequencing and Combinations

Chapter 4: Baseline Forecast and Gravity Model Results

This chapter presents the gravity-model results and baseline domestic air-cargo projections used as the reference case for the emissions scenario analysis in Chapter 5. The baseline represents a "do-nothing" scenario in which domestic air-cargo activity grows according to the gravity-model forecast while aircraft operations continue to rely on conventional Jet-A fuel. This scenario introduces no SAF blending, alternative propulsion, or modal shift.

Gravity-model estimates and forecasts are presented by commodity and service type because these segmented forecasts provide the demand inputs used in the modal-shift scenarios evaluated in Chapter 5. Commodity forecasts are summed up to form the main aggregate baseline for total cargo demand and emissions. Service categories are evaluated separately because individual shipments may be associated with multiple service tags and therefore cannot be summed up to construct a separate national total. Section 4.1 presents the segmented gravity-model results, Section 4.2 presents the baseline cargo forecasts, and Section 4.3 presents the resulting WTWa emissions projection.

4.1 Segmented gravity model results

Separate PPML gravity models are estimated for each commodity and service category to capture differences in air-cargo demand patterns across freight types. Each model relates OD-level cargo flows to origin GDP, destination GDP, and air-route distance, while controlling for year effects and regional origin and destination effects. The segmented models are used to generate the commodity- and service-level cargo forecasts presented in Section 4.2.

4.1.1 Commodity-level PPML gravity-model results

Table 4.1 summarizes the commodity-level gravity-model results. To keep the main results chapter focused, the table reports only the key variables used for forecasting: origin GDP, destination GDP, OD distance, the intercept, and the model fit statistic. Additional control variables, fixed effects, standard errors, and the full regression output for each commodity model are provided in Appendix S.

Table 4-1. Summary of commodity-level PPML gravity-model results

Commodity category	Intercept	Ln (Origin GDP)	Ln (Destination GDP)	Ln (OD distance)	R^2
Biological Commodity	**-38.99*****	**0.79*****	**0.75*****	**-0.13*****	**0.49**

Dangerous Goods	**-101.29*** **	**2.34*** **	**1.38*** **	**0.69*** **	**0.86**
General Cargo	**-60.79*** **	**1.64*** **	**0.85*** **	**0.28*** **	**0.77**
High Value Goods	**-67.99*** **	**1.52*** **	**0.92*** **	**0.73*** **	**0.68**
Live Animals	**-90.31*** **	**2.61*** **	**0.92*** **	**0.18*** **	**0.77**
Perishable	**-86.48*** **	**2.10*** **	**0.94*** **	**1.36*** **	**0.80**
Pharmaceuticals	**-124.6*** **	**2.52*** **	**1.81*** **	**1.51*** **	**0.79**
Commodity Information Pending	**-88.46*** **	**2.84*** **	**0.69*** **	**0.41*** **	**0.70**
Other Special Cargo	**-109.67*** **	**2.93*** **	**0.85*** **	**1.97*** **	**0.79**

Note: *** indicates statistical significance at the 1% level.

Across all commodity groups, origin and destination GDP coefficients are positive and statistically significant, indicating that domestic air-cargo flows are strongly associated with economic activity at both ends of the OD pair. In most cases, the origin GDP coefficient is larger than the destination GDP coefficient, suggesting that outbound cargo generation is particularly sensitive to the economic scale of the origin city. Distance is statistically significant for all commodity groups, but the sign is mostly positive. Only Biological Commodity shows the negative distance effect. Most other commodities have positive distance coefficients, suggesting that domestic air cargo in Canada is often concentrated on longer-distance corridors. The R^2 values indicate that the segmented models provide a reasonable fit for most commodity categories, particularly for dangerous goods, perishables, pharmaceuticals, and other special cargo. The lower value for Biological Commodity suggests that this category may be more specialized and less consistently explained by GDP and distance alone.

4.1.2 Service-level PPML gravity-model results

Table 4.2 summarizes the service-level PPML gravity model results in the same reporting format. The table reports the key forecasting variables, while the full regression results for each service category are provided in Appendix T.

Table 4-2. Summary of service-level PPML gravity-model results

	Intercept	Ln (Origin GDP)	Ln (Destination GDP)	Ln (OD distance)	R^2
Express & Time-Sensitive	**-78.01*** **	**1.87*** **	**0.93*** **	**1.19*** **	**0.79**
General Cargo Service	**-60.72*** **	**1.64*** **	**0.85*** **	**0.28*** **	**0.77**
Oversized & Heavy	**-119.31*** **	**3.34*** **	**0.83*** **	**1.92*** **	**0.78**
Commodity Information Pending	**-99.76*** **	**3.09*** **	**0.89*** **	**0.43*** **	**0.75**
Temperature Sensitive	**-73.23*** **	**1.44*** **	**1.20*** **	**0.67*** **	**0.81**
Vulnerable Cargo	**-76.03*** **	**1.36*** **	**1.27*** **	**0.60*** **	**0.68**
Other Special Cargo - No Service	**-78.02*** **	**1.94*** **	**1.06*** **	**0.39*** **	**0.80**

Note: *** indicates statistical significance at the 1% level.

Across all service categories, origin and destination GDP coefficients are positive and statistically significant, indicating that service-tagged domestic air-cargo flows are strongly associated with economic activity at both ends of the OD pair. In most cases, the origin GDP coefficient is larger than the destination GDP coefficient, suggesting that outbound service-specific cargo generation is particularly sensitive to the economic scale of the origin city. The distance coefficients are also positive and statistically significant across all service categories. This suggests that service-tagged air cargo is concentrated on longer-distance domestic corridors. This pattern is especially relevant for express & time-sensitive, temperature sensitive, and vulnerable cargo, where delivery speed, handling requirements, or shipment characteristics may make air transport more attractive over longer distances. The model fit values indicate reasonable performance across the service-level models, with R^2 values ranging from approximately 0.68 to 0.80.

4.2 Baseline cargo forecast by commodity and service type

The commodity-level forecasts are first generated at the OD level and then summed across the nine commodity categories to estimate total domestic air-cargo demand to 2050. Figure 4.1 shows the forecasted cargo demand by commodity category, while figure 4.2 shows the combined commodity-based baseline forecast. Since CargoIS does not provide complete coverage of domestic air cargo activity in Canada, the forecasted volumes should be interpreted with caution. In this study, the forecast is used primarily to establish a consistent baseline for comparing scenario outcomes, rather than to provide a complete national inventory of domestic air-cargo tonnes.

The service-level forecasts are also generated at the OD level and are presented in figure 4.3. These forecasts are included because the modal-shift scenarios are also evaluated by service type. However, as mentioned above, unlike the commodity categories, service categories are treated as overlapping tags rather than mutually exclusive cargo groups. Therefore, the service-level forecasts are not summed up to estimate total domestic air-cargo demand. Instead, they are interpreted as tag-specific demand patterns that support service-based modal-shift scenarios.

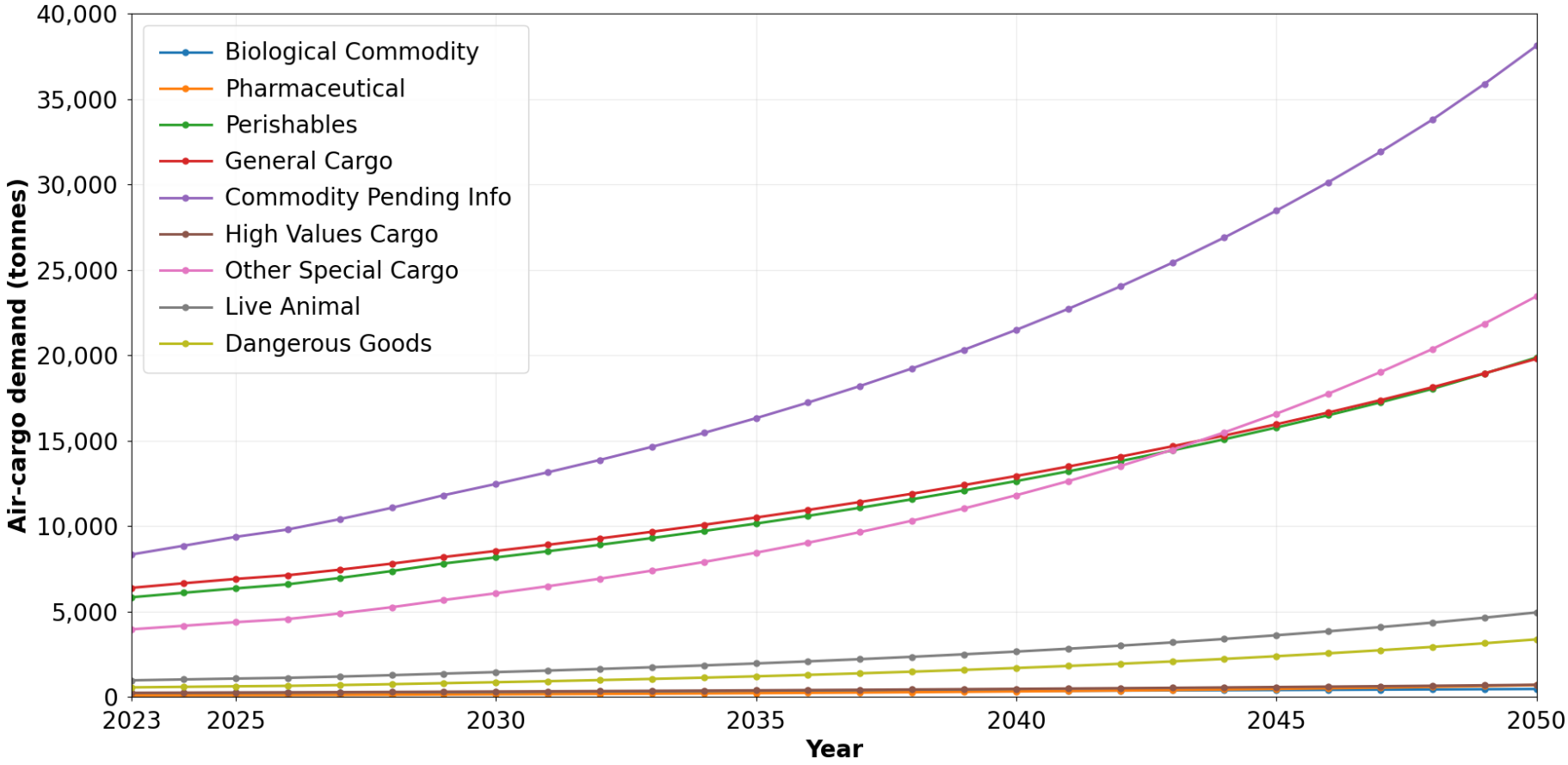


Figure 4-1. Domestic air-cargo demand by commodity category, 2023-2050

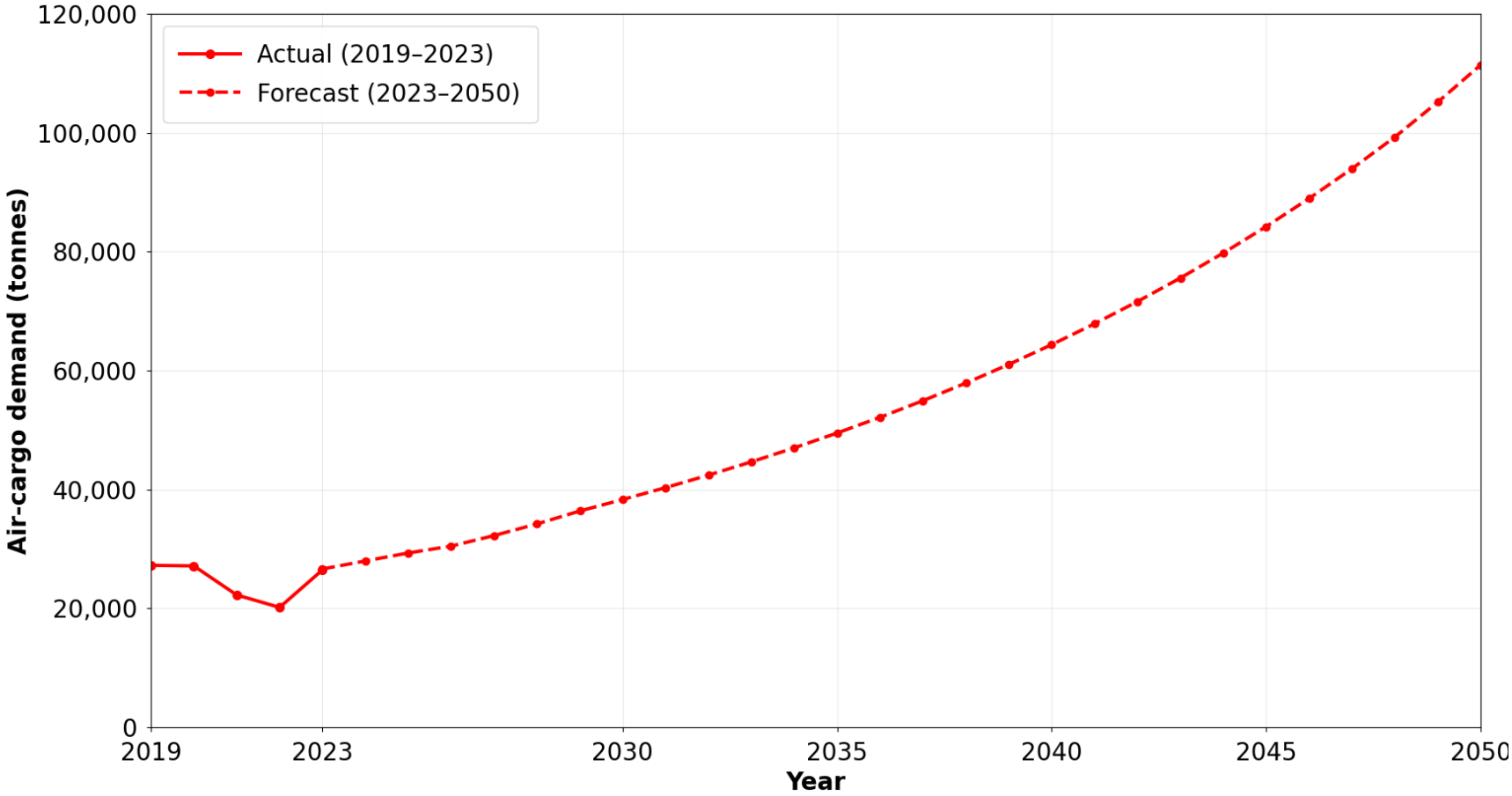


Figure 4-2. Total commodity-based baseline cargo forecast demand, 2023-2050

As shown in Figure 4.1, forecasted cargo demand increases across all commodity categories between 2023 and 2050. Growth is concentrated in a few large categories, particularly “Commodity Information Pending”, Other Special Cargo, Perishable, and General Cargo. By 2050, Commodity Information Pending reaches approximately 38,107 tonnes, followed by Other Special Cargo at 23,450 tonnes, Perishables at 19,866 tonnes, and General Cargo at 19,792 tonnes.

Figure 4.2 presents the combined commodity-based baseline forecast. The combined commodity-based baseline forecast shows steady growth over the analysis period. Annual growth in projected domestic air-cargo demand ranges from approximately 3.9% to 6.0%, with an average annual growth rate of about 5.4%. This is slightly higher than the historical growth observed in Statistics Canada domestic air-cargo data from 2008 to 2023, which shows an average annual growth rate of approximately 4.5% (Statistics Canada, 2025). The difference could partly be due to incomplete coverage of CargoIS and partly to the forecasting method, which is driven by projected GDP growth in the origin and destination cities. As GDP is assumed to increase over time, the baseline forecast produces a smoother upward trend, while the historical data include actual annual fluctuations and occasional declines. Therefore, this comparison should be interpreted as a reasonableness check rather than a direct validation of the absolute forecasted volumes.

Then, Figure 4.3 presents the forecasted cargo demand by service type from 2023 to 2050.

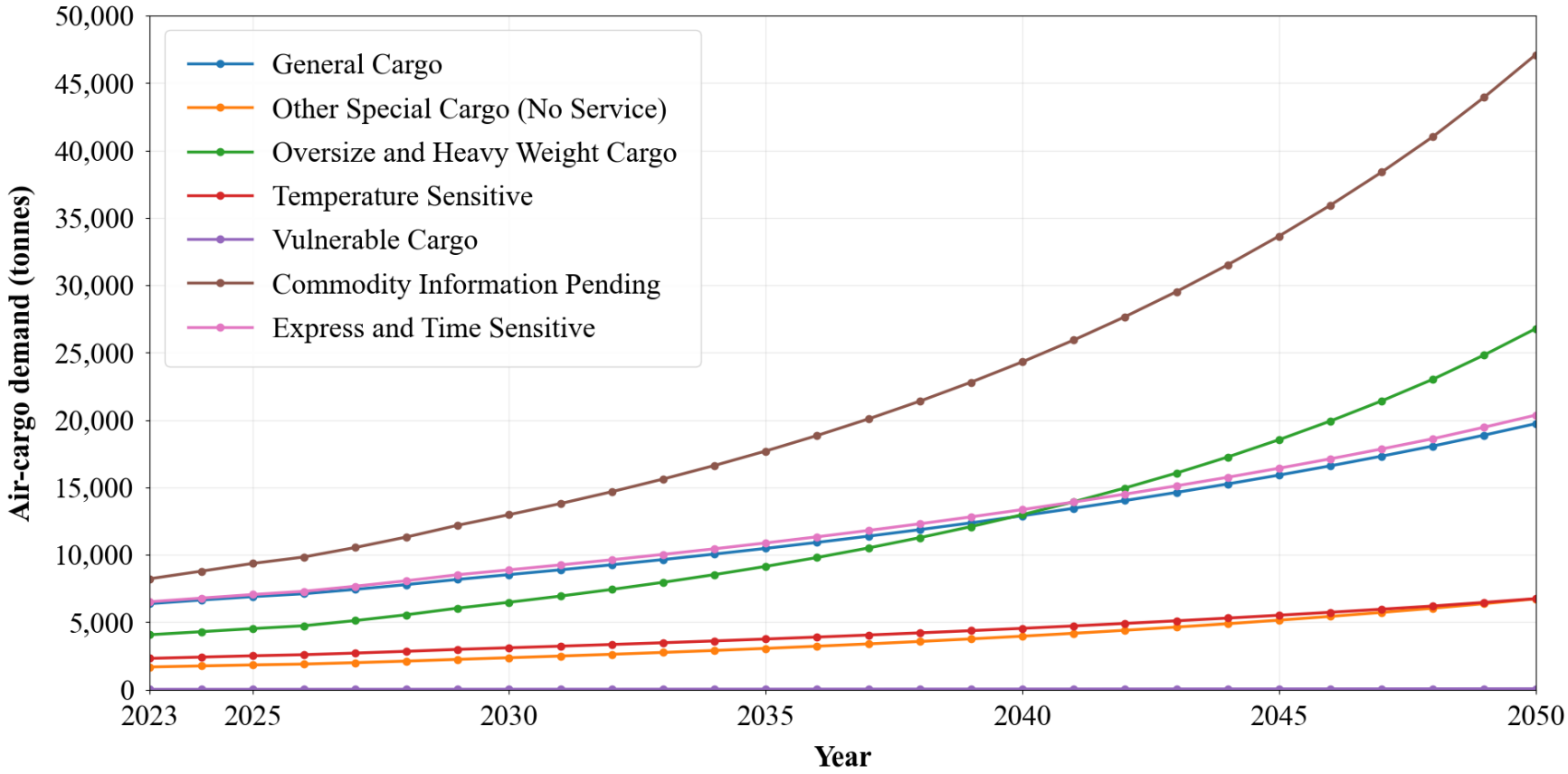


Figure 4-3. Domestic air-cargo demand by service category, 2023-2050

The service-level forecasts show an overall increase across all service categories. The largest forecasted service categories are Commodity Information Pending, General Cargo, and Oversized and Heavy Weight Cargo. Commodity information pending increases from approximately 8,200 tonnes in 2023 to 47,100 tonnes in 2050, while General Cargo increases from approximately 6,400 tonnes to 19,700 tonnes over the same period. Oversized and Heavy Weight Cargo also shows substantial growth, increasing from approximately 4,100 tonnes in 2023 to 26,800 tonnes in 2050.

4.3 Baseline WTWa emissions projection

The commodity-based cargo forecast is used to estimate baseline WTWa emissions for domestic air cargo to 2050. For each OD pair and commodity category, emissions are calculated using forecasted cargo volume, air-route distance, and the WTWa emission factor for conventional Jet-A fuel. The emission factor is adjusted over time to account for the projected decline in electricity-grid emissions intensity under the Current Measures scenario from Canada's Energy Future 2023. Therefore, the baseline reflects changes in upstream electricity-related emissions while assuming no SAF blending, alternative propulsion, or modal shift.

Figure 4.4 presents the baseline WTWa emissions projection under the no-mitigation or "do nothing" scenario.

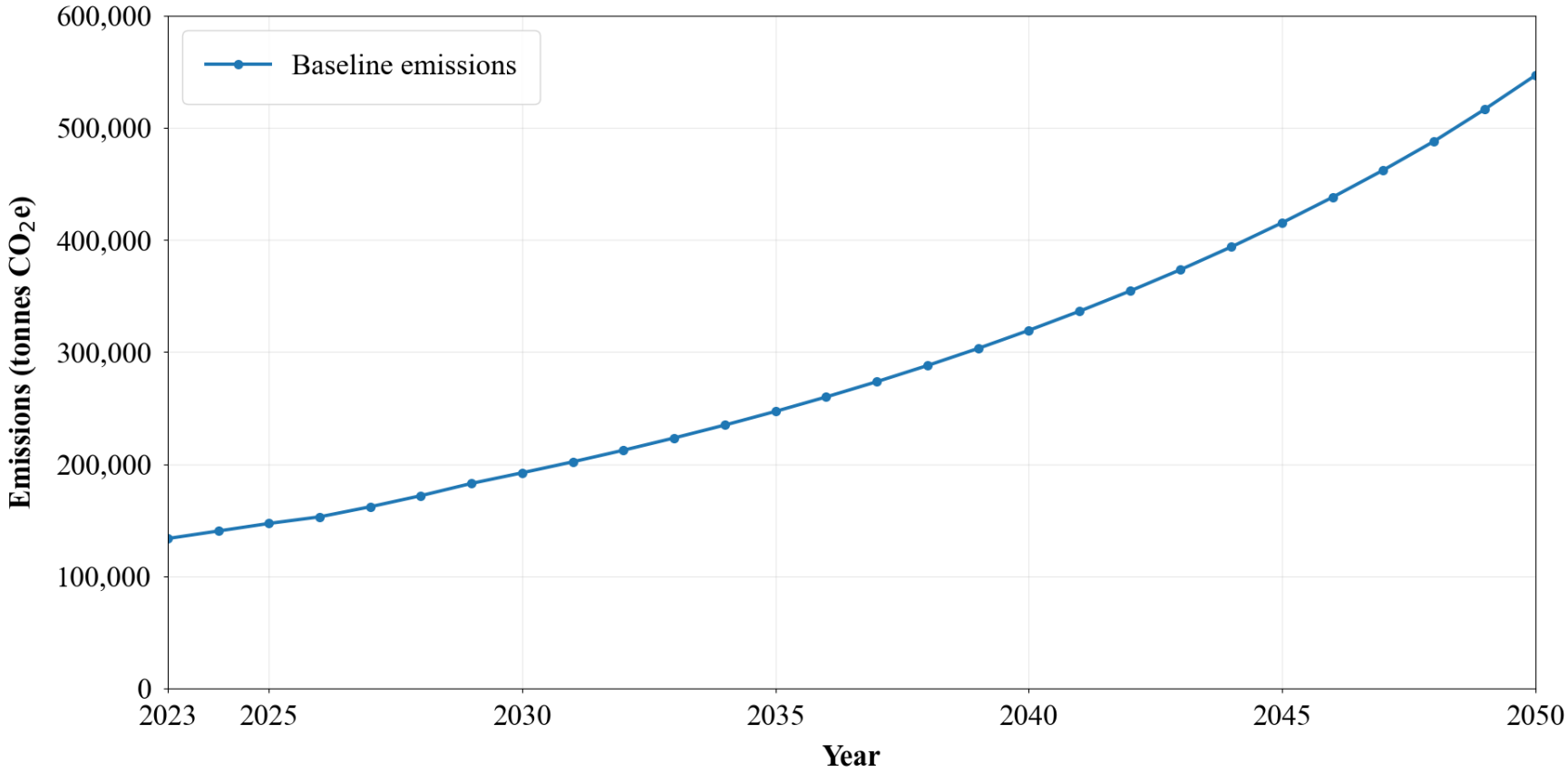


Figure 4-4. Baseline WTWa emissions projection for domestic air cargo, 2023-2050

The results show that baseline emissions increase over the forecast period, following the growth in projected domestic air-cargo demand. The baseline emissions pathway is not intended to represent a policy target, but rather a reference case for evaluating mitigation scenarios.

Chapter 5: Emissions Scenario Results

This chapter presents the emissions-reduction results for the decarbonization scenarios evaluated in this study. Section 5.1 examines sustainable aviation fuel scenarios, Section 5.2 evaluates alternative aircraft propulsion, and Section 5.3 presents the selective modal-shift scenarios, both with and without surface freight decarbonization. Section 5.4 presents the combined mitigation scenarios and compares their emissions trajectories with national and global climate-aligned benchmarks. Finally, Section 5.5 summarizes the principal findings across the scenarios.

5.1 Sustainable aviation fuel-only scenario results

This section presents the emissions results for the SAF-only scenarios. In these scenarios, domestic cargo demand follows the commodity-based baseline forecast presented in chapter 4, while conventional Jet-A fuel is partially replaced by SAF, as described in Section 3.5.4. This section does not introduce alternative propulsion or modal shift, allowing the effect of SAF adoption to be evaluated independently of the other mitigation strategies considered in this study. Figure 5.1 presents the WTWa emissions under the SAF-only scenarios from 2023 to 2050.

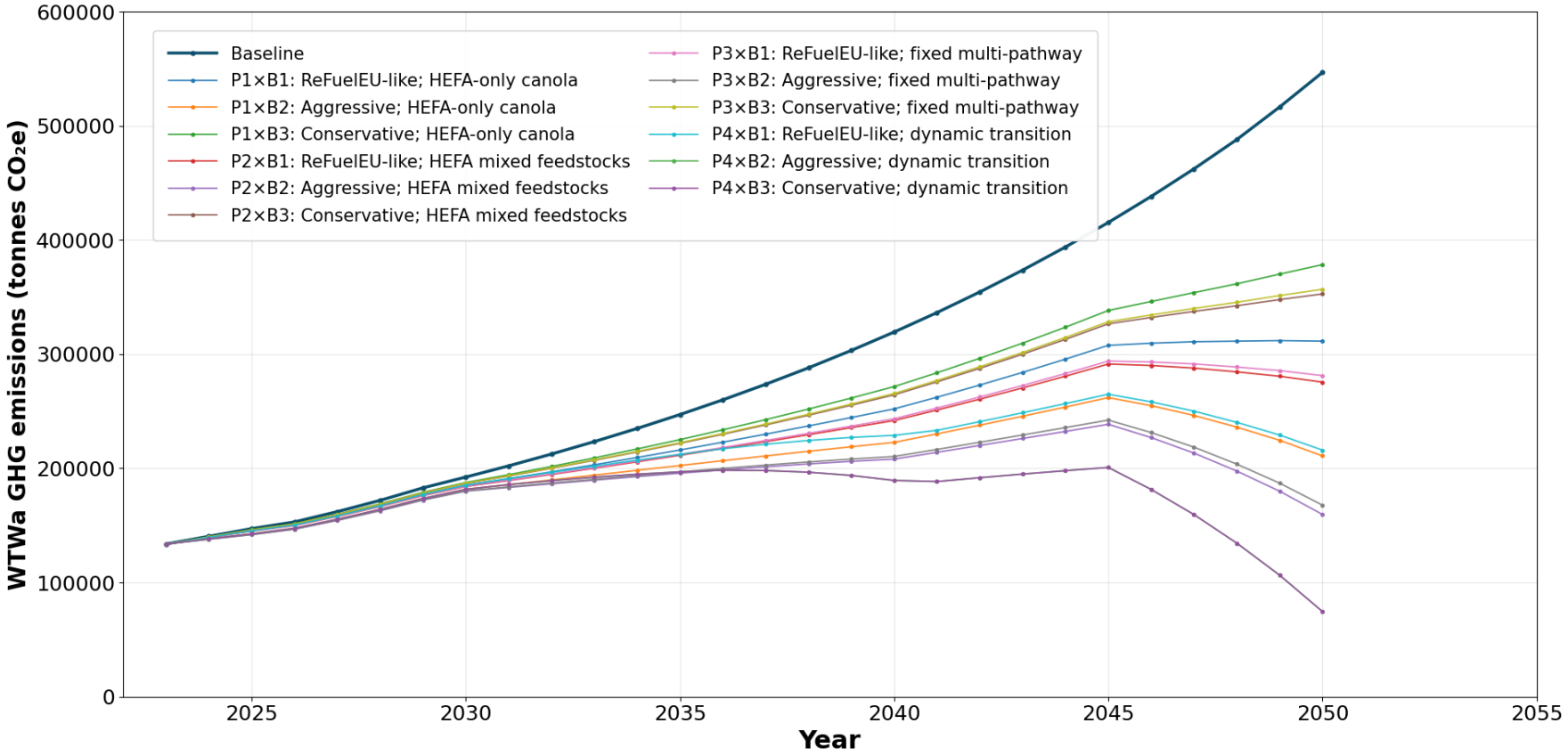


Figure 5-1. GHG Emissions under SAF scenarios (2023 - 2050)

All SAF scenarios reduce emissions relative to this baseline, but the magnitude of reduction depends strongly on both the SAF blending rate and the SAF production portfolio. In the early years, the SAF scenarios are close to the baseline because blending shares remain low. The scenarios diverge more clearly after 2030, especially after 2035, as SAF blending rates increase. Within each SAF portfolio, the aggressive blending case generally provides the largest reduction, followed by the ReFuelEU-style case and then the conservative case.

By 2050, SAF-only emissions reductions range from approximately 30.8% to 86.4% relative to the baseline. The weakest outcome is observed in scenario SAF 3 (P1*B3), which applies the conservative blending pathway to the single-feedstock HEFA portfolio. The strongest outcome is observed in scenario SAF 11 (P4*B2), where aggressive SAF blending is combined with the dynamic transition portfolio. This indicates that SAF can provide substantial emissions reductions, but the deepest reductions require both high blending rates and a lower-carbon SAF production mix.

The results also indicate that the SAF blending rate has a larger effect than the SAF feedstock on emissions reduction. In 2050, moving from the conservative blending case to the aggressive blending case within the same SAF portfolio reduces emissions by approximately 167,500-235,700 tonnes CO_2e. By comparison, shifting from the single-feedstock HEFA portfolio to the more diverse dynamic transition portfolio reduces emissions by approximately 68,200-136,400 tonnes CO_2e, depending on the blending case. This finding on the relative impact of SAF blending rates and pathway mix should be interpreted within the assumptions of this scenario set, including the selected blending pathways, SAF portfolio compositions, and lifecycle emission factors. Figures 5.2 and 5.3 compare the SAF-only emissions results against the illustrative IPCC 1.5°C and Canada net-zero climate target ranges.

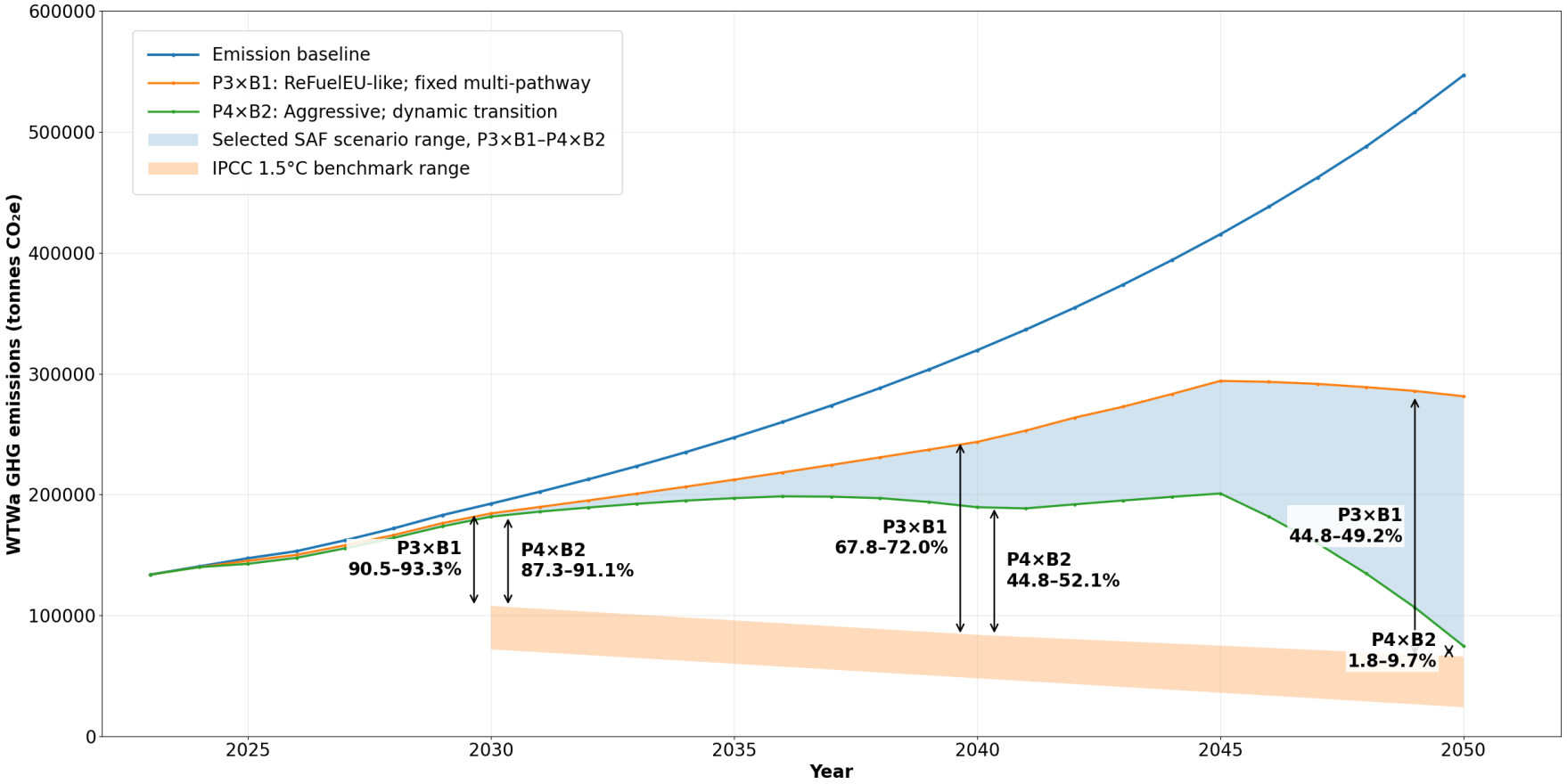


Figure 5-2. SAF scenarios compared with Canada IPCC 1.5 climate target

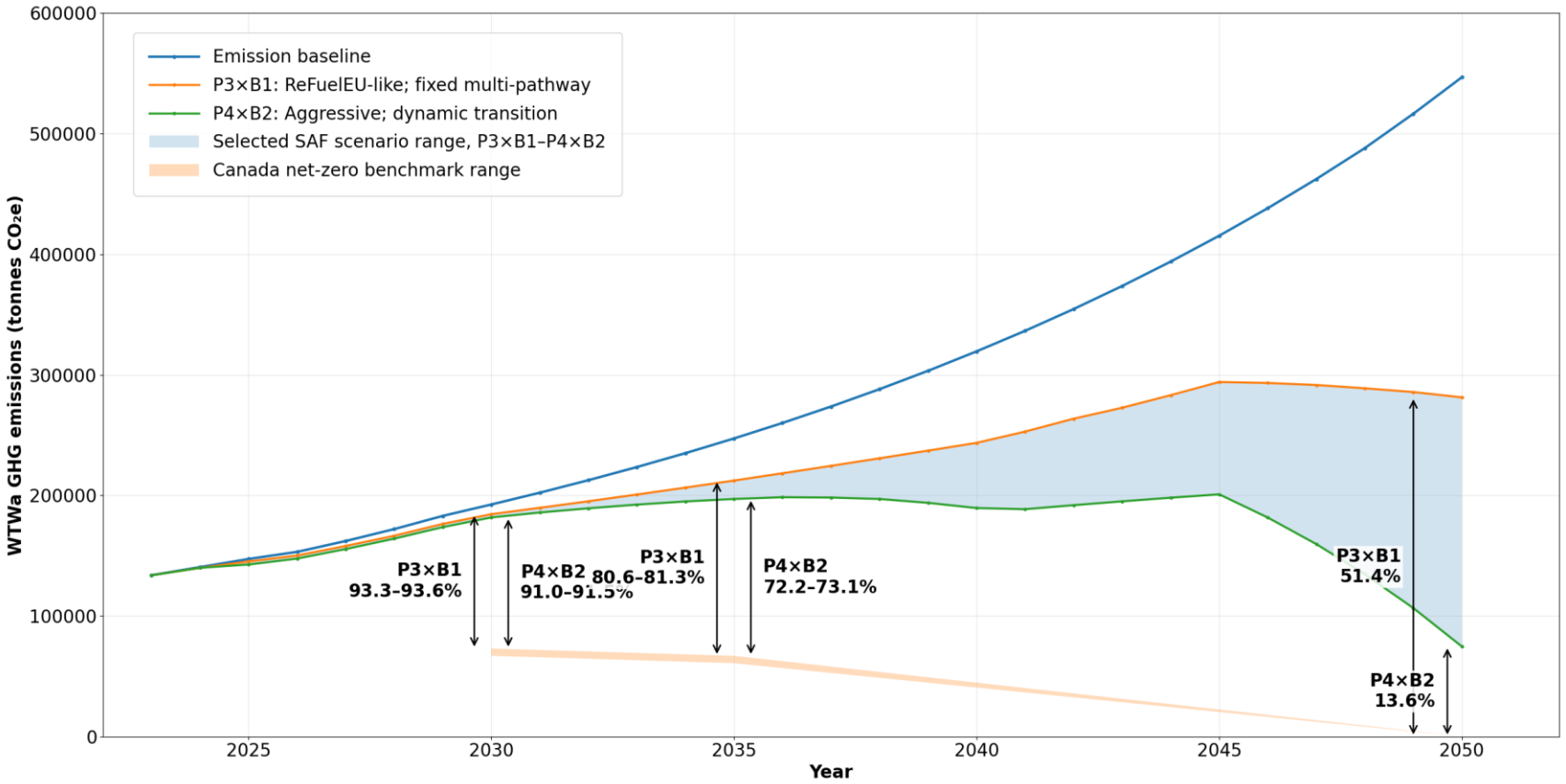


Figure 5-3. SAF scenarios compared with Canada net-zero climate target

The figures 5.2 and 5.3 focus on SAF 7 and SAF 11 to represent two different levels of SAF ambition. SAF 7 is treated as the more moderate and policy-aligned scenario because it uses the fixed multi-pathway SAF portfolio based on the C-SAF Roadmap and applies a ReFuelEU-style blending pathway. This makes SAF 7 a useful central comparison case, since it reflects a more gradual SAF adoption trajectory and a fixed portfolio mix rather than assuming a major transformation in the SAF supply structure. In contrast, SAF 11 represents a high-ambition or upper-bound case. This scenario combines the dynamic transition SAF portfolio with an aggressive blending pathway, reaching 100% SAF blending by 2050. It also assumes a major shift in the SAF supply mix over time, moving away from a HEFA-dominated portfolio based on bio-based feedstocks toward greater shares of lower-carbon pathways such as FT, ATJ, and especially PtL.

The results show that SAF 11 closes a much larger share of the climate targets gap than SAF 7. Under the IPCC 1.5°C benchmark, SAF 11 leaves only about 1.8-9.7% of the gap remaining by 2050, while SAF 7 leaves approximately 44.8-49.2% of the gap remaining. Similarly, under the Canada net-zero target, SAF 11 leaves approximately 13.6% of the 2050 gap remaining, compared with about 51.4% for SAF 7. This demonstrates that very high SAF adoption, combined with a lower-carbon transition portfolio, can significantly reduce emissions. However, the stronger performance of SAF 11 should be interpreted cautiously because it depends on ambitious assumptions about SAF availability, neat SAF (pure, 100% SAF) by 2050, PtL scale-up, and low-carbon hydrogen supply. By comparison, SAF 7 represents a more moderate pathway, although it may still be ambitious in the Canadian context. The large remaining gap under SAF 7 suggests that a gradual SAF deployment pathway would likely need to be combined with additional mitigation measures to align domestic air-cargo emissions with deep decarbonization targets by 2050.

5.2 Alternative propulsion systems-only scenario results

This section presents the emissions results for the alternative propulsion systems-only scenarios. In these scenarios, domestic air-cargo demand follows the baseline forecast presented in Chapter 4, while eligible corridors are gradually served by alternative propulsion technologies according to the adoption assumptions described in Section 3.5.4. This section does not introduce sustainable aviation fuels or mode shift, allowing the effect of alternative propulsion to be evaluated independently. The results are first presented at the network level to show the overall emissions trajectory and the remaining gap to climate targets, followed by an aggregate OD-level analysis to identify where alternative propulsion provides the greatest reductions and where its impact remains limited.

5.2.1 Network-level emissions results

At the network level, the AP-only scenarios produce relatively modest emissions reductions compared with the baseline. As shown in Figure 5.4 and 5.5, all AP scenarios follow a similar upward trend to the baseline throughout the analysis period. In the early years, the AP scenarios are almost indistinguishable from the baseline. By 2030, emissions reductions relative to the baseline remain very small, ranging from approximately 0.02% to 0.29% across the AP scenarios. This reflects the limited near-term availability of alternative propulsion technologies and the restricted number of corridors eligible for early adoption.

The scenarios begin to diverge more clearly after 2035 as additional aircraft categories and stage-length ranges become eligible for alternative propulsion. By 2040, the AP-only scenarios reduce emissions by approximately 0.4% to 4.9% relative to the baseline. By 2050, emissions under the AP scenarios range from approximately 507,923 to 527,341 tonnes CO_2e, compared with 546,822 tonnes CO_2e in the baseline. This corresponds to a 2050 reduction of only 3.6% to 7.1% relative to the baseline. Therefore, while AP adoption provides some emissions benefits, its network-level impact remains limited over the study period. Figures 5.4 and 5.5 compare the AP-only emissions pathways with the illustrative IPCC 1.5°C target and the Canada net-zero climate target.

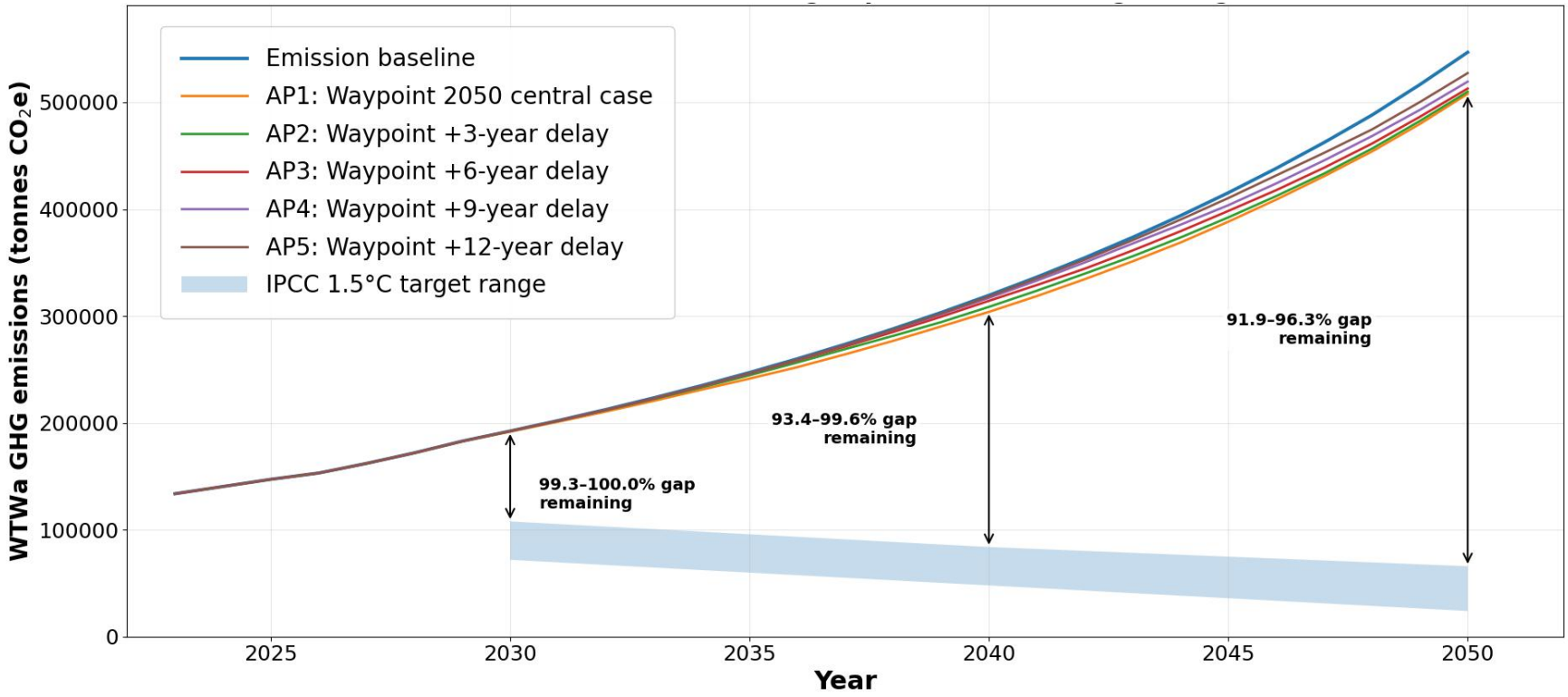


Figure 5-4. AP scenarios and the remaining gap to IPCC 1.5 climate target

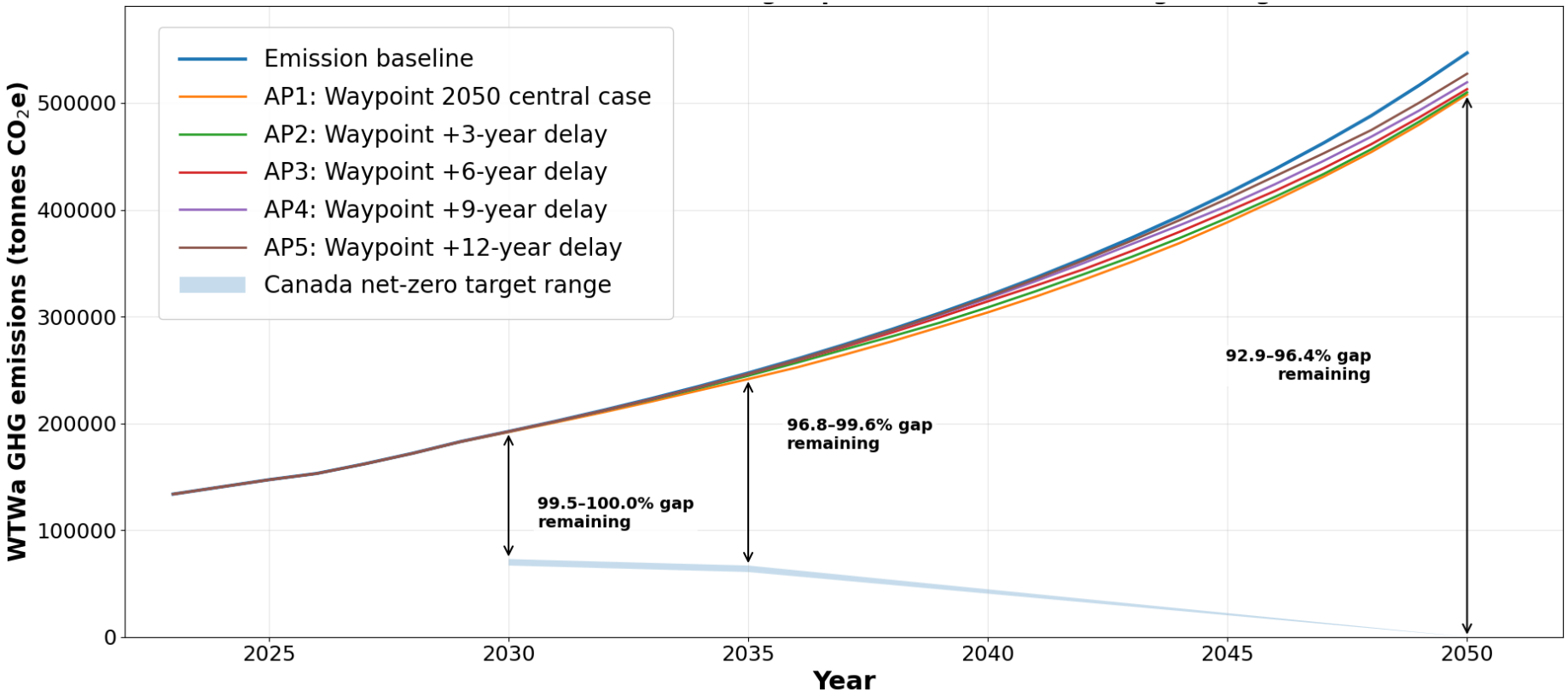


Figure 5-5. AP scenarios and the remaining gap to Canada's net-zero climate target

The results show that AP-only adoption leaves a substantial remaining gap to both climate targets. Relative to the IPCC 1.5°C target range, approximately 99.3%-100.0% of the baseline-to-target gap remains in 2030, 93.4%-99.6% remains in 2040, and 91.9%-96.3% remains in 2050. Relative to the Canada net-zero pathway, approximately 99.5%-100.0% of the gap remains in 2030, 96.8%-99.6% remains in 2035, and 92.9%-96.4% remains in 2050.

The remaining 100% gap in the early milestone years is mainly due to conservative adoption timelines assumed in some AP scenarios. In these scenarios, alternative propulsion technologies have not yet reached meaningful deployment by 2030, so their network-level emissions impact remains very limited or minimal. As a result, the AP-only pathways remain close to the baseline and therefore leave almost the entire baseline-to-target gap unresolved. However, in practice, some near-term reductions could occur through conventional fleet turnover and incremental aircraft efficiency improvements, such as improved aerodynamics, weight reduction, and operational efficiency gains. However, these improvements are not included in the AP-only scenario or this thesis as a whole. Broader fleet-replacement effects are excluded due to data limitations and the difficulty of assigning aircraft-level efficiency improvements to specific OD flows.

5.2.2 Disaggregate OD-level results

While the network-level results show that AP-only scenarios reduce total emissions by only 3.6%-7.1% relative to the baseline by 2050, the OD-level results reveal that the impact of alternative propulsion varies substantially by corridor. This variation is mainly driven by the assumed aircraft range thresholds and technology deployment timelines. As a result, shorter and medium-distance corridors can achieve large reductions in emissions, while longer corridors remain largely unaffected. This distinction is important in the Canadian domestic air-cargo context because a large share of activity and emissions is concentrated on longer-haul corridors, where alternative propulsion technologies remain less feasible within the study period. Figure 5.6 presents selected OD corridors in 2050 to illustrate how AP impacts differ across route distances.

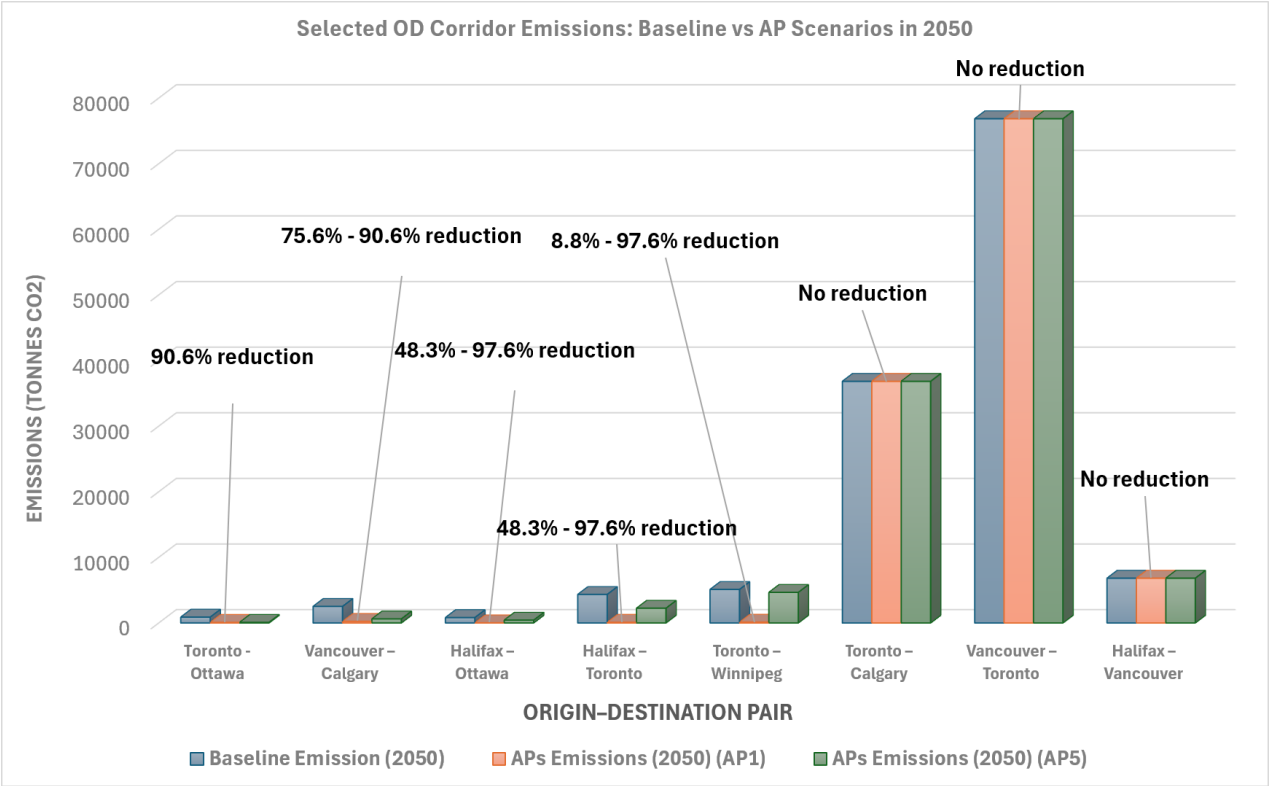


Figure 5-6. Selected OD corridor emissions: Baseline vs AP scenarios in 2050

The selected corridors are ordered from shorter to longer flight distance and were chosen to cover the assumed AP distance thresholds described in Section 3.5.4.2.2, as well as longer-haul corridors that fall outside the assumed feasible range of the technologies. The figure compares the baseline with AP1 and AP5. AP1 represents the more optimistic Waypoint-based adoption timeline, while AP5 represents a more conservative timeline with a 12-year delay relative to the Waypoint-based assumptions. The results show that shorter and medium-distance corridors generally experience the largest reductions. For example, Toronto-Ottawa shows a reduction of approximately 90.6%, while Vancouver-Calgary shows reductions of approximately 75.6%-90.6% across the selected AP scenarios. Other medium-distance corridors, such as Halifax-Ottawa, Halifax-Toronto, and Toronto-Winnipeg, also show reductions, although the magnitude depends on the scenario and the timing of AP adoption, and the assumed propulsion technologies.

Longer corridors, such as Toronto-Calgary, Vancouver-Toronto, and Halifax-Vancouver, show no emissions reduction under the AP scenarios as modelled in this study. These corridors exceed the assumed feasible range of the alternative propulsion technologies considered and therefore continue to rely on conventional aircraft within the scenario framework. However, this result should not be interpreted as meaning that no emissions improvements are possible on longer corridors in practice. As mentioned in section 5.2.1, some reductions could occur through conventional fleet turnover and incremental aircraft efficiency improvements, such as improved aerodynamics, lighter aircraft structures, more efficient engines, and operational improvements. These effects are excluded in this thesis due to data availability at the OD level.

Overall, the OD-level results show that alternative propulsion can provide meaningful emissions reductions on eligible short- and medium-distance corridors. However, because many high-emission Canadian domestic air-cargo corridors are longer-haul routes, AP-only scenarios remain insufficient to deliver deep network-wide decarbonization. This suggests that alternative propulsion should be viewed as a targeted corridor-level mitigation strategy rather than a stand-alone solution for the full domestic air-cargo system.

5.3 Modal shift scenario results

5.3.1 Modal shift-only results

This subsection presents the emissions results for the modal shift-only scenarios. In these scenarios, eligible air-cargo flows are shifted to surface transport modes in accordance with the modal shift assumptions described in Section 3.5. The remaining air-cargo flows continue to be served by conventional aircraft using Jet-A fuel, with no SAF adoption or alternative propulsion introduced. For the shifted flows, surface transportation is represented using conventional truck and rail technologies, without additional truck or rail decarbonization. Therefore, this scenario set isolates the emissions impact of modal shift alone.

Modal shift is applied at the commodity and service-category level because these categories provide the most detailed available information on shipment characteristics in the CargoIS data. However, this is a simplified representation of modal shift. In practice, modal shift decisions depend not only on commodity or service type, but also on shipment-level factors such as delivery time requirements,

transport cost, reliability, cargo value, handling requirements, and the availability of truck or rail alternatives. A more detailed modal choice model based on generalized cost or shipper behavior would be preferable, but the required shipment-level data are not available for air cargo.

Figures 5.7 to 5.10 compare the modal shift-only scenarios with the baseline and the two climate benchmark ranges. Figures 5.7 and 5.10 present the commodity-based modal shift results relative to the IPCC 1.5°C and Canada's net-zero target ranges, respectively.

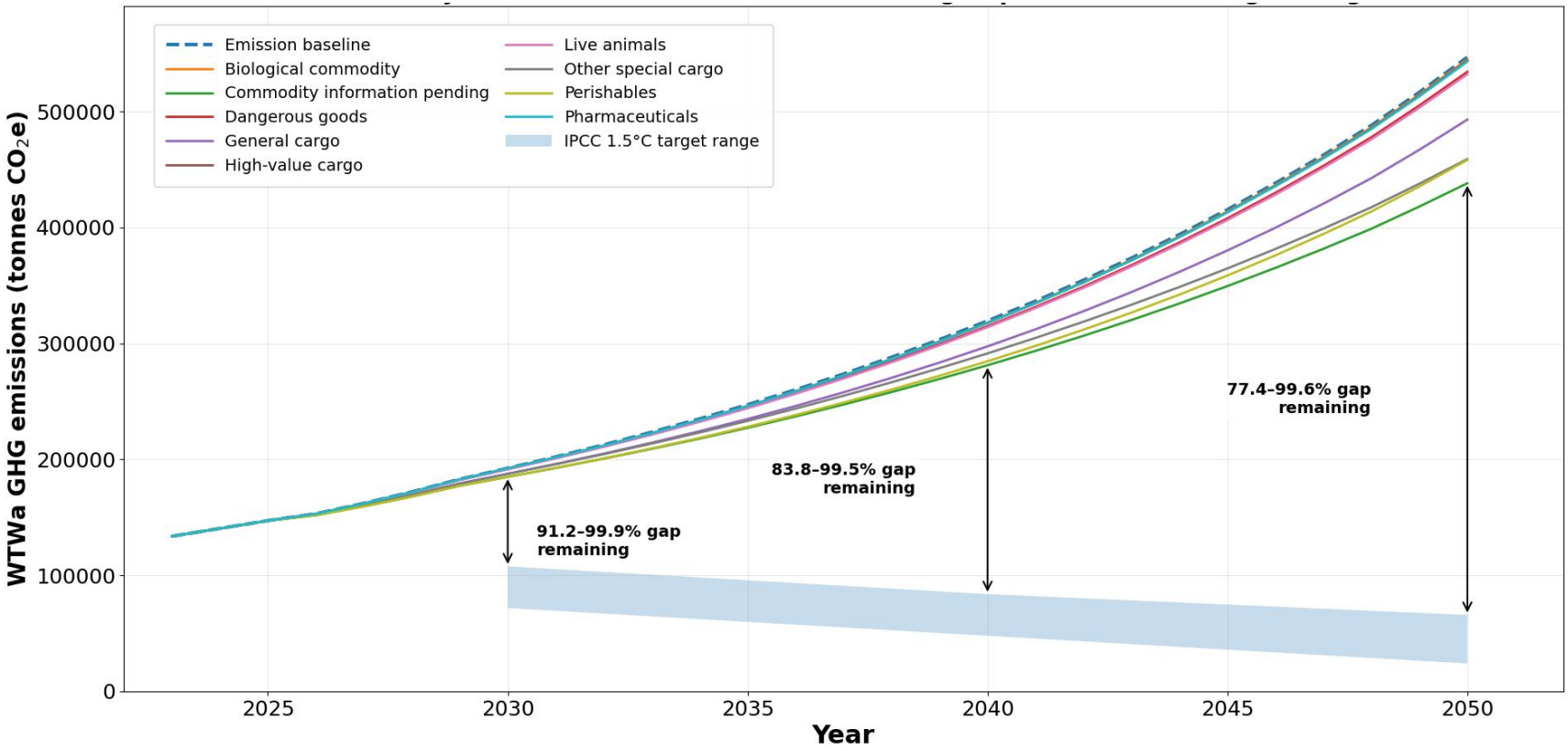


Figure 5-7. Modal shift-only scenarios and remaining gap to the IPCC 1.5°C target range: commodity-based shifts.

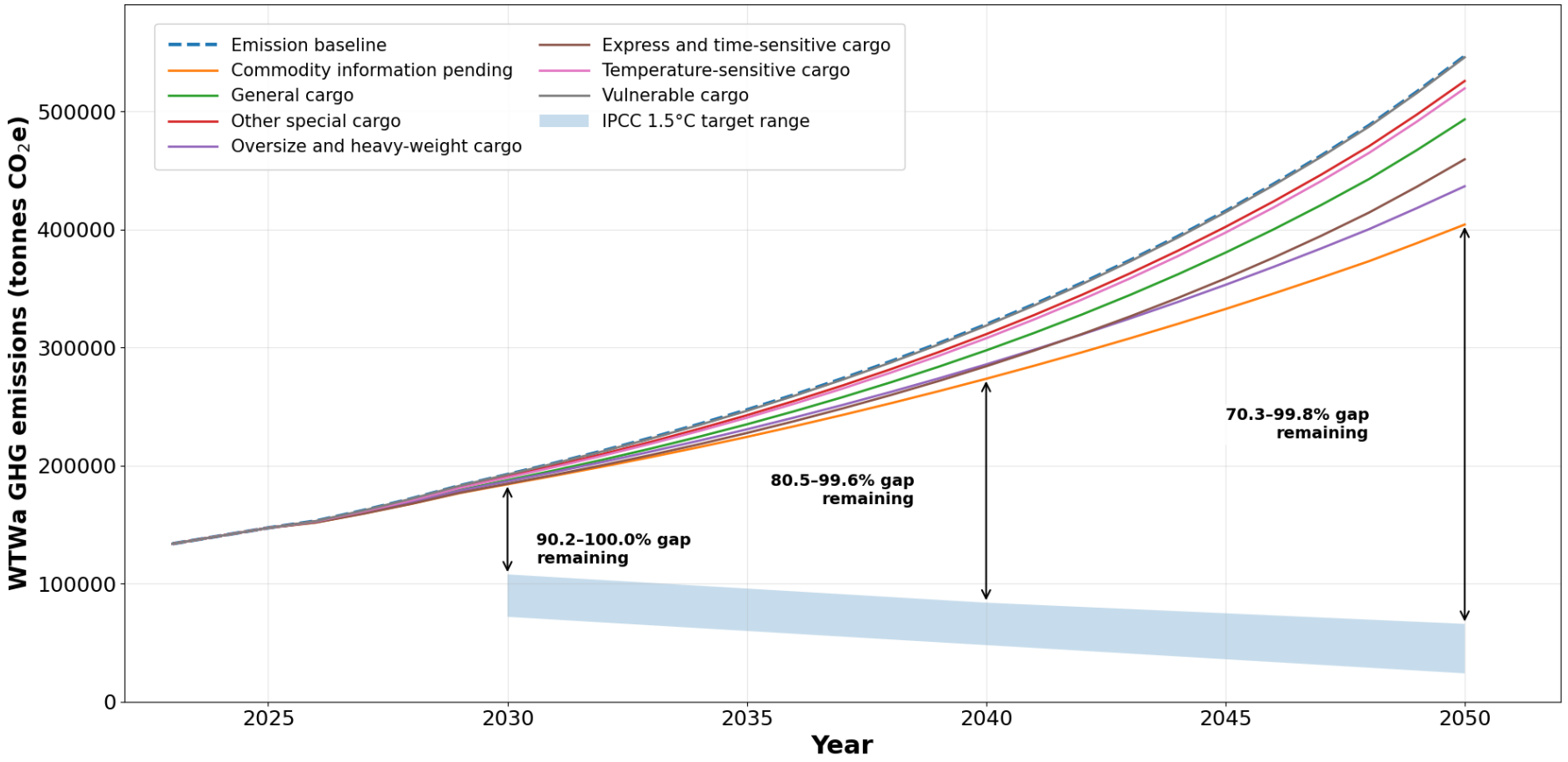


Figure 5-8. Modal shift-only scenarios and remaining gap to the IPCC 1.5°C target range: service-tag shifts.

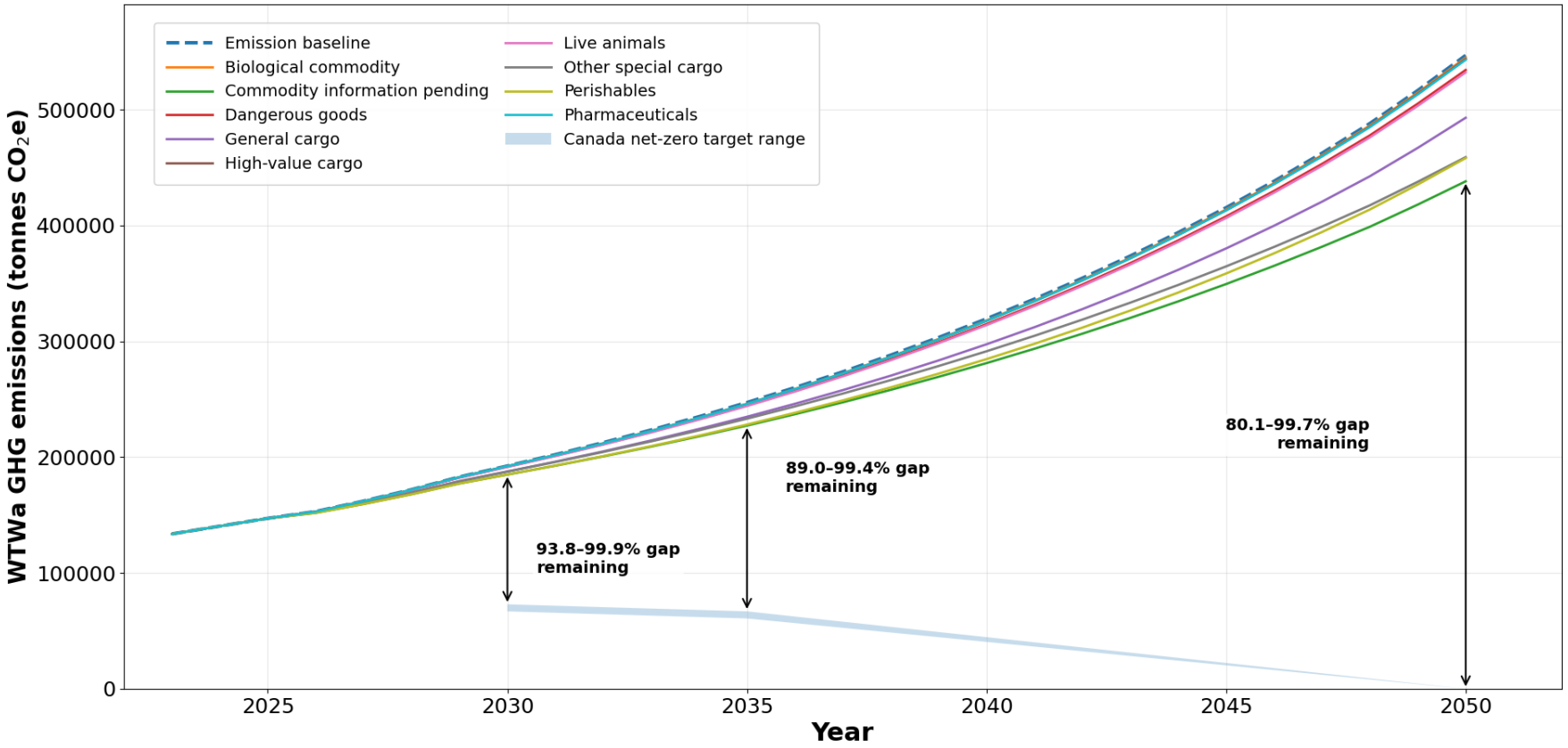


Figure 5-9. Modal shift-only scenarios and remaining gap to the Canada net-zero target range: commodity-based shifts.

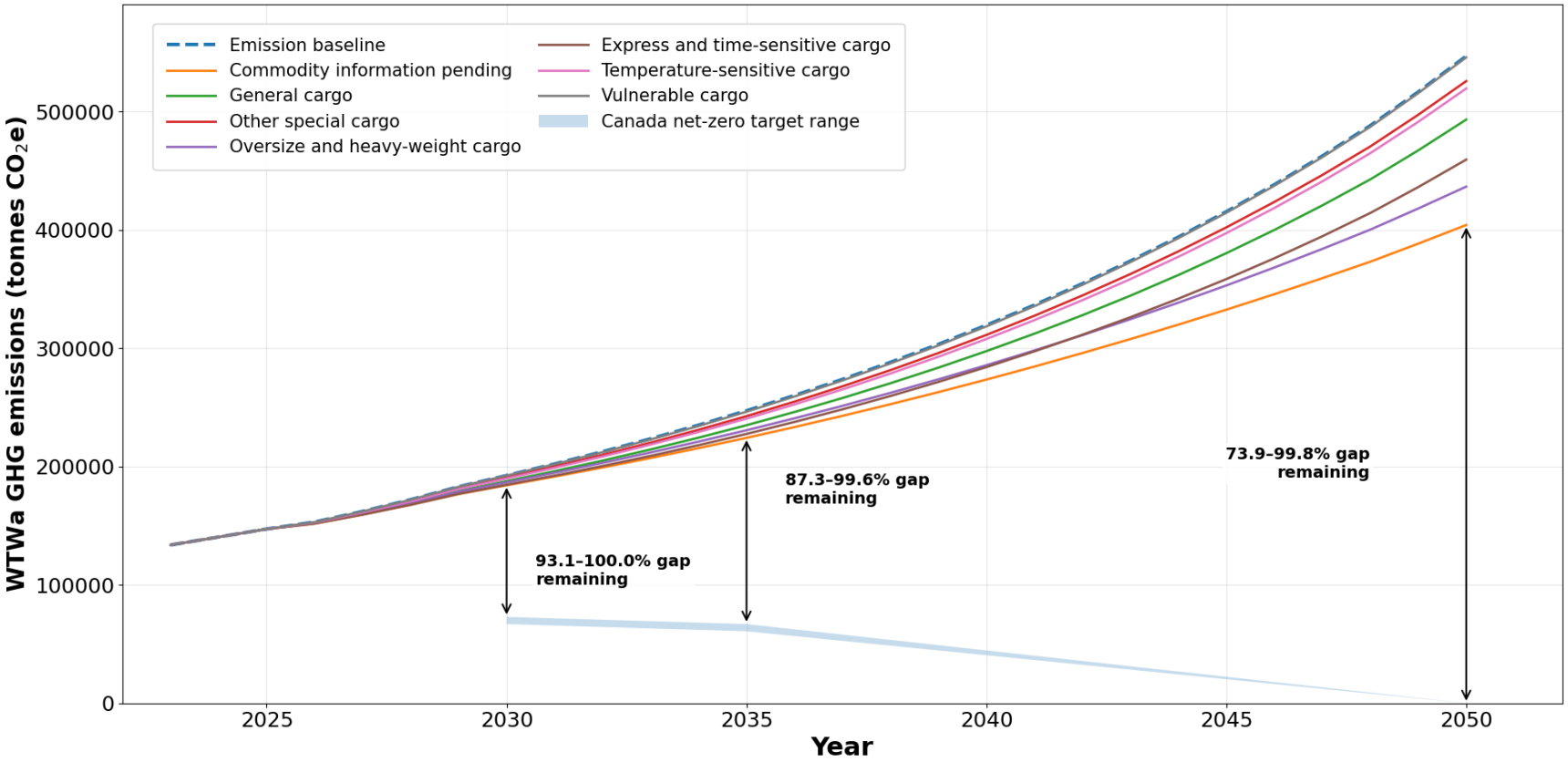


Figure 5-10. Modal shift-only scenarios and remaining gap to the Canada net-zero target range: service-tag shifts.

Figures 5.8 and 5.10 present the corresponding service-tag modal shift results. The results show that modal shift-only scenarios reduce emissions relative to the baseline, but the remaining gaps to both climate targets remain large. For commodity-based shifts, the remaining gap by 2050 is approximately 77.4%-99.6% relative to the IPCC 1.5°C target range and 80.1%-99.7% relative to the Canada net-zero target range. For service-tag shifts, the remaining gap by 2050 is approximately 70.3%-99.8% relative to the IPCC 1.5°C target range and 73.9%-99.8% relative to the Canada net-zero target range. This indicates that modal shift can provide emissions benefits, but it is not sufficient as a stand-alone strategy. The remaining gap is large because only selected cargo categories or service tags are shifted, and shifted freight still produces emissions when transported by conventional truck or rail. The following subsection examines whether the emissions benefits of modal shift increase when it is combined with surface transportation decarbonization.

5.3.2 Modal shift with surface transportation decarbonization results

This subsection extends the modal-shift-only analysis by incorporating surface transportation decarbonization. The amount of freight shifted remains the same as in Section 5.3.1, but truck and rail emission factors change over time based on the decarbonization assumptions described in Section 3.5.3. This allows the analysis to test whether modal shift becomes more effective when cleaner surface modes carry shifted freight.

Truck decarbonization is represented through fleet turnover and the gradual adoption of zero-emission heavy-duty vehicles, while rail decarbonization is represented by four roadmap-based pathways guided by the Rail Pathways Initiative. These surface decarbonization assumptions are applied to each of the 16 modal shift categories, including nine commodity-based shifts and seven service-tag shifts, producing 64 emission outputs. Because the results follow similar patterns and differ only modestly across many cases, this section presents selected representative results; Appendix U provides the full set.

Figures 5.11 to 5.14 present a representative set of modal shifts with surface transportation decarbonization results for both commodity-based and service-tag shifts. For this selected set of outputs, truck decarbonization follows the fleet-turnover pathway based on ZEV sales targets described in Section 3.5.3.1, while rail decarbonization follows Rail Technology Scenario 4 in Section 3.5.3.2.5, with alternative fuel represented by biofuel and alternative propulsion by hydrogen rail.

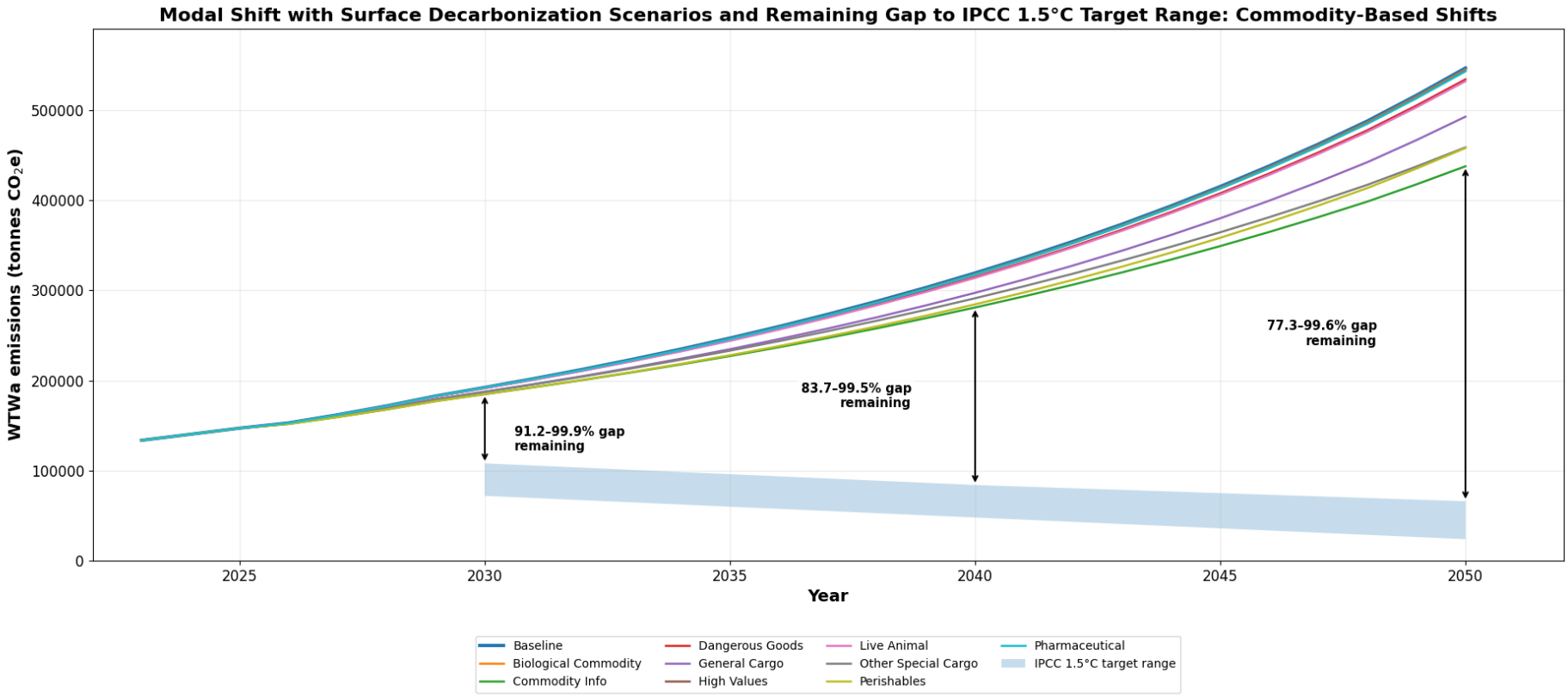


Figure 5-11. Modal Shift with Surface Decarbonization Scenarios and Remaining Gap to IPCC 1.5°C target range: commodity-based shifts

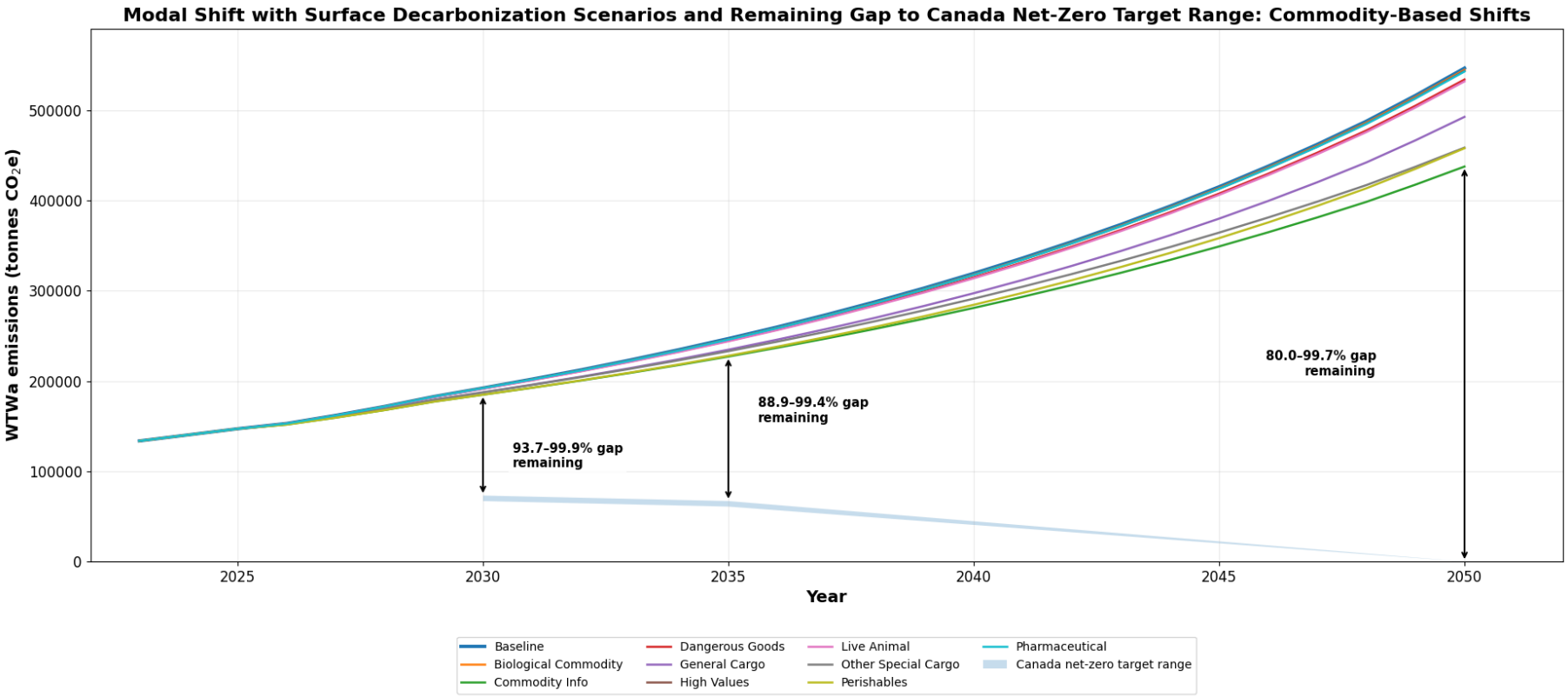


Figure 5-12. Modal Shift with Surface Decarbonization Scenarios and Remaining Gap to Canada Net Zero target range: commodity-based shifts.

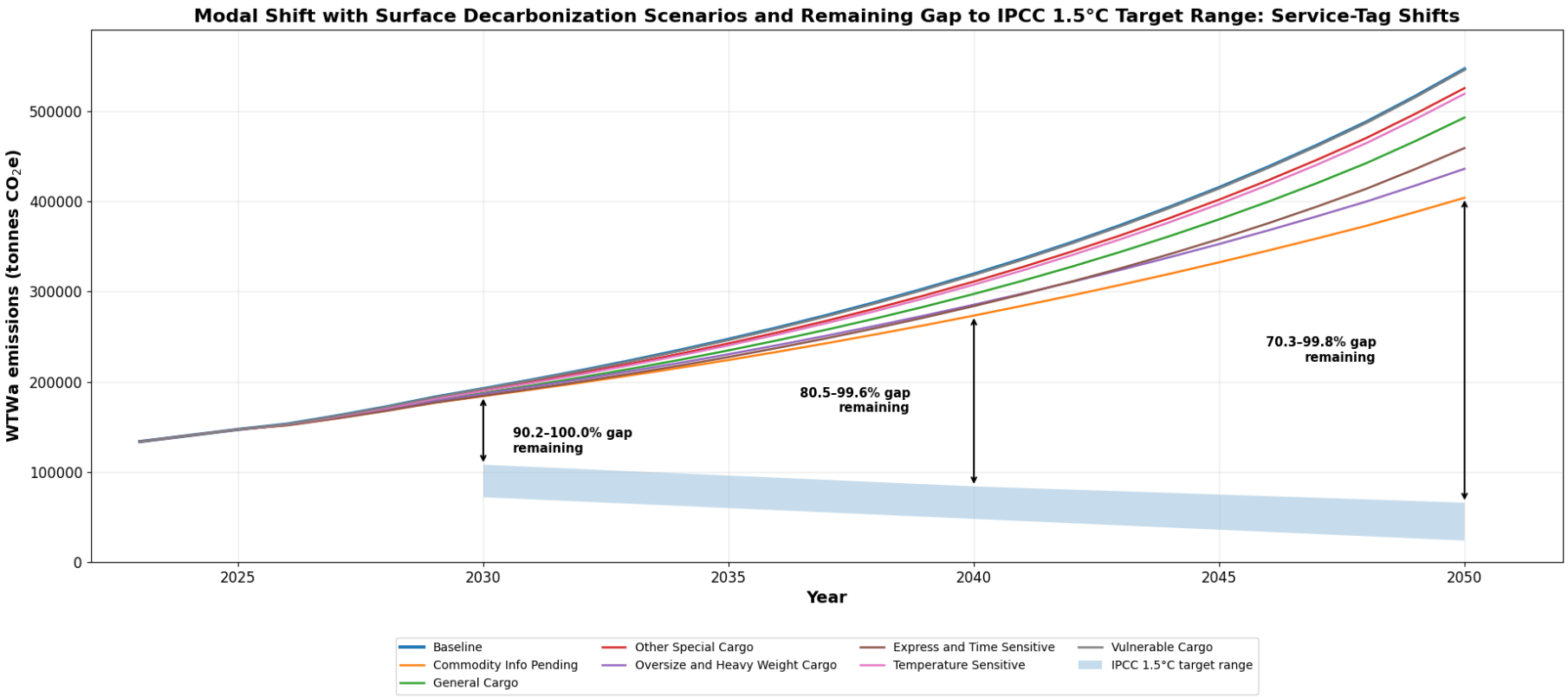


Figure 5-13. Modal Shift with Surface Decarbonization Scenarios and Remaining Gap to IPCC 1.5°C target range: service-tag shifts

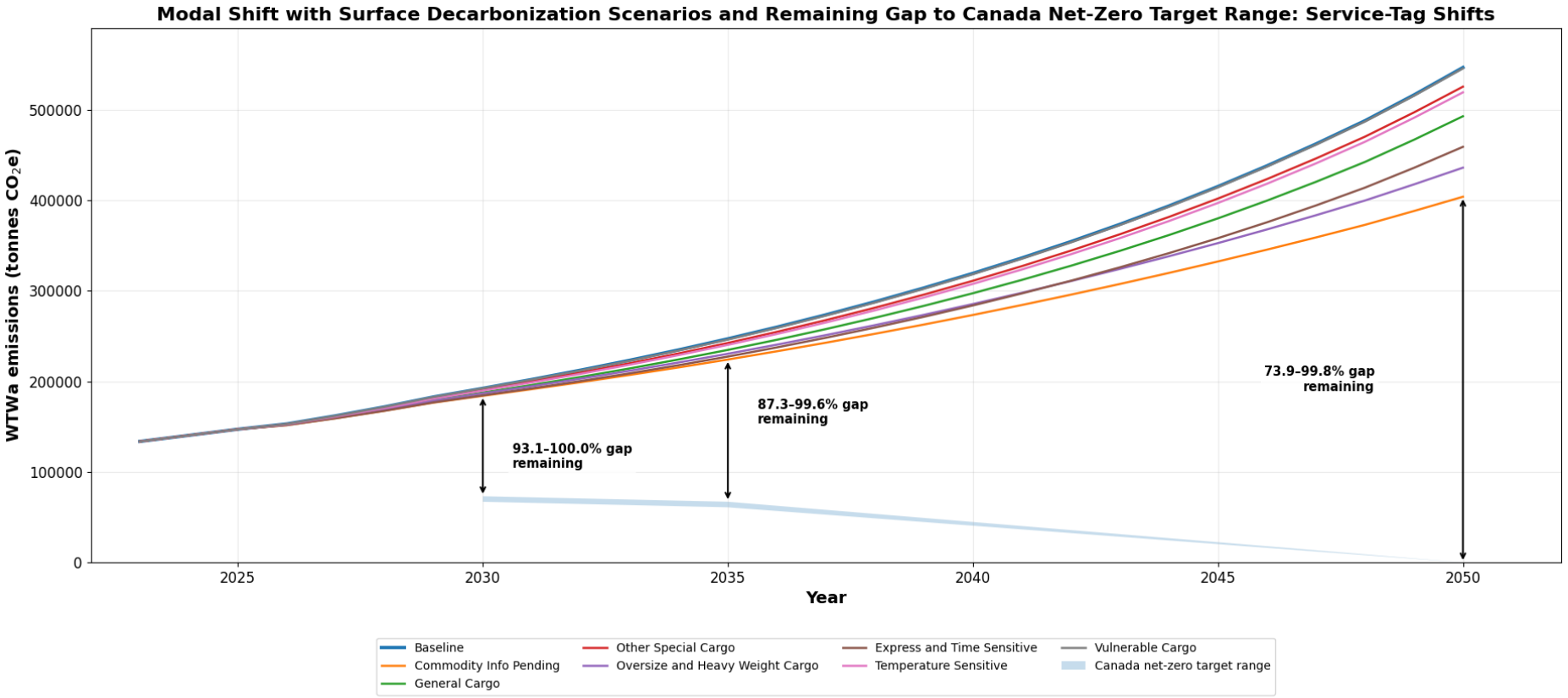


Figure 5-14. Modal Shift with Surface Decarbonization Scenarios and Remaining Gap to Canada Net Zero target range: service-tag shifts

Compared with the modal shift-only results, the overall emissions pathways show only minimal change when surface transportation decarbonization is added. The percentage reductions relative to the baseline and the remaining gaps to the climate target ranges are either unchanged or differ by only about 0.1 percentage points for both commodity-based and service-tag shifts. For example, under the commodity-based Commodity Information Pending shift, 2050 emissions decrease by about 388 tonnes CO_2e when surface transportation decarbonization is included. This represents only about 0.09% of the modal shift-only emissions for that category in 2050, or about 0.07% of the 2050 baseline emissions. This small relative change explains why the surface decarbonization results appear very similar to the modal shift-only results in the figures.

This small difference occurs because the modal shift scenarios shift only selected commodity or service-tag flows, rather than the full air-cargo network. Even the largest shifted categories account for only a portion of total domestic air-cargo activity. In addition, the modal shift-only scenario already captures the major emissions reduction from replacing aviation activity with lower-emission truck or rail transport. Therefore, although surface transportation decarbonization can substantially reduce the emission intensity of trucks and rail relative to conventional diesel technologies, its additional effect is small when measured against the full aviation network. As a result, surface transportation decarbonization slightly improves modal shift outcomes, but it does not substantially alter the overall conclusion that modal shift alone is insufficient to close the remaining gap to deep decarbonization targets.

5.3.3 Illustrative OD-level comparison

Because this thesis is based on an OD-level emissions framework, the modal shift results can also be examined at the corridor level. While the network-level results show the aggregate impact across all domestic air-cargo flows, the OD-level comparison helps isolate the effects of modal shift and surface transportation decarbonization on specific corridors. Even if the network-level reduction is insufficient to reverse the overall upward emissions trend, individual corridors where modal shift is applied can show much larger emissions benefits.

Figure 5-15 shows the OD-level emissions reduction from modal shift scenarios

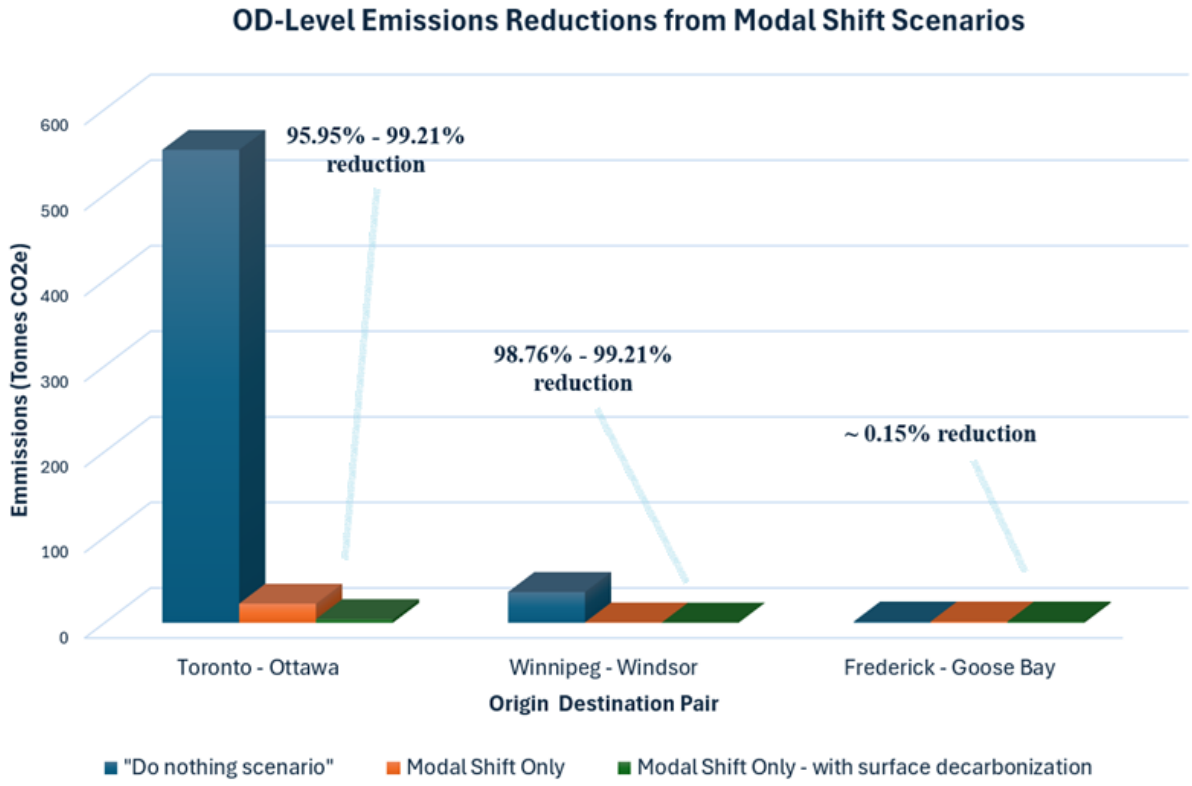


Figure 5-15. OD-Level Emissions Reduction from Modal Shift Scenarios

For the Toronto-Ottawa corridor, shifting air cargo to surface modes reduces emissions by approximately 95.95% to 99.21% relative to the do-nothing scenario. A similarly large reduction is observed for the Winnipeg-Windsor corridor, where emissions decrease by approximately 98.76% to 99.21%. These reductions show that modal shifts can be highly effective on corridors where air cargo can be replaced by truck or rail. In these cases, a substantial reduction occurs even before additional surface transportation decarbonization is applied, because conventional truck and rail technologies are already considerably less emissions-intensive than aviation on a tonne-kilometre basis.

In contrast, the Fredericton-Goose Bay corridor shows only a very small reduction of approximately 0.15%. This is because no rail alternative is available for this OD pair, which limits the potential benefit of modal shift. The small reduction observed is therefore not mainly due to modal substitution, but rather to gradual improvements in the emissions intensity over time, including a cleaner electricity grid and lower-emission hydrogen production.

These OD-level results provide a different perspective from the network-level results. At the corridor level, modal shifts can produce substantial emissions reductions when suitable surface alternatives are available. However, at the network level, the aggregate effect is more limited because many domestic air-cargo flows remain served by aircraft, and the total amount of freight shifted depends strongly on the commodity- or service-based scenario assumptions. Therefore, Figure 5.15 highlights the potential benefits of modal shift on selected corridors, while the broader network-level results show that these benefits do not necessarily translate into a large system-wide reduction unless modal shift is applied to a wider share of domestic air-cargo activity.

5.4 Combined mitigation scenario results

This subsection presents the combined mitigation scenario results, in which the main mitigation strategies examined in this thesis are applied together: sustainable aviation fuel (SAF) adoption, alternative propulsion (AP), and modal shift with surface transportation decarbonization. Unlike the previous subsections, which evaluated each strategy independently, this subsection assesses the overall emissions pathway when multiple mitigation options are implemented simultaneously.

There are many possible combinations of SAF adoption, alternative propulsion, modal shift, and surface transportation decarbonization. However, this subsection focuses on the combined impact of applying all the main strategies. Other strategy combinations, such as SAF adoption with alternative propulsion, SAF adoption with modal shift, and alternative propulsion with modal shift and surface transportation decarbonization, are provided in Appendix V.

Figure 5.16 presents the WTWa emissions pathway for the combined mitigation scenario, where modal shift, surface transportation decarbonization, APs, and SAF adoption are applied together and evaluated against the baseline, the Canada Net Zero-aligned target, and the IPCC 1.5°C-aligned target.

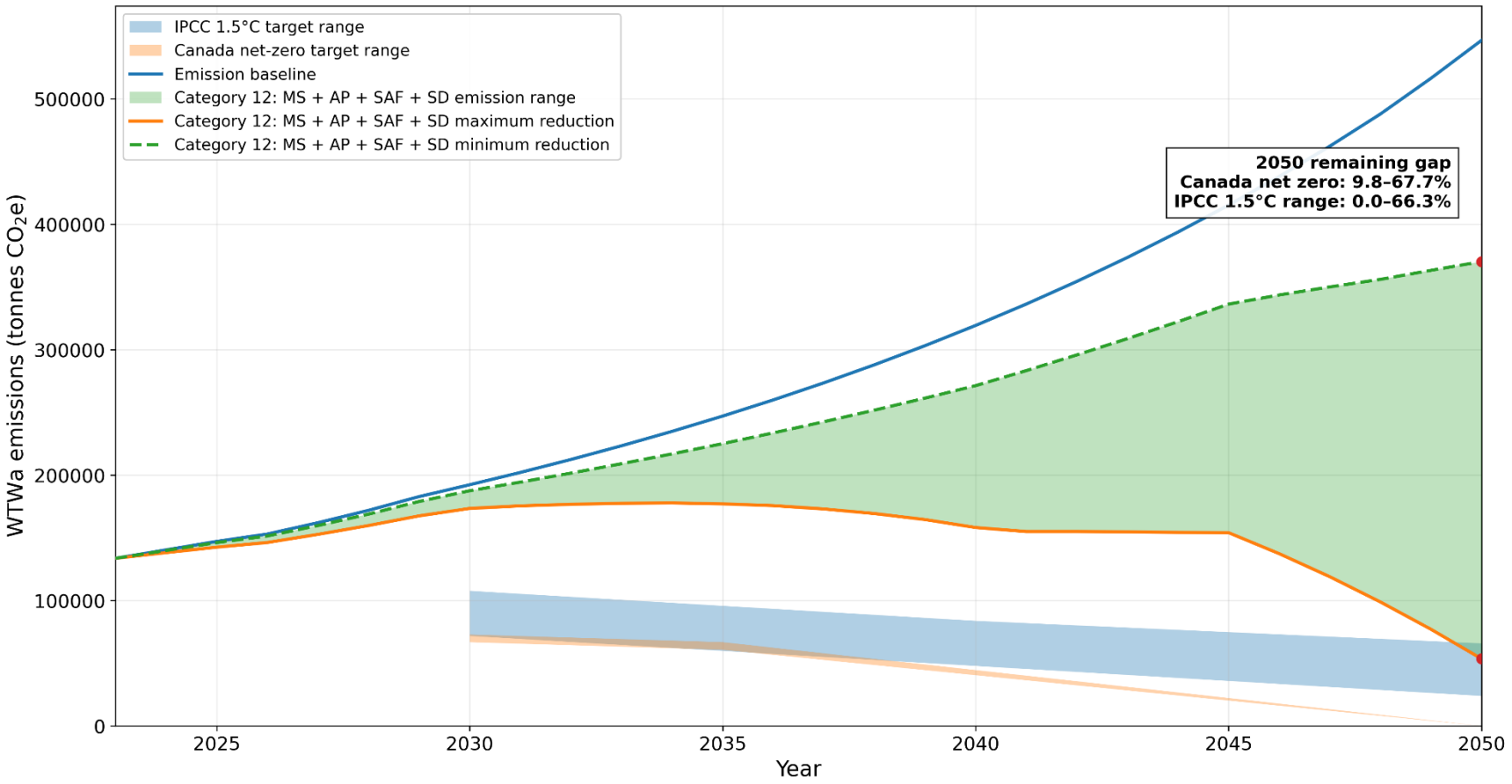


Figure 5-16. Combined Mitigation Scenarios Compared with the IPCC 1.5°C-Aligned and Canada Net-Zero Benchmark Ranges, 2023-2050

The results show that the combined mitigation pathway can substantially reduce emissions relative to the baseline, especially under the maximum mitigation case. However, emissions remain above the climate target in most milestone years, meaning that the combined strategies do not fully close the gap to climate alignment in the near and medium term.

In 2030, the maximum mitigation case reduces emissions by 9.8% relative to the baseline, while the minimum mitigation case reduces emissions by only 2.5%. Despite these reductions, a large share of the climate-target gap remains. For the Net Zero-aligned benchmark, 84.2%-84.9% of the original baseline-to-target gap remains under the maximum case, while 96.0%-96.2% remains under the minimum case. For the IPCC 1.5°C-aligned benchmark, 77.6%-84.3% of the gap remains under the maximum case, and 94.3%-96.0% remains under the minimum case. This shows that the combined strategies have a limited near-term impact because adoption levels remain relatively low in the early years.

The reductions become stronger after 2030. By 2035, the maximum mitigation case reduces emissions by 28.3% relative to the baseline, leaving 61.1%-62.4% of the Net Zero-aligned gap remaining. The minimum case reduces emissions by only 8.9%, leaving 87.8%-88.2% of the gap unresolved. By 2040, the maximum case achieves a 50.5% reduction relative to the baseline, leaving 31.5%-40.6% of the IPCC-aligned gap remaining. In contrast, the minimum case achieves only a 15.0% reduction, leaving 79.6%-82.3% of the IPCC-aligned gap unaddressed.

By 2050, the maximum mitigation case achieves a 90.2% reduction relative to the baseline. This pathway falls within the IPCC 1.5°C-aligned benchmark range, indicating no remaining gap relative to it. However, it still leaves 9.8% of the baseline-to-net-zero gap remaining. The minimum mitigation case achieves a much smaller 32.3% reduction relative to the baseline, leaving 67.7% of the baseline-to-net-zero gap and 63.3%-66.3% of the baseline-to-IPCC gap remaining.

Overall, Figure 5.16 shows that combining the main mitigation strategies can produce significant long-term reductions, but the outcome depends strongly on the level of ambition assumed. The maximum mitigation case should not be interpreted as the most realistic pathway, but rather as an optimistic upper-bound case that illustrates the highest level of emissions reduction achievable under the assumptions tested in this thesis. Under this upper-bound case, the pathway approaches the lower-bound of the IPCC 1.5°C-aligned climate target by 2050, although a remaining gap persists relative to the Canada Net Zero-aligned target. In contrast, the minimum mitigation case represents a more conservative/realistic lower bound and remains far from both the Net Zero and the IPCC 1.5°C-

aligned targets. This suggests that partial or delayed implementation of SAF adoption, AP deployment, modal shift, and surface transportation decarbonization is unlikely to fully align domestic air-cargo emissions with long-term climate targets. Closing the remaining gap would likely require a broader mitigation portfolio, including conventional fleet turnover, operational improvements, infrastructure improvements, and out-of-sector measures to address residual emissions that cannot be eliminated through the strategies modelled in this thesis.

5.5 Summary of key findings

The results indicate that domestic Canadian air-cargo demand and baseline emissions will continue to increase through 2050 without additional mitigation/decarbonization lever. Among the individual strategies evaluated, SAF provides the largest emissions-reduction potential, with 2050 reductions ranging from approximately 30.8% to 86.4% relative to the baseline. Alternative propulsion produces smaller network-level reductions of approximately 3.6% to 7.1% by 2050 but provides meaningful benefits on eligible short- and medium-distance routes. Selective modal shift can also generate corridor-level reductions, particularly where freight can be transferred to truck and rail. Surface-mode decarbonization further improves these outcomes, though its additional emissions-reduction effect is relatively limited at the network level.

Combined mitigation portfolios consistently outperform individual strategies. By 2050, the maximum combined case reduces emissions by approximately 90.2% relative to the baseline, compared with approximately 32.3% under the minimum case. The maximum case approaches the upper bound of the IPCC 1.5°C-aligned climate target but remains above the Canada net-zero benchmark, while the minimum case remains far from both pathways. These results provide the basis for the conclusions, implications, limitations, and recommendations discussed in Chapter 6.

Chapter 6 : Conclusions, Limitations, and Future Research

6.1 Conclusion

This thesis developed a Canada-focused, freight-oriented framework for forecasting domestic air-cargo activity and evaluating well-to-wake emissions-reduction pathways to 2050. The gravity-model forecast indicates that domestic air-cargo demand will continue to grow, with an average annual growth rate of approximately 5.4%. This is broadly consistent with, although slightly higher than, the historical average annual growth rate of approximately 4.5% observed in Statistics Canada's domestic air-cargo data from 2008 to 2023. This comparison provides a reasonableness check on the projected growth trend rather than a direct validation of the forecast.

Among the strategies considered in this thesis, SAF provides the largest emissions-reduction potential over the study period. By 2050, the SAF-only scenarios reduce emissions by approximately 30.8% to 86.4% relative to the baseline. The assumed blending rate has a greater influence on emissions than the composition of the SAF production portfolio, although the deepest reductions require both aggressive blending and a transition from a predominantly single-feedstock pathway toward a more diverse portfolio of lower-carbon production pathways. These high-ambition scenarios should be interpreted cautiously because SAF production capacity, feedstock availability, infrastructure requirements, and supply-chain constraints were not explicitly modelled.

Alternative propulsion produces smaller network-level reductions, particularly in the near and medium term, because battery-electric, hybrid-electric, and hydrogen aircraft are introduced gradually and are restricted to eligible flight distances. By 2050, alternative-propulsion scenarios reduce baseline emissions by approximately 3.6% to 7.1%. Nevertheless, these technologies can produce meaningful reductions on eligible short- and medium-distance corridors and are therefore more effective as complementary long-term measures than as stand-alone pathways.

Selective modal shift can also result in reductions in suitable corridors, particularly when freight can be transferred to rail and truck. Surface-freight decarbonization further improves these outcomes as lower-carbon truck and rail technologies enter the fleet, although its additional effect on the overall modal-shift results is relatively limited at the network level.

The combined-scenario results demonstrate that no single mitigation strategy is sufficient to achieve deep decarbonization of domestic air cargo. Portfolios integrating SAF, alternative propulsion, modal shift, and surface-freight decarbonization obviously outperform individual measures. By 2050, the maximum combined case reduces emissions by approximately 90.2% relative to the baseline, compared with approximately 32.3% under the minimum case. The maximum case approaches the IPCC 1.5°C-aligned benchmark range by 2050 but remains above the Canada net-zero benchmark, while the minimum case remains far from both pathways.

Overall, the study concludes that Canadian domestic air-cargo decarbonization will require a coordinated portfolio rather than reliance on a single technology. SAF is likely to provide the largest near- to medium-term contribution, while alternative propulsion and selective modal shift can provide complementary reductions on suitable routes and corridors. Achieving deeper alignment with climate objectives will likely require additional measures beyond those explicitly modelled, including fleet renewal, infrastructure and operational improvements, demand-management strategies, and out-of-sector emissions reductions or removals.

6.2 Study limitations and future research

The limitations of this study are primarily related to data availability, modelling assumptions, and the scope of the analysis. The framework was designed to compare and evaluate the relative emissions impacts of different domestic air-cargo decarbonization pathways rather than to predict a single most likely future. Accordingly, the results depend on assumptions regarding future freight demand, technology availability, adoption rates, eligible route distances, fuel-production pathways, and surface-mode substitution.

For example, future air-cargo demand is projected using assumed provincial and regional GDP growth, while the relationships estimated from the 2019-2023 CargoIS data are assumed to remain applicable through 2050. The demand model does not capture possible changes in freight rates, fuel prices, trade patterns, e-commerce activity, service frequency, or supply-chain structure. It also does not model endogenous demand responses to mitigation policies. For instance, higher costs associated with SAF, alternative aircraft, or new infrastructure could increase air-freight rates and reduce demand, while government subsidies or other policy support could limit these effects. The analysis does not estimate these price responses, determine who would bear the additional costs, or quantify

the level of public support that may be required. As more detailed data become available, future research could incorporate aircraft-level fleet turnover, probabilistic technology-entry dates, nonlinear adoption curves, and route-specific operational constraints.

The alternative-propulsion scenarios assume specific technology-entry years, estimated aircraft operating ranges, and a seven-year linear penetration period. As discussed in the methodology, the seven-year period is relatively optimistic and represents penetration within eligible distance-based operations rather than complete replacement of the aircraft fleet. Hybrid-electric aircraft are treated as an initial transition technology before battery-electric or hydrogen-powered aircraft progressively assume a larger share of eligible operations. Once the successor technology reaches fully assumed penetration within the applicable distance bin, hybrid-electric aircraft are modelled as being removed from that segment. This phase-out is a simplifying upper-bound assumption used to estimate the maximum potential emissions reductions rather than a prediction of future fleet composition. Actual adoption may be slower, uneven across operators, or influenced by aircraft costs, certification, payload limitations, infrastructure readiness, energy availability, and fleet-retirement schedules. Future research could incorporate aircraft-level fleet turnover, probabilistic technology-entry dates, nonlinear adoption curves, and route-specific operating constraints.

The SAF scenarios assume that sufficient feedstock, production capacity, processing facilities, transportation infrastructure, and low-carbon energy are available to meet the blending levels specified for each milestone year. Although the C-SAF Roadmap identifies potential Canadian SAF facilities and Antony et al. (2024) examine the production potential of canola-based SAF, the available evidence is insufficient to develop a comprehensive national SAF supply forecast through 2050. Therefore, the study estimates the emissions reductions achievable if the assumed blending levels and production portfolios are realized, without assessing whether the required SAF volumes could be supplied domestically or through imports. Future research could develop a national SAF supply model incorporating project-level production plans, feedstock availability, refinery capacity, imports, costs, and regional infrastructure.

The modal-shift analysis applies simplified eligibility rules based on route distance and commodity or service classifications. Shorter eligible routes are assigned to truck, while longer eligible routes are assigned to rail where rail service is available. This approach provides a transparent hypothetical

method for estimating potential emissions reductions, but it does not represent the full decision-making process of shippers and carriers. Actual mode choice also depends on freight rates, shipment size, reliability, delivery windows, transfer requirements, terminal access, service frequency, risk of damage, and the value of travel time. Consequently, some shipments classified as shiftable may remain in air transport, while some shipments excluded from the analysis may be suitable for surface modes. This study does not have access to these factors at the OD-pair level. As more detailed data become available, future research could develop a behavioural freight mode-choice model to estimate the probability of shifting individual shipments rather than assigning modes using fixed eligibility rules.

Surface freight decarbonization is also represented by using simplified technology-adoption assumptions. Truck adoption is estimated using assumed zero-emission vehicle sales and fleet-turnover relationships, while rail adoption follows high-level technology pathways identified by the Rail Pathways Initiative. These assumptions do not explicitly account for vehicle purchase costs, charging or hydrogen refueling infrastructure, operator preferences, or regional operating conditions. Thus, the assumed penetration of lower-carbon surface technologies may occur more rapidly than would be supported by market-driven adoption. Future research could apply a bass diffusion model, discrete-choice model, or more detailed stock-turnover framework to represent technology adoption more realistically. These approaches could distinguish between vehicle classes and account for regional infrastructure availability, total cost of ownership, operational suitability, policy incentives, and uncertainty regarding compliance with zero-emission vehicle sales mandates. An example of this type of market-adoption analysis was conducted by Foda et al. (2026) in their study, Market Potential of Personal and Commercial Zero-Emission Vehicles in Ontario.

Overall, the results should be interpreted as scenario-based estimates of the potential emissions reductions achievable under the stated assumptions, rather than forecasts of future actual deployment. Nevertheless, the study provides a transparent, replicable, and extensible modelling framework that can support future research. As more detailed data become available, the framework can be updated to incorporate improved demand forecasts, technology-adoption models, fuel-supply constraints, economic considerations, and more detailed operational characteristics.

References

Abu Salem, K., Palaia, G., & Quarta, A. A. (2023). Review of hybrid-electric aircraft technologies and designs: Critical analysis and novel solutions. *Progress in Aerospace Sciences, Special Issue on Green Aviation*, *141*, 100924. https://doi.org/10.1016/j.paerosci.2023.100924

ADB. (2011). *Methodology for Impact Assessment of Free Trade Agreements*. ADB.

Adu-Gyamfi, B. A., & Good, C. (2022). Electric aviation: A review of concepts and enabling technologies. *Transportation Engineering*, *9*, 100134. https://doi.org/10.1016/j.treng.2022.100134

Air Charter Service. (n.d.). *Boeing 767-300F*. Retrieved June 16, 2026, from https://www.aircharterservice.com/aircraft-guide/cargo/boeing-usa/boeingb767-300f

Air Inuit. (2026, June 3). *De Havilland Dash-8 Cargo 300*. Air Inuit. https://www.airinuit.com/en/charter/fleet/de-havilland-dash-8-cargo-300

Airbus Aircraft. (2024, July 24). *A330-300P2F | Airbus*. https://www.aircraft.airbus.com/en/aircraft/freighters/a330-300p2f

Airliners. (n.d.). *ATR ATR-42*. Airliners.Net. Retrieved June 16, 2026, from https://www.airliners.net/aircraft-data/atr-atr-42/41?utm_source=google&utm_medium=organic

Airlines Inform. (n.d.). *Airbus A321 commercial aircraft. Pictures, specifications, reviews.* Retrieved June 16, 2026, from https://www.airlines-inform.com/commercial-aircraft/airbus-a321.html

Alexander, D. W., & Merkert, R. (2017). Challenges to domestic air freight in Australia: Evaluating air traffic markets with gravity modelling. *Journal of Air Transport Management, Special Issue on Air Cargo: A By-Product or Success Factor?*, *61*, 41–52. https://doi.org/10.1016/j.jairtraman.2016.11.008

Alexander, D. W., & Merkert, R. (2021). Applications of gravity models to evaluate and forecast US international air freight markets post-GFC. *Transport Policy*, *104*, 52–62. https://doi.org/10.1016/j.tranpol.2020.04.004

Alsayed, A. R. M., & Cameletti, M. (2026). Air demand forecasting for passengers and freight in Italy: A comparison of two statistical models. *Journal of Air Transport Management*, *134*, 102975. https://doi.org/10.1016/j.jairtraman.2026.102975

Alternative Fuels Data Center: Sustainable Aviation Fuel. (n.d.). Retrieved March 3, 2026, from https://afdc.energy.gov/fuels/sustainable-aviation-fuel

Anderson, J. E., & van Wincoop, E. (2003). Gravity with Gravitas: A Solution to the Border Puzzle. *American Economic Review*, *93*(1), 170–192. https://doi.org/10.1257/000282803321455214

Anderson, S., Allen, J., & Browne, M. (2005). Urban logistics—how can it meet policy makers' sustainability objectives? *Journal of Transport Geography, Sustainability and the Interaction Between External Effects of Transport (Part Special Issue, Pp. 23-99)*, *13*(1), 71–81. https://doi.org/10.1016/j.jtrangeo.2004.11.002

Antony, P. S., Vanderghem, C., L. MacLean, H., A. Saville, B., & Daniel Posen, I. (2024). A framework to estimate national biofuel potential by siting production facilities: A case study for canola sustainable aviation fuel in Canada. *Energy Advances*, *3*(7), 1612–1631. https://doi.org/10.1039/D3YA00579H

Arvidsson, R., Nordelöf, A., & Brynolf, S. (2024). Life cycle assessment of a two-seater all-electric aircraft. *The International Journal of Life Cycle Assessment*, *29*(2), 240–254. https://doi.org/10.1007/s11367-023-02244-z

ATAG. (2021). *Waypoint 2050*. https://aviationbenefits.org/media/167417/w2050_v2021_27sept_full.pdf

AXON Aviation Group. (n.d.). *Boeing 777F*. AXON Aviation. Retrieved June 16, 2026, from https://www.axonaviation.com/commercial-aircraft/aircraft-data/boeing-777f

Aydın, U., & Ülengin, B. (2022). Analyzing air cargo flows of Turkish domestic routes: A comparative analysis of gravity models. *Journal of Air Transport Management*, *102*, 102217. https://doi.org/10.1016/j.jairtraman.2022.102217

Baccalá, L. A., & Sameshima, K. (2022). Partial Directed Coherence and the Vector Autoregressive Modelling Myth and a Caveat. *Frontiers in Network Physiology*, *2*. https://doi.org/10.3389/fnetp.2022.845327

BaFail, A. O. (2004). Applying Data Mining Techniques to Forecast Number of Airline Passengers in Saudi Arabia (domestic and International Travels). *Journal of Air Transportation*, *9*(1), 100–115.

Baier, F., Berster, P., & Gelhausen, M. (2022a). Global cargo gravitation model: Airports matter for forecasts. *International Economics and Economic Policy*, *19*(1), 219–238. https://doi.org/10.1007/s10368-021-00525-2

Baier, F., Berster, P., & Gelhausen, M. (2022b). Global cargo gravitation model: Airports matter for forecasts. *International Economics and Economic Policy*, *19*(1), 219–238. https://doi.org/10.1007/s10368-021-00525-2

Baier, S. L., & Bergstrand, J. H. (2007). Do free trade agreements actually increase members' international trade? *Journal of International Economics*, *71*(1), 72–95. https://doi.org/10.1016/j.jinteco.2006.02.005

Barbosa, F. C. (2022). *Battery Electric Rail Technology Review—A Technical and Operational Assessment. Current Status, Challenges and Perspectives*. ASME/IEEE Joint Rail Conference. https://doi.org/10.1115/JRC2022-78133

Barkova, L., Cléophat, R., Creighton, M., Kho, A., Laurin, M., Matier, C., Nahornick, N., Nicol, C., & Stanton, J. (2024). Fiscal Sustainability Report 2024. In *Office of the Parliamentary Budget Officer*. Office of the Parliamentary Budget Officer. https://www.pbo-dpb.ca/en/publications/RP-2425-014-S--fiscal-sustainability-report-2024--rapport-viabilite-financiere-2024

Barros Pintos, P., Ulloa Sande, C., & Castro Álvarez, Ó. (2023). Sustainable propulsion alternatives in regional aviation: The case of the Canary Islands. *Transportation Research Part D: Transport and Environment*, *120*, 103779. https://doi.org/10.1016/j.trd.2023.103779

Bauen, A., Bitossi, N., German, L., Harris, A., & Leow, K. (2020). Sustainable aviation fuels status, challenges and prospects of drop-in liquid fuels, hydrogen and electrification in aviation. *Johnson Matthey Technology Review*, *64*(3), 263–278. https://doi.org/10.1595/205651320x15816756012040

Beil, D., Putz-Egger, L.-M., & Dopler, S. (2025a). Freight mode choices for eco-friendly transport modes: An impact-analysis of modal shift measures. *Transportation Research Procedia, World Conference on Transport Research - WCTR 2023 Montreal 17-21 July 2023*, *82*, 1004–1022. https://doi.org/10.1016/j.trpro.2024.12.108

Beil, D., Putz-Egger, L.-M., & Dopler, S. (2025b). Freight mode choices for eco-friendly transport modes: An impact-analysis of modal shift measures. *Transportation Research Procedia, World Conference on Transport Research - WCTR 2023 Montreal 17-21 July 2023*, *82*, 1004–1022. https://doi.org/10.1016/j.trpro.2024.12.108

Bentéjac, C., Csörgő, A., & Martínez-Muñoz, G. (2021). A comparative analysis of gradient boosting algorithms. *Artificial Intelligence Review*, *54*(3), 1937–1967. https://doi.org/10.1007/s10462-020-09896-5

Bentley, A., Jonas, G., & Geoff, T. (2023). The C-SAF Roadmap Building a feedstocks-to-fuels SAF supply chain in Canada. *Canadian Council for Sustainable Aviation Fuels*. https://transitionaccelerator.ca/wp-content/uploads/2023/07/CSAF_Roadmap_Full_Report_Digital-1.pdf

Bhardwaj, C. (2026). *Planning to charge: Electric truck charging infrastructure and electricity demand in the GTHA*. https://www.pembina.org/sites/default/files/2026-01/Planning_to_Charge.pdf

Björk, L., Vierth, I., & Cullinane, K. (2023). Freight modal shift: A means or an objective in achieving lower emission targets? The case of Sweden. *Transport Policy*, *142*, 125–136. https://doi.org/10.1016/j.tranpol.2023.08.013

Blauwens, G., Vandaele, N., Van De Voorde, E., Vernimmen, B., & Witlox, F. (2006). Towards a Modal Shift in Freight Transport? A Business Logistics Analysis of Some Policy Measures. *Transport Reviews*, *26*(2), 239–251. https://doi.org/10.1080/01441640500335565

Bombardier. (n.d.). *CRJ specifications*. https://web.archive.org/web/20220131032627/https://www2.bombardier.com/Used_Aircraft/en/CRJ_Specifications.jsp.

Booto, G. K., Aamodt Espegren, K., & Hancke, R. (2021). Comparative life cycle assessment of heavy-duty drivetrains: A Norwegian study case. *Transportation Research Part D: Transport and Environment*, *95*, 102836. https://doi.org/10.1016/j.trd.2021.102836

Borrill, E., Koh, S. C. L., & Yuan, R. (2024). Review of technological developments and LCA applications on biobased SAF conversion processes. *Frontiers in Fuels*, *2*. https://doi.org/10.3389/ffuel.2024.1397962

Box, G. E. P., Gwilym, J. M., Gregory, R. C., & Greta, L. (2016). *Time Series Analysis—Forecasting and Control (fifth edition)*. https://repo.darmajaya.ac.id/4781/1/Time%20Series%20Analysis_%20Forecasting%20and%20Control%20%28%20PDFDrive%20%29.pdf

Breiman, L. (2001). Random Forests. *Machine Learning*, *45*(1), 5–32. https://doi.org/10.1023/A:1010933404324

Brelje, B. J., & Martins, J. R. R. A. (2019). Electric, hybrid, and turboelectric fixed-wing aircraft: A review of concepts, models, and design approaches. *Progress in Aerospace Sciences*, *104*, 1–19. https://doi.org/10.1016/j.paerosci.2018.06.004

British Columbia. Ministry of Finance. (2025, September 15). *First Quarterly Report 2025/26* [Quarterly report (Fiscal Plan Update / Financial Forecast)]. Government of British Columbia. https://www2.gov.bc.ca/assets/gov/british-columbians-our-governments/government-finances/quarterly-reports/2025-26_first_quarterly_sept_2025_web_secured_f9e4ab62-584b-4902-b450-b924182d7fb8.pdf

Bruno, F., Maghrour Zefreh, M., Fröidh, O., & Cats, O. (2025). Replacing short-haul flights with train travel: Exploring impacts, capacity requirements and policy implications. *Transport Policy*, *171*, 326–343. https://doi.org/10.1016/j.tranpol.2025.05.031

Cabrera, E., & Sousa, J. M. M. de. (2022). Use of Sustainable Fuels in Aviation—A Review. *Energies*, *15*(7). https://doi.org/10.3390/en15072440

Cabrera-Jiménez, R., Mateo, J. M., Jiménez, L., & Pozo, C. (2025). Prospective life-cycle assessment of sustainable alternatives for road freight transport. *Renewable and Sustainable Energy Reviews*, *211*, 115243. https://doi.org/10.1016/j.rser.2024.115243

Canada. (2026). *Environment and Climate Change Canada, National Inventory Report* [National inventory document (NID)]. https://unfccc.int/documents/656424

Canada, S. (2022, June 22). *Canada's 2030 Emissions Reduction Plan—Overview*. https://www.canada.ca/en/services/environment/weather/climatechange/climate-plan/climate-plan-overview/emissions-reduction-2030/plan/overview.html

Çatuk, C. (2025). Forecasting Turkey's Air Cargo Tonnage: A Comparative Analysis of Statistical Techniques and Machine Learning Methods. *Journal of Aviation*, *9*(1), 109–117. https://doi.org/10.30518/jav.1582814

Centobelli, P., Cerchione, R., & Esposito, E. (2017). Environmental sustainability in the service industry of transportation and logistics service providers: Systematic literature review and research directions. *Transportation Research Part D: Transport and Environment*, *53*, 454–470. https://doi.org/10.1016/j.trd.2017.04.032

Cessna. (2011, March). *Skyhawk Model 172R -Specification & Description*. Cessna Aircraft Company.

Charles, L., Larry, H., Jonathon, R., & Lee, K. (2016). *Parallel Hybrid Gas-Electric Geared Turbofan Engine Conceptual Design and Benefits Analysis*. AIAA Propulsion and Energy Forum. https://arc.aiaa.org/doi/10.2514/6.2016-4610

Chatfield, C. (2000). *Time-Series Forecasting*. Chapman and Hall/CRC. https://doi.org/10.1201/9781420036206

Chen, P. H., Lee, U., Liu, X., Cai, H., & Wang, M. (2024). Life-cycle analysis of sustainable aviation fuel production through catalytic hydrothermolysis. *Biofuels, Bioproducts and Biorefining*, *18*(1), 42–54. https://doi.org/10.1002/bbb.2574

Chen, S.-C., Kuo, S.-Y., Chang, K.-W., & Wang, Y.-T. (2012). Improving the forecasting accuracy of air passenger and air cargo demand: The application of back-propagation neural networks. *Transportation Planning and Technology*, *35*(3), 373–392. https://doi.org/10.1080/03081060.2012.673272

City Population. (n.d.-a). *City Population—Help & Information*. Retrieved January 14, 2026, from https://www.citypopulation.de/en/help/

City Population. (n.d.-b). *City Population—Population Statistics in Maps and Charts for Cities, Agglomerations and Administrative Divisions of all Countries of the World*. Retrieved January 14, 2026, from https://www.citypopulation.de/

Dahl, G., & Suttrop, F. (1998). *ENGINE CONTROL AND LOW-NO, COMBUSTION FOR HYDROGEN FUELLED AIRCRAFT GAS TURBINES*. *23*(8), 695–704.

Data Sources—FlightAware. (n.d.). Retrieved January 15, 2026, from https://www.flightaware.com/about/data-sources/

Day, G. (1994). The Capabilities of Market-Driven Organizations on JSTOR. In *Closing the Marketing Capabilities Gap* (Vol. 75, pp. 183–195). https://www.jstor.org/stable/1251915?seq=1 (Original work published SAGE Publications, Inc)

De Havilland Canada. (2021, July 15). De Havilland Canada Working with Pratt & Whitney Canada to Support the Development of Sustainable Hybrid-Electric Aircraft Propulsion Technology. *De Havilland Canada*. https://dehavilland.com/corporate-initiatives/de-havilland-canada-working-with-pratt-whitney-canada-to-support-the-development-of-sustainable-hybrid-electric-aircraft-propulsion-technology/

De Jong, G., Kouwenhoven, M., Bates, J., Koster, P., Verhoef, E., Tavasszy, L., & Warffemius, P. (2014). New SP-values of time and reliability for freight transport in the Netherlands. *Transportation Research Part E: Logistics and Transportation Review*, *64*, 71–87. https://doi.org/10.1016/j.tre.2014.01.008

Department of Finance Canada. (2025, March 22). *Removing the consumer carbon price, effective April 1, 2025* [Backgrounder]. https://www.canada.ca/en/department-finance/news/2025/03/removing-the-consumer-carbon-price-effective-april-1-2025.html

Deuber, R. de S., Bressanin, J. M., Fernandes, D. S., Guimarães, H. R., Chagas, M. F., Bonomi, A., Fregolente, L. V., & Watanabe, M. D. B. (2023). Production of Sustainable Aviation Fuels from Lignocellulosic Residues in Brazil through Hydrothermal Liquefaction: Techno-Economic and Environmental Assessments. *Energies*, *16*(6). https://doi.org/10.3390/en16062723

Drone Delivery Canada. (n.d.). Retrieved April 30, 2026, from https://dronedeliverycanada.com/

Drucker, H., Burges, C. J. C., Kaufman, L., Smola, A., & Vapnik, V. (1996). Support Vector Regression Machines. *Advances in Neural Information Processing Systems*, *9*. https://proceedings.neurips.cc/paper_files/paper/1996/hash/d38901788c533e8286cb6400b40b386d-Abstract.html

Düker, M.-C., Matteson, D., Tsay, R., & Wilms, I. (2025). Vector AutoRegressive Moving Average Models: A Review. *WIREs Computational Statistics*, *17*(1). https://doi.org/https://doi.org/10.1002/wics.70009

Durbin, J., & Koopman, S. J. (2012). *Time Series Analysis by State Space Methods*. Oxford University Press. https://doi.org/10.1093/acprof:oso/9780199641178.001.0001

Economou, J. T., Tsourdos, A., & Wang, S. (2019). Design of a Distributed Hybrid Electric Propulsion System for a Light Aircraft based on genetic algorithm. In *AIAA Propulsion and Energy 2019 Forum*. American Institute of Aeronautics and Astronautics. https://doi.org/10.2514/6.2019-4305

Eelco, B., Sanne, A., Florian, K., & Johannes, P. (2013). *Zero emissions trucks*. https://theicct.org/wp-content/uploads/2021/06/CE_Delft_4841_Zero_emissions_trucks_Def.pdf

El-Adawy, M., Hamdy, M., Khedr, A. M., Ismael, M. A., Elserfy, K., Moral, A., & Nemitallah, M. A. (2025). Hydrogen-Powered Aviation: Status and Perspectives. *Energy & Fuels*, *39*(24), 11469–11503. https://doi.org/10.1021/acs.energyfuels.5c01319

Elshehawy, M. A., Shen, H., & Ahmed, R. A. (2014). The Factors Affecting Egypt's Exports: Evidence from the Gravity Model Analysis. *Open Journal of Social Sciences*, *2*(11), 138–148. https://doi.org/10.4236/jss.2014.211020

Emami Javanmard, M., Tang, Y., & Martínez-Hernández, J. A. (2024). Forecasting air transportation demand and its impacts on energy consumption and emission. *Applied Energy*, *364*, 123031. https://doi.org/10.1016/j.apenergy.2024.123031

Eng-Larsson, F., & Kohn, C. (2012). Modal shift for greener logistics – the shipper's perspective. *International Journal of Physical Distribution & Logistics Management*, *42*(1), 36–59. https://doi.org/10.1108/09600031211202463

Engle, R., & Granger, C. (1987). *Co-Integration and Error Correction: Representation, Estimation, and Testing*. *55*(2), 251–276. https://doi.org/https://doi.org/10.2307/1913236

Environment and Climate Change Canada. (2021). *National Inventory Report 1990–2019: Greenhouse Gas Sources and Sinks in Canada*. Government of Canada. https://publications.gc.ca/collections/collection_2021/eccc/En81-4-2019-1-eng.pdf

Epstein, A. H., & O'Flarity, S. M. (2019). Considerations for Reducing Aviation's CO2 with Aircraft Electric Propulsion. *Journal of Propulsion and Power*, *35*(3), 572–582. https://doi.org/10.2514/1.B37015

EUROCONTROL Air Transport Association. (2022). *EUROCONTROL – Aviation Outlook 2050*. https://www.eurocontrol.int/sites/default/files/2022-04/eurocontrol-aviation-outlook-2050-main-report.pdf

European Union. (2023). *REGULATION (EU) 2023/2405 OF THE EUROPEAN PARLIAMENT AND OF THE COUNCIL*. https://eur-lex.europa.eu/eli/reg/2023/2405/2023-10-31/eng

Evon, R. B., Weyand, J., Juschus, D., Schröder, M., Gentner, C., Dietrich, R.-U., & Ansar, S. A. (2026). Life cycle assessment of hydrogen-powered fuel cell system for regional aviation—Methodology development and preliminary results. *International Journal of Hydrogen Energy*, *202*, 152527. https://doi.org/10.1016/j.ijhydene.2025.152527

Fernández, F. J., & Harvey, A. C. (1990). Seemingly Unrelated Time Series Equations and a Test for Homogeneity. *Journal of Business & Economic Statistics*, *8*(1), 71–81. https://doi.org/10.1080/07350015.1990.10509778

Flugzeuginfo. (n.d.). *Boeing 777 Freighter (777F)—Specifications—Technical Data / Description*. Retrieved June 16, 2026, from https://www.flugzeuginfo.net/acdata_php/acdata_boeing_777f_en.php

Foda, A., Shehabeldeen, A., & Mohamed, M. (2026). *Market Potential of Personal and Commercial Zero-Emission Vehicles in Ontario*. Canadian Transportation Research Forum.

Fox, E. B., Liu, Z.-W., & Liu, Z.-T. (2013). Ultraclean Fuels Production and Utilization for the Twenty-First Century: Advances toward Sustainable Transportation Fuels. *Energy & Fuels*, *27*(11), 6335–6338. https://doi.org/10.1021/ef401094t

Fries, H. (2009). *Market potential and value of sustainable freight transport chains*. ETH Zürich.

Funke, H. H.-W., Beckmann, N., Keinz, J., & Horikawa, A. (2021). 30 Years of Dry-Low-NOx Micromix Combustor Research for Hydrogen-Rich Fuels—An Overview of Past and Present Activities. *Journal of Engineering for Gas Turbines and Power*, *143*(071002). https://doi.org/10.1115/1.4049764

Garrido, C., De Oña, R., & De Oña, J. (2014). Neural networks for analyzing service quality in public transportation. *Expert Systems with Applications*, *41*(15), 6830–6838. https://doi.org/10.1016/j.eswa.2014.04.045

Gary Grim, R., Ravikumar, D., D. Tan, E. C., Huang, Z., R. Ferrell, J., Resch, M., Li, Z., Mevawala, C., D. Phillips, S., Snowden-Swan, L., Tao, L., & A. Schaidle, J. (2022). Electrifying the production of sustainable aviation fuel: The risks, economics, and environmental benefits of emerging pathways including CO 2. *Energy & Environmental Science*, *15*(11), 4798–4812. https://doi.org/10.1039/D2EE02439J

Gaspari, F., Trainelli, L., Rolando, A., & Perkon, I. (2017). *Concept of modular architecture for hybrid electric propulsion of aircraft*.

Gladstein, N., & Associates. (2020). *Sustainable aviation fuel: Greenhouse gas reductions from Bay Area commercial aircraft*. Bay Area Air Quality Management District. https://www.baaqmd.gov/~/media/files/planning-and-research/research-and-modeling/saf-report-final-for-distribution-to-baaqmd-pdf.pdf?la=en

Glenn, B., & Panarat. (2018a). THE USE OF AN ARTIFICIAL NEURAL NETWORK TO PREDICT AUSTRALIA'S EXPORT AIR CARGO DEMAND. *INTERNATIONAL JOURNAL FOR TRAFFIC AND TRANSPORT ENGINEERING*, *8*(1), 15–30. https://doi.org/10.7708/ijtte.2018.8(1).02

Glenn, B., & Panarat, S. (2018b). THE USE OF AN ARTIFICIAL NEURAL NETWORK TO PREDICT AUSTRALIA'S EXPORT AIR CARGO DEMAND. *INTERNATIONAL JOURNAL FOR TRAFFIC AND TRANSPORT ENGINEERING*, *8*(1), 15–30. https://doi.org/10.7708/ijtte.2018.8(1).02

Gong, Q., Wang, K., Fan, X., & Fu, X. (2014). *Why Chinese airlines haven't become leading cargo carriers—Analyzing air freight network and international trade drivers for mainland China*. https://ses.library.usyd.edu.au/handle/2123/19255

Government of Alberta. (2025, February 27). *2025-28 Fiscal Plan, Strategic Plan and Ministry Business Plans, Budget Highlights and Budget Addres* [Budget (Fiscal Plan / Business Plans)]. Government of Alberta. https://open.alberta.ca/dataset/5ebd05dc-d598-440b-9da2-25f37cd99a49/resource/43bccd72-36fa-41a4-becd-cb8c28da9683/download/budget-2025-fiscal-plan-2025-28.pdf

Government of British Columbia. (2022). *Low Carbon Fuels Act*. King's Printer. BC Laws. https://www.bclaws.gov.bc.ca/civix/document/id/complete/statreg/22021

Government of Canada. (2023, April 17). *Types of zero-emission vehicles*. https://natural-resources.canada.ca/energy-efficiency/transportation-energy-efficiency/zero-emission-vehicles/types-zero-emission-vehicles

Government of Canada. (2024a, September 3). *Net-zero emissions by 2050*. Canada.Ca. https://www.canada.ca/en/services/environment/weather/climatechange/climate-plan/net-zero-emissions-2050.html

Government of Canada. (2024b, September 30). *Clean Fuel Regulations, SOR/2022-140*. Department of Justice Canada. Justice Laws Website. https://laws-lois.justice.gc.ca/eng/regulations/sor-2022-140/FullText.html

Government of Canada. (2026a). *Canadian Aviation Regulations (SOR/96-433)*. AARBH. AARBH 14882767. https://laws-lois.justice.gc.ca/eng/regulations/SOR-96-433/

Government of Canada, S. C. (2011). *Geography*. https://www150.statcan.gc.ca/n1/pub/11-402-x/2011000/chap/geo/geo-eng.htm

Government of Canada, S. C. (2024c, June 7). *Gross domestic product, 2023: An in-depth look at provincial and territorial economies*. https://www150.statcan.gc.ca/n1/pub/11-621-m/11-621-m2024004-eng.htm

Government of Canada, S. C. (2025a). *Air passenger traffic at Canadian airports, annual*. https://www150.statcan.gc.ca/t1/tbl1/en/tv.action?pid=2310025301

Government of Canada, S. C. (2025b). *Gross domestic product (GDP) at basic prices, by census metropolitan area (CMA)*. https://www150.statcan.gc.ca/t1/tbl1/en/tv.action?pid=3610046801

Government of Canada, S. C. (2025c). *Population estimates, quarterly*. https://www150.statcan.gc.ca/t1/tbl1/en/tv.action?pid=1710000901

Government of Canada, S. C. (2025d, November 6). *Gross domestic product (GDP) at basic prices, by industry, provinces and territories, growth rates*. https://www150.statcan.gc.ca/t1/tbl1/en/tv.action?pid=3610071102

Government of Canada, S. C. (2026b). *Population estimates, July 1, by census metropolitan area and census agglomeration, 2021 boundaries*. https://www150.statcan.gc.ca/t1/tbl1/en/tv.action?pid=1710014801

Government of Saskatchewan. (2025, November 25). *2025-26 Mid-Year Report* [Mid-year report (fiscal update)]. Government of Saskatchewan. https://www.saskatchewan.ca/-/media/news-release-backgrounders/2025/nov/2025-26-mid-year-report---final.pdf

Government of the Northwest Territories (NWT Finance). (2025, February 6). *Economic Review 2025-2026* [Economic review]. Government of the Northwest Territories. https://www.fin.gov.nt.ca/sites/fin/files/resources/2025-26_budget_economic_review.pdf

GraphHopper Directions API. (n.d.). Retrieved January 15, 2026, from https://docs.graphhopper.com/openapi

Grimme, W. (2023a). The Introduction of Sustainable Aviation Fuels—A Discussion of Challenges, Options and Alternatives. *Aerospace*, *10*(3). https://doi.org/10.3390/aerospace10030218

Grimme, W. (2023b). The Introduction of Sustainable Aviation Fuels—A Discussion of Challenges, Options and Alternatives. *Aerospace*, *10*(3). https://doi.org/10.3390/aerospace10030218

Grue, B., & Ludvigsen, J. (2006). *Decision factors underlying transport mode choice in international European freight transport*. European Transport Conference.

Gudmundsson, S. V., Cattaneo, M., & Redondi, R. (2021). Forecasting temporal world recovery in air transport markets in the presence of large economic shocks: The case of COVID-19. *Journal of Air Transport Management*, *91*, 102007. https://doi.org/10.1016/j.jairtraman.2020.102007

Gupta, D., & Dhar, S. (2022). Exploring the freight transportation transitions for mitigation and development pathways of India. *Transport Policy*, *129*, 156–175. https://doi.org/10.1016/j.tranpol.2022.10.013

Harbour Air. (2025). In *Wikipedia*. https://en.wikipedia.org/w/index.php?title=Harbour_Air&oldid=1320784402#cite_note-28

Harvey, A., & Koopman, S. J. (2014). Structural Time Series Models. In *Wiley StatsRef: Statistics Reference Online*. John Wiley & Sons, Ltd. https://doi.org/10.1002/9781118445112.stat05808

Head, K., & Mayer, T. (2014). Gravity Equations: Workhorse,Toolkit, and Cookbook. In *Handbook of International Economics* (Vol. 4, pp. 131–195). Elsevier. https://doi.org/10.1016/B978-0-444-54314-1.00003-3

Helijet. (2025, November 4). Helijet Hosts BETA Technologies' First All-Electric Passenger Demonstration Flight In Western Canada. *Helijet.Com*. https://helijet.com/helijet-hosts-beta-technologies-first-all-electric-passenger-demonstration-flight-in-western-canada/

Hollanda, D. L. D. R., & Miranda, P. E. V. de. (2024). New analysis strategy for hydrail freight locomotives: Case study and replication. *International Journal of Hydrogen Energy*, *53*, 1149–1154. https://doi.org/10.1016/j.ijhydene.2023.12.124

Hong Tsui, K. W., Wang, H., & Liu, Y. (2025). Gravity models of airfreight exports during the pre-COVID era: Evidence from New Zealand. *Case Studies on Transport Policy*, *19*, 101336. https://doi.org/10.1016/j.cstp.2024.101336

Horizon Aircraft. (n.d.). *A hybrid that aims higher.* Horizon Aircraft. Retrieved April 30, 2026, from https://www.horizonaircraft.com/

Hu, Y.-J., Yang, L., Cui, H., Wang, H., Li, C., & Tang, B.-J. (2022). Strategies to Mitigate Carbon Emissions for Sustainable Aviation: A Critical Review From a Life-cycle Perspective. *Sustainable Production and Consumption*, *33*, 788–808. https://doi.org/10.1016/j.spc.2022.08.009

Huang, T.-Y., Masum, F. H., Jiang, Y., Li, S., Curran, S. J., Biruduganti, M. S., & Hawkins, T. R. (2025). Techno-Economic Analysis and Life Cycle Assessment of Alternative Fuels for Locomotives in the U.S. Freight Rail Sector. *Environmental Science & Technology*, *59*(30), 15741–15750. https://doi.org/10.1021/acs.est.4c11029

Hussain, M. M., & Alidrisi, M. (2025). Forecasting Air Cargo Demand of Saudia Cargo Company. *ISSN*, *9*(1).

Hwang, C.-C., & Shiao, G.-C. (2011). Analyzing air cargo flows of international routes: An empirical study of Taiwan Taoyuan International Airport. *Journal of Transport Geography*, *19*(4), 738–744. https://doi.org/10.1016/j.jtrangeo.2010.09.001

IATA. (2024). *Disappointingly Slow Growth in SAF Production*. https://www.iata.org/en/pressroom/2024-releases/2024-12-10-03/

ICAO. (n.d.). *SAF Conversion processes*. Retrieved April 16, 2026, from https://www.icao.int/SAF/saf-conversion-processes

ICAO. (2022). *Long-Term Aspirational Goal*. https://www.icao.int/sites/default/files/environmental-protection/Documents/EnvironmentalReports/2022/ENVReport2022_Special-Supplement-on-LTAG.pdf

IMARC. (n.d.). *Canada Air Freight Market Size, Share, Trends and Forecast by Service, Destination, End-User, and Region, 2025-2033*. Retrieved January 24, 2026, from https://www.imarcgroup.com/canada-air-freight-market

International Air Transport Association. (n.d.-a). *Cargo CO2 Emissions Measurement*. Retrieved January 20, 2026, from https://www.iata.org/en/programs/cargo/sustainability/carbon-footprint/

International Air Transport Association. (n.d.-b). *CargoIS*. Retrieved January 14, 2026, from https://www.iata.org/en/services/data/cargo/cargois/

International Air Transport Association. (n.d.-c). *CargoIS Data Unleashed: The Data Behind US$32 Billion Worth of Air Freight Charges*. IATA. Retrieved https://www.iata.org/en/services/data/cargo/cargois/cargois-guide-with-data-samples/

International Air Transport Association. (2019). *The Value of Air Transport to Canada*. https://www.iata.org/en/iata-repository/publications/economic-reports/the-value-of-air-transport-to-canada

IPCC. (2023). *Climate Change 2023: Synthesis Report. Contribution of Working Groups I, II and III to the Sixth Assessment Report of the Intergovernmental Panel on Climate Change*. IPCC. https://doi.org/10.59327/IPCC/AR6-9789291691647

Jahangir Samet, M., Liimatainen, H., & van Vliet, O. P. R. (2023). GHG emission reduction potential of road freight transport by using battery electric trucks in Finland and Switzerland. *Applied Energy*, *347*, 121361. https://doi.org/10.1016/j.apenergy.2023.121361

Kapetanović, M., Núñez, A., van Oort, N., & Goverde, R. M. P. (2024). Energy use and greenhouse gas emissions of traction alternatives for regional railways. *Energy Conversion and Management*, *303*, 118202. https://doi.org/10.1016/j.enconman.2024.118202

Kaya, G., Aydın, U., & Ülengin, B. (2023). A Comparison of Forecasting Performance of PPML and OLS estimators: The Gravity Model in the Air Cargo Market. *EKOIST Journal of Econometrics and Statistics*, *0*(39), 112–128.

Kennes, D., Abubackar, H. N., Diaz, M., Veiga, M. C., & Kennes, C. (2016). Bioethanol production from biomass: Carbohydrate vs syngas fermentation. *Journal of Chemical Technology & Biotechnology*, *91*(2), 304–317. https://doi.org/10.1002/jctb.4842

Kenneth, S. (2024, July 4). Out From the Shadows: EVIO's hybrid-electric aircraft plan. *Skies Mag*. https://skiesmag.com/features/out-from-the-shadows-evios-hybrid-electric-aircraft-plan/

Kerr, W. A., & Gaisford, J. D. (2007). *Handbook on International Trade Policy*. Edward Elgar Publishing.

Kim, H. C. (2014). *Developing a mode choice model for New Zealand freight transportation.* http://hdl.handle.net/10092/10031

Kim, H. K., & Lee, C. W. (2019). Development of a Cost Forecasting Model for Air Cargo Service Delay Due to Low Visibility. *Sustainability*, *11*(16). https://doi.org/10.3390/su11164390

Klimczyk, W., Jasiński, R., Niklas, J., Siedlecki, M., & Ziółkowski, A. (2025). Sustainable Aviation Fuels: A Comprehensive Review of Production Pathways, Environmental Impacts, Lifecycle Assessment, and Certification Frameworks. *Energies*, *18*(14). https://doi.org/10.3390/en18143705

KLRI. (2018). *SUSTAINABLE TRANSPORTATION LOGISTICS DEVELOPMENT ACT*. Korean Legislation Research Institute. https://elaw.klri.re.kr/eng_service/lawView.do?hseq=51298&lang=ENG

Klug, H. G., & Faass, R. (2001). CRYOPLANE: Hydrogen fuelled aircraft -status and challenges. *Air & Space Europe*, *3*(3), 252–254. https://doi.org/10.1016/S1290-0958(01)90110-8

Knibbe, R., Harding, D., Cooper, E., Burton, J., Liu, S., Amirzadeh, Z., Buckley, R., & Meehan, P. A. (2022). Application and limitations of batteries and hydrogen in heavy haul rail using Australian case studies. *Journal of Energy Storage*, *56*, 105813. https://doi.org/10.1016/j.est.2022.105813

Kock, A. B., & Teräsvirta, T. (2011). Forecasting With Nonlinear Time Series Models. In M. P. Clements & D. F. Hendry (Eds.), *The Oxford Handbook of Economic Forecasting* (p. 0). Oxford University Press. https://doi.org/10.1093/oxfordhb/9780195398649.013.0004

Konstantinus, A., & Mark, Z. (2018). *Freight transport decisions and their considerations in the Southern African Development Community (SADC)*. VREF Urban Freight Conference, Gothernburg.

Kossarev, K., Scholz, A. E., & Hornung, M. (2023). Comparative environmental life cycle assessment and operating cost analysis of long-range hydrogen and biofuel fueled transport aircraft. *CEAS Aeronautical Journal*, *14*(1), 3–28. https://doi.org/10.1007/s13272-022-00627-w

Kowalska, S., & Bonk, D. (2021). Evaluation of Modal Shift in Freight Transport: Case Study of Poland. *European Research Studies*, *XXIV*(3-Part 2), 851–862.

Kramer, S., Andac, G., Heyne, J., Ellsworth, J., Herzig, P., & Lewis, K. C. (2022). Perspectives on Fully Synthesized Sustainable Aviation Fuels: Direction and Opportunities. *Frontiers in Energy Research*, *9*. https://doi.org/10.3389/fenrg.2021.782823

Kreutzberger, E. D. (2003). Impact of Innovative Technical Concepts for Load Unit Exchange on the Design of Intermodal Freight Networks. *Transportation Research Record*, *1820*(1), 1–10. https://doi.org/10.3141/1820-01

Kunst, R. (2012). *Econometric Forecasting*. University of Vienna. https://homepage.univie.ac.at/robert.kunst/prognos.pdf

Kunt, M. M., Aghayan, I., & Noii, N. (2012). Prediction for traffic accident severity: Comparing the artificial neural network, genetic algorithm, combined genetic algorithm and pattern search methods. *TRANSPORT*, *26*(4), 353–366. https://doi.org/10.3846/16484142.2011.635465

Kurtuluş, E., & Çetin, İ. B. (2020). Analysis of modal shift potential towards intermodal transportation in short-distance inland container transport. *Transport Policy*, *89*, 24–37. https://doi.org/10.1016/j.tranpol.2020.01.017

Kurzawska-Pietrowicz, P. (2023). Life Cycle emission of selected Sustainable Aviation Fuels – A review. *Transportation Research Procedia*, *75*, 77–85. https://doi.org/10.1016/j.trpro.2023.12.010

Lai, Y. Y., & Björklund, A. (2025). Prospective life cycle assessment of future Swedish hydrogen-powered aviation pathways. *Transportation Research Part D: Transport and Environment*, *146*, 104887. https://doi.org/10.1016/j.trd.2025.104887

Lau, J. I. C., Wang, Y. S., Ang, T., Seo, J. C. F., Khadaroo, S. N. B. A., Chew, J. J., Ng Kay Lup, A., & Sunarso, J. (2024). Emerging technologies, policies and challenges toward implementing sustainable aviation fuel (SAF). *Biomass and Bioenergy*, *186*, 107277. https://doi.org/10.1016/j.biombioe.2024.107277

Leckel, D. (2009). Diesel Production from Fischer−Tropsch: The Past, the Present, and New Concepts. *Energy & Fuels*, *23*(5), 2342–2358. https://doi.org/10.1021/ef900064c

Lee, D.-Y., Elgowainy, A., Kotz, A., Vijayagopal, R., & Marcinkoski, J. (2018). Life-cycle implications of hydrogen fuel cell electric vehicle technology for medium- and heavy-duty trucks. *Journal of Power Sources*, *393*, 217–229. https://doi.org/10.1016/j.jpowsour.2018.05.012

Leitão, A. B. de V., Bringhenti, C., Tomita, J. T., dos Santos Silva, F. J., Xisto, C., & Grönstedt, T. (2025). A review of hydrogen aircraft propulsion systems: Recent advances and environmental perspectives. *International Journal of Hydrogen Energy*, *176*, 151489. https://doi.org/10.1016/j.ijhydene.2025.151489

Li. (2025). Decarbonizing China's Express Freight Market Using High-Speed Rail Services and Carbon Taxes: A Bi-Level Optimization Approach. *Symmetry*, *17*(8), 1364. https://doi.org/10.3390/sym17081364

Li, H., Bai, J., Cui, X., Li, Y., & Sun, S. (2020). A new secondary decomposition-ensemble approach with cuckoo search optimization for air cargo forecasting. *Applied Soft Computing*, *90*, 106161. https://doi.org/10.1016/j.asoc.2020.106161

Linders, G.-J., & De Groot, H. L. F. (2006). Estimation of the Gravity Equation in the Presence of Zero Flows. *SSRN Electronic Journal*. https://doi.org/10.2139/ssrn.924160

Linders, G.-J., & de Groot, H. L. F. (2006). *Estimation of the Gravity Equation in the Presence of Zero Flows* (SSRN Scholarly Paper No. 924160). Social Science Research Network. https://doi.org/10.2139/ssrn.924160

Liu, F., Mauzerall, D. L., Zhao, F., & Hao, H. (2021). Deployment of fuel cell vehicles in China: Greenhouse gas emission reductions from converting the heavy-duty truck fleet from diesel and natural gas to hydrogen. *International Journal of Hydrogen Energy, Special Issue on the 2nd International Symposium on Hydrogen Energy and Energy Technologies (HEET 2019)*, *46*(34), 17982–17997. https://doi.org/10.1016/j.ijhydene.2021.02.198

Liu, J., Ding, L., Guan, X., Gui, J., & Xu, J. (2020a). Comparative analysis of forecasting for air cargo volume: Statistical techniques vs. machine learning. *Journal of Data, Information and Management*, *2*(4), 243–255. https://doi.org/10.1007/s42488-020-00031-1

Liu, J., Ding, L., Guan, X., Gui, J., & Xu, J. (2020b). Comparative analysis of forecasting for air cargo volume: Statistical techniques vs. machine learning. *Journal of Data, Information and Management*, *2*(4), 243–255. https://doi.org/10.1007/s42488-020-00031-1

Loprespub. (2025, July 2). Mapping Canada's Urban and Rural Landscape. *HillNotes*. https://hillnotes.ca/2025/07/02/mapping-canadas-urban-and-rural-landscape/

Lütkepohl, H. (2005). *New Introduction to Multiple Time Series Analysis*. Springer. https://doi.org/10.1007/978-3-540-27752-1

Lyu, Z., Pons, D., & Zhang, Y. (2023). Emissions and Total Cost of Ownership for Diesel and Battery Electric Freight Pickup and Delivery Trucks in New Zealand: Implications for Transition. *Sustainability*, *15*(10), 7902. https://doi.org/10.3390/su15107902

Madhavan, M., Ali Sharafuddin, M., Piboonrungroj, P., & Yang, C.-C. (2023). Short-term Forecasting for Airline Industry: The Case of Indian Air Passenger and Air Cargo. *Global Business Review*, *24*(6), 1145–1179. https://doi.org/10.1177/0972150920923316

Mancaruso, E., Meccariello, G., & Rossetti, S. (2024). *Investigation of Plug-In Hybrid Light Duty Commercial Vehicle in Real-World Conditions by Simulation*. SAE International. Conference on Sustainable Mobility. https://doi.org/10.4271/2024-24-0016

Mandegari, M., Ebadian, M., & Saddler, J. (John). (2023). Decarbonizing North America's rail sector, international initiatives and local opportunities. *Transportation Research Interdisciplinary Perspectives*, *21*, 100859. https://doi.org/10.1016/j.trip.2023.100859

Marek, C., Smith, T., & Kundu, K. (2005). Low Emission Hydrogen Combustors for Gas Turbines Using Lean Direct Injection. In *41st AIAA/ASME/SAE/ASEE Joint Propulsion Conference & Exhibit*. American Institute of Aeronautics and Astronautics. https://doi.org/10.2514/6.2005-3776

Martinez-Boggio, S., Monsalve-Serrano, J., García, A., & Curto-Risso, P. (2023). High Degree of Electrification in Heavy-Duty Vehicles. *Energies*, *16*(8), 3565. https://doi.org/10.3390/en16083565

Mary, B., Sean, P., David, H., & Adrian, S. (2012). Understanding mode choice decisions: A study of Australian freight shippers. In *Maritime Economics & Logistics* (Vols. 1–14, pp. 274–299). https://link.springer.com/article/10.1057/mel.2012.8

Massiani, J., Danielis, R., & Marcucci, E. (2007). *THE HETEROGENEITY IN SHIPPER'S VALUE OF TIME, RESULTS FROM AN SP EXPERIMENT USING MIXED LOGIT AND LATENT CLASS*.

Matsumoto, H., & Domae, K. (2019). Assessment of competitive hub status of cities in Europe and Asia from an international air traffic perspective. *Journal of Air Transport Management*, *78*, 88–95. https://doi.org/10.1016/j.jairtraman.2019.01.006

Merkus, Henk. G., & Meesters, G. M. H. (2013). *2014 Book ParticulateProducts | PDF | Pharmacy | Paint*. Springer International Publishing, Switzerland: 1-19. Scribd. https://www.scribd.com/document/492703044/2014-Book-ParticulateProducts

Mohd Noor, C. W., Noor, M. M., & Mamat, R. (2018). Biodiesel as alternative fuel for marine diesel engine applications: A review. *Renewable and Sustainable Energy Reviews*, *94*, 127–142. https://doi.org/10.1016/j.rser.2018.05.031

Mukhopadhaya, J., & Graver, B. (2022). PERFORMANCE ANALYSIS OF REGIONAL ELECTRIC AIRCRAFT. *Washington*. https://theicct.org/wp-content/uploads/2022/07/global-aviation-performance-analysis-regional-electric-aircraft-jul22-1.pdf-1.pdf

Müller, K.-R., Smola, A. J., Rätsch, G., Schölkopf, B., Kohlmorgen, J., & Vapnik, V. (1997). Predicting time series with support vector machines. In W. Gerstner, A. Germond, M. Hasler, & J.-D. Nicoud (Eds.), *Artificial Neural Networks—ICANN'97* (pp. 999–1004). Springer. https://doi.org/10.1007/BFb0020283

Nasoulis, C. P., Protopapadakis, G., Ntouvelos, E. G., Gkoutzamanis, V. G., & Kalfas, A. I. (2023). Environmental and techno-economic evaluation for hybrid-electric propulsion architectures. *The Aeronautical Journal*, *127*(1317), 1904–1926. https://doi.org/10.1017/aer.2023.27

National Institute of Standards and Technology. (n.d.-a). *6.4.4. Univariate Time Series Models. NIST/SEMATECH e-Handbook of Statistical Methods*. Retrieved April 1, 2026, from https://www.itl.nist.gov/div898/handbook/pmc/section4/pmc44.htm

National Institute of Standards and Technology. (n.d.-b). *6.4.4.3. Seasonality. NIST/SEMATECH e-Handbook of Statistical Methods*. Retrieved April 1, 2026, from https://www.itl.nist.gov/div898/handbook/pmc/section4/pmc443.htm

Natural Resources Canada. (2026, March 10). *Transportation Sector Canada Table 60: Truck Explanatory Variables*. Government of Canada, Natural Resources Canada. https://oee.nrcan.gc.ca/corporate/statistics/neud/dpa/showTable.cfm?type=CP&sector=tran&juris=ca&year=2023&rn=60&page=0

Nemitallah, M. A., El-Adawy, M., Abdulrahman, G. A. Q., Mansour, S., Habib, M. A., & Khalifa, A. (2025). Hydrogen Mobility toward Affordable and Clean Energy Production in Gas Turbines: State-of-the-Art and Perspectives. *Energy & Fuels*, *39*(13), 6045–6077. https://doi.org/10.1021/acs.energyfuels.4c05875

New Brunswick. Department of Finance and Treasury Board. (2025, March 18). *Economic Outlook 2025-2026* [Economic outlook report]. Department of Finance and Treasury Board, Province of New Brunswick. https://legnb.ca/content/house_business/61/1/tabled_documents/2025-03-18%20Economic%20Outlook%202025-2026.pdf

Ng, K. S., Farooq, D., & Yang, A. (2021). Global biorenewable development strategies for sustainable aviation fuel production. *Renewable and Sustainable Energy Reviews*, *150*, 111502. https://doi.org/10.1016/j.rser.2021.111502

Nguyen, D. D., Kale, U., & Wangai, A. W. (2020). *TOTAL LIFE CYCLE COST AND EMISSION OF ELECTRIC, HYBRID- ELECTRIC AIRCRAFT*.

Nguyen, Q. H. (2024). Modeling the volatility of international air freight: A case study of Singapore using the SARIMAX-EGARCH model. *Journal of Air Transport Management*, *117*, 102593. https://doi.org/10.1016/j.jairtraman.2024.102593

Nguyen, Q. H., Tran, P. Q., & Ngo, P. D. (2025). Air cargo traffic forecasting model: An empirical study in Vietnam using the SARIMA-X/(E)GARCH model. *Research in Transportation Business & Management*, *59*, 101268. https://doi.org/10.1016/j.rtbm.2024.101268

Nova Scotia. Department of Finance and Treasury Board. (2025, September 22). *Forecast Update* [Forecast update]. Province of Nova Scotia. https://notices.novascotia.ca/files/budget-forecast-notices/budget-forecast-update-september-2025.pdf

Oehmichen, K., Majer, S., Müller-Langer, F., & Thrän, D. (2022). Comprehensive LCA of Biobased Sustainable Aviation Fuels and JET A-1 Multiblend. *Applied Sciences*, *12*(7). https://doi.org/10.3390/app12073372

Oesingmann, K., Grimme, W., & Scheelhaase, J. (2024). Hydrogen in aviation: A simulation of demand, price dynamics, and CO2 emission reduction potentials. *International Journal of Hydrogen Energy*, *64*, 633–642. https://doi.org/10.1016/j.ijhydene.2024.03.241

Ontario. Ministry of Finance. (2025, November 6). *2025 Ontario Economic Outlook and Fiscal Review: A Plan to Protect Ontario* [Fall Economic Statement / Fiscal review]. Government of Ontario. https://budget.ontario.ca/2025/fallstatement/brief.html

OpenStreetMap. (n.d.-a). *Copyright and License*. OpenStreetMap. Retrieved January 15, 2026, from https://www.openstreetmap.org/copyright

OpenStreetMap. (n.d.-b). *OpenStreetMap*. OpenStreetMap. Retrieved January 15, 2026, from https://www.openstreetmap.org/

Ordinary least squares. (2025). In *Wikipedia*. https://en.wikipedia.org/w/index.php?title=Ordinary_least_squares&oldid=1327870412

Park, M., Regan, A., & Yang, C.-H. (2007). Emissions impacts of a modal shift: A case study of the Southern California ports region. *Journal of International Logistics and Trade*, *5*(2), 67–81. https://doi.org/10.24006/jilt.2007.5.2.67

Patrao, A. C., Jonsson, I., Xisto, C., Lundbladh, A., & Grönstedt, T. (2024). Compact heat exchangers for hydrogen-fueled aero engine intercooling and recuperation. *Applied Thermal Engineering*, *243*, 122538. https://doi.org/10.1016/j.applthermaleng.2024.122538

PCJ. (n.d.). *Boeing 737-800BCF: Specs, Cargo Conversion & Freight Capacity Guide*. Private Jets Connect. Retrieved June 16, 2026, from https://private-jets-connect.com/en/cargo/guide/boeing-737-800bcf-fiche-technique/

Perullo, C., & Mavris, D. N. (2014). Assessment of Vehicle Performance Using Integrated NPSS Hybrid Electric Propulsion Models. In *50th AIAA/ASME/SAE/ASEE Joint Propulsion Conference*. American Institute of Aeronautics and Astronautics. https://doi.org/10.2514/6.2014-3489

Peters, J. F., Iribarren, D., & Dufour, J. (2015). Life cycle assessment of pyrolysis oil applications. *Biomass Conversion and Biorefinery*, *5*(1), 1–19. https://doi.org/10.1007/s13399-014-0120-z

Piepenbrink, H., Flämig, H., & Menger, A. (2025). CO2e Life-Cycle Assessment: Twin Comparison of Battery–Electric and Diesel Heavy-Duty Tractor Units with Real-World Data. *Future Transportation*, *5*(1), 12. https://doi.org/10.3390/futuretransp5010012

Piermartini, R., & Teh, R. (2005). *Demystifying modelling methods for trade policy* (Working Paper No. 10). WTO Discussion Paper. https://www.econstor.eu/handle/10419/107045

Pipitone, G., Zoppi, G., Pirone, R., & Bensaid, S. (2023). Sustainable aviation fuel production using in-situ hydrogen supply via aqueous phase reforming: A techno-economic and life-cycle greenhouse gas emissions assessment. *Journal of Cleaner Production*, *418*, 138141. https://doi.org/10.1016/j.jclepro.2023.138141

Popovich, N. D., Rajagopal, D., Tasar, E., & Phadke, A. (2021). Economic, environmental and grid-resilience benefits of converting diesel trains to battery-electric. *Nature Energy*, *6*(11), 1017–1025. https://doi.org/10.1038/s41560-021-00915-5

Pornet, C., & Isikveren, A. T. (2015). Conceptual design of hybrid-electric transport aircraft. *Progress in Aerospace Sciences*, *79*, 114–135. https://doi.org/10.1016/j.paerosci.2015.09.002

Pöyhönen, P. (1963). A Tentative Model for the Volume of Trade between Countries. *Weltwirtschaftliches Archiv*, *90*, 93–100.

Qiu, X., Zhang, L., Nagaratnam Suganthan, P., & Amaratunga, G. A. J. (2017). Oblique random forest ensemble via Least Square Estimation for time series forecasting. *Information Sciences*, *420*, 249–262. https://doi.org/10.1016/j.ins.2017.08.060

Québec. Ministère des Finances. (2025, November 25). *Update on Québec's Economic and Financial Situation – Fall 2025* [Economic and financial update]. Gouvernement du Québec. https://www.finances.gouv.qc.ca/Budget_and_update/maj/documents/AUTEN_updateNov2025.pdf

Railway Association of Canada. (2020). *Canada's Railways: Helping Canada Stay on Track to Fight Climate Change*. Railway Association of Canada. https://www.railcan.ca/wp-content/uploads/2020/05/RailCan_EnvironmentalBrief_Final.pdf

Ram, A., & Rafael, P.-P. (2020). Role of Comparative Advantage in Biofuel Policy Adoption in Latin America. *Sustainability*. https://doi.org/https://doi.org/10.3390/su12041411

Reinsel, G. C. (1993). *Elements of Multivariate Time Series Analysis*. Springer US. https://doi.org/10.1007/978-1-4684-0198-1

Ren, L., Zhou, S., Peng, T., & Ou, X. (2022). Greenhouse gas life cycle analysis of China's fuel cell medium- and heavy-duty trucks under segmented usage scenarios and vehicle types. *Energy*, *249*, 123628. https://doi.org/10.1016/j.energy.2022.123628

Renouard-Vallet, G., Saballus, M., Schmithals, G., Schirmer, J., Kallo, J., & Friedrich, K. A. (2010). Improving the environmental impact of civil aircraft by fuel cell technology: Concepts and technological progress. *Energy and Environmental Science*, *3*(10), 1458–1468. https://doi.org/10.1039/b925930a

Ribeiro, J., Afonso, F., Ribeiro, I., Ferreira, B., Policarpo, H., Peças, P., & Lau, F. (2020). Environmental assessment of hybrid-electric propulsion in conceptual aircraft design. *Journal of Cleaner Production*, *247*, 119477. https://doi.org/10.1016/j.jclepro.2019.119477

Rodrigue, J.-P. (2017). Principles of Modal Shift. In *The Geography of Transport Systems*. Routledge. https://doi.org/10.4324/9781003343196

Rodríguez, Y., & Olariaga, O. D. (2024). Air Traffic Demand Forecasting with a Bayesian Structural Time Series Approach. *Periodica Polytechnica Transportation Engineering*, *52*(1). https://trid.trb.org/View/2475805

Rogachuk, B. E., & Okolie, J. A. (2024). Comparative assessment of pyrolysis and Gasification-Fischer Tropsch for sustainable aviation fuel production from waste tires. *Energy Conversion and Management*, *302*, 118110. https://doi.org/10.1016/j.enconman.2024.118110

Rosales Calderon, O., Tao, L., Abdullah, Z., Talmadge, M., Milbrandt, A., Smolinski, S., Moriarty, K., Bhatt, A., Zhang, Y., Ravi, V., Skangos, C., Davis, R., & Payne, C. (2024). *Sustainable Aviation Fuel State-of-Industry Report: Hydroprocessed Esters and Fatty Acids Pathway* (NREL/TP--5100-87803, 2426563, MainId:88578; p. NREL/TP--5100-87803, 2426563, MainId:88578). https://doi.org/10.2172/2426563

Royal Netherlands Aerospace Centre, & SEO Amsterdam Economics. (2021). *Destination 2050: Roadmap 2025 – A Route to Net Zero European Aviation* (NLR-CR-2020-510). A4E, ACI-EUROPE, ASD, CANSO, ERA. https://www.destination2050.eu/wp-content/uploads/2021/03/Destination2050_Report.pdf

Sahoo, S., Zhao, X., & Kyprianidis, K. (2020). A Review of Concepts, Benefits, and Challenges for Future Electrical Propulsion-Based Aircraft. *Aerospace*, *7*(4). https://doi.org/10.3390/aerospace7040044

Schäfer, A. W., Barrett, S. R. H., Doyme, K., Dray, L. M., Gnadt, A. R., Self, R., O'Sullivan, A., Synodinos, A. P., & Torija, A. J. (2019). Technological, economic and environmental prospects of all-electric aircraft. *Nature Energy*, *4*(2), 160–166. https://doi.org/10.1038/s41560-018-0294-x

Schlunk, A., & Shurland, M. (2022, February 1). *Proceedings of FRA Workshops on Environmentally Sustainable Energy Technologies Powering Future of Rai*. https://rosap.ntl.bts.gov

Scholz, A. E., Trifonov, D., & Hornung, M. (2022). Environmental life cycle assessment and operating cost analysis of a conceptual battery hybrid-electric transport aircraft. *CEAS Aeronautical Journal*, *13*(1), 215–235. https://doi.org/10.1007/s13272-021-00556-0

Scott, S. L., & Varian, H. R. (2014). Predicting the present with Bayesian structural time series. *International Journal of Mathematical Modelling and Numerical Optimisation*, *5*(1–2), 4–23. https://doi.org/10.1504/IJMMNO.2014.059942

Sen, B., Ercan, T., & Tatari, O. (2017). Does a battery-electric truck make a difference? – Life cycle emissions, costs, and externality analysis of alternative fuel-powered Class 8 heavy-duty trucks in the United States. *Journal of Cleaner Production*, *141*, 110–121. https://doi.org/10.1016/j.jclepro.2016.09.046

Service Canada. (2024, December 12). *Canada's 2035 emissions reduction target*. https://www.canada.ca/en/services/environment/weather/climatechange/climate-plan/2035-emissions-reduction-target.html

Shahriar, M. F., & Khanal, A. (2022). The current techno-economic, environmental, policy status and perspectives of sustainable aviation fuel (SAF). *Fuel*, *325*, 124905. https://doi.org/10.1016/j.fuel.2022.124905

Shepherd, B. (2013). *The gravity model of international trade: A user guide. ARTNeT, United Nations ESCAP*. https://repository.unescap.org/server/api/core/bitstreams/ab15dad9-de4e-4c7d-b981-1dd9c5b6640c/content

Siliverstovs, B., & Schumacher, D. (2006). *To log or not to log, or How to estimate a gravity model?* 8th Annual Conference of the European Trade Study Group. https://www.etsg.org/ETSG2006/papers/SiliverstovsSchumacher.pdf

Silva, J. M. C. S., & Tenreyro, S. (2006). The Log of Gravity. *The Review of Economics and Statistics*, *88*(4), 641–658. https://doi.org/10.1162/rest.88.4.641

Sineglazov, V., Chumachenko, E., & Gorbatyuk, V. (2013). An algorithm for solving the problem of forecasting. *Aviation*, *17*(1), 9–13. https://doi.org/10.3846/16487788.2013.777219

Sirikhorn, K., Peter, N., Yue, W., Udechukwu, O., Max, C., & Alasdair, M. (2014). *Evaluation of forecasting models for air cargo—ProQuest*. https://doi.org/10.1108/IJLM-05-2013-0049

SLOCAT. (2024). *Zooming In: Freight Transport and Logistics*. https://tcc-gsr.com/wp-content/uploads/2024/02/Freight-GSR-summary_final.pdf

Smit, R., Helmers, E., Schwingshackl, M., Opetnik, M., & Kennedy, D. (2024). Greenhouse Gas Emissions Performance of Electric, Hydrogen and Fossil-Fuelled Freight Trucks with Uncertainty Estimates Using a Probabilistic Life-Cycle Assessment (pLCA). *Sustainability*, *16*(2), 762. https://doi.org/10.3390/su16020762

Smith, P. M., Gaffney, M. J., Shi, W., Hoard, S., Armendariz, I. I., & Mueller, D. W. (2017). Drivers and barriers to the adoption and diffusion of Sustainable Jet Fuel (SJF) in the U.S. Pacific Northwest. *Journal of Air Transport Management*, *58*, 113–124. https://doi.org/10.1016/j.jairtraman.2016.10.004

Snyder, C. A., Berton, J. J., Brown, G. V., Dolce, J. L., Dravid, N. V., & Eichenberg, D. J. (2009). *Propulsion Investigation for Zero and Near-Zero Emissions Aircraft—NASA Technical Reports Server (NTRS)*. https://ntrs.nasa.gov/citations/20090023315

Soleymani, M., Mostafavi, V., Hebert, M., Kelouwani, S., & Boulon, L. (2024). Hydrogen propulsion systems for aircraft, a review on recent advances and ongoing challenges. *International Journal of Hydrogen Energy*, *91*, 137–171. https://doi.org/10.1016/j.ijhydene.2024.10.131

Statistics Canada. (2025, July 29). *Air Cargo Traffic at Canadian Airports, Annual (Table 23-10-0254-01)*. Statistics Canada. https://doi.org/https://doi.org/10.25318/2310025401-eng

Statistics Canada, S. C. (2022a, December 1). *Vehicle registrations, by type of vehicle and fuel type*. https://www150.statcan.gc.ca/t1/tbl1/en/tv.action?pid=2310030801

Statistics Canada, S. C. (2022b, December 1). *Vehicle registrations, by type of vehicle and fuel type*. https://www150.statcan.gc.ca/t1/tbl1/en/tv.action?pid=2310030801

Stine, T., Peter, M. H., & Tomas, F. (2020). *Life cycle assessment of hydrogen fuel in aviation* [Master Thesis]. University of Bergen. https://nva.sikt.no/registration/0198f19eebe5-64e89328-6651-4980-8243-ce955c5c9ba8

Strack, M., Chiozzotto, G. P., Iwanizki, M., Plohr, M., & Kuhn, M. (2017). Conceptual Design Assessment of Advanced Hybrid Electric Turboprop Aircraft Configurations. In *17th AIAA Aviation Technology, Integration, and Operations Conference*. American Institute of Aeronautics and Astronautics. https://doi.org/10.2514/6.2017-3068

Sulistyowati, R., Suhartono, Kuswanto, H., Setiawan, & Astuti, E. T. (2018). Hybrid forecasting model to predict air passenger and cargo in Indonesia. *2018 International Conference on Information and Communications Technology (ICOIACT)*, 442–447. https://doi.org/10.1109/ICOIACT.2018.8350816

Tavasszy, L., Kaa, G. van de, & Liu, W. (2020). Importance of freight mode choice criteria: An MCDA approach. *Journal of Supply Chain Management Science*, *1*(1–2), 27–44. https://doi.org/10.18757/jscms.2020.4651

TD Economics. (2025, September 22). *Provincial Economic Forecast: Crawl Before You Walk* [Provincial economic forecast]. TD Economics.

https://economics.td.com/domains/economics.td.com/documents/reports/pef/ProvincialEconomicForecast_Sep2025.pdf

The Delphi Group, & Pollution Probe. (2022). *Towards Net Zero: Developing a Rail Decarbonization Roadmap for Canada*. https://www.railcan.ca/wp-content/uploads/2022/12/Rail-Pathways-Decarbonization-Roadmap.pdf

Thomson, R., Weichenhain, U., Sachdeva, N., & Kaufmann, M. (2020). *Hydrogen: A future fuel for aviation?* [National College of Ireland]. https://www.rolandberger.com/publications/publication_pdf/roland_berger_hydrogen_the_future_fuel_for_aviation.pdf

Thonemann, N., Pierrat, E., Dudka, K. M., Saavedra-Rubio, K., Tromer Dragsdahl, A. L. S., & Laurent, A. (2024). Towards sustainable regional aviation: Environmental potential of hybrid-electric aircraft and alternative fuels. *Sustainable Production and Consumption*, *45*, 371–385. https://doi.org/10.1016/j.spc.2024.01.013

Tinbergen, J. (1962). *Shaping the World Economy*. The Twentieth Century Fund, New York.

Tobit model. (2025). In *Wikipedia*. https://en.wikipedia.org/w/index.php?title=Tobit_model&oldid=1301725476#The_likelihood_function

Transport Canada. (2022a). *Canada's aviation climate action plan 2022–2030* (Nos. T42-29/2022E-PDF). Transport Canada. https://tc.canada.ca/sites/default/files/2022-11/canada-aviation-climate-action-plan-2022-2030.pdf

Transport Canada. (2024, July 12). *43. Incentives for Medium and Heavy Duty Zero-Emission Vehicles Program (IMHZEV)*. Transport Canada. https://tc.canada.ca/en/binder/43-incentives-medium-heavy-duty-zero-emission-vehicles-program-imhzev

Transport Canada. (2025a, July 23). *Carbon Offsetting and Reduction Scheme for International Aviation (CORSIA)*. AART. Transport Canada. https://tc.canada.ca/en/aviation/carbon-offsetting-reduction-scheme-international-aviation-corsia

Transport Canada, & Sustainable Aviation Task Force. (2025). *Aviation Climate Action Plan: 2022 and 2023 Report* (Nos. T40-3E-PDF). Transport Canada. https://tc.canada.ca/sites/default/files/2025-09/Aviation%20Report%202022%202023%20EN-accessible_0.pdf

Transport Canada, T. (2022b). *Transportation in Canada annual report 2021*. Transport Canada. https://tc.canada.ca/en/corporate-services/transparency/corporate-management-reporting/transportation-canada-annual-reports/2021/freight-0

Transport Canada, T. (2025b, September 26). *19. Regional Connectivity*. Transport Canada. https://tc.canada.ca/en/binder/19-regional-connectivity

Turner, S. A. (2002). *An application of a gravity model to air cargo at Vancouver International Airport* [University of British Columbia]. https://doi.org/10.14288/1.0090306

Tzanetis, K. F., Posada, J. A., & Ramirez, A. (2017). Analysis of biomass hydrothermal liquefaction and biocrude-oil upgrading for renewable jet fuel production: The impact of reaction conditions on production costs and GHG emissions performance. *Renewable Energy*, *113*, 1388–1398. https://doi.org/10.1016/j.renene.2017.06.104

Unither Bioelectronics. (n.d.). Retrieved April 30, 2026, from https://www.unither.aero/en/

University of Waterloo. (n.d.). *Geospatial Centre*. University of Waterloo. Retrieved January 15, 2026, from https://uwaterloo.ca/lib-geospatial/collections/canadian-geospatial-data-resources/canada

Uyaroğlu, A., & Unaldi, M. (2023). Alternative Aviation Fuel Types Used in Aircraft Engine. *The Eurasia Proceedings of Science Technology Engineering and Mathematics*, *23*, 85–92. https://doi.org/10.55549/epstem.1361715

van den Oever, A. E. M., Costa, D., & Messagie, M. (2023). Prospective life cycle assessment of alternatively fueled heavy-duty trucks. *Applied Energy*, *336*, 120834. https://doi.org/10.1016/j.apenergy.2023.120834

van Dyk, S., Su, J., Mcmillan, J. D., & Saddler, J. (John). (2019). Potential synergies of drop-in biofuel production with further co-processing at oil refineries. *Biofuels, Bioproducts and Biorefining*, *13*(3), 760–775. https://doi.org/10.1002/bbb.1974

Verma, N. (2023). *Air Passenger and Freight Demand Forecast for Ireland*.

Wandelt, S., Zhang, Y., & Sun, X. (2025). Sustainable aviation fuels: A meta-review of surveys and key challenges. *Journal of the Air Transport Research Society*, *4*, 100056. https://doi.org/10.1016/j.jatrs.2024.100056

Wang, B., Ting, Z. J., & Zhao, M. (2024). Sustainable aviation fuels: Key opportunities and challenges in lowering carbon emissions for aviation industry. *Carbon Capture Science & Technology*, *13*, 100263. https://doi.org/10.1016/j.ccst.2024.100263

Watts, M. J., & Worner, S. P. (2008). Using artificial neural networks to determine the relative contribution of abiotic factors influencing the establishment of insect pest species. *Ecological Informatics*, *3*(1), 64–74. https://doi.org/10.1016/j.ecoinf.2007.06.004

Wei, H., Liu, W., Chen, X., Yang, Q., Li, J., & Chen, H. (2019). Renewable bio-jet fuel production for aviation: A review. *Fuel*, *254*, 115599. https://doi.org/10.1016/j.fuel.2019.06.007

Weiss, R., Karimijafarbigloo, S., Roggenbuck, D., & Rödiger, S. (2022). Applications of Neural Networks in Biomedical Data Analysis. *Biomedicines*, *10*(7), 1469. https://doi.org/10.3390/biomedicines10071469

Witlox, F., & Vandaele, E. (2005). Determining the Monetary Value of Quality Attributes in Freight Transportation Using a Stated Preference Approach. *Transportation Planning and Technology*, *28*(2), 77–92.

Wooldridge, J. M. (2009). *Introductory econometrics: A modern approach* (4. ed., student ed). South-Western. https://commecsinstitute.edu.pk/wp-content/uploads/2024/08/IntroductoryEconometrics_AModernApproach_FourthEdition_Jeffrey_Wooldridge.pdf

Wu, M., Ko, H., & Chaiboonsri, C. (2024). Forecasting China's Air Cargo Volume by ARIMA vs Holt-Winters. *International Journal of Science and Social Science Research*, *2*(3), 123–128. https://doi.org/10.5281/zenodo.14171114

Wu, Z., Wang, M., Zheng, J., Sun, X., Zhao, M., & Wang, X. (2018). Life cycle greenhouse gas emission reduction potential of battery electric vehicle. *Journal of Cleaner Production*, *190*, 462–470. https://doi.org/10.1016/j.jclepro.2018.04.036

Xie, Y., Savvarisal, A., Tsourdos, A., Zhang, D., & Gu, J. (2021). Review of hybrid electric powered aircraft, its conceptual design and energy management methodologies. *Chinese Journal of Aeronautics*, *34*(4), 432–450. https://doi.org/10.1016/j.cja.2020.07.017

Xu, S., Chan, H. K., & Zhang, T. (2019). Forecasting the demand of the aviation industry using hybrid time series SARIMA-SVR approach. *Transportation Research Part E: Logistics and Transportation Review*, *122*, 169–180. https://doi.org/10.1016/j.tre.2018.12.005

Xu, X., Yang, H.-C., Jeong, K., Bui, W., Ravulaparthy, S., Laarabi, H., Needell, Z. A., & Spurlock, C. A. (2024). Teaching freight mode choice models new tricks using interpretable machine learning methods. *Frontiers in Future Transportation*, *5*. https://doi.org/10.3389/ffutr.2024.1339273

Yang, C.-H., Shao, J.-C., Liu, Y.-H., Jou, P.-H., & Lin, Y.-D. (2022). Application of Fuzzy-Based Support Vector Regression to Forecast of International Airport Freight Volumes. *Mathematics*, *10*(14). https://doi.org/10.3390/math10142399

Yao, Z., Gan, M., Li, X., & Liu, X. (2023). Strategic plan for China's air high-speed rail express freight network and its carbon reduction potential. *Environmental Science and Pollution Research*, *30*(11), 29110–29124. https://doi.org/10.1007/s11356-022-24244-6

Yeow, L. W., Yan, Y., & Cheah, L. (2022). Life cycle greenhouse gas emissions of alternative fuels and powertrains for medium-duty trucks: A Singapore case study. *Transportation Research Part D: Transport and Environment*, *105*, 103258. https://doi.org/10.1016/j.trd.2022.103258

Yotov, Y. V., Piermartini, R., Monteiro, J.-A., & Larch, M. (2016). *An Advanced Guide to Trade Policy Analysis: The Structural Gravity Model*. WTO iLibrary. https://doi.org/10.30875/abc0167e-en

Zenith, F., Isaac, R., Hoffrichter, A., Thomassen, M. S., & Møller-Holst, S. (2020). Techno-economic analysis of freight railway electrification by overhead line, hydrogen and batteries: Case studies in Norway and USA. *Proceedings of the Institution of Mechanical Engineers, Part F: Journal of Rail and Rapid Transit*, *234*(7), 791–802. https://doi.org/10.1177/0954409719867495

Zhang, Z., Li, J., Wang, Z., Liu, H., & Wei, K. (2023). Estimating Soil Carbon Sequestration of Jatropha for Sustainable Aviation Fuel Pathway. *Water, Air, & Soil Pollution*, *235*(1), 47. https://doi.org/10.1007/s11270-023-06832-5

Zhao, X., Sahoo, S., Kyprianidis, K., Rantzer, J., & Sielemann, M. (2019). Off-design performance analysis of hybridised aircraft gas turbine. *The Aeronautical Journal*, *123*(1270), 1999–2018. https://doi.org/10.1017/aer.2019.75

Zheng, X. S., Mukhopadhya, J., Benoit, J., Kumar, S. N., Rutherford, D., Rhode, D., & Sitompul, D. (2025). *Aviation Vision 2050: The potential for climate-neutral growth* (ID-445). International Council on Clean Transportation (ICCT). https://theicct.org/wp-content/uploads/2025/09/ID-445-–-Aviation-Vision-2050_report_final.pdf

Zhou, Y., Vyas, A. D., & Guo, Z. (2017). *An Evaluation of the Potential for Shifting of Freight from Truck to Rail and Its Impacts on Energy Use and GHG Emissions* (ANL/ESD--17/12, 1375453; p. ANL/ESD--17/12, 1375453). https://doi.org/10.2172/1375453

Appendix A: Gravity Trade Model Estimation

Model estimation refers to the process of identifying the coefficients that link explanatory variables to the dependent variable in a gravity model. Several estimators have been applied in gravity-model research, including Ordinary Least Squares (OLS), Tobit models, the Heckman sample-selection estimator, Two-Stage Least Squares (TSLS), and Poisson Pseudo-Maximum Likelihood (PPML). This appendix reviews these estimation approaches.

A.1 Ordinary Least Squares

Ordinary Least Squares (OLS) has historically been widely used to estimate log-linear gravity models by minimizing the sum of squared residuals (or the squared errors between the actual and predicted log-trade) ("Ordinary Least Squares," 2025; Siliverstovs & Schumacher, 2006). However, OLS has two major limitations in the gravity model context:

- It cannot directly accommodate zero trade flows because the logarithm of zero is undefined. Dropping zero-flow observations may result in sample-selection bias when those observations are not randomly distributed (Linders & De Groot, 2006).
- Log-linear OLS estimates may be biased and inconsistent in the presence of heteroskedasticity (Silva & Tenreyro, 2006).

A.2 Tobit model and the Heckman sample selection estimator (Tobit II)

To address the issue of zero flows, the Tobit and the Heckman sample selection estimator (Tobit Type II) have been proposed as alternatives to deal with the limitations of using OLS in a log-log model (Linders & De Groot, 2006).

Tobit models assume an unobserved latent variable y_i^*, where observed y_i is a censored version of y_i^*. When y_i^* falls at or below a censoring threshold (often 0 in gravity model application), the observation is recorded as $y_i = 0$; when y_i^* exceeds the threshold, the observed value equals the latent value, $y_i = y_i^*$ (Linders & De Groot, 2006; "Tobit Model," 2025). However, there are a few limitations of the Tobit model in gravity trade model applications:

- Gravity theory provides little guidance on what the appropriate Tobit censoring threshold should be, which creates a mismatch between estimation and theory (Yotov et al., 2016).

- In practice, standard Tobit implementations often require ad hoc data adjustments (adding 1 before taking logs), making results sensitive to measurement units and undermining the usual elasticity interpretation of coefficients (Head & Mayer, 2014).
- Related variants such as ET-Tobit have also been criticized for lacking a clear structural interpretation, and empirical evidence suggests estimates can be sensitive to how the threshold is defined (Head & Mayer, 2014).

Heckman sample selection (Tobit Type II) is a two-step approach for estimating gravity models with many zero flows. It first estimates a selection equation, typically a probit model, to explain the probability of a positive flow. In the second step, it estimates an outcome equation for the volume of positive flows while including a correction term for non-random sample selection (Shepherd, 2013). The selection equation can provide an economic explanation for zero flows by representing the fixed costs associated with establishing a trading relationship (Yotov et al., 2016). This approach may be preferred over the standard Tobit model because zero flows often represent a discrete decision to trade or not to trade, rather than the censoring of an underlying continuous flow (Linders & de Groot, 2006).

A.3 Two-Stage Least Squares

Endogeneity occurs when an explanatory variable is correlated with the regression error term, leading to biased and inconsistent coefficient estimates (Wooldridge, 2009). This problem can arise from omitted variables in the model specification that are correlated with both the explanatory and dependent variables or from measurement error in the explanatory variable (Wooldridge, 2009). Two-Stage Least Squares (TSLS) addresses endogeneity by using instrumental variables (IVs). In the first stage, the endogenous explanatory variable is regressed on all valid instruments and the remaining exogenous variables to obtain its fitted values. In the second stage, the dependent variable is regressed on these fitted values and the other exogenous covariates (Wooldridge, 2009).

Moreover, a valid IV must satisfy two key conditions: (i) relevance (it is sufficiently correlated with the endogenous regressor), and (ii) exogeneity (it is uncorrelated with the structural error term). In practice, finding instruments that satisfy both conditions is difficult (Wooldridge, 2009; Yotov et al., 2016). In panel gravity models, country-pair fixed effects can help reduce omitted-variable bias by

controlling for unobserved time-invariant bilateral characteristics that may be correlated with the explanatory variables (S. L. Baier & Bergstrand, 2007; Wooldridge, 2009). However, they are not a general substitute for valid instruments and do not necessarily address endogeneity arising from measurement error or time-varying omitted variables. Pair fixed effects also absorb all time-invariant bilateral regressors, such as distance, common language, and shared borders, preventing their coefficients from being identified separately (Yotov et al., 2016).

A.4 Poisson Pseudo-Maximum Likelihood

Heteroscedasticity and frequent zero trade/flow observations are common in gravity-model data, making log-linear OLS problematic (Silva & Tenreyro, 2006; Yotov et al., 2016). For this reason, the Poisson Pseudo-Maximum Likelihood (PPML) estimator is widely recommended for gravity model estimation (Head & Mayer, 2014; Silva & Tenreyro, 2006; Yotov et al., 2016). PPML is a quasi-likelihood estimator for multiplicative gravity models and is consistent when the conditional mean is correctly specified (typically $E[y|X] = \exp(X\beta)$), even when the dependent variable is non-integer and not Poisson distributed (Silva & Tenreyro, 2006; Wooldridge, 2009).

Under the PPML framework, the estimating equations are derived from the Poisson assumption that the conditional variance is proportional to the conditional mean. However, this variance relationship is not required for consistency; PPML remains consistent as long as the conditional mean is correctly specified, although heteroskedasticity-robust standard errors should be used when the variance assumption does not hold (Silva & Tenreyro, 2006). Another key advantage is that PPML estimates the dependent variable in levels without applying a logarithmic transformation, allowing zero trade or flow observations to be retained naturally (Silva & Tenreyro, 2006; Yotov et al., 2016). Head & Mayer (2014) show that even a large share of zeros does not necessarily undermine the performance of PML estimators, including PPML. Silva & Tenreyro (2006) provides simulation evidence that PPML performs well across a wide range of settings and is robust to certain types of measurement error in the dependent variable.

Appendix B: Time-Series Forecasting Models

This appendix provides an overview of the univariate and multivariate time-series models.

B.1 Univariate Time-Series Models

A univariate time series is a series of individual observations recorded sequentially over time (National Institute of Standards and Technology, n.d.-a). Univariate time-series models are forecasting approaches that rely solely on the historical values of the demand series itself to identify temporal patterns and predict future demand (Verma, 2023). As such, they do not require additional explanatory variables such as GDP, income, prices, or distance. Most classical univariate time-series applications are based on linear models. These include autoregressive (AR), moving-average (MA), and autoregressive moving-average (ARMA) for stationary series (Kunst, 2012). Autoregressive integrated moving-average (ARIMA) models and seasonal autoregressive integrated moving-average (SARIMA) models extend this framework to non-stationary series through differencing (Box et al., 2016). In addition to these classical linear models, the univariate time series also includes more advanced extensions, such as fractional and nonlinear models (Kunst, 2012).

B.1.1 Autoregressive model

The AR model is among the most common time-series models and is widely used because it can be estimated and tested within the framework of least-squares regression (Kunst, 2012). An AR model represents the current value of a series as a function of its own past values and a random error term (Kunst, 2012). The general AR(p) specification is:

$$X_t = \phi_1 X_{t-1} + \phi_2 X_{t-2} + \cdots + \phi_p X_{t-p} + \varepsilon_t$$

where X_t is the current value of the series, $X_{t-1}, X_{t-2}, \ldots, X_{t-p}$ are past values of the series, p is the number of lagged terms included, $\phi_1, \phi_2, \ldots, \phi_p$ are parameters to be estimated, and ε_t is the random shock at time t and is typically assumed to be white noise (it has mean zero, constant variance, and no serial correlation over time) (Box et al., 2016; Kunst, 2012). AR models are formulated for stationary processes and are useful when the variable being forecast shows persistence over time or the current demand is influenced by its own past behavior (Box et al., 2016).

B.1.2 Moving-average model

The MA model is another common type of univariate time-series model. In an MA model, the current value of a series is expressed as a function of the current random error term and a finite number of past error terms (Box et al., 2016; Kunst, 2012). Simply put, the model explains the current value using present and past shocks, rather than past values of the series itself, as in the AR model. The general MA(q) specification is:

$$X_t = \varepsilon_t + \theta_1 \varepsilon_{t-1} + \theta_2 \varepsilon_{t-2} + \cdots + \theta_q \varepsilon_{t-q}$$

where q denotes the number of lagged error terms, $\theta_1, \theta_2, \ldots, \theta_q$ are moving-average coefficients, and ε_t is a white-noise error or random shock at time t (Box et al., 2016; Kunst, 2012). The MA model is typically useful for representing series in which the current value depends on the current shock and a limited number of past shocks (Box et al., 2016).

B.1.3 Autoregressive moving-average model

The ARMA model combines the autoregressive and moving-average components in a single framework (Box et al., 2016). In an ARMA model, the current value of a series is expressed as a function of both its own past values, and current and past random shocks. The general ARMA(p, q) specification is

$$X_t = \phi_1 X_{t-1} + \phi_2 X_{t-2} + \cdots + \phi_p X_{t-p} + \varepsilon_t + \theta_1 \varepsilon_{t-1} + \theta_2 \varepsilon_{t-2} + \cdots + \theta_q \varepsilon_{t-q}$$

where p denotes the number of autoregressive lags, q denotes the number of moving-average lags, $\phi_1, \phi_2, \ldots, \phi_p$ are autoregressive coefficients, $\theta_1, \theta_2, \ldots, \theta_q$ are moving-average coefficients, and ε_t is a white-noise error term or random shock at time t (Kunst, 2012).

B.1.4 Autoregressive integrated moving-average model

In practice, the assumption of stationarity is often violated in many time-series datasets due to growth trends, cyclical fluctuations, volatility changes, or level shifts (Kunst, 2012). The ARIMA model extends the ARMA framework to non-stationary time series by introducing an integration component (Box et al., 2016). In an ARIMA model, the original series is differenced one or more times to achieve stationarity before the autoregressive and moving-average terms are estimated. The general ARIMA(p, d, q) specification is

$$\Delta^d X_t = \phi_1 \Delta^d X_{t-1} + \phi_2 \Delta^d X_{t-2} + \cdots + \phi_p \Delta^d X_{t-p} + \varepsilon_t + \theta_1 \varepsilon_{t-1} + \theta_2 \varepsilon_{t-2} + \cdots + \theta_q \varepsilon_{t-q}$$

where p denotes the number of autoregressive lags, d denotes the order of differencing, q denotes the number of moving-average lags, $\phi_1, \phi_2, \ldots, \phi_p$ are autoregressive coefficients, $\theta_1, \theta_2, \ldots, \theta_q$ are moving-average coefficients, and ε_t is a white-noise error term (Box et al., 2016). ARIMA models are useful when the original series exhibits non-stationary behavior, such as trend, but can be transformed into a stationary series through differencing.

B.1.5 Seasonal autoregressive integrated moving-average model

Many time-series datasets display seasonality, which is common in economic data. This refers to periodic fluctuations that recur at regular intervals over time (National Institute of Standards and Technology, n.d.-b). When such patterns are present, they should be incorporated into the time-series model to ensure the model adequately captures the data's underlying structure and produces more reliable forecasts. The SARIMA model extends the ARIMA framework to time series with seasonal patterns. Box et al. (2016) expressed this model as SARIMA $(P, D, Q) \times (p, d, q)$, where (p, d, q) denote the non-seasonal autoregressive, differencing, and moving-average orders, and (P, D, Q) denote the corresponding seasonal components. SARIMA models are therefore useful when the observed series exhibits both non-stationary behavior and systematic seasonal fluctuations.

B.1.6 Other models

In addition to the models discussed above, the univariate time-series models also include fractional, nonlinear, and state-space models (Kunst, 2012). Fractional or long-memory models are used to describe time series that exhibit persistent dependence over time, with autocorrelations that decay more slowly than in standard ARIMA models. A common example of this type of model is fractionally integrated ARMA (ARFIMA), which extends ARIMA by allowing non-integer differencing orders (Box et al., 2016).

On the other hand, nonlinear time-series models are used when the behavior of a series cannot be adequately captured by standard linear models. They are intended to represent features such as regime changes, asymmetric responses, nonlinear dependence, and time-varying volatility. Examples of this type of model include bilinear models, threshold autoregression models, smooth transition models, switching regression models, and random coefficient models (Box et al., 2016; Kock & Teräsvirta, 2011). These models, however, generally require large datasets for reliable identification and meaningful improvements in forecasting accuracy (Kunst, 2012).

State-space models provide an alternative framework for time-series analysis in which the observed series is represented as the output of an underlying unobserved dynamic system (Chatfield, 2000). Rather than modelling only the patterns in the observed series directly, this approach represents the series via latent components, thereby improving interpretability. The model will consist of an observation equation and a state-transition equation:

$$X_t = h_t'\theta_t + n_t$$
$$\theta_t = G_t\theta_{t-1} + w_t$$

where X_t denotes the observed time series, θ_t is the vector of unobserved state variables, h_t' links the hidden states to the observed series, G_t governs the evolution of the state variables over time, and n_t and w_t are disturbance terms (Chatfield, 2000). In the context of air-cargo forecasting, one state-space approach that has been applied is the Bayesian Structural Time Series (BSTS) model (Madhavan et al., 2023; Rodríguez & Olariaga, 2024). BSTS is classified as a state-space model because it is built around observation and state equations (Scott & Varian, 2014).

B.2 Multivariate Time-Series Models

While univariate models rely only on the historical values of a single series, multivariate time-series models jointly analyze two or more series to capture dynamic relationships among them and potentially improve forecasting performance (Verma, 2023). The common approaches in this time series category include vector autoregression (VAR) models, vector autoregressive-moving average (VARMA), cointegration-based models, and multivariate state-space models (Box et al., 2016)

B.2.1 Vector autoregression model

VAR models are widely used multivariate time series models because they are straightforward to estimate and closely resemble ordinary regression (Box et al., 2016). In a VAR model, each variable in the system is expressed as a function of its own past values and the past values of the other variables in the system (Reinsel, 1993). A VAR model can be viewed as a multivariate extension of the univariate AR model. The general VAR(p) specification is:

$$(\mathbf{X}_t - \boldsymbol{\mu}) = \sum_{j=1}^{p} \Phi_j \, (\mathbf{X}_{t-j} - \boldsymbol{\mu}) + \boldsymbol{\varepsilon}_t$$

where $\mathbf{X}_t$ is the vector of variables at time t, $\boldsymbol{\mu}$ is the mean vector, p denotes the number of lagged terms included in the model, $\boldsymbol{\Phi}_1, \boldsymbol{\Phi}_2, \ldots, \boldsymbol{\Phi}_p$ are coefficient matrices to be estimated, and $\boldsymbol{\varepsilon}_t$ is a vector white-noise error term (Reinsel, 1993). Standard VAR models are generally applied to stationary time series. When the variables are non-stationary but cointegrated, a vector error-correction specification may be more appropriate.

B.2.2 Vector autoregressive-moving average model

Although VAR models are widely used in practice, representing complex dynamic relationships may require a high lag order, thereby substantially increasing the number of parameters. VARMA models may provide a more parsimonious representation by combining autoregressive terms with lagged innovations. However, they are generally more difficult to identify and estimate than VAR models (Düker et al., 2025; Lütkepohl, 2005). The general VARMA(p, q) model is:

$$(\mathbf{X}_t - \boldsymbol{\mu}) - \sum_{j=1}^{p} \boldsymbol{\Phi}_j \, (\mathbf{X}_{t-j} - \boldsymbol{\mu}) = \boldsymbol{\varepsilon}_t - \sum_{j=1}^{q} \boldsymbol{\Theta}_j \, \boldsymbol{\varepsilon}_{t-j}$$

where $\mathbf{X}_t$ is the vector of variables at time t, $\boldsymbol{\mu}$ is the mean vector, p is the number of autoregressive lags, $q$is the number of moving-average lags, $\boldsymbol{\Phi}_1, \ldots, \boldsymbol{\Phi}_p$ are autoregressive coefficient matrices, $\boldsymbol{\Theta}_1, \ldots, \boldsymbol{\Theta}_q$ are moving-average coefficient matrices, and $\boldsymbol{\varepsilon}_t$ is a zero-mean vector white-noise error term. A vector moving-average model (VMA) is obtained as a special case when $p = 0$ (Baccalá & Sameshima, 2022; Lütkepohl, 2005).

B.2.3 Cointegration-based model

In univariate settings, non-stationarity is often addressed through differencing. In multivariate systems, however, differencing each series separately may remove important information about long-run relationships among the variables. A set of variables that are individually non-stationary and integrated of order one, $I(1)$, is said to be cointegrated if one or more nonzero linear combinations of those variables are stationary (Box et al., 2016; Engle & Granger, 1987). Although cointegration is not limited to vector autoregressive models, a VAR system containing cointegrated variables can be represented in vector error-correction form. This representation captures both short-run dynamics and adjustment toward the long-run equilibrium relationships (Box et al., 2016):

$$\Delta \mathbf{X}_t = \mathbf{C}\mathbf{X}_{t-1} + \sum_{j=1}^{p-1} \mathbf{\Phi}_j^* \, \Delta \mathbf{X}_{t-j} + \boldsymbol{\varepsilon}_t$$

where $\Delta \mathbf{X}_t$ is the differenced vector series, $\mathbf{C}\mathbf{X}_{t-1}$ is the error-correction term, $\mathbf{\Phi}_j^*$ are coefficient matrices for short-run dynamics, and $\boldsymbol{\varepsilon}_t$ is a vector white-noise error term. The rank of $\mathbf{C}$ determines the number of cointegrating relationships in the system. When $rank(C) = 0$, no cointegrating relationship is present, and, provided that all variables are $I(1)$, the system may instead be estimated as a VAR model in first differences (Box et al., 2016).

B.2.4 Multivariate state-space model

Multivariate state-space models extend the univariate state-space framework by jointly representing multiple related time series through vectors of observed variables and unobserved state variables. This framework allows relationships among the observed series to be modelled while representing their underlying latent components, such as trends, seasonal patterns, and cycles (Durbin & Koopman, 2012; Harvey & Koopman, 2014).

One example is the seemingly unrelated time-series equations (SUTSE) model (Chatfield, 2000). In a SUTSE model, each series may have its own unobserved components, while disturbances associated with corresponding components may be contemporaneously correlated across the series (Fernández & Harvey, 1990). This structure allows information from related time series to be jointly incorporated into model estimation and forecasting.

Appendix C: Machine-Learning Forecasting Models

C.1 Support vector regression

Support Vector Regression (SVR) is a supervised learning method derived from Support Vector Machine algorithms and used for predicting continuous outcomes (Drucker et al., 1996; Müller et al., 1997). Unlike classical regression models, which penalize all prediction errors, SVR applies an ϵ-insensitive loss function, meaning that errors within a predefined margin ϵ are ignored, and only larger deviations are penalized (Drucker et al., 1996; Liu et al., 2020). The method, therefore, seeks a prediction function that is as flat as possible while keeping most observations within an acceptable error band. The SVR function can be written as:

$$f(x_i) = \omega^T \phi(x_i) + b$$

where x_i is the input vector, $\phi(x_i)$ is the feature mapping, ω is the weight vector, and b is the intercept (Yang et al., 2022). The primal optimization problem is the mathematical step SVR uses to find the best regression function:

$$\min_{w,b,\xi_i,\xi_i^*} \frac{1}{2} \| \omega \|^2 + C \sum_{i=1}^{n} (\xi_i + \xi_i^*)$$

subject to:

$$y_i - (\omega^T \phi(x_i) + b) \leq \varepsilon + \xi_i$$
$$(\omega^T \phi(x_i) + b) - y_i \leq \varepsilon + \xi_i^*$$
$$\xi_i, \xi_i^* \geq 0$$

where y_i is the observed target, ε defines the width of the error-insensitive region, ξ_i and ξ_i^* are slack variables, and C is a penalty parameter that controls the trade-off between model flatness and prediction errors outside the ε margin (Yang et al., 2022). For nonlinear relationships, SVR uses kernel functions to represent similarities between observations in a higher-dimensional feature space. Common kernel functions include polynomial, sigmoid, and radial basis function kernels (Liu et al., 2020).

C.2 Artificial neural networks

ANN is one of the most widely used supervised learning models and is capable of capturing complex relationships between the input and output data (Sineglazov et al., 2013; Verma, 2023). It predicts the output variable by learning the underlying patterns in the input data, even when the data contains noise or random variation (Garrido et al., 2014). Unlike traditional models, ANNs do not require the functional form between inputs and outputs to be specified in advance (Merkus & Meesters, 2013; Watts & Worner, 2008). Instead, they learn this relationship directly from the data by adjusting the connection weights between variables during training (Kunt et al., 2012). Once trained, the network can generate forecasts for new data by identifying patterns similar to those observed in the training sample (BaFail, 2004). In the most general form, ANN forecasting model can be represented as a nonlinear mapping from a vector of input variables to an output variable:

$$X_t = F(H_1(\mathbf{z}_t), H_2(\mathbf{z}_t), \dots, H_n(\mathbf{z}_t)) + \varepsilon_t$$

where X_t denotes the forecasted demand at time t, $\mathbf{z}_t$ is the vector of input variables, $H_1(\cdot), \dots, H_n(\cdot)$ represent hidden-layer transformations, $F(\cdot)$ is the output mapping, and ε_t is an error term (BaFail, 2004). The most widely used ANN structure in forecasting is the multi-layer perception (MLP), which typically consists of an input layer, one or more hidden layers, and an output layer, as shown in the figure below (Glenn & Panarat, 2018; Weiss et al., 2022). Each layer contains a set of nodes, or neurons, connected to nodes in adjacent layers (S.-C. Chen et al., 2012). These layers are responsible for receiving the input variables, processing the inputs and learning patterns, and producing the predicted values (Glenn & Panarat, 2018)

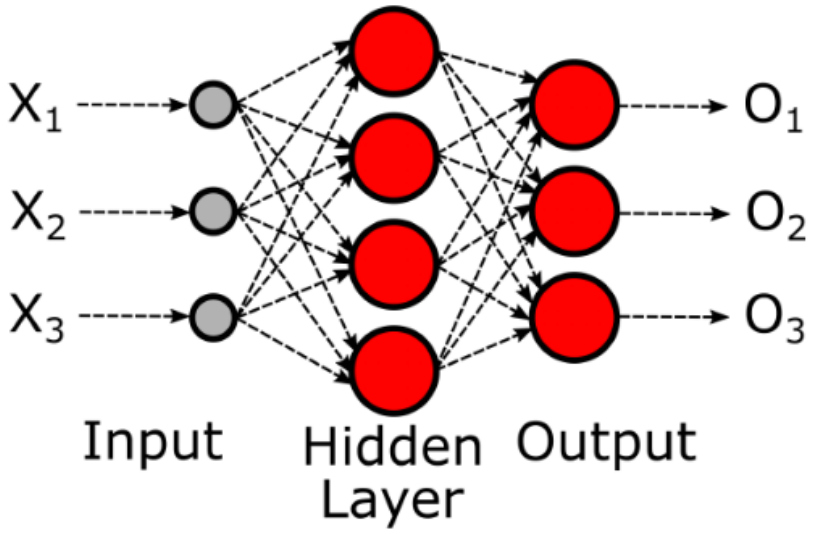


Figure C 1. Structure of an artificial neural network with input, hidden, and output layers (Weiss et al., 2022)

The general form of the MLP output can be expressed as:

$$X_t = g\left(\theta + \sum_{j=1}^{m} v_j \, f\left(\sum_{i=1}^{n} W_{ij} \, z_{it} + \beta_j\right)\right) + \varepsilon_t$$

Where X_t denotes the predicted output at time t, $\mathbf{z}_t$ is the vector of input variables, W_{ij} is the weight connecting input i to hidden neuron j, β_j is the bias term of hidden neuron j, v_j is the weight connecting hidden neuron j to the output layer, and θ is the output-layer bias. The functions $f(\cdot)$ and $g(\cdot)$ represent the activation functions in the hidden and output layers, respectively, while ε_t is the error term (Glenn & Panarat, 2018).

C.3 Random forest

Random forests (RFs) are ensemble learning methods that construct multiple decision trees using bootstrap samples of the training data and randomly selected subsets of input features (Breiman, 2001). Each decision tree is a model that predicts an outcome by splitting the data through a sequence of decision rules. Starting from the root node or the most fundamental question, the tree applies a series of questions based on the input variables, with each answer directing the observation to a new branch until a terminal node is reached, where the final prediction is assigned (Çatuk, 2025). Each

tree is grown independently, and the final prediction is obtained by aggregating the outputs of all trees, typically by majority vote for classification and averaging for regression (Breiman, 2001; Qiu et al., 2017). The general Random Forest model can be expressed as:

$$F(x) = S(T_1(x), T_2(x), T_3(x), \dots, T_B(x))$$

where $F(x)$ is the final model prediction for input x, $T_b(x)$ is the prediction produced by the b-th decision tree, B is the total number of trees in the forest, and $S(\cdot)$ is the aggregation function used to combine individual tree outputs (Çatuk, 2025)

C.4 Gradient boosting methods

Gradient Boosting Regression Tree (GBRT) is an ensemble learning method in which multiple weak learners, typically decision trees, are combined sequentially to improve predictive performance (Bentéjac et al., 2021; Çatuk, 2025). GBRT builds trees iteratively, where each new tree is trained to reduce the residual errors of the existing model (Çatuk, 2025; Liu et al., 2020). The model at iteration m can be expressed as:

$$F_m(x) = F_{m-1}(x) + \gamma_m h_m(x)$$

where $F_{m-1}(x)$ is the prediction from the previous iteration, $h_m(x)$ is the weak learner fitted at iteration m, and γ_m is the learning rate that controls the contribution of the new tree (Liu et al., 2020). The objective of $h_m(x)$ is to minimize the difference between the updated prediction and the observed target value, which can be written as:

$$h_m(x) = \arg\min_h \sum_{i=1}^{n} L(y_i, F_{m-1}(x_i) + h(x_i))$$

where L is the loss function, $y_i$is the observed value for observation i, and $F_{m-1}(x_i) + h(x_i)$ is the updated prediction (Liu et al., 2020). In other words, each new tree is selected so that, when added to the current model, it reduces the overall prediction error as much as possible. Through this iterative process, GBRT gradually improves prediction accuracy and captures complex relationships in the data.

Appendix D: Sustainable Aviation Fuel Production Pathways

This appendix provides technical background on the major sustainable aviation fuel production pathways. These pathways differ in their eligible feedstocks, conversion processes, technological maturity, lifecycle greenhouse gas emissions, and compatibility with conventional jet fuel. The discussion includes hydroprocessed esters and fatty acids, fischer-tropsch, alcohol-to-jet, hydroprocessed fermented sugars, catalytic hydrothermolysis, and power-to-liquid pathways.

D.1 Hydroprocessed Esters and Fatty Acids (HEFA)

HEFA-SPK is the most mature SAF production pathway and is currently the only commercially deployed method producing the majority of SAF. The conversion of HEFA feedstocks into aviation fuel generally involves three main stages: pretreatment, hydroprocessing, and product separation, as illustrated in figure D-1 below (Rosales Calderon et al., 2024).

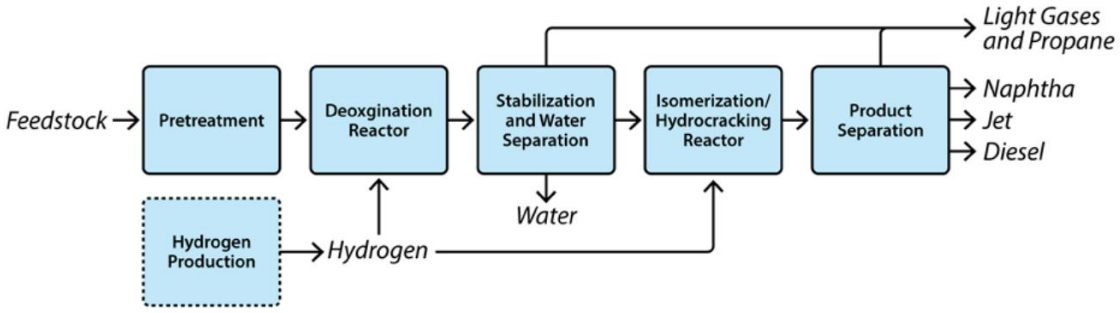


Figure D 1. HEFA-SPK production process flow diagram (Rosales Calderon et al., 2024)

In the pretreatment stage, impurities such as insoluble solids, gums, metals, phosphorus, and other contaminants are removed to protect downstream catalysts, ensure stable processing and improve feed quality (Rosales Calderon et al., 2024). Typical pretreatment operations include filtration, degumming, adsorption/bleaching, and neutralization, although the exact configuration depends on feedstock quality and the requirements of the downstream upgrading system (Rosales Calderon et al., 2024).

After pretreatment, the feedstock undergoes hydroprocessing, in which oxygen is removed, and the molecular structure is transformed into hydrocarbons (Rosales Calderon et al., 2024; Wei et al.,

2019). In a standalone HEFA process, the main conversion steps typically include hydrotreating/deoxygenation, followed by isomerization and hydrocracking (Rosales Calderon et al., 2024). The resulting products are then separated into different fractions, including jet fuel, as well as co-products such as diesel, naphtha, and light gases (Wei et al., 2019).

D.2 Fischer-Tropsch pathways (FT-SPK & FT-SKA)

FT is a SAF production pathway that converts syngas into liquid hydrocarbon fuels. The overall process includes six main steps: feedstock pretreatment, gasification, syngas cleaning, acid-gas removal and conditioning, FT synthesis, and syncrude refining, as illustrated in figure D-2 below (Wei et al., 2019).

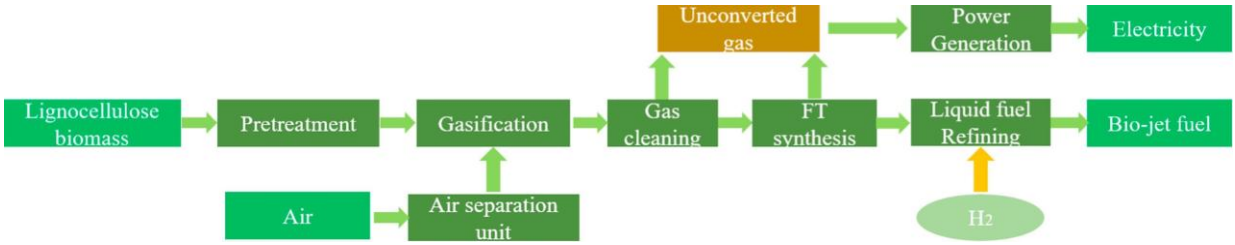


Figure D 2. Fischer-Tropsch (FT) process flow diagram (Wei et al., 2019)

In the pretreatment stage, the feedstock is dried and milled to reduce its particle size and moisture content (Wei et al., 2019). The pretreated feedstock is then gasified at high temperature (approximately 1300 °C), in the presence of oxygen and steam, to produce syngas (Wei et al., 2019). Then, after gasification, the raw syngas undergoes cleaning and acid-gas removal to eliminate ash, tars, carbon dioxide, hydrogen sulfide, and other impurities that could reduce process efficiency or poison downstream catalysts (Wei et al., 2019). The cleaned syngas is then conditioned to achieve an appropriate H_2/CO ratio before entering the FT reactor, where it is converted into hydrocarbon products (Wei et al., 2019).

FT synthesis can be conducted at either high or low temperatures, with lower-temperature conditions generally more favorable for producing kerosene and diesel fuels (Leckel, 2009; Wei et al., 2019). FT-derived aviation fuels generally have very low sulfur and nitrogen content, high thermal stability, and the potential to reduce sulfur oxide and particulate emissions during combustion (Fox et al.,

2013). However, FT-SPK has a low aromatic content, slightly lower volumetric energy density than conventional jet fuel, and relatively high production costs (Wei et al., 2019).

The FT pathway includes both FT-SPK and FT-SKA. Both pathways generally rely on similar feedstocks, such as biomass and municipal solid waste, and follow the same core conversion route, as described above. The main distinction is that FT-SKA contains aromatic compounds in the final fuel product, whereas FT-SPK is primarily paraffinic (Klimczyk et al., 2025; Wandelt et al., 2025). In particular, FT-SKA includes light aromatics, mainly benzene, which help maintain seal compatibility and proper sealing performance within engine fuel system components (Klimczyk et al., 2025).

D.3 Alcohol-to-Jet pathways (ATJ-SPK & ATJ-SKA)

ATJ pathways convert various types of alcohols, such as ethanol, methanol, and isobutanol, derived from a wide range of sources, including sugarcane, corn, wheat, woody biomass, grassy feedstocks, and wastes, into jet fuel as well as other hydrocarbons (Bauen et al., 2020). Depending on the feedstocks, alcohol production may involve direct fermentation of sugars, hydrolysis of starches, or additional pretreatment and conversion steps for lignocellulosic biomass (Kennes et al., 2016; Wei et al., 2019). Once the feedstocks have been converted into alcohol intermediates, figure D-3 illustrates the main upgrading steps in the ATJ pathway from alcohol to jet fuel

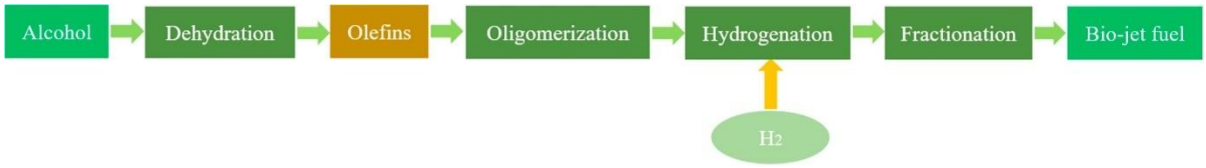


Figure D 3. Alcohol-to-Jet production process flow diagram (Wei et al., 2019)

The ATJ process generally involves alcohol dehydration to form olefins, followed by oligomerization to produce a middle distillate. These distillates are hydrogenated to produce jet-fuel-range hydrocarbons. The final step is fractionation, which separates the jet-fuel fraction (Wei et al., 2019). In addition, ATJ-SKA is a variant of the ATJ pathway in which aromatic compounds are incorporated after base hydrocarbons form, thereby improving fuel properties such as energy density, lubricity, and chemical stability (Borrill et al., 2024; Klimczyk et al., 2025).

D.4 Hydroprocessed Fermented Sugars Synthetic Isoparaffin (HFS-SIP)

Direct sugar-to-hydrocarbon (DSHC) pathways convert sugars into hydrocarbons or lipids that can later be upgraded into aviation fuel (Bauen et al., 2020). Three main DSHC routes are currently under development: sugar conversion to lipids, sugar conversion to long-chain alkenes such as farnesene, and sugar conversion to short-chain gaseous alkenes such as isobutene (Bauen et al., 2020). Among these routes, the pathway based on farnesane production has been certified as HFS-SIP under ASTM D7566 Annex A3 and is currently approved for blending with conventional jet fuel at up to 10% by volume (Uyaroğlu & Unaldi, 2023). In this pathway, sugars derived from sugarcane or other sugar-based feedstocks are converted into hydrocarbon fuel through fermentation, as shown in the figure below (Borrill et al., 2024; Ng et al., 2021)

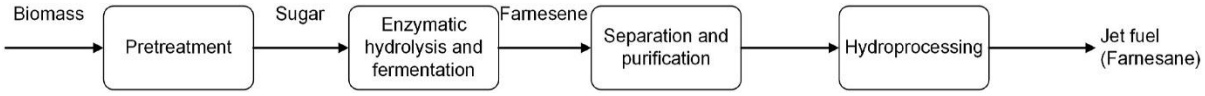


Figure D 4. Hydroprocessing of fermented sugars to jet fuel process flow diagram (Ng et al., 2021)

First, the feedstock/biomass undergoes pretreatment to separate sugars from lignin. This is followed by enzymatic hydrolysis and fermentation, during which the sugars are converted into farnesene ($C_{15}H_{24}$). The farnesene is then recovered through solid-liquid separation and subsequently hydroprocessed into farnesane ($C_{15}H_{32}$), which is the biojet fuel (Ng et al., 2021).

D.5 Catalytic Hydrothermolysis Synthetic Paraffinic Kerosene (CH-SK)

Similar to HEFA, CH-SK is a SAF pathway that produces jet fuel from oils and fats, such as vegetable oils, animal fats, and used cooking oil (Klimczyk et al., 2025). However, CH-SK uses high-temperature, high-pressure hydrothermal conditions with water and a catalyst to convert the feedstock into hydrocarbons suitable for jet fuel (Klimczyk et al., 2025; Lau et al., 2024). The process generally involves three main stages: preconditioning, CH-SK conversion, and post-refining (Lau et al., 2024)

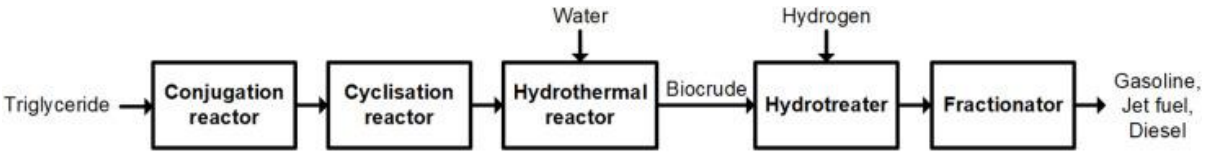


Figure D 5. Catalytic hydrothermolysis synthetic paraffinic kerosene process flow diagram (Lau et al., 2024)

During these stages, the feedstock is broken down and chemically rearranged through reactions such as cracking, hydrolysis, decarboxylation, dehydration, and isomerization, producing biocrude that is then hydrotreated and fractionated into jet fuel and other products such as diesel and gasoline (Klimczyk et al., 2025; Lau et al., 2024).

D.6 Power-to-Liquid (PtL)

PtL is a SAF pathway that produces synthetic liquid fuels using renewable electricity, water, and a carbon source such as captured CO_2 (Bauen et al., 2020). The figure below presents a simplified process flow diagram of the PtL pathway, which mainly involves two key steps: electrolysis and FT synthesis.

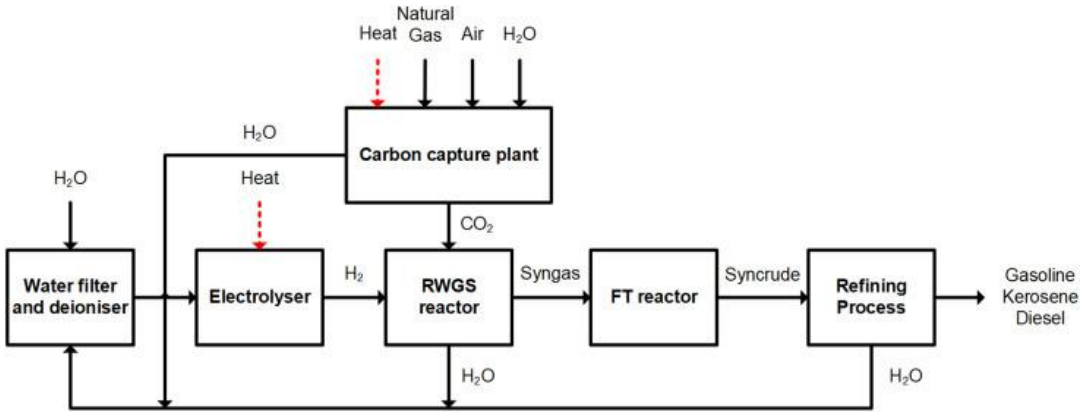


Figure D 6. Power-to-Liquid Route with FT-SPK Process Flow Diagram (Lau et al., 2024)

Within this pathway, hydrogen is first produced through water electrolysis, while CO_2 is captured either from the atmosphere or from concentrated industrial sources (Lau et al., 2024). The hydrogen and CO_2 are then converted into syngas through the reverse water-gas shift reaction, after which FT synthesis is used to produce liquid hydrocarbons (Lau et al., 2024). After synthesis, the resulting mixture undergoes further conditioning and refining, including distillation and cracking or hydrocracking, to produce jet-fuel-range products with suitable fuel properties (Klimczyk et al., 2025; Lau et al., 2024). Although the pathway is still at an early stage of deployment, it has attracted significant interest due to its potential to achieve very low life-cycle GHG emissions and to avoid some of the feedstock constraints associated with bio-based SAF pathways (Bauen et al., 2020).

Appendix E: Alternative Aircraft Propulsion Technologies

This appendix provides technical background on alternative aircraft propulsion technologies, including hybrid-electric and fully electric aircraft configurations, selected Canadian demonstration and development initiatives, and the two principal hydrogen-propulsion pathways: direct hydrogen combustion and hydrogen fuel-cell electric propulsion.

E.1 Hybrid-Electric and Fully Electric Aircraft

Aviation electrification has developed over several decades, initially through the gradual electrification of auxiliary onboard systems. This shift has been driven by the potential for electric systems to be lighter and more efficient than conventional mechanical systems (Bauen et al., 2020). Although electrically assisted propulsion has the potential to reduce fuel consumption, GHG emissions, and noise levels, its practical application remains limited by significant technical barriers, particularly the low energy and power density of current battery technologies (Bauen et al., 2020).

The electrification of aircraft propulsion has led to a range of propulsion-system configurations, which are broadly classified into three primary categories: fully electric, turboelectric, and hybrid-electric aircraft (Sahoo et al., 2020). This subsection focuses specifically on fully electric and hybrid-electric aircraft

E.1.1 Hybrid-electric aircraft:

Hybrid electric aircraft combine conventional thermal propulsion with electric power systems to reduce fuel burn, emissions, and noise while improving overall propulsion efficiency (Abu Salem et al., 2023). Hybrid-electric aircraft can generally be categorized into parallel and series configurations depending on how propulsion power is distributed between the conventional engine and the electric system.

In a parallel-hybrid configuration, the gas turbine engine (fuel tank and turboshaft) and electric motor are connected to the propeller, allowing both systems to provide propulsion either together or separately (Adu-Gyamfi & Good, 2022; Sahoo et al., 2020; Xie et al., 2021). This configuration can reduce fuel use by allowing electrical power to assist the engine during high-demand phases such as takeoff and climb (Charles et al., 2016; Perullo & Mavris, 2014) and by enabling battery charging

during low-thrust conditions (Zhao et al., 2019). A key advantage of this configuration is that system weight can be reduced by downsizing the electric motor or the gas turbine while maintaining similar performance (Adu-Gyamfi & Good, 2022). However, the mechanical coupling between the engine, electric motor, and propeller introduces operational and control complexity (Sahoo et al., 2020), and the engine may not always operate at its most efficient condition, thereby reducing some of the expected fuel-saving benefits (Adu-Gyamfi & Good, 2022). The parallel hybrid-electric configuration is illustrated in figure E-1 below.

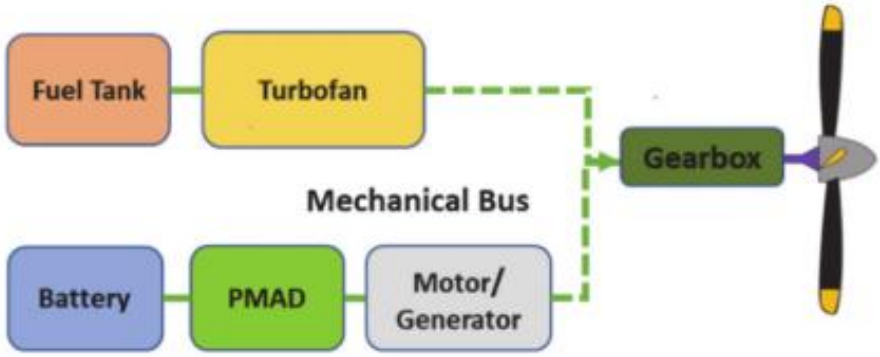


Figure E 1. Parallel Hybrid-Electric Configuration (Sahoo et al., 2020)

In a series-hybrid configuration, the gas turbine engine is not mechanically connected to the propeller. Instead, it is used primarily to drive a generator, which produces electricity to power the electric motor, while the battery can also supply or store electrical energy (Adu-Gyamfi & Good, 2022). A key advantage of this configuration is that the gas turbine can operate closer to its optimal efficiency across different flight phases, as there is no direct linkage between the propeller and the gas turbine, potentially improving fuel efficiency and allowing greater flexibility in engine placement. However, compared with parallel hybrid-electric configurations, series-hybrid systems require an additional generator, which increases system weight and can introduce energy-conversion losses (Adu-Gyamfi & Good, 2022; Economou et al., 2019). It may also provide less redundancy in the event of motor failure (Adu-Gyamfi & Good, 2022). The series hybrid-electric configuration is illustrated in figure E-2 below.

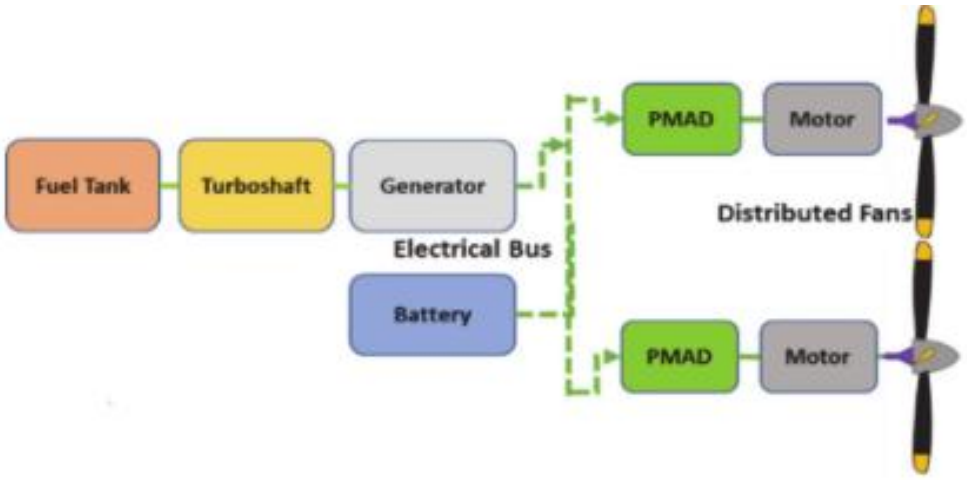


Figure E 2. Series Hybrid-Electric Configuration (Sahoo et al., 2020)

In addition to series and parallel configurations, a combined series-parallel hybrid configuration has also been proposed. This architecture combines both mechanical and electrical power pathways, allowing the propulsor to be driven either directly by the gas turbine or electrically through a generator and battery system (Sahoo et al., 2020). By decoupling the propulsor from the power-generation system, this configuration provides greater flexibility in engine sizing and operation compared to the series and parallel configurations, allowing engine performance to be optimized across different flight segments (Pornet & Isikveren, 2015; Strack et al., 2017). The series/parallel hybrid electric configuration is illustrated in figure E-3 shown below.

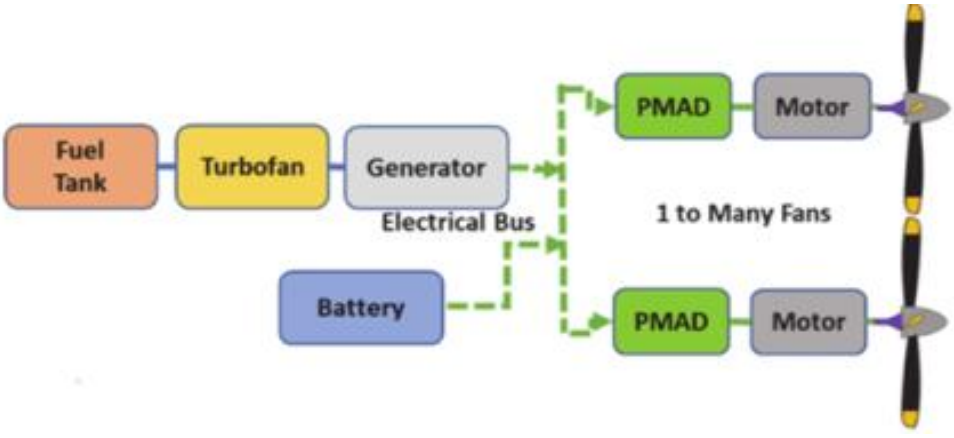


Figure E 3. Series-Parallel Hybrid configuration (Sahoo et al., 2020)

E.1.2 Full-electric aircraft:

Compared with hybrid-electric configurations, fully electric aircraft have the simplest propulsion layout because the battery is the only onboard energy source and directly supplies electricity to the electric motor through a power-management system (Adu-Gyamfi & Good, 2022). However, this configuration does not allow in-flight battery charging; therefore, the batteries must be charged on the ground before each flight mission (Adu-Gyamfi & Good, 2022). Full-electric aircraft offer many advantages, including zero direct in-flight emissions, reduced noise levels, and the potential for lower operating and maintenance costs due to fewer moving parts. However, their application remains constrained as the current battery technology lacks sufficient energy density to match the range and payload capabilities of conventional fuel-powered aircraft (Epstein & O'Flarity, 2019). As a result, fully electric aircraft are currently limited to small aircraft, eVTOL applications, and retrofitted platforms (Adu-Gyamfi & Good, 2022). Current development of fully electric aircraft is primarily focused on urban air mobility and general aviation, which serve as early-stage applications for electrification due to their lower weight and shorter-range requirements (Bauen et al., 2020). This suggests that the application of fully electric propulsion to air cargo remains limited under current technological constraints. The full electric configuration is illustrated in figure shown below

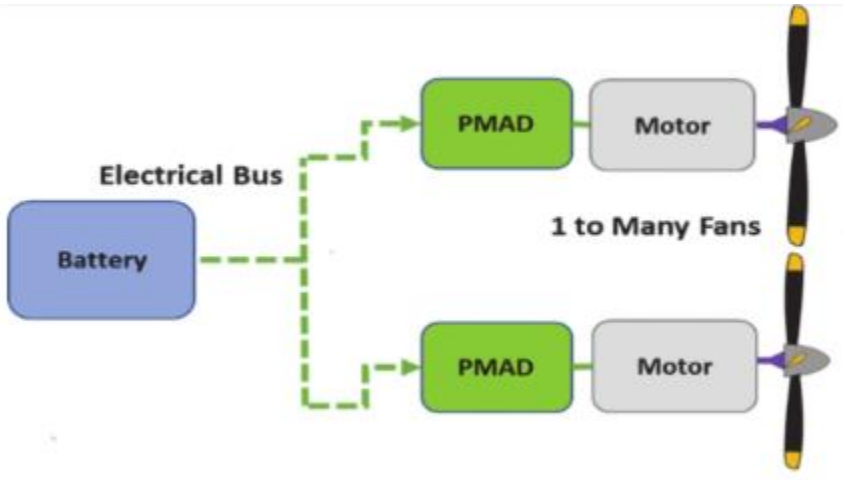


Figure E 4. Full-Electric Configuration (Sahoo et al., 2020)

E.1.3 Canadian context and current developments:

In Canada, electrified aviation remains largely at the demonstration, certification, and early-deployment stage. Some Canada-related full-electric activities, projects, demonstrations, and test programs include:

- **Harbour Air ePlane**: electric retrofit of a DHC-2 Beaver seaplane, with a successful test flight over the Fraser River near Vancouver in 2019 ("Harbour Air," 2025).
- **Drone Delivery Canada**: battery-electric cargo drones for healthcare, remote communities, and logistics (*Drone Delivery Canada*, n.d.).
- **Unither Bioelectronics**: Quebec project developing electric aircraft/eVTOL concepts for organ transport (*Unither Bioelectronics*, n.d.).
- **Helijet:** BETA's all-electric ALIA CTOL (CX300) completed a passenger demonstration flight at Vancouver International Airport in 2025, supporting Helijet's plan to introduce quiet, lower-cost electric passenger, cargo, healthcare, and remote-community air services in BC (Helijet, 2025).

On the other hand, Canada-related hybrid-electric activities, projects, demonstrations, and test programs include:

- **Pratt & Whitney Canada-De Havilland Canada-Collins Aerospace:** hybrid-electric flight demonstrator using a Dash 8-400 platform, with support from the governments of Canada and Quebec; a high-voltage mobile charging unit was announced in 2024 for testing (De Havilland Canada, 2021).
- **EVIO Inc.:** developing the EVIO 810, a 76-seat hybrid-electric regional aircraft targeted for entry into service in the early 2030s, with Boeing support and collaboration with Pratt & Whitney Canada (Kenneth, 2024).
- **Horizon Aircraft:** Canadian company developing the Cavorite X7, a hybrid-electric VTOL aircraft aimed at passenger (Horizon Aircraft, n.d.).

E.2 Hydrogen-powered aircraft

While hybrid-electric and full-electric aircraft provide important pathways for aviation electrification, their application remains constrained by battery energy density, aircraft weight, and range limitations.

Therefore, hydrogen has received increasing attention as an alternative propulsion pathway because it offers much higher specific energy than batteries and can reduce or eliminate direct CO_2 emissions (El-Adawy et al., 2025; Soleymani et al., 2024). Hydrogen can be utilized in aviation through two primary pathways: direct combustion in modified gas turbine engines and fuel-cell-based electric propulsion systems (El-Adawy et al., 2025; Soleymani et al., 2024).

E.2.1 Hydrogen combustion

In hydrogen combustion systems, hydrogen is used as an alternative to kerosene in modified gas turbine engines (El-Adawy et al., 2025). This approach builds on existing aircraft engine technology while taking advantage of hydrogen's high energy content and zero direct CO_2 emissions (El-Adawy et al., 2025; Soleymani et al., 2024). Typically, liquid hydrogen is stored onboard in a cryogenic tank, vaporized through a heat exchanger, and then injected into the engine combustion chamber as gaseous hydrogen (Klug & Faass, 2001; Nemitallah et al., 2025; Soleymani et al., 2024). This allows hydrogen to be used as the combustion fuel in modified gas turbine or piston-engine systems (El-Adawy et al., 2025). A key advantage of this pathway is that it can make use of existing gas-turbine knowledge, design tools, and engine-manufacturing experience, while also offering high specific power potential for larger aircraft (Leitão et al., 2025). However, hydrogen combustion still requires engines optimized specifically for hydrogen (Dahl & Suttrop, 1998; Funke et al., 2021; Marek et al., 2005; Oesingmann et al., 2024), along with new fuel delivery and conditioning systems (Patrao et al., 2024). It also presents operational challenges, including combustion instability due to hydrogen's high flame speed, potential NO_x formation, and the need for high-pressure or cryogenic tanks because hydrogen has lower volumetric energy density than Jet-A fuel (Nemitallah et al., 2025).

E.2.2 Fuel cells

Another hydrogen propulsion pathway involves fuel-cell-based electric systems, in which hydrogen is converted to electricity via an electrochemical reaction to power electric motors (El-Adawy et al., 2025; Thomson et al., 2020). This system acts as continuous energy converters, generating electricity as long as hydrogen is supplied, unlike batteries which store a finite amount of energy (El-Adawy et al., 2025). Moreover, unlike combustion systems, fuel cells do not burn fuel, and therefore produce only water as a byproduct, resulting in zero direct CO_2 emissions during operation (Barros Pintos et al., 2023; Brelje & Martins, 2019; Renouard-Vallet et al., 2010; Snyder et al., 2009). Hydrogen fuel-

cell propulsion can be implemented in either fully electric or hybrid-electric configurations, in which fuel cells can be combined with electric motors to improve system performance and flexibility (El-Adawy et al., 2025; Gaspari et al., 2017). Key advantages of fuel-cell system also include higher efficiency, fewer moving parts, improved reliability and the potential to eliminate auxiliary power units or ram air turbines (Leitão et al., 2025). However, fuel-cell propulsion remains difficult to scale for high-power aircraft applications due to specific power and thermal limitations (Leitão et al., 2025). Other challenges include complex thermal management, hydrogen and water purity requirements for proton exchange membrane fuel cells, longer start-ups and shut-down times, and low power-to-weight ratios (Leitão et al., 2025).

Appendix F: Surface Freight Decarbonization Pathways

This appendix provides additional background on surface freight decarbonization pathways relevant to the modal-shift scenarios assessed in this study. It reviews the principal technologies and fuel pathways available for reducing greenhouse gas emissions from truck and rail freight, including battery-electric vehicles, hydrogen fuel-cell vehicles, plug-in hybrid electric vehicles, biodiesel, renewable diesel, battery-electric locomotives, and hydrogen fuel-cell locomotives

F.1 Truck freight decarbonization pathways

In Canada, surface freight emissions are dominated by road freight, particularly heavy-duty trucks (Environment and Climate Change Canada, 2021). In 2019, on-road freight generated approximately 64.83 Mt CO_2e, making it the largest freight-related source of transportation emissions (Transport Canada, 2022b). Heavy-duty vehicles, including both freight and passenger applications, are also a major contributor to the broader transportation sector, accounting for about 30% of total transportation emissions (Environment and Climate Change Canada, 2021). Emissions from this segment have continued to increase over time; for example, heavy-duty diesel vehicle emissions increased by about 41% between 2005 and 2019, rising from approximately 37 Mt CO_2e to 52 Mt CO_2e (Environment and Climate Change Canada, 2021).

Although global interest in electric medium- and heavy-duty vehicles (MHDVs), also known as electric trucks, has grown in recent years, large-scale adoption in Canada remains limited. Several jurisdictions have introduced sales targets for electric and other zero-emission MHDVs (Bhardwaj, 2026). Canada's 2030 Emissions Reduction Plan, for example, sets a target for 35% of new MHDV sales to be zero-emission by 2030 and 100% by 2040 (Canada, 2022; Transport Canada, 2024). However, the existing medium- and heavy-duty truck fleet in Canada remains largely dependent on conventional fuels (Statistics Canada, 2022b). Statistics Canada vehicle-registration data show that, up to 2024, most registered MHDVs continued to operate on diesel or gasoline (Statistics Canada, 2022b). Battery-electric, hybrid-electric, plug-in hybrid-electric, and other fuel types represented only a very small share of medium-duty vehicles and were not reported for heavy-duty trucks in the dataset (Statistics Canada, 2022b). This indicates that surface freight decarbonization is still in its early stages and that large-scale emissions reductions will require substantial fleet turnover, infrastructure

investment, and policy support. Zero-emission vehicles (ZEVs) are defined as vehicles that do not produce tailpipe emissions or have the potential to operate without tailpipe emissions. The main types of ZEVs include battery-electric vehicles (BEVs), plug-in hybrid electric vehicles (PHEVs), and hydrogen fuel-cell vehicles (FCVs) (Government of Canada, 2023).

F.1.1 Battery-electric vehicles:

Battery-electric trucks use rechargeable batteries to power an electric motor and produce no tailpipe emissions during operation (Eelco et al., 2013; Government of Canada, 2023). They are most suitable for urban, regional, and return-to-base operations, where daily travel distances are shorter and depot charging is feasible (Eelco et al., 2013). Previous literature shows that battery-electric trucks can reduce life cycle GHG emissions relative to diesel trucks, with reported reductions ranging from 12% in carbon-intensive or near-term scenarios to more than 90% in regions with low-carbon electricity or future decarbonized electricity systems. The magnitude of reduction is highly context dependent, particularly on electricity generation mix, battery production emissions, vehicle duty cycle, operating range, and charging infrastructure availability (Booto et al., 2021; Jahangir Samet et al., 2023; Lyu et al., 2023; Piepenbrink et al., 2025; Sen et al., 2017; Smit et al., 2024; Z. Wu et al., 2018). In addition, the application of battery-electric trucks to long-haul freight remains constrained because large battery packs can increase vehicle weight, reduce payload capacity, and require high-power charging or corridor-level charging infrastructure (Eelco et al., 2013).

F.1.2 Hydrogen fuel-cell vehicles:

Hydrogen fuel-cell trucks use hydrogen to generate electricity onboard, which then powers an electric motor (Eelco et al., 2013; Government of Canada, 2023). They are considered zero-emission vehicles because they produce no tailpipe emissions during operation, other than water vapor and warm air (Government of Canada, 2023). Previous studies show that hydrogen fuel-cell trucks can reduce life cycle or well-to-wheel GHG emissions relative to diesel trucks, with reported reductions ranging from about 20-45% for hydrogen produced from steam methane reforming to more than 50% when low-carbon or renewable hydrogen pathways are used (Booto et al., 2021; Cabrera-Jiménez et al., 2025; Lee et al., 2018; Liu et al., 2021; Ren et al., 2022; Yeow et al., 2022). Although hydrogen fuel-cell trucks may be particularly suitable for heavier-duty and long-haul applications because they can provide longer driving ranges and shorter refueling times than battery-electric trucks, large-scale

deployment remains constrained by high fuel-cell and hydrogen costs, durability concerns, onboard hydrogen storage requirements, and the need for dedicated refueling infrastructure. (Eelco et al., 2013)

F.1.3 Plug-in hybrid electric vehicles:

Plug-in hybrid electric trucks combine a rechargeable battery with a conventional internal combustion engine, allowing them to operate in electric-only mode for part of a trip. In this mode, they produce no tailpipe emissions (Government of Canada, 2023). They are often viewed as a transitional pathway between conventional diesel trucks and fully battery-electric trucks (Eelco et al., 2013; Mancaruso et al., 2024). PHEVs require smaller batteries than fully battery-electric trucks and can maintain longer driving ranges by using both grid electricity and a combustion engine. Existing studies show that PHEVs can reduce CO_2e emissions compared with conventional diesel trucks. However, their emissions benefits depend strongly on battery size, charging behavior, duty cycle, electricity grid mix, fuel pathway, and vehicle control strategy (Mancaruso et al., 2024; Martinez-Boggio et al., 2023; van den Oever et al., 2023)

F.2 Rail freight decarbonization pathways

Rail freight is widely recognized as one of the most energy-efficient and lowest-emissions freight modes in Canada. On a tonne-kilometre basis, rail carries about 44% of domestic freight, compared with 33% by truck, while producing only about 4% of Canada's transportation-related GHG emissions (The Delphi Group & Pollution Probe, 2022). Most rail-sector emissions, approximately 93%, come from freight rail operations (Environment and Climate Change Canada, 2021). Since 1990, Canadian railways have reduced emissions intensity through locomotive upgrades and operational efficiency improvements, with freight rail emissions intensity declining by more than 40% and intercity passenger rail emissions intensity declining by about 55% (Railway Association of Canada, 2020; The Delphi Group & Pollution Probe, 2022). However, these efficiency gains alone are not sufficient to achieve deep decarbonization or net-zero targets (The Delphi Group & Pollution Probe, 2022).

The *Towards Net Zero: Developing a Rail Decarbonization Roadmap for Canada* report, developed with support from Transport Canada and the Railway Association of Canada, identifies three

overlapping phases for rail decarbonization: continued efficiency improvements, low-carbon fuels, and alternative propulsion technologies (The Delphi Group & Pollution Probe, 2022). Since efficiency measures have already played a major role and are unlikely to deliver deep reductions on their own, this subsection focuses on the latter two pathways. It briefly reviews low-carbon fuel alternatives, such as biodiesel and renewable diesel, as well as alternative propulsion options, including battery-electric and hydrogen fuel-cell locomotives.

F.2.1 Biodiesel:

Biodiesel is produced from fats and oils through transesterification and is commonly derived from vegetable oils, used cooking oil, yellow grease, and animal fats (Mandegari et al., 2023). Biodiesel offers several advantages over conventional petroleum diesel, including its renewable origin, biodegradability, compatibility with existing diesel engines at approved blend levels, and potential GHG emissions reductions (Mohd Noor et al., 2018). However, its use also presents several limitations, including variability in fuel quality, poorer cold-weather performance, higher cost relative to petroleum diesel, and competition with food production (Mohd Noor et al., 2018).

Biodiesel is commonly blended with petroleum diesel at relatively low blend levels, such as B2, B5, or B20 (Mohd Noor et al., 2018). Although neat biodiesel (B100) can provide significant CO_2 emissions reductions, with reported reductions of up to approximately 80%, its use in rail has been limited. This is partly due to OEM warranty restrictions, as many manufacturers limit biodiesel blends to B5, although Progress Rail has approved B20 for some locomotive engines in the United States (Mandegari et al., 2023; The Delphi Group & Pollution Probe, 2022). In Canada, cold-weather performance also remains an important barrier to wider biodiesel deployment (The Delphi Group & Pollution Probe, 2022).

F.2.2 Renewable diesel:

Renewable diesel is a low-carbon diesel substitute produced from lipid-based feedstocks, such as vegetable oils, animal fats, and used cooking oils (van Dyk et al., 2019). Because its properties are similar to petroleum diesel, it can be blended with conventional diesel or used as a direct substitute in existing diesel engines and fueling infrastructure with limited modifications (Mandegari et al., 2023; Ram & Rafael, 2020; Schlunk & Shurland, 2022). Wider deployment in Canadian rail is, however,

constrained by original equipment manufacturer warranty restrictions; while Progress Rail in the United States has approved the use of neat renewable diesel in certain locomotive models, most OEM warranties applicable to the Canadian fleet currently cap renewable diesel blending at 20% (Mandegari et al., 2023; Schlunk & Shurland, 2022).

Although renewable diesel has been shown to provide significant GHG reductions, the magnitude of these reductions depends strongly on the feedstock and conversion process (Huang et al., 2025; Mandegari et al., 2023). Its wider deployment in the rail sector is also constrained by several challenges, including higher costs relative to conventional diesel and competition with other long-distance transport sectors, such as trucking, marine transport, and aviation, for lipid-based feedstocks (Mandegari et al., 2023). In the Canadian context, renewable diesel is reported to be more chemically similar to petroleum diesel and to offer better cold-weather performance than biodiesel. However, at the time of the 2022 report, deployment remained limited by domestic availability, as Canada had no large-scale renewable diesel production facilities and relied mainly on imports from the United States, Finland, the Netherlands, and Singapore (The Delphi Group & Pollution Probe, 2022).

F.2.3 Battery-electric and hydrogen fuel-cells:

Alternative propulsion technologies, including battery-electric and hydrogen fuel-cell locomotives, are considered potential long-term pathways for rail decarbonization. The Canadian rail roadmap indicates that these technologies are technically feasible, but their relative suitability remains uncertain and depends on continued development, testing, infrastructure requirements, and cost (The Delphi Group & Pollution Probe, 2022). Battery-electric rail systems use onboard batteries to supply traction power, allowing trains to operate without relying entirely on continuous external electricity from overhead wires or third-rail systems (The Delphi Group & Pollution Probe, 2022). These systems are similar to conventional electric trains but require additional onboard battery storage, power conversion equipment, and battery temperature-management systems (The Delphi Group & Pollution Probe, 2022). Battery-electric rail can provide lower operating costs, reduced local air pollution and noise and large GHG reductions, especially when powered by low-carbon electricity. However, wider use in freight rail is limited by high capital costs, battery weight and range constraints, charging infrastructure needs, long charging times, and safety/regulatory requirements,

and dependence on the carbon intensity of the electricity grid (Barbosa, 2022; Kapetanović et al., 2024; Popovich et al., 2021; The Delphi Group & Pollution Probe, 2022).

Hydrogen fuel-cell rail systems use onboard hydrogen, fuel cells, and batteries to generate electricity for traction power (The Delphi Group & Pollution Probe, 2022). They offer potential long-term emissions reductions because they produce no direct emissions during operation and can achieve large lifecycle GHG reductions when supplied with green hydrogen (Hollanda & Miranda, 2024; Knibbe et al., 2022; Zenith et al., 2020). They are generally considered more suitable for yard, switcher, and passenger applications, where refueling can occur at fixed locations and duty cycles are more manageable (The Delphi Group & Pollution Probe, 2022). However, their application to mainline freight remains uncertain due to high costs, hydrogen storage requirements, low volumetric energy density, limited refueling infrastructure, regulatory challenges, and the dependence of lifecycle emissions on the hydrogen production pathway (Knibbe et al., 2022; The Delphi Group & Pollution Probe, 2022).

Appendix G: Population Data for CMA and CA Cities

This appendix presents annual population estimates for the 55 Canadian cities in the origin-destination dataset that are classified by Statistics Canada as either a Census Metropolitan Area (CMA) or a Census Agglomeration (CA). Only cities that appear directly in Statistics Canada Table 17-10-0148-01 are included in table G-1. For Ottawa, the Ontario portion of the Ottawa-Gatineau CMA is reported. For Sudbury, the Greater Sudbury CMA boundary is used. For Sydney (NS), Statistics Canada reports this area as the Cape Breton CA.

Table G 1. Annual Population for CMA and CA Cities in the Origin-Destination Dataset

City	Province	Type	2019	2020	2021	2022	2023
Census Metropolitan Areas (CMA) - 34 cities							
Abbotsford	British Columbia	CMA	201,792	203,004	204,670	207,369	214,099
Calgary	Alberta	CMA	1,503,295	1,528,262	1,540,242	1,586,947	1,678,702
Edmonton	Alberta	CMA	1,438,636	1,461,697	1,472,402	1,499,878	1,559,106
Fredericton	New Brunswick	CMA	109,092	110,168	111,017	114,495	118,800
Grande Prairie	Alberta	CMA	67,497	67,514	66,628	66,026	67,811
Halifax	Nova Scotia	CMA	462,737	473,565	482,144	498,943	517,981
Kamloops	British Columbia	CMA	116,906	118,389	119,049	122,117	125,546
Kelowna	British Columbia	CMA	220,517	226,205	232,150	239,748	246,766
Kingston	Ontario	CMA	176,279	178,343	179,707	184,063	188,247
Lethbridge	Alberta	CMA	125,885	127,455	128,503	130,751	134,714
London	Ontario	CMA	548,743	559,067	567,539	585,834	606,986
Medicine Hat	Alberta	CMA	78,781	78,847	78,780	79,051	80,065
Moncton	New Brunswick	CMA	155,078	158,135	161,376	168,581	178,599
Montreal	Quebec	CMA	4,327,976	4,356,853	4,330,143	4,374,055	4,483,155

Nanaimo	British Columbia	CMA	117,004	118,556	120,213	122,968	125,591
North Bay	Ontario	CMA	73,645	73,974	74,521	76,774	79,745
Ottawa	Ontario	CMA	348,380	352,896	355,971	359,041	364,106
Prince George	British Columbia	CMA	93,530	94,041	93,542	94,767	96,931
Quebec	Quebec	CMA	832,966	840,396	844,774	858,197	878,116
Regina	Saskatchewan	CMA	256,646	257,598	257,368	260,515	271,516
Saguenay-Bagotville	Quebec	CMA	161,894	162,285	162,376	164,255	166,854
Saint John	New Brunswick	CMA	131,349	132,226	133,140	135,557	139,095
Sarnia	Ontario	CMA	100,975	101,233	101,251	104,135	106,371
Saskatoon	Saskatchewan	CMA	323,519	327,547	328,256	335,938	352,436
Sault Ste Marie	Ontario	CMA	80,527	80,757	80,202	81,955	84,741
St John's	Newfoundland and Labrador	CMA	217,821	219,282	220,052	224,712	232,699
St-Hyacinthe	Quebec	CMA	59,500	59,800	57,239	60,500	61,000
Sudbury	Ontario	CMA	175,351	176,580	177,415	180,100	185,005
Thunder Bay	Ontario	CMA	128,291	128,815	128,040	128,931	131,031
Toronto	Ontario	CMA	6,426,293	6,491,939	6,472,951	6,582,012	6,837,468
Vancouver	British Columbia	CMA	2,715,494	2,750,966	2,771,430	2,853,203	2,981,253
Victoria	British Columbia	CMA	403,868	409,898	414,596	426,397	434,085
Windsor	Ontario	CMA	433,979	438,328	439,473	452,394	468,529
Winnipeg	Manitoba	CMA	847,015	852,805	860,237	875,837	910,729
Census Agglomerations (CA) - 21 cities							
Baie-Comeau	Quebec	CA	26,892	26,719	26,730	26,661	26,571
Bathurst	New Brunswick	CA	31,720	31,799	31,876	32,184	32,636
Brandon	Manitoba	CA	55,465	55,816	55,877	56,975	59,097

Campbell River	British Columbia	CA	41,266	41,722	42,231	43,175	43,421
Charlottetown	Prince Edward Island	CA	80,008	81,853	83,104	86,412	90,528
Cranbrook	British Columbia	CA	27,932	28,034	28,197	28,612	29,269
Fort St John	British Columbia	CA	30,161	30,162	30,216	30,117	30,385
Gander	Newfoundland and Labrador	CA	13,628	13,677	13,817	13,849	14,112
Penticton	British Columbia	CA	47,564	48,349	48,924	49,426	49,533
Powell River	British Columbia	CA	17,869	18,107	18,381	18,650	18,852
Prince Rupert	British Columbia	CA	14,043	14,039	14,181	14,118	14,122
Rouyn-Noranda	Quebec	CA	42,738	42,667	42,565	42,677	42,832
Sept-Iles	Quebec	CA	27,904	27,895	27,892	27,811	27,815
Sydney	Nova Scotia	CA	102,560	102,356	100,754	103,110	109,271
Terrace	British Columbia	CA	20,153	20,378	20,496	20,738	21,215
Thompson	Manitoba	CA	13,691	13,408	13,459	13,405	13,264
Timmins	Ontario	CA	43,001	42,984	42,763	43,108	44,790
Val d'Or	Quebec	CA	34,089	34,208	34,234	34,292	34,421
Whitehorse	Yukon	CA	32,498	33,332	34,233	35,235	36,743
Williams Lake	British Columbia	CA	24,285	24,378	24,532	24,883	25,029
Yellowknife	Northwest Territories	CA	21,491	21,658	21,904	22,147	22,481

CMA = Census Metropolitan Area; CA = Census Agglomeration

Appendix H: Supplementary City-Level Population Data for the Origin-Destination Dataset

This appendix presents population estimates for the 42 cities in the Origin-Destination dataset that do not appear in Statistics Canada Table 17-10-0148-01.

Table H 1 Supplementary Population Estimates and Data Sources for Cities and Years Not Covered by Statistics Canada

City	Province	2019	2020	2021	2022	2023
Arctic Bay	Nunavut	963	998	1,032	1,066	1,114
Baker Lake	Nunavut	2,167	2,187	2,206	2,226	2,236
Bella Coola	British Columbia	890	911	933	955	998
Cambridge Bay	Nunavut	1,888	1,901	1,915	1,929	1,982
Castlegar	British Columbia	8,595	8,702	8,808	8,915	9,071
Churchill	Manitoba	916	895	874	853	888
Clyde River	Nunavut	668	668	669	669	695
Comox	British Columbia	14,981	15,134	15,288	15,441	15,702
Dawson City	Yukon	2,263	2,217	2,320	2,351	2,380
Deer Lake	Newfoundland and Labrador	5,203	5,149	5,094	5,039	5,059
Flin Flon	Manitoba	5,084	5,061	5,037	5,014	4,909
Fort MacKay	Alberta	649	646	642	639	654
Fort McMurray	Alberta	75,009	74,270	68,002	74,809	76,000

City	Province	2019	2020	2021	2022	2023
Fort Simpson	Northwest Territories	1,310	1,313	1,316	1,319	1,316
Gaspe	Quebec	14,860	14,969	15,077	15,185	15,362
Gillam	Manitoba	1,100	1,067	1,035	1,003	969
Gjoa Haven	Nunavut	1,411	1,427	1,442	1,458	1,429
Goose Bay	Newfoundland and Labrador	8,303	8,276	8,248	8,220	8,209
Grise Fiord	Nunavut	146	150	155	159	162
Hay River	Northwest Territories	3,584	3,512	3,440	3,368	3,359
Iles de La Madeleine	Quebec	12,101	12,210	12,320	12,429	12,455
Inuvik	Northwest Territories	3,394	3,373	3,351	3,330	3,306
Iqaluit	Nunavut	8,300	8,400	7,429	8,600	8,428
Kinngait	Nunavut	1,532	1,537	1,543	1,548	1,559
Kugluktuk	Nunavut	1,513	1,513	1,514	1,515	1,497
Kuujjuaq	Quebec	2,749	2,750	2,750	2,751	2,735
Masset	British Columbia	859	876	894	912	915
Mont-Joli	Quebec	6,329	6,375	6,420	6,465	6,455
Norman Wells	Northwest Territories	797	782	766	751	725
Old Crow	Yukon	228	232	236	238	240
Pangnirtung	Nunavut	1,545	1,575	1,604	1,633	1,605

City	Province	2019	2020	2021	2022	2023
Pond Inlet	Nunavut	1,688	1,700	1,713	1,725	1,708
Port Hardy	British Columbia	4,253	4,240	4,226	4,213	4,181
Qikiqtarjuaq	Nunavut	628	639	649	659	670
Rankin Inlet	Nunavut	3,119	3,173	3,226	3,280	3,280
Sandspit	British Columbia	304	307	310	312	315
Sioux Lookout	Ontario	5,786	5,885	5,983	6,081	6,086
Smithers	British Columbia	5,476	5,427	5,378	5,410	5,450
Taloyoak	Nunavut	1,021	1,022	1,023	1,024	1,041
The Pas	Manitoba	5,676	5,722	5,767	5,813	5,773
Ulukhaktok	Northwest Territories	401	405	408	440	471
Wabush	Newfoundland and Labrador	1,980	2,008	2,036	2,064	2,077

Appendix I: Provincial GDP Inputs Used for City-Level GDP Estimation

This appendix presents provincial and territorial GDP inputs for 2019-2023 at basic prices for all industries, reported in millions of current Canadian dollars. Values for 2019-2022 are official Statistics Canada figures retrieved from Table 36-10-0711-01 via the StatCan API. The 2023 values are estimated because complete current-dollar GDP figures were unavailable. The 2023 nominal GDP growth rate was estimated using the Fisher equation shown in section 3.2.3.1, using the province-specific 2023 real GDP growth rates reported by Statistics Canada and an assumed CPI inflation rate of 3.9%.

Table I 1. Provincial and Territorial GDP Used for City-Level GDP Estimation, 2019-2023

Province / Territory	2019	2020	2021	2022	2023 (est.)
Newfoundland and Labrador	33,159.5	29,626.5	35,730.4	39,102.4	39,611.7
Prince Edward Island	6,778.3	6,810.4	7,760.6	8,602.0	9,080.5
Nova Scotia	42,703.6	42,217.8	46,618.2	50,952.8	53,628.2
New Brunswick	34,495.2	33,820.4	37,290.0	40,416.7	42,538.9
Quebec	425,277.0	420,699.4	468,856.5	512,822.6	544,544.8
Ontario	833,628.9	820,962.5	903,203.1	987,790.7	1,061,209.2
Manitoba	69,243.3	67,965.2	73,459.4	81,892.1	86,192.0
Saskatchewan	79,002.0	72,672.0	82,682.3	110,789.5	115,340.5
Alberta	339,674.6	290,154.2	366,736.1	456,439.6	481,354.4
British Columbia	286,182.3	287,202.1	330,874.0	372,203.6	392,907.1

Province / Territory	2019	2020	2021	2022	2023 (est.)
Yukon	2,960.0	3,131.2	3,495.9	3,739.4	3,947.4
Northwest Territories	4,502.9	4,017.5	4,577.2	5,121.0	5,315.4
Nunavut	3,507.1	3,993.1	4,323.3	4,310.2	4,550.0

Appendix J: City-Level GDP Estimates

This appendix presents the estimated city-level GDP inputs for the 97 cities represented in the CargoIS dataset and used in the gravity model estimation.

Table J 1. Annual Origin- and Destination-City GDP Estimates Used in the Gravity Model, 2019-2023

City	2019	2020	2021	2022	202
Alberta					
Calgary	$111,259,000,000	$102,663,000,000	$115,136,000,000	$121,008,000,000	$122,823,000,000
Edmonton	$91,568,000,000	$87,484,000,000	$93,271,000,000	$98,027,820,000	$99,498,240,000
Fort McKay	$52,000,000	$54,652,000	$55,471,780	$58,245,000	$59,990,000
Fort McMurray	$5,946,637,000	$5,067,194,000	$6,362,771,000	$6,687,272,000	$6,787,581,000
Grande Prairie	$5,272,369,000	$4,447,621,000	$5,513,469,000	$5,794,656,000	$5,881,576,000
Lethbridge	$6,743,000,000	$6,785,000,000	$7,071,000,000	$7,768,000,000	$8,192,016,280
Medicine Hat	$6,147,543,000	$5,194,205,000	$6,519,341,000	$6,851,827,000	$6,954,604,000
British Columbia					
Abbotsford	$8,148,000,000	$8,367,000,000	$9,294,000,000	$9,628,584,000	$9,782,641,000
Bella Coola	$237,599,900	$237,599,900	$136,700,000	$141,621,200	$143,887,139
Campbell River	$2,230,000,000	$2,150,000,000	$2,580,000,000	$2,683,000,000	$2,725,000,000
Castlegar	$467,863,000	$472,267,000	$545,208,000	$564,835,000	$573,873,000
Comox	$3,567,442,000	$3,578,728,000	$4,153,659,000	$4,303,191,000	$4,372,042,000
Cranbrook	$1,567,325,000	$1,557,592,000	$1,787,584,000	$1,851,937,000	$1,881,568,000

City	2019	2020	2021	2022	202
Fort St John	$1,692,399,000	$1,675,826,000	$1,915,581,000	$1,984,542,000	$2,016,295,000
Kamloops	$6,011,174,000	$6,027,617,000	$6,916,000,000	$7,164,976,000	$7,279,616,000
Kelowna	$10,911,000,000	$11,267,000,000	$12,278,000,000	$12,720,010,000	$12,923,530,000
Masset	$134,000,000	$138,422,000	$53,000,000	$54,908,000	$55,786,528
Nanaimo	$4,987,077,000	$5,003,578,000	$5,789,000,000	$5,997,404,000	$6,093,362,000
Penticton	$2,668,918,000	$2,686,310,000	$3,101,598,000	$3,213,256,000	$3,264,668,000
Port Hardy	$231,855,000	$227,799,000	$253,585,000	$262,714,000	$266,918,000
Powell River	$1,021,904,700	$999,444,300	$1,122,975,000	$1,224,042,700	$1,257,732,000
Prince George	$5,248,169,000	$5,224,995,000	$5,930,213,000	$6,143,700,000	$6,241,999,000
Prince Rupert	$787,983,000	$780,018,000	$899,022,000	$931,387,000	$946,289,000
Sandspit	$16,609,000	$16,668,000	$19,019,000	$19,704,000	$20,019,000
Smithers	$300,256,000	$300,028,000	$342,340,000	$354,664,000	$360,339,000
Terrace	$1,130,828,000	$1,132,218,000	$1,299,370,000	$1,346,147,000	$1,367,685,000
Vancouver	$163,475,000,000	$163,772,000,000	$183,140,000,000	$189,733,000,000	$192,769,000,000
Victoria	$22,758,000,000	$22,517,000,000	$24,285,000,000	$25,159,260,000	$25,561,810,000
Williams Lake	$646,759,619	$634,928,420	$691,900,000	$716,808,400	$728,277,334
Manitoba					
Brandon	$2,900,000,000	$2,750,000,000	$2,900,000,000	$3,013,100,000	$3,052,270,300

City	2019	2020	2021	2022	202
Churchill	$46,248,500	$42,797,400	$44,115,000	$46,455,000	$47,430,000
Flin Flon	$257,949,000	$240,143,000	$250,207,000	$263,480,000	$269,010,000
Gillam	$61,475,000	$53,247,000	$50,931,000	$53,633,000	$54,757,000
The Pas	$290,140,000	$271,468,000	$286,122,000	$300,302,000	$306,600,000
Thompson	$697,450,000	$645,130,000	$660,220,000	$694,415,000	$709,000,000
Winnipeg	$46,301,000,000	$45,005,000,000	$48,388,000,000	$50,275,130,000	$50,928,710,000
New Brunswick					
Bathurst	$1,408,526,000	$1,376,874,000	$1,506,105,000	$1,533,215,000	$1,553,147,000
Fredericton	$5,805,212,000	$5,716,493,000	$6,286,000,000	$6,399,148,000	$6,482,337,000
Moncton	$8,149,000,000	$8,089,000,000	$8,893,000,000	$9,053,074,000	$9,170,764,000
Saint John	$6,521,000,000	$6,367,000,000	$6,800,000,000	$6,922,400,000	$7,012,391,000
Newfoundland and Labrador					
Deer Lake	$333,838,000	$295,169,000	$348,502,000	$342,578,000	$334,013,000
Gander	$866,746,000	$776,351,000	$944,167,000	$928,116,000	$904,913,000
Goose Bay	$515,735,000	$465,459,000	$567,170,000	$557,528,000	$543,590,000
St John's	$13,272,000,000	$12,912,000,000	$13,744,000,000	$13,510,350,000	$13,172,590,000
Wabush	$124,911,000	$107,850,000	$129,834,000	$127,627,000	$124,436,000

City	2019	2020	2021	2022	202
Northwest Territories					
Fort Simpson	$129,450,000	$110,961,000	$108,459,000	$121,290,000	$121,900,000
Hay River	$379,000,000	$327,241,000	$309,580,000	$349,438,000	$351,195,000
Inuvik	$362,980,000	$310,105,000	$306,633,000	$344,950,000	$346,685,000
Norman Wells	$69,657,300	$68,109,400	$77,395,000	$89,004,200	$88,230,300
Ulukhaktok	$41,000,000	$37,000,000	$38,000,000	$40,500,000	$41,300,000
Yellowknife	$2,172,402,000	$1,955,104,000	$2,249,576,000	$2,283,320,000	$2,281,036,000
Nova Scotia					
Halifax	$24,098,000,000	$24,447,000,000	$26,967,000,000	$27,668,140,000	$28,027,830,000
Sydney	$4,529,740,000	$4,420,927,000	$4,751,877,000	$4,875,426,000	$4,938,806,000
Nunavut					
Arctic Bay	$106,878,299	$108,267,717	$110,000,000	$111,100,000	$111,655,500
Baker Lake	$237,599,900	$237,599,900	$269,991,000	$302,389,900	$337,488,700
Cambridge Bay	$188,494,454	$190,944,882	$194,000,000	$195,940,000	$196,919,700
Clyde River	$124,367,475	$125,984,252	$128,000,000	$129,280,000	$129,926,400
Gjoa Haven	$136,773,000	$136,312,000	$149,218,000	$161,593,000	$168,210,000
Grise Fiord	$14,336,635	$13,341,900	$15,937,507	$17,448,243	$18,189,753
Iqaluit	$802,558,861	$812,992,126	$826,000,000	$834,260,000	$838,431,300

City	2019	2020	2021	2022	202
Kinngait	$177,900,000	$180,700,000	$183,700,000	$186,639,200	$192,984,933
Kugluktuk	$159,317,400	$159,317,400	$181,042,000	$202,767,000	$226,302,500
Pangnirtung	$173,382,400	$173,382,400	$197,024,000	$220,666,800	$246,280,000
Pond Inlet	$163,285,000	$160,142,000	$174,174,000	$188,620,000	$196,345,000
Qikiqtarjuaq	$61,582,000	$60,980,000	$65,764,000	$71,220,000	$74,137,000
Rankin Inlet	$303,450,000	$299,985,000	$329,800,000	$357,148,000	$371,775,000
Taloyoak	$106,000,000	$107,696,000	$111,357,664	$115,250,000	$118,130,000
Ontario					
Kingston	$9,409,000,000	$9,218,000,000	$10,132,000,000	$10,496,750,000	$10,664,700,000
London	$29,040,000,000	$27,492,000,000	$31,368,000,000	$34,502,000,000	$35,156,000,000
North Bay	$4,232,053,000	$4,117,981,000	$4,534,733,000	$4,697,983,000	$4,773,151,000
Ottawa	$73,878,000,000	$74,821,000,000	$82,014,000,000	$84,966,500,000	$86,325,970,000
Sarnia	$5,786,872,000	$5,635,433,000	$6,161,300,000	$6,383,107,000	$6,485,236,000
Sault Ste Marie	$4,614,998,000	$4,496,133,000	$4,880,431,000	$5,056,127,000	$5,137,025,000
Sioux Lookout	$356,712,900	$345,329,800	$379,481,800	$413,635,100	$428,814,400
Sudbury	$10,142,000,000	$9,713,000,000	$10,324,000,000	$10,695,660,000	$10,866,790,000
Thunder Bay	$6,554,000,000	$6,247,000,000	$7,256,000,000	$7,517,216,000	$7,637,491,000
Timmins	$2,464,385,000	$2,392,831,000	$2,602,203,000	$2,695,882,000	$2,739,016,000

City	2019	2020	2021	2022	202
Toronto	$442,180,000,000	$430,935,000,000	$473,663,000,000	$490,715,000,000	$498,566,000,000
Windsor	$16,359,000,000	$16,420,000,000	$18,026,000,000	$18,674,940,000	$18,973,730,000
Prince Edward Island					
Charlottetown	$3,431,742,000	$3,473,621,000	$3,925,134,000	$4,038,963,000	$4,127,820,000
Quebec					
Baie-Comeau	$1,345,615,000	$1,315,034,000	$1,462,239,000	$1,500,257,000	$1,503,257,000
Gaspe	$731,398,000	$723,493,000	$809,620,000	$830,670,000	$832,331,000
Iles de la Madeleine	$602,971,000	$595,528,000	$667,389,000	$684,741,000	$686,111,000
Kuujjuaq	$135,238,000	$122,100,000	$132,000,000	$145,300,000	$148,800,000
Mont-Joli	$315,342,000	$310,068,000	$350,106,000	$359,209,000	$359,927,000
Montreal	$233,996,000,000	$228,707,000,000	$253,901,000,000	$260,502,000,000	$261,023,000,000
Quebec	$48,544,000,000	$47,935,000,000	$52,555,000,000	$53,921,430,000	$54,029,270,000
Rouyn-Noranda	$2,145,694,000	$2,099,949,000	$2,328,477,000	$2,389,018,000	$2,393,796,000
Saguenay-Bagotville	$8,364,000,000	$8,509,000,000	$10,143,000,000	$10,406,720,000	$10,427,530,000
Sept-Iles	$1,400,942,000	$1,372,913,000	$1,525,805,000	$1,565,476,000	$1,568,607,000
St-Hyacinthe	$2,940,000,000	$2,850,000,000	$3,200,000,000	$3,456,000,000	$3,628,000,000
Val d'Or	$1,711,464,000	$1,683,621,000	$1,872,191,000	$1,920,868,000	$1,924,709,000

City	2019	2020	2021	2022	202
Saskatchewan					
Regina	$18,460,000,000	$17,462,000,000	$19,637,000,000	$20,756,310,000	$21,088,410,000
Saskatoon	$20,691,000,000	$20,196,000,000	$21,859,000,000	$23,104,960,000	$23,474,640,000
Yukon					
Dawson City	$134,000,000	$138,422,000	$134,000,000	$143,333,505	$151,306,288
Old Crow	$17,018,793	$18,003,124	$20,100,000	$20,763,300	$21,095,513
Whitehorse	$2,344,139,000	$2,494,025,000	$2,804,550,000	$2,897,100,000	$2,943,454,000

Appendix K: Provincial and Territorial GDP Growth Rates and Projection Sources, 2023-2050

This appendix presents the sources and assumptions used to develop provincial and territorial GDP growth rates for the 2023-2050 forecast period. Historical 2023 growth rates are obtained from Statistics Canada. Near- and medium-term projections are compiled from provincial and territorial fiscal plans and budget reports, supplemented by forecasts from major Canadian banks where necessary. Long-term growth rates are based primarily on the Parliamentary Budget Officer's Fiscal Sustainability Report. The first table presents annual GDP growth rates for 2024-2036, while the second table presents growth rates for 2037-2050.

Table K 1. Annual real GDP growth rates (%) by province and territory, 2024-2036

Province / Territory	2024	2025	2026	2027	2028	2029	2030	2031	2032	2033	2034	2035	2036
Alberta	+2.70%	+1.80%	+1.70%	+2.10%	+2.20%	+2.20%	+2.20%	+2.20%	+2.20%	+2.20%	+2.20%	+2.20%	+2.20%
British Columbia	+1.20%	+1.50%	+1.30%	+2.10%	+2.10%	+2.10%	+1.10%	+1.10%	+1.10%	+1.10%	+1.10%	+1.10%	+1.10%
Manitoba	+1.10%	+1.00%	+1.20%	+1.90%	+1.80%	+1.80%	+1.80%	+1.80%	+1.80%	+1.80%	+1.80%	+1.80%	+1.80%
New Brunswick	+1.80%	+1.10%	+1.30%	+1.50%	+1.50%	+1.50%	+0.90%	+0.90%	+0.90%	+0.90%	+0.90%	+0.90%	+0.90%
Newfoundland and Labrador	+3.40%	+3.30%	+1.40%	+0.90%	+1.00%	+1.00%	+1.00%	+1.00%	+1.00%	+1.00%	+1.00%	+1.00%	+1.00%
Northwest Territories	-1.10%	-4.70%	+1.60%	+1.60%	+1.60%	+1.60%	+1.60%	+1.60%	+1.60%	+1.60%	+1.60%	+1.60%	+1.60%
Nova Scotia	+2.70%	+1.40%	+1.70%	+0.90%	+0.90%	+0.90%	+0.90%	+0.90%	+0.90%	+0.90%	+0.90%	+0.90%	+0.90%
Ontario	+1.20%	+0.80%	+0.90%	+1.80%	+1.90%	+2.10%	+2.10%	+2.10%	+2.10%	+2.10%	+2.10%	+2.10%	+2.10%
Prince Edward Island	+3.60%	+2.20%	+1.40%	+1.60%	+1.50%	+1.50%	+1.50%	+1.50%	+1.50%	+1.50%	+1.50%	+1.50%	+1.50%
Quebec	+1.30%	+1.70%	+0.90%	+1.10%	+1.40%	+1.50%	+1.50%	+0.90%	+0.90%	+0.90%	+0.90%	+0.90%	+0.90%
Saskatchewan	+3.00%	+1.70%	+1.60%	+2.10%	+2.10%	+2.10%	+2.10%	+2.10%	+2.10%	+2.10%	+2.10%	+2.10%	+2.10%
Yukon	-3.30%	+1.60%	+1.60%	+1.60%	+1.60%	+1.60%	+1.60%	+1.60%	+1.60%	+1.60%	+1.60%	+1.60%	+1.60%
Nunavut	+7.50%	+1.60%	+1.60%	+1.60%	+1.60%	+1.60%	+1.60%	+1.60%	+1.60%	+1.60%	+1.60%	+1.60%	+1.60%

Table K 2. Annual real GDP growth rates (%) by province and territory, 2037-2050

Province / Territory	2037	2038	2039	2040	2041	2042	2043	2044	2045	2046	2047	2048	2049	2050
Alberta	+2.20%	+2.20%	+2.20%	+2.20%	+2.20%	+2.20%	+2.20%	+2.20%	+2.20%	+2.20%	+2.20%	+2.20%	+2.10%	+2.10%
British Columbia	+1.10%	+1.10%	+1.10%	+1.10%	+1.10%	+1.10%	+1.10%	+1.10%	+1.10%	+1.10%	+1.10%	+1.10%	+1.30%	+1.30%
Manitoba	+1.80%	+1.80%	+1.80%	+1.80%	+1.80%	+1.80%	+1.80%	+1.80%	+1.80%	+1.80%	+1.80%	+1.80%	+1.80%	+1.80%
New Brunswick	+0.90%	+0.90%	+0.90%	+0.90%	+0.90%	+0.90%	+0.90%	+0.90%	+0.90%	+0.90%	+0.90%	+0.90%	+1.00%	+1.00%
Newfoundland and Labrador	+1.00%	+1.00%	+1.00%	+1.00%	+1.00%	+1.00%	+1.00%	+1.00%	+1.00%	+1.00%	+1.00%	+1.00%	+1.20%	+1.20%
Northwest Territories	+1.60%	+1.60%	+1.60%	+1.60%	+1.60%	+1.60%	+1.60%	+1.60%	+1.60%	+1.60%	+1.60%	+1.60%	+1.60%	+1.60%
Nova Scotia	+0.90%	+0.90%	+0.90%	+0.90%	+0.90%	+0.90%	+0.90%	+0.90%	+0.90%	+0.90%	+0.90%	+0.90%	+1.10%	+1.10%
Ontario	+2.10%	+2.10%	+2.10%	+2.10%	+2.10%	+2.10%	+2.10%	+2.10%	+2.10%	+2.10%	+2.10%	+2.10%	+2.10%	+2.10%
Prince Edward Island	+1.50%	+1.50%	+1.50%	+1.50%	+1.50%	+1.50%	+1.50%	+1.50%	+1.50%	+1.50%	+1.50%	+1.50%	+1.60%	+1.60%
Quebec	+0.90%	+0.90%	+0.90%	+0.90%	+0.90%	+0.90%	+0.90%	+0.90%	+0.90%	+0.90%	+0.90%	+0.90%	+1.20%	+1.20%
Saskatchewan	+2.10%	+2.10%	+2.10%	+2.10%	+2.10%	+2.10%	+2.10%	+2.10%	+2.10%	+2.10%	+2.10%	+2.10%	+2.00%	+2.00%
Yukon	+1.60%	+1.60%	+1.60%	+1.60%	+1.60%	+1.60%	+1.60%	+1.60%	+1.60%	+1.60%	+1.60%	+1.60%	+1.70%	+1.70%
Nunavut	+1.60%	+1.60%	+1.60%	+1.60%	+1.60%	+1.60%	+1.60%	+1.60%	+1.60%	+1.60%	+1.60%	+1.60%	+1.70%	+1.70%

Appendix L: Python Workflow for Extracting FlightAware Air-Route Distances

This appendix presents the Python-based automated workflow used to retrieve a representative non-stop flight observation for each OD pair from FlightAware. The script uses Selenium to open the route-search page, identify available scheduled airline flights, extract route distance, convert distance from miles to kilometers, and export the results to CSV and Excel files.

```
import time
import re
import pandas as pd
from selenium import webdriver
from selenium.webdriver.common.by import By
from selenium.webdriver.chrome.service import Service
from selenium.webdriver.support.ui import WebDriverWait
from selenium.webdriver.support import expected_conditions as EC
from selenium.common.exceptions import TimeoutException, NoSuchElementException
from webdriver_manager.chrome import ChromeDriverManager


# Configuration
BASE_URL     = "https://www.flightaware.com/live/findflight/"
HEADLESS     = False     # Keep False until confirmed working, then set True
WAIT_SEC     = 8         # Max wait (timeout) -page usually loads much faster
PAUSE_SEC    = 0.5       # Polite pause between requests
OUTPUT_CSV   = "od_distances_raw.csv"
OUTPUT_EXCEL = "od_distances_raw.xlsx"

# Set to True to dump page HTML on timeout (helps debug selectors)
DEBUG_ON_FAIL = True

# Skip the General Aviation filter click (saves a page reload per pair).
# The first result row is almost always a scheduled airline anyway, and
# get_first_flight_row() already skips non-airline rows.
APPLY_AIRLINE_FILTER = True

# Internal flag -dumps the flight detail page structure once for tuning
_detail_debug_done = False


# OD Pairs – Toronto to Vancouver is a sample OD pair
OD_PAIRS = [
   ("CYYZ", "CYVR", "Toronto”,      "Vancouver"),

]
```

```
#  Driver Setup
def init_driver(headless=False):
    opts = webdriver.ChromeOptions()
    if headless:
        opts.add_argument("--headless=new")
    opts.add_argument("--no-sandbox")
    opts.add_argument("--disable-dev-shm-usage")
    opts.add_argument("--window-size=1400,900")
    opts.add_argument("--disable-blink-features=AutomationControlled")
    opts.add_argument("--log-level=3")          # suppress DevTools noise
    opts.add_experimental_option("excludeSwitches", ["enable-automation", "enable-logging"])
    opts.add_experimental_option("useAutomationExtension", False)
    opts.add_argument(
        "user-agent=Mozilla/5.0 (Windows NT 10.0; Win64; x64) "
        "AppleWebKit/537.36 (KHTML, like Gecko) "
        "Chrome/124.0.0.0 Safari/537.36"
    )
    driver = webdriver.Chrome(
        service=Service(ChromeDriverManager().install()),
        options=opts
    )
    driver.execute_script(
        "Object.defineProperty(navigator, 'webdriver', {get: () => undefined})"
    )
    return driver


#  Wait Helper: any table or flight-list element
# FlightAware has changed its class names -we wait for ANY <table> or known
# container to appear, then inspect what we actually got.
RESULT_SELECTORS = [
    "table.prettyTable",
    "table.flightTable",
    "table",                        # any table at all
    "div.flightRow",
    "div[class*='flight']",
    "div[class*='result']",
]

def wait_for_results(driver):
    """Wait until any flight-result element appears. Returns True/False."""
    wait = WebDriverWait(driver, WAIT_SEC)
    for sel in RESULT_SELECTORS:
```

```
        try:
            wait.until(EC.presence_of_element_located((By.CSS_SELECTOR, sel)))
            time.sleep(0.6)   # brief settle for dynamic rows
            return True
        except TimeoutException:
            continue
    return False


# Load Results Page
def load_findflight(driver, origin_icao, dest_icao):
    url = f"{BASE_URL}?origin={origin_icao}&destination={dest_icao}"
    print(f"    → Loading: {url}")
    driver.get(url)
    ok = wait_for_results(driver)
    if not ok and DEBUG_ON_FAIL:
        # Dump page title and first 2000 chars of HTML for debugging
        print(f"    ✗ Page title: {driver.title}")
        print(f"    ✗ HTML snippet:\n{driver.page_source[:2000]}\n")
    return ok


# Airline-Only Filter
def select_airline_only(driver):
    """Uncheck General Aviation checkbox if present."""
    try:
        # Try multiple XPath approaches
        xpaths = [
            "//label[contains(text(),'General Aviation')]/../input[@type='checkbox']",
            "//label[contains(text(),'General Aviation')]/input[@type='checkbox']",
            "//input[@type='checkbox'][following-sibling::label[contains(text(),'General Aviation')]]",
            "//input[@type='checkbox'][preceding-sibling::label[contains(text(),'General Aviation')]]",
        ]
        for xp in xpaths:
            try:
                cb = driver.find_element(By.XPATH, xp)
                if cb.is_selected():
                    cb.click()
                    time.sleep(0.5)
                return
            except NoSuchElementException:
                continue
    except Exception:
        pass
```

```
# Discover Table Structure
def discover_and_print_table(driver):
    """Debug helper -prints first table found and its structure."""
    tables = driver.find_elements(By.TAG_NAME, "table")
    print(f"    ℹ Found {len(tables)} table(s) on page")
    for i, tbl in enumerate(tables[:3]):
        rows = tbl.find_elements(By.TAG_NAME, "tr")
        print(f"    Table {i}: {len(rows)} rows, class='{tbl.get_attribute('class')}'")
        for j, row in enumerate(rows[:4]):
            cells = row.find_elements(By.TAG_NAME, "td")
            ths   = row.find_elements(By.TAG_NAME, "th")
            texts = [c.text.strip()[:30] for c in (ths or cells)]
            print(f"      Row {j} ({len(cells)} td, {len(ths)} th): {texts}")


# Extract First Flight Row
def get_first_flight_row(driver):
    """
    Try multiple strategies to get the first airline flight row.
    Prints table structure on first call to help tune selectors.
    """
    # Strategy 1: any <tr> with 5+ <td> cells where first cell looks like an airline
    tables = driver.find_elements(By.TAG_NAME, "table")
    for tbl in tables:
        rows = tbl.find_elements(By.TAG_NAME, "tr")
        for row in rows:
            cells = row.find_elements(By.TAG_NAME, "td")
            if len(cells) >= 4:
                airline_text = cells[0].text.strip()
                # Skip empty rows, header rows, and non-airline rows
                if not airline_text or airline_text.lower() in (
                    "airline", "type", "flight", "status", ""
                ):
                    continue
                # The ident (flight number) is usually in cell[1] as a link
                ident_text = cells[1].text.strip() if len(cells) > 1 else ""
                ident_href = None
                try:
                    link = cells[1].find_element(By.TAG_NAME, "a")
                    ident_href = link.get_attribute("href")
                except NoSuchElementException:
                    pass

                if ident_text:
                    return {
```

```
                "airline":    airline_text,
                "ident":      ident_text,
                "ident_href": ident_href,
                "aircraft":   cells[2].text.strip() if len(cells) > 2 else "",
                "status":     cells[3].text.strip() if len(cells) > 3 else "",
                "departure":  cells[4].text.strip() if len(cells) > 4 else "",
                "arrival":    cells[5].text.strip() if len(cells) > 5 else "",
            }

    # Strategy 2: look for any element with a flight-number-like href
    links = driver.find_elements(By.XPATH, "//a[contains(@href,'/live/flight/')]")
    if links:
        href = links[0].get_attribute("href")
        ident = href.rstrip("/").split("/")[-1]
        # Try to get parent row context
        try:
            row = links[0].find_element(By.XPATH, "./ancestor::tr")
            cells = row.find_elements(By.TAG_NAME, "td")
            return {
                "airline":    cells[0].text.strip() if cells else "Unknown",
                "ident":      ident,
                "ident_href": href,
                "aircraft":   cells[2].text.strip() if len(cells) > 2 else "",
                "status":     cells[3].text.strip() if len(cells) > 3 else "",
                "departure":  cells[4].text.strip() if len(cells) > 4 else "",
                "arrival":    cells[5].text.strip() if len(cells) > 5 else "",
            }
        except NoSuchElementException:
            return {
                "airline": "Unknown", "ident": ident,
                "ident_href": href, "aircraft": "",
                "status": "", "departure": "", "arrival": "",
            }
    return None
# Flight Detail Page
def get_flight_details(driver, ident, ident_href=None):
    result = {"distance_km": None, "flight_time_min": None}
    try:
        if ident_href:
            driver.get(ident_href)
        else:
            driver.get(f"https://www.flightaware.com/live/flight/{ident}")

        # Single combined-selector wait instead of looping 7 separate waits.
        # Any one of these matching means the page has rendered enough.
```

```
    combined = (
        "div.flightPageSummaryTableContainer, div.flightSummaryContainer, "
        "section.flightPageSummary, div[class*='summary'], "
        "div[class*='Summary'], div[class*='flightPage'], "
        "div[class*='FlightPage']"
    )
    try:
        WebDriverWait(driver, WAIT_SEC).until(
            EC.presence_of_element_located((By.CSS_SELECTOR, combined))
        )
    except TimeoutException:
        pass   # proceed anyway; body text may still contain the data
    time.sleep(0.8)   # short settle for JS-rendered fields

except Exception as e:
    print(f"      Could not load detail page for {ident}: {e}")
    return result

# Read ONLY the visible text of the page body, not raw page_source.
# page_source contains FlightAware's JS localization dictionary
# (FP_Duration_Hours_Minutes etc.) which pollutes regex matches.
try:
    body_text = driver.find_element(By.TAG_NAME, "body").text
except Exception:
    body_text = ""

# DEBUG: dump visible-text distance/time context once
global _detail_debug_done
if DEBUG_ON_FAIL and not _detail_debug_done:
    _detail_debug_done = True
    print(f"      ── DETAIL PAGE DEBUG ({ident}) ──")
    print(f"      URL: {driver.current_url}")
    for line in body_text.split("\n"):
        low = line.lower()
        if any(k in low for k in ("distance", "direct", "takeoff", "landing",
                                  "gate departure", "gate arrival", " mi", " km")):
            if len(line.strip()) < 80:
                print(f"        · {line.strip()}")
    print(f"      ── END DEBUG ──")

# Distance
# FlightAware "Flight Data" section shows:  Distance  Direct: 2,082 mi
# (sometimes also "Planned: X mi"). We capture the Direct value in miles
# and convert to km. Falls back to any km value if present.
MI_TO_KM = 1.60934
```

```
def parse_distance(text):
    # 1. Preferred: "Direct: 2,082 mi"
    m = re.search(r'direct\s*:?\s*([\d,]+)\s*mi', text, re.IGNORECASE)
    if m:
        mi = int(m.group(1).replace(",", ""))
        if 0 < mi < 12000:
            return round(mi * MI_TO_KM)
    # 2. "Planned: X mi"
    m = re.search(r'planned\s*:?\s*([\d,]+)\s*mi', text, re.IGNORECASE)
    if m:
        mi = int(m.group(1).replace(",", ""))
        if 0 < mi < 12000:
            return round(mi * MI_TO_KM)
    # 3. Any "Distance ... N mi"
    m = re.search(r'distance[^\d]{0,40}?([\d,]+)\s*mi', text, re.IGNORECASE)
    if m:
        mi = int(m.group(1).replace(",", ""))
        if 0 < mi < 12000:
            return round(mi * MI_TO_KM)
    # 4. km fallback
    m = re.search(r'([\d,]+)\s*km', text, re.IGNORECASE)
    if m:
        v = int(m.group(1).replace(",", ""))
        if 0 < v < 20000:
            return v
    return None

result["distance_km"] = parse_distance(body_text)
# Also store the raw miles value for reference
m_mi = re.search(r'direct\s*:?\s*([\d,]+)\s*mi', body_text, re.IGNORECASE)
if m_mi:
    result["distance_mi"] = int(m_mi.group(1).replace(",", ""))

# Flight time: compute from Takeoff and Landing times
TZ_OFFSETS = {   # hours relative to UTC (standard + daylight)
    "EDT": -4, "EST": -5, "CDT": -5, "CST": -6,
    "MDT": -6, "MST": -7, "PDT": -7, "PST": -8,
    "ADT": -3, "AST": -4, "NDT": -2.5, "NST": -3.5,
    "UTC":  0, "GMT":  0,
}

def to_utc_minutes(timestr, tz):
    """Convert '04:30PM' + 'EDT' to minutes-since-midnight in UTC."""
    m = re.match(r'(\d{1,2}):(\d{2})\s*([AP]M)', timestr, re.IGNORECASE)
```

```
    if not m or tz not in TZ_OFFSETS:
        return None
    hh = int(m.group(1)) % 12
    mm = int(m.group(2))
    if m.group(3).upper() == "PM":
        hh += 12
    local_min = hh * 60 + mm
    utc_min = local_min - int(TZ_OFFSETS[tz] * 60)
    return utc_min

def parse_flight_time(text):
    # Find Takeoff time + tz, and Landing time + tz
    tk = re.search(r'takeoff\s*\n?\s*(\d{1,2}:\d{2}\s*[AP]M)\s*([A-Z]{3})',
                   text, re.IGNORECASE)
    ld = re.search(r'landing\s*\n?\s*(\d{1,2}:\d{2}\s*[AP]M)\s*([A-Z]{3})',
                   text, re.IGNORECASE)
    # Fall back to Gate Departure / Gate Arrival
    if not tk:
        tk = re.search(r'gate departure\s*\n?\s*(\d{1,2}:\d{2}\s*[AP]M)\s*([A-Z]{3})',
                       text, re.IGNORECASE)
    if not ld:
        ld = re.search(r'gate arrival\s*\n?\s*(\d{1,2}:\d{2}\s*[AP]M)\s*([A-Z]{3})',
                       text, re.IGNORECASE)
    if tk and ld:
        dep = to_utc_minutes(tk.group(1), tk.group(2).upper())
        arr = to_utc_minutes(ld.group(1), ld.group(2).upper())
        if dep is not None and arr is not None:
            diff = arr - dep
            if diff < 0:
                diff += 24 * 60   # crossed midnight UTC
            if 25 < diff < 900:
                return diff
    return None

result["flight_time_min"] = parse_flight_time(body_text)

# ── Targeted element fallback -ONLY if body-text parse missed distance ──
if result["distance_km"] is None:
    try:
        blocks = driver.find_elements(
            By.CSS_SELECTOR,
            "div[class*='flightPageData'], li[class*='flightPageData'], "
            "div[class*='summaryBlock'], div[class*='detailBlock']"
        )
        for blk in blocks[:30]:   # cap to avoid scanning huge tables
```

```
            txt = blk.text
            if "distance" in txt.lower() and "mi" in txt.lower():
                d = parse_distance(txt)
                if d:
                    result["distance_km"] = d
                    break
        except Exception:
            pass

    print(f"      → distance={result['distance_km']} km  "
          f"time={result['flight_time_min']} min")

    # No driver.back() needed -the next iteration loads a fresh URL directly.
    return result

# Main Loop
def scrape_all_pairs(od_pairs, headless=False):
    driver  = init_driver(headless)
    results = []
    total   = len(od_pairs)
    debug_printed = False

    for idx, (origin_icao, dest_icao, origin_city, dest_city) in enumerate(od_pairs, 1):
        print(f"\n[{idx}/{total}] {origin_icao} → {dest_icao}  "
              f"({origin_city} → {dest_city})")
        record = {
            "origin_city":      origin_city,
            "dest_city":        dest_city,
            "origin_icao":      origin_icao,
            "dest_icao":        dest_icao,
            "airline":          None,
            "flight_number":    None,
            "aircraft":         None,
            "status":           None,
            "departure":        None,
            "arrival":          None,
            "distance_mi":      None,
            "distance_km":      None,
            "flight_time_min":  None,
            "error":            None,
        }
        try:
            ok = load_findflight(driver, origin_icao, dest_icao)
            if not ok:
                record["error"] = "page load timeout"
```

```
            results.append(record)
            continue

        # Print table structure on first successful load to help debug
        if not debug_printed:
            discover_and_print_table(driver)
            debug_printed = True

        if APPLY_AIRLINE_FILTER:
            select_airline_only(driver)
        first = get_first_flight_row(driver)

        if first:
            record["airline"]       = first["airline"]
            record["flight_number"] = first["ident"]
            record["aircraft"]      = first["aircraft"]
            record["status"]        = first["status"]
            record["departure"]     = first["departure"]
            record["arrival"]       = first["arrival"]
            print(f"    ✓ Airline: {first['airline']}  "
                  f"Flight: {first['ident']}  Aircraft: {first['aircraft']}")

            details = get_flight_details(
                driver, first["ident"], first.get("ident_href")
            )
            record["distance_mi"]     = details.get("distance_mi")
            record["distance_km"]     = details["distance_km"]
            record["flight_time_min"] = details["flight_time_min"]
        else:
            record["error"] = "no flights found"
            print(f"    No airline flights found -check page manually")
            discover_and_print_table(driver)

    except TimeoutException:
        record["error"] = "timeout"
        print(f"    Timeout")
    except Exception as e:
        record["error"] = str(e)
        print(f"    Error: {e}")

    results.append(record)

    # Save progress after every pair so you don't lose data
    pd.DataFrame(results).to_csv(OUTPUT_CSV, index=False)
    time.sleep(PAUSE_SEC)
```

```
    driver.quit()
    return pd.DataFrame(results)


# Entry Point
if __name__ == "__main__":
    print("=" * 60)
    print("  FlightAware Distance Extractor")
    print(f"  {len(OD_PAIRS)} OD pairs queued")
    print(f"  Headless: {HEADLESS}")
    print("=" * 60)

    df = scrape_all_pairs(OD_PAIRS, headless=HEADLESS)

    df.to_csv(OUTPUT_CSV, index=False)
    df.to_excel(OUTPUT_EXCEL, index=False)
    print(f"\n✓ Saved: {OUTPUT_CSV}  and  {OUTPUT_EXCEL}")

    success = df["distance_km"].notna().sum()
    print(f"Results: {success}/{len(df)} pairs with distance extracted")

    if df["error"].notna().any():
        print("\nFailed pairs:")
        print(df[df["error"].notna()][
            ["origin_city","dest_city","error"]
        ].to_string(index=False))

    print("\nSample output:")
    cols = ["origin_city","dest_city","airline","flight_number",
            "distance_km","flight_time_min"]
    print(df[cols].head(10).to_string(index=False))
```

Appendix M: Representative Sample of FlightAware-Derived OD Flight Distances

This appendix presents a representative sample of the air-route distances derived from FlightAware and used in the gravity model estimation. The complete dataset contains 5760 OD records and is therefore too large to reproduce in its entirety in this thesis. The sample below includes selected OD pairs spanning different geographic regions and flight distance ranges. For each OD pair, the table reports the origin, destination, and representative FlightAware-derived flight distance.

Table M 1. Representative Sample of Flight Distances from FlightAware

Origin	Destination	Flight Distance (km)
Vancouver	Victoria	63.3
Ottawa	Montreal	151.5
Halifax	Charlottetown	159.6
Yellowknife	Hay River	193.9
St John's	Gander	198.9
Toronto	Ottawa	363.5
Calgary	Saskatoon	518.4
Regina	Winnipeg	531.8
Vancouver	Calgary	686.4
Quebec	Iles de La Madeleine	730.6
Whitehorse	Old Crow	796.7

Origin	Destination	Flight Distance (km)
Yellowknife	Cambridge Bay	850.0
Fredericton	Goose Bay	937.5
Winnipeg	Churchill	1002.8
Toronto	Halifax	1288.3
Winnipeg	Toronto	1504.0
Ottawa	Iqaluit	2097.4
Toronto	St John's	2123.5
Yellowknife	Iqaluit	2262.2
Toronto	Calgary	2689.2
Vancouver	Toronto	3345.5
Vancouver	Iqaluit	3580.6
Halifax	Yellowknife	3744.9
Montreal	Whitehorse	4242.4
St John's	Whitehorse	5170.8

Appendix N: Python Workflow for Extracting Road Distances Using OpenStreetMap

This appendix documents the Python script used to automate the collection of truck route data from OpenStreetMap. The script uses Selenium to control a Chrome browser, enter OD pairs into the OSM directions interface, and scrape the resulting distance and travel time into a CSV file. The table below lists each library used and its specific role in the automation.

```
import os, re, time, csv
from selenium import webdriver
from selenium.webdriver.common.by import By
from selenium.webdriver.chrome.service import Service
from selenium.webdriver.chrome.options import Options
from selenium.webdriver.support.ui import WebDriverWait
from selenium.webdriver.support import expected_conditions as EC
from selenium.webdriver.common.keys import Keys
from webdriver_manager.chrome import ChromeDriverManager
#   ENTER YOUR ORIGIN/DESTINATION PAIRS HERE
OD_PAIRS = [

]
#  CONFIG
# engine=graphhopper_truck forces Truck routing.
# We DO NOT click any mode buttons to avoid resetting this.
URL = "https://www.openstreetmap.org/directions?engine=graphhopper_truck&route="
HEADLESS = True  # Set to True for background running
RESULT_CSV = "osm_results.csv"
```

```
WAIT_SEC = 5
PAIR_RETRIES = 1
#  Setup Browser
def make_driver():
    opts = Options()
    if HEADLESS:
        opts.add_argument("--headless=new")
    opts.add_argument("--window-size=1400,1000")
    opts.add_argument("--no-sandbox")
    opts.add_argument("--disable-dev-shm-usage")
    # NEW: Suppress those scary "google_apis" and "Authentication Failed" logs
    opts.add_argument("--log-level=3")

    prefs = {"profile.default_content_setting_values.notifications": 2}
    opts.add_experimental_option("prefs", prefs)
    opts.add_experimental_option("excludeSwitches", ["enable-logging"])

    driver = webdriver.Chrome(service=Service(ChromeDriverManager().install()), options=opts)
    driver.set_page_load_timeout(WAIT_SEC)
    return driver

#  HELPER: VISUAL HIGHLIGHT
def highlight_element(driver, element):
    """
    Draws a red border and yellow background around the element
    so you can see exactly what the script is interacting with.
```

```
    """
    try:
        driver.execute_script("arguments[0].setAttribute('style', 'border: 3px solid red; background:
yellow;');", element)
        time.sleep(0.5) # Pause briefly so human can see it
    except:
        pass
#  FORCE INPUT METHOD (OSM compatible)
def set_osm_input(driver, element_id, text, stay_focused=False):
    """
    Fills the input field using JS.
    stay_focused=False -> Tabs away (good for Origin).
    stay_focused=True  -> Stays in field (good for Destination so Enter submits).
    """
    try:
        wait = WebDriverWait(driver, 10)

        # Revert to presence first, then ensure visibility.
        inp = wait.until(EC.presence_of_element_located((By.ID, element_id)))
        # HIGHLIGHT DEBUG
        # Show exactly which box we are about to type into
        highlight_element(driver, inp)
        # Scroll + Click to ensure real focus
        driver.execute_script("arguments[0].scrollIntoView(true);", inp)
        try:
            inp.click()
        except:
```

```
    driver.execute_script("arguments[0].click();", inp)

time.sleep(0.5)

# Clear and input via JS + trigger events
driver.execute_script("""
    arguments[0].value = '';
    arguments[0].value = arguments[1];
    arguments[0].dispatchEvent(new Event('input', { bubbles: true }));
    arguments[0].dispatchEvent(new Event('change', { bubbles: true }));
    arguments[0].focus();
""", inp, text)

time.sleep(1.5) # Wait for OSM dropdown to appear

# Select the suggestion using ARROW DOWN
active_el = driver.switch_to.active_element
active_el.send_keys(Keys.ARROW_DOWN)
time.sleep(0.5)

# CONFIRM SELECTION WITH ENTER
# This selects the city from the dropdown.
# If it's the destination field, this usually triggers the route calculation.
active_el.send_keys(Keys.ENTER)
time.sleep(0.5)

if not stay_focused:
```

```
            # Tab away (only for Origin)
            active_el.send_keys(Keys.TAB)
            time.sleep(0.5)
        # Else: Stay in the box

    except Exception as e:
        print(f"    ! Error setting input {element_id}: {e}")
        return False
    return True

#  READ RESULTS
def parse_osm_results(driver):
    """
    Scrapes the text independently to find Distance and Time.
    """
    try:
        wait = WebDriverWait(driver, 5)
        # Try finding the summary by ID first
        try:
            summary = wait.until(EC.presence_of_element_located((By.ID, "routing_summary")))
            text = summary.text
        except:
            # Fallback: Look for any sidebar text containing "Distance:"
            # This helps if the ID changes or isn't found immediately
            summary = driver.find_element(By.XPATH, "//*[contains(text(), 'Distance:')]")
            text = summary.text
```

```
        # Debug print to see what the scraper actually sees
        # print(f"    (DEBUG: Saw text -> '{text.strip()}')")
        # We search for them separately now to be more robust
        # Look for "Distance: 123 km" or "Distance: 123km"
        dist_match = re.search(r"Distance:?\s*([\d\.,]+\s*\w+)", text, re.I)

        # Look for "Time: 12:30" or "Time: 4h 5m" or "Time: 7:04"
        time_match = re.search(r"Time:?\s*([\d:hmin\s]+)", text, re.I)
        dist_val = dist_match.group(1).strip() if dist_match else None
        time_val = time_match.group(1).strip().rstrip('.') if time_match else None
        return time_val, dist_val
    except:
        return None, None
#  RUN SINGLE PAIR
def run_pair(driver, origin, dest):
    print(f"\nProcessing: {origin} -> {dest}")
    driver.get(URL)
    time.sleep(3)
    # Wait for page init
    try:
        WebDriverWait(driver, 20).until(
            EC.presence_of_element_located((By.ID, "route_from"))
        )
    except:
        print("  ! 'route_from' not found immediately, refreshing...")
        driver.refresh()
        time.sleep(3)
```

```
try:
    # Just unconditionally click it to be safe
    print("  > DEBUG: Initial Car Mode check...")
    el = driver.find_element(By.ID, "modes_car")
    highlight_element(driver, el)
    driver.execute_script("arguments[0].click();", el)
    time.sleep(1)
except Exception as e:
    print(f"  ! DEBUG: Initial mode set warning: {e}")

# 1. Put in Origin City (Arrow Down -> Enter -> Tab)
print("  > Setting Origin...")
if not set_osm_input(driver, "route_from", origin, stay_focused=False):
    return {"Status": "Failed", "Error_Log": "Could not set origin"}

# 2. Put in Destination City (Arrow Down -> Enter -> Stay Focused)
print("  > Setting Destination...")
# The 'Enter' inside set_osm_input should trigger the calculation automatically
if not set_osm_input(driver, "route_to", dest, stay_focused=True):
    return {"Status": "Failed", "Error_Log": "Could not set destination"}

print("  > Calculation triggered via Input...")

# --- NEW: UNCONDITIONALLY FORCE CAR MODE BEFORE RESULTS ---
# We force click "Car" now to ensure the result we read is for Car/Truck.
try:
```

```
    print("  > Enforcing Car Mode before reading results...")
    car_btn = driver.find_element(By.ID, "modes_car")
    highlight_element(driver, car_btn) # Show user
    driver.execute_script("arguments[0].click();", car_btn)
    time.sleep(2) # Give it time to re-calc if needed
except Exception as e:
    print(f"  ! Warning: Could not force Car Mode: {e}")

# 4. Result
print("  > Waiting for results...")
duration, distance = "", ""

# Loop 20 times (20 seconds) to ensure we catch slow loading results
for _ in range(2):
    dur, dist = parse_osm_results(driver)

    # Only break if we found BOTH, or if we found at least Distance (sometimes time is missing)
    if dist:
        duration = dur if dur else "N/A"
        distance = dist
        break
    time.sleep(1)

if not distance:
    print("  > No results found (or regex mismatch).")
    # Print what the text actually was for debugging
    try:
```

```
            raw_text = driver.find_element(By.ID, "routing_summary").text
            print(f"    (Scraper saw this text: '{raw_text}')")
        except:
            print("    (Could not find 'routing_summary' element to read text)")
            pass
        return {"Status": "Failed", "Error_Log": "No summary text found"}

    print(f" > Success: {duration} | {distance}")
    return {
        "Origin": origin,
        "Destination": dest,
        "Duration": duration,
        "Distance": distance,
        "Status": "Success",
        "Error_Log": ""
    }

# MAIN
def main():

    # Check if file exists to write header (safe creation)
    if not os.path.exists(RESULT_CSV):
        try:
            with open(RESULT_CSV, "w", newline="", encoding="utf-8") as f:
                csv.writer(f).writerow([
                    "Origin", "Destination", "Duration", "Distance", "Status", "Error_Log"
                ])
```

```
        except PermissionError:
            print(f" ERROR: Could not create {RESULT_CSV}. Please close the file if it is open in
Excel.")
            return

    print(f"\nStarting OpenStreetMap scraper for {len(OD_PAIRS)} pairs...")

    driver = make_driver()
    try:
        for idx, (origin, dest) in enumerate(OD_PAIRS, 1):
            print(f"\n--- Pair {idx}/{len(OD_PAIRS)} ---")
            success = False
            for attempt in range(PAIR_RETRIES):
                try:
                    data = run_pair(driver, origin, dest)

                    if data["Status"] == "Success":
                        # Write SUCCESS immediately to file
                        try:
                            with open(RESULT_CSV, "a", newline="", encoding="utf-8") as f:
                                writer = csv.DictWriter(f, fieldnames=data.keys())
                                writer.writerow(data)
                            print("    >  Saved result to CSV.")
                        except PermissionError:
                            print("    !  ERROR SAVING: Is the CSV file open in Excel? Close it to save data!")
                        success = True
                        break
```

```
                else:
                    print("    Retrying due to failure status...")
                    time.sleep(2)
            except Exception as e:
                print(f"    ! Error during attempt {attempt+1}: {e}")
                time.sleep(2)
        if not success:
            print("    x Failed after retries. Saving as 'no road'.")
            # Write FAILURE with "no road" result
            try:
                with open(RESULT_CSV, "a", newline="", encoding="utf-8") as f:
                    # Changed: Writes "no road" instead of empty string
                    csv.writer(f).writerow([origin, dest, "no road", "no road", "no road", "Max retries"])
                print("    > Saved 'no road' result to CSV.")
            except PermissionError:
                 print("    ERROR SAVING: Is the CSV file open in Excel? Close it to save data!")
        time.sleep(2)
    except KeyboardInterrupt:
        print("\nProcess interrupted by user.")
    finally:
        driver.quit()
        print(f"\nDone! Results saved to: {RESULT_CSV}")
if __name__ == "__main__":
    main()
```

Appendix O: Representative Sample of OSM-Derived Truck-Route Distances

This appendix presents a representative sample of truck distances obtained from OpenStreetMap. The complete dataset contains approximately 5,760 OD records and is therefore too large to reproduce in its entirety in this thesis. The sample below includes selected OD pairs spanning different geographic regions and distance ranges. For each OD pair, the table reports the origin, destination, and representative truck distance.

Table O 1. Representative Sample of OpenStreetMap Truck Distances by Origin–Destination Pair

#	Origin	Destination	Truck Distance (km)
1	Vancouver	Victoria	**112**
2	Ottawa	Montreal	**199**
3	Halifax	Charlottetown	**326**
4	Yellowknife	Hay River	**482**
5	St John's	Gander	**335**
6	Toronto	Ottawa	**450**
7	Calgary	Saskatoon	**614**
8	Regina	Winnipeg	**574**
9	Vancouver	Calgary	**972**
10	Quebec	Iles de La Madeleine	**1173**
11	Whitehorse	Old Crow	**no road**
12	Yellowknife	Cambridge Bay	**no road**

#	Origin	Destination	Truck Distance (km)
13	Fredericton	Goose Bay	**1696**
14	Winnipeg	Churchill	**no road**
15	Toronto	Halifax	**1683**
16	Winnipeg	Toronto	**2229**
17	Ottawa	Iqaluit	**no road**
18	Toronto	St John's	**3893**
19	Yellowknife	Iqaluit	**no road**
20	Toronto	Calgary	**3409**
21	Vancouver	Toronto	**4348**
22	Vancouver	Iqaluit	**no road**
23	Halifax	Yellowknife	**6272**
24	Montreal	Whitehorse	**5593**
25	St John's	Whitehorse	**8926**

Appendix P: Representative Sample Rail Distances

This appendix presents a representative sample of the resulting rail distances for the same origin-destination pairs shown in Appendix M and O. Rail-route distances for each OD pair were derived using a GIS network-based approach. Rail line network data and rail terminal/hub layers were obtained from the University of Waterloo Geospatial Centre data library. The complete dataset contains approximately 5,760 OD records and is therefore too large to reproduce in its entirety in this thesis. Because Canada's rail network is far sparser than its road network, many pairs have no rail connection and are reported as "no rail." For each OD pair, the table reports the origin, destination, and representative rail distance.

Table P 1. Representative Sample of GIS-Derived Rail Distances by Origin–Destination Pair

#	Origin	Destination	Rails Distance (km)
1	Vancouver	Victoria	**no rail**
2	Ottawa	Montreal	**187**
3	Halifax	Charlottetown	**no rail**
4	Yellowknife	Hay River	**no rail**
5	St John's	Gander	**no rail**
6	Toronto	Ottawa	**450**
7	Calgary	Saskatoon	**624**
8	Regina	Winnipeg	**583**
9	Vancouver	Calgary	**no rail**
10	Quebec	Iles de La Madeleine	**no rail**
11	Whitehorse	Old Crow	**no rail**

#	Origin	Destination	Rails Distance (km)
12	Yellowknife	Cambridge Bay	**no rail**
13	Fredericton	Goose Bay	**no rail**
14	Winnipeg	Churchill	**1697**
15	Toronto	Halifax	**1888**
16	Winnipeg	Toronto	**2320**
17	Ottawa	Iqaluit	**no rail**
18	Toronto	St John's	**no rail**
19	Yellowknife	Iqaluit	**no rail**
20	Toronto	Calgary	**3465**
21	Vancouver	Toronto	**4466**
22	Vancouver	Iqaluit	**no rail**
23	Halifax	Yellowknife	**no rail**
24	Montreal	Whitehorse	**no rail**
25	St John's	Whitehorse	**no rail**

Appendix Q: Summary of Reference Emission Factors

This appendix summarizes the reference emission factors used to estimate greenhouse-gas emissions for aviation, truck, and rail freight technologies. Emission factors are expressed in grams of carbon-dioxide equivalent per tonne-kilometre (g CO_2e/t-km). Aviation factors use a well-to-wake (WTWa) boundary, while truck and rail factors use a well-to-wheel (WTW) boundary. GREET 2024 is the principal source of fuel- and technology-specific emission factors. Alternative aircraft propulsion factors are derived using literature-based assumptions within the GREET-based framework.

Table Q 1. Summary of 2023 reference emission factors by mode and technology

Mode	Representative category	Fuel or technology pathway	2023 reference EF (g CO_2e/t-km)	Boundary	2023 energy-supply basis	Source
Air	GREET single-aisle aircraft	Conventional Jet-A	1,423.76	WTWa	Current Measures	GREET 2024
Air	GREET single-aisle aircraft	HEFA-canola SAF	541.33	WTWa	Canada Net-Zero inputs where applicable	GREET 2024
Air	GREET single-aisle aircraft	HEFA-soybean SAF	390.47	WTWa	Canada Net-Zero inputs where applicable	GREET 2024
Air	GREET single-aisle aircraft	HEFA-corn-oil SAF	292.53	WTWa	Canada Net-Zero inputs where applicable	GREET 2024
Air	GREET single-aisle aircraft	FT biomass SAF - municipal solid waste and forestry waste	77.79	WTWa	Canada Net-Zero inputs where applicable	GREET 2024
Air	GREET single-aisle aircraft	ATJ-corn SAF	1,072.27	WTWa	Canada Net-Zero inputs where applicable	GREET 2024
Air	GREET single-aisle aircraft	PtL/e-SAF using industrial CO_2 and hydrogen	16.87	WTWa	Canada Net-Zero electricity and hydrogen assumptions	GREET 2024
Air	Single-aisle reference aircraft	Hybrid-electric aircraft (50% hybridization assumption)	137.46	WTWa	Literature-based technology assumption	Literature applied to GREET reference
Air	Single-aisle reference aircraft	Battery-electric aircraft	1,204.50	WTWa	Canada Net-Zero electricity assumption	Literature applied to GREET reference
Air	Single-aisle reference aircraft	Hydrogen aircraft	34.71	WTWa	Canada Net-Zero hydrogen assumption	Literature applied to GREET reference
Truck	GREET combination long-haul truck	Conventional diesel	57.71	WTW	Current Measures	GREET 2024

Mode	Representative category	Fuel or technology pathway	2023 reference EF (g CO_2e/t-km)	Boundary	2023 energy-supply basis	Source
Truck	GREET combination long-haul truck	Battery-electric	17.78	WTW	Canada Net-Zero electricity assumption	GREET 2024
Rail	GREET freight rail	Conventional diesel	17.67	WTW	Current Measures	GREET 2024
Rail	GREET freight rail	Biodiesel blend (B20)	15.79	WTW	Canada Net-Zero inputs where applicable	GREET 2024
Rail	GREET freight rail	Renewable diesel blend (HDRD30)	13.92	WTW	Canada Net-Zero inputs where applicable	GREET 2024
Rail	GREET freight rail	Electric propulsion	8.23	WTW	Canada Net-Zero electricity assumption	GREET 2024
Rail	GREET freight rail	Hydrogen fuel-cell propulsion	11.46	WTW	Canada Net-Zero hydrogen assumption	GREET 2024

Appendix R: Annual Alternative-Propulsion Eligibility and Penetration Schedules for the Waypoint-Based and Delayed-Deployment Scenarios

This appendix presents the annual alternative-propulsion eligibility and penetration schedules used in the scenario analysis. It includes the original Waypoint-based deployment timeline and the +3-, +6-, +9-, and +12-year delayed variants. For each scenario, the tables identify the eligible distance bins, applicable aircraft technology mix, and annual penetration rate used to assign alternative-propulsion technologies to eligible OD pairs.

Table R 1. Alternative-Propulsion Eligibility and Annual Penetration Rates under the Waypoint-Based Timeline (Scenario AP1)

Year	Commuter bin	Commuter mix	Penetration Rate	Regional bin	Regional mix	Penetration Rate
2025	0 – 480km	(100% Hybrid)	14%			
2026	0 – 480km	(90% Hybrid + 10% Electric)	29%			
2027	0 – 480km	(80% Hybrid + 20% Electric)	43%			
2028	0 – 480km	(70% Hybrid + 30% Electric)	57%			
2029	0 – 480km	(60% Hybrid + 40% Electric)	71%			
2030	0 – 480km	(50% Hybrid + 50% Electric)	86%	480–1306.5 km	(100% Hybrid)	14%
2031	0 – 480km	(40% Hybrid + 60% Electric)	86%	480–1306.5 km	(90% Hybrid + 10% Electric)	29%
2032	0 – 480km	(30% Hybrid + 70% Electric)	100%	480–1306.5 km	(80% Hybrid + 20% Electric)	43%
2033	0 – 480km	(20% Hybrid + 80% Electric)	100%	480–1306.5 km	(70% Hybrid + 30% Electric)	57%
2034	0 – 480km	(10% Hybrid + 90% Electric)	100%	480–1306.5 km	(60% Hybrid + 40% Electric)	71%
2035	0 – 480km	(0% Hybrid + 100% Electric)	100%	480–1306.5 km	(50% Hybrid + 50% Electric)	86%
2036				480–1306.5 km	(40% Hybrid + 60% Electric)	100%
2037				480–1306.5 km	(30% Hybrid + 70% Electric)	100%
2038				480–1306.5 km	(20% Hybrid + 80% Electric)	100%
2039				480–1306.5 km	(10% Hybrid + 90% Electric)	100%
2040				480–1306.5 km	(0% Hybrid + 100% Electric)	100%
2041						
2042						
2043						
2044						
2045						
2046						
2047						
2048						
2049						
2050						

Year	Short Haul	Short Haul Mix	Penetration Rate	Medium Haul	Medium Haul Mix	Penetration Rate
2025						
2026						
2027						
2028						
2029						
2030	1306.5-1800 km	(100% Hybrid)	14%			
2031	1306.5-1800 km	(100% Hybrid)	29%			
2032	1306.5-1800 km	(100% Hybrid)	43%			
2033	1306.5-1800 km	(100% Hybrid)	57%			
2034	1306.5-1800 km	(100% Hybrid)	71%			
2035	1306.5-1800 km	(90% Hybrid + 10% Hydrogen)	86%	1800 km - 2300 km	(100% Hybrid)	14%
2036	1306.5-1800 km	(80% Hybrid + 20% Hydrogen)	100%	1800 km - 2300 km	(100% Hybrid)	29%
2037	1306.5-1800 km	(70% Hybrid + 30% Hydrogen)	100%	1800 km - 2300 km	(100% Hybrid)	43%
2038	1306.5-1800 km	(60% Hybrid + 40% Hydrogen)	100%	1800 km - 2300 km	(100% Hybrid)	57%
2039	1306.5-1800 km	(50% Hybrid + 50% Hydrogen)	100%	1800 km - 2300 km	(100% Hybrid)	71%
2040	1306.5-1800 km	(40% Hybrid + 60% Hydrogen)	100%	1800 km - 2300 km	(90% Hybrid + 10% Hydrogen)	86%
2041	1306.5-1800 km	(30% Hybrid + 70% Hydrogen)	100%	1800 km - 2300 km	(80% Hybrid + 20% Hydrogen)	100%
2042	1306.5-1800 km	(20% Hybrid + 80% Hydrogen)	100%	1800 km - 2300 km	(70% Hybrid + 30% Hydrogen)	100%
2043	1306.5-1800 km	(10% Hybrid + 90% Hydrogen)		1800 km - 2300 km	(60% Hybrid + 40% Hydrogen)	100%
2044	1306.5-1800 km	100% Hydrogen		1800 km - 2300 km	(50% Hybrid + 50% Hydrogen)	100%
2045				1800 km - 2300 km	(40% Hybrid + 60% Hydrogen)	100%
2046				1800 km - 2300 km	(30% Hybrid + 70% Hydrogen)	100%
2047					(20% Hybrid + 80% Hydrogen)	
2048					(10% Hybrid + 90% Hydrogen)	
2049					100% Hydrogen	
2050					100% Hydrogen	

Table R 2. Alternative-Propulsion Eligibility and Annual Penetration Rates under the Three-Year Deployment Delay

Year	Commuter bin	Commuter mix	Penetration Rate	Regional bin	Regional mix	Penetration Rate
2025						
2026						
2027						
2028	0 – 480km	(100% Hybrid)	14%			
2029	0 – 480km	(90% Hybrid + 10% Electric)	29%			
2030	0 – 480km	(80% Hybrid + 20% Electric)	43%			
2031	0 – 480km	(70% Hybrid + 30% Electric)	57%			
2032	0 – 480km	(60% Hybrid + 40% Electric)	71%			
2033	0 – 480km	(50% Hybrid + 50% Electric)	86%	480–1306.5 km	(100% Hybrid)	14%
2034	0 – 480km	(40% Hybrid + 60% Electric)	100%	480–1306.5 km	(90% Hybrid + 10% Electric)	29%
2035	0 – 480km	(30% Hybrid + 70% Electric)	100%	480–1306.5 km	(80% Hybrid + 20% Electric)	43%
2036	0 – 480km	(20% Hybrid + 80% Electric)	100%	480–1306.5 km	(70% Hybrid + 30% Electric)	57%
2037	0 – 480km	(10% Hybrid + 90% Electric)	100%	480–1306.5 km	(60% Hybrid + 40% Electric)	71%
2038				480–1306.5 km	(50% Hybrid + 50% Electric)	86%
2039				480–1306.5 km	(40% Hybrid + 60% Electric)	100%
2040				480–1306.5 km	(30% Hybrid + 70% Electric)	100%
2041				480–1306.5 km	(20% Hybrid + 80% Electric)	100%
2042				480–1306.5 km	(10% Hybrid + 90% Electric)	100%
2043						
2044	0 – 480km	(0% Hybrid + 100% Electric)	100%			
2045						
2046				480–1306.5 km	(0% Hybrid + 100% Electric)	100%
2047						
2048						
2049						
2050						

Year	Short Haul	Short Haul Mix	Penetration Rate	Medium Haul	Short Haul Mix	Penetration Rate
2025						
2026						
2027						
2028						
2029						
2030						
2031						
2032						
2033	1306.5-1800 km	(100% Hybrid)	14%			
2034	1306.5-1800 km	(100% Hybrid)	29%			
2035	1306.5-1800 km	(100% Hybrid)	43%			
2036	1306.5-1800 km	(100% Hybrid)	57%			
2037	1306.5-1800 km	(100% Hybrid)	71%			
2038	1306.5-1800 km	(90% Hybrid + 10% Hydrogen)	86%	1800 km - 2300 km	(100% Hybrid)	14%
2039	1306.5-1800 km	(80% Hybrid + 20% Hydrogen)	100%	1800 km - 2300 km	(100% Hybrid)	29%
2040	1306.5-1800 km	(70% Hybrid + 30% Hydrogen)	100%	1800 km - 2300 km	(100% Hybrid)	43%
2041	1306.5-1800 km	(60% Hybrid + 40% Hydrogen)	100%	1800 km - 2300 km	(100% Hybrid)	57%
2042	1306.5-1800 km	(50% Hybrid + 50% Hydrogen)	100%	1800 km - 2300 km	(100% Hybrid)	71%
2043	1306.5-1800 km	(40% Hybrid + 60% Hydrogen)	100%	1800 km - 2300 km	(90% Hybrid + 10% Hydrogen)	86%
2044	1306.5-1800 km	(30% Hybrid + 70% Hydrogen)	100%	1800 km - 2300 km	(80% Hybrid + 20% Hydrogen)	100%
2045	1306.5-1800 km	(20% Hybrid + 80% Hydrogen)	100%	1800 km - 2300 km	(70% Hybrid + 30% Hydrogen)	100%
2046	1306.5-1800 km	(10% Hybrid + 90% Hydrogen)	100%	1800 km - 2300 km	(60% Hybrid + 40% Hydrogen)	100%
2047	1306.5-1800 km	100% Hydrogen	100%	1800 km - 2300 km	(50% Hybrid + 50% Hydrogen)	100%
2048				1800 km - 2300 km	(40% Hybrid + 60% Hydrogen)	100%
2049				1800 km - 2300 km	(30% Hybrid + 70% Hydrogen)	100%
2050				1800 km - 2300 km	(20% Hybrid + 80% Hydrogen)	100%

Table R 3. Alternative-Propulsion Eligibility and Annual Penetration Rates under the Six-Year Deployment Delay

Year	Commuter bin	Commuter mix	Penetration Rate	Regional bin	Regional mix	Penetration Rate
2025						
2026						
2027						
2028						
2029						
2030						
2031	0 – 480km	(100% Hybrid)	14%			
2032	0 – 480km	(90% Hybrid + 10% Electric)	29%			
2033	0 – 480km	(80% Hybrid + 20% Electric)	43%			
2034	0 – 480km	(70% Hybrid + 30% Electric)	57%			
2035	0 – 480km	(60% Hybrid + 40% Electric)	71%			
2036	0 – 480km	(50% Hybrid + 50% Electric)	86%	480–1306.5 km	(100% Hybrid)	14%
2037	0 – 480km	(40% Hybrid + 60% Electric)	100%	480–1306.5 km	(90% Hybrid + 10% Electric)	29%
2038	0 – 480km	(30% Hybrid + 70% Electric)	100%	480–1306.5 km	(80% Hybrid + 20% Electric)	43%
2039	0 – 480km	(20% Hybrid + 80% Electric)	100%	480–1306.5 km	(70% Hybrid + 30% Electric)	57%
2040	0 – 480km	(10% Hybrid + 90% Electric)	100%	480–1306.5 km	(60% Hybrid + 40% Electric)	71%
2041	0 – 480km	(0% Hybrid + 100% Electric)	100%	480–1306.5 km	(50% Hybrid + 50% Electric)	86%
2042				480–1306.5 km	(40% Hybrid + 60% Electric)	100%
2043				480–1306.5 km	(30% Hybrid + 70% Electric)	100%
2044				480–1306.5 km	(20% Hybrid + 80% Electric)	100%
2045				480–1306.5 km	(10% Hybrid + 90% Electric)	100%
2046				480–1306.5 km	(0% Hybrid + 100% Electric)	100%
2047						
2048						
2049						
2050						

Year	Short Haul	Short Haul Mix	Penetration Rate	Medium Haul	Short Haul Mix	Penetration Rate
2025						
2026						
2027						
2028						
2029						
2030						
2031						
2032						
2033						
2034						
2035						
2036	1306.5-1800 km	(100% Hybrid)	14%			
2037	1306.5-1800 km	(100% Hybrid)	29%			
2038	1306.5-1800 km	(100% Hybrid)	43%			
2039	1306.5-1800 km	(100% Hybrid)	57%			
2040	1306.5-1800 km	(100% Hybrid)	71%			
2041	1306.5-1800 km	(90% Hybrid + 10% Hydrogen)	86%	1800 km - 2300 km	(100% Hybrid)	14%
2042	1306.5-1800 km	(80% Hybrid + 20% Hydrogen)	100%	1800 km - 2300 km	(100% Hybrid)	29%
2043	1306.5-1800 km	(70% Hybrid + 30% Hydrogen)	100%	1800 km - 2300 km	(100% Hybrid)	43%
2044	1306.5-1800 km	(60% Hybrid + 40% Hydrogen)	100%	1800 km - 2300 km	(100% Hybrid)	57%
2045	1306.5-1800 km	(50% Hybrid + 50% Hydrogen)	100%	1800 km - 2300 km	(100% Hybrid)	71%
2046	1306.5-1800 km	(40% Hybrid + 60% Hydrogen)	100%	1800 km - 2300 km	(90% Hybrid + 10% Hydrogen)	86%
2047	1306.5-1800 km	(30% Hybrid + 70% Hydrogen)	100%	1800 km - 2300 km	(80% Hybrid + 20% Hydrogen)	100%
2048	1306.5-1800 km	(20% Hybrid + 80% Hydrogen)	100%	1800 km - 2300 km	(70% Hybrid + 30% Hydrogen)	100%
2049	1312.5-1800 km	(10% Hybrid + 90% Hydrogen)	100%	1800 km - 2300 km	(60% Hybrid + 40% Hydrogen)	100%
2050	1306.5-1800 km	100% Hydrogen	100%	1800 km - 2300 km	(50% Hybrid + 50% Hydrogen)	100%

Table R 4. Alternative-Propulsion Eligibility and Annual Penetration Rates under the Nine-Year Deployment Delay

Year	Commuter bin	Commuter mix	Penetration Rate	Regional bin	Regional mix	Penetration Rate
2025						
2026						
2027						
2028						
2029						
2030						
2031						
2032						
2033						
2034	0 – 480km	(100% Hybrid)	14%			
2035	0 – 480km	(90% Hybrid + 10% Electric)	29%			
2036	0 – 480km	(80% Hybrid + 20% Electric)	43%			
2037	0 – 480km	(70% Hybrid + 30% Electric)	57%			
2038	0 – 480km	(60% Hybrid + 40% Electric)	71%			
2039	0 – 480km	(50% Hybrid + 50% Electric)	86%	480–1306.5 km	(100% Hybrid)	14%
2040	0 – 480km	(40% Hybrid + 60% Electric)	100%	480–1306.5 km	(90% Hybrid + 10% Electric)	29%
2041	0 – 480km	(30% Hybrid + 70% Electric)	100%	480–1306.5 km	(80% Hybrid + 20% Electric)	43%
2042	0 – 480km	(20% Hybrid + 80% Electric)	100%	480–1306.5 km	(70% Hybrid + 30% Electric)	57%
2043	0 – 480km	(10% Hybrid + 90% Electric)	100%	480–1306.5 km	(60% Hybrid + 40% Electric)	71%
2044	0 – 480km	(0% Hybrid + 100% Electric)	100%	480–1306.5 km	(50% Hybrid + 50% Electric)	86%
2045				480–1306.5 km	(40% Hybrid + 60% Electric)	100%
2046				480–1306.5 km	(30% Hybrid + 70% Electric)	100%
2047				480–1306.5 km	(20% Hybrid + 80% Electric)	100%
2048				480–1306.5 km	(10% Hybrid + 90% Electric)	100%
2049				480–1306.5 km	(0% Hybrid + 100% Electric)	100%
2050						

Year	Short Haul	Short Haul Mix	Penetration Rat	Medium Haul	Short Haul Mix	Penetration Rate
2025						
2026						
2027						
2028						
2029						
2030						
2031						
2032						
2033						
2034						
2035						
2036						
2037						
2038						
2039	1306.5-1800 km	(100% Hybrid)	14%			
2040	1306.5-1800 km	(100% Hybrid)	29%			
2041	1306.5-1800 km	(100% Hybrid)	43%			
2042	1306.5-1800 km	(100% Hybrid)	57%			
2043	1306.5-1800 km	(100% Hybrid)	71%			
2044	1306.5-1800 km	(90% Hybrid + 10% Hydrogen)	86%	1800 km - 2300 km	(100% Hybrid)	14%
2045	1306.5-1800 km	(80% Hybrid + 20% Hydrogen)	100%	1800 km - 2300 km	(100% Hybrid)	29%
2046	1306.5-1800 km	(70% Hybrid + 30% Hydrogen)	100%	1800 km - 2300 km	(100% Hybrid)	43%
2047	1306.5-1800 km	(60% Hybrid + 40% Hydrogen)	100%	1800 km - 2300 km	(100% Hybrid)	57%
2048	1306.5-1800 km	(50% Hybrid + 50% Hydrogen)	100%	1800 km - 2300 km	(100% Hybrid)	71%
2049	1306.5-1800 km	(40% Hybrid + 60% Hydrogen)	100%	1800 km - 2300 km	(90% Hybrid + 10% Hydrogen)	86%
2050	1306.5-1800 km	(30% Hybrid + 70% Hydrogen)	100%	1800 km - 2300 km	(80% Hybrid + 20% Hydrogen)	100%

Table R 5. Alternative-Propulsion Eligibility and Annual Penetration Rates under the Twelve-Year Deployment Delay

Year	Commuter bin	Commuter mix	Penetration Rate	Regional bin	Regional mix	Penetration Rate
2025						
2026						
2027						
2028						
2029						
2030						
2031						
2032						
2033						
2034						
2035						
2036						
2037	0 – 480km	(100% Hybrid)	14%			
2038	0 – 480km	(90% Hybrid + 10% Electric)	29%			
2039	0 – 480km	(80% Hybrid + 20% Electric)	43%			
2040	0 – 480km	(70% Hybrid + 30% Electric)	57%			
2041	0 – 480km	(60% Hybrid + 40% Electric)	71%			
2042	0 – 480km	(50% Hybrid + 50% Electric)	86%	480–1312.5 km	(100% Hybrid)	14%
2043	0 – 480km	(40% Hybrid + 60% Electric)	100%	480–1312.5 km	(90% Hybrid + 10% Electric)	29%
2044	0 – 480km	(30% Hybrid + 70% Electric)	100%	480–1312.5 km	(80% Hybrid + 20% Electric)	43%
2045	0 – 480km	(20% Hybrid + 80% Electric)	100%	480–1312.5 km	(70% Hybrid + 30% Electric)	57%
2046	0 – 480km	(10% Hybrid + 90% Electric)	100%	480–1312.5 km	(60% Hybrid + 40% Electric)	71%
2047	0 – 480km	(0% Hybrid + 100% Electric)	100%	480–1312.5 km	(50% Hybrid + 50% Electric)	86%
2048				480–1312.5 km	(40% Hybrid + 60% Electric)	100%
2049				480–1312.5 km	(30% Hybrid + 70% Electric)	100%
2050				480–1312.5 km	(20% Hybrid + 80% Electric)	100%

Year	Short Haul	Short Haul Mix	Penetration Rate	Medium Haul	Short Haul Mix	Penetration Rate
2025						
2026						
2027						
2028						
2029						
2030						
2031						
2032						
2033						
2034						
2035						
2036						
2037						
2038						
2039						
2040						
2041						
2042	1312.5-1800 km	(100% Hybrid)	14%			
2043	1312.5-1800 km	(100% Hybrid)	29%			
2044	1312.5-1800 km	(100% Hybrid)	43%			
2045	1312.5-1800 km	(100% Hybrid)	57%			
2046	1312.5-1800 km	(100% Hybrid)	71%			
2047	1312.5-1800 km	(90% Hybrid + 10% Hydrogen)	86%	1800 km - 2300 km	(100% Hybrid)	14%
2048	1312.5-1800 km	(80% Hybrid + 20% Hydrogen)	100%	1800 km - 2300 km	(100% Hybrid)	29%
2049	1312.5-1800 km	(70% Hybrid + 30% Hydrogen)	100%	1800 km - 2300 km	(100% Hybrid)	43%
2050	1312.5-1800 km	(60% Hybrid + 40% Hydrogen)	100%	1800 km - 2300 km	(100% Hybrid)	57%

Appendix S: Full Commodity-Level PPML Gravity-Model Estimation Results

This appendix reports the complete Poisson pseudo-maximum-likelihood (PPML) gravity-model estimates for each of the nine cargo commodity groups. All models share the same specification, log origin GDP, log destination GDP, log air distance, year fixed effects, and origin- and destination-province fixed effects.

Table S 1. Biological Commodity - PPML gravity-model estimates.

Variable	Coefficient	Std. err.
Intercept	-38.9891***	(1.344)
C(Year) [2020]	-0.4712	(0.327)
C(Year) [2021]	-0.6722*	(0.361)
C(Year) [2022]	-0.4480	(0.358)
C(Year) [2023]	-0.3159	(0.352)
C(Origin_Prov) [British Columbia (BC)]	0.7870***	(0.161)
C(Origin_Prov) [Manitoba (MB)]	0.4744	(0.324)
C(Origin_Prov) [New Brunswick (NB)]	-0.2577	(0.705)
C(Origin_Prov) [Newfoundland and Labrador (NL)]	-0.1197	(0.381)
C(Origin_Prov) [Northwest Territories (NT)]	-20.5003***	(0.417)
C(Origin_Prov) [Nova Scotia (NS)]	0.3497	(0.271)
C(Origin_Prov) [Ontario (ON)]	0.7679**	(0.373)
C(Origin_Prov) [Prince Edward Island (PE)]	-8.0380***	(1.049)
C(Origin_Prov) [Quebec (QC)]	-1.4554***	(0.195)
C(Origin_Prov) [Saskatchewan (SK)]	-0.8640***	(0.221)
C(Origin_Prov) [Yukon (YT)]	-20.7033***	(0.404)
C(Dest_Prov) [British Columbia (BC)]	0.5433**	(0.222)
C(Dest_Prov) [Manitoba (MB)]	1.0806***	(0.333)
C(Dest_Prov) [New Brunswick (NB)]	-0.0982	(0.294)
C(Dest_Prov) [Newfoundland and Labrador (NL)]	1.4339***	(0.251)
C(Dest_Prov) [Northwest Territories (NT)]	-2.8523***	(0.748)
C(Dest_Prov) [Nova Scotia (NS)]	1.1052***	(0.217)
C(Dest_Prov) [Nunavut (NU)]	-2.8626***	(0.505)
C(Dest_Prov) [Ontario (ON)]	1.3579***	(0.266)
C(Dest_Prov) [Prince Edward Island (PE)]	0.4910	(0.370)
C(Dest_Prov) [Quebec (QC)]	-0.5356***	(0.202)
C(Dest_Prov) [Saskatchewan (SK)]	0.5804***	(0.223)
C(Dest_Prov) [Yukon (YT)]	-20.4828***	(0.363)
ln_GDP_Origin	0.7925***	(0.102)
ln_GDP_Dest	0.7465***	(0.074)
ln_Air_Distance	-0.1337***	(0.077)

Notes: *** $p < 0.01$, ** $p < 0.05$, * $p < 0.10$. N = 28,800. $R^2 = 0.4888$.

Table S 2. General Cargo - PPML gravity-model estimates.

Variable	Coefficient	Std. err.
Intercept	-60.7876***	(2.464)
C(Year) [2020]	-0.6573***	(0.236)
C(Year) [2021]	-0.0062	(0.241)
C(Year) [2022]	-0.2337	(0.234)
C(Year) [2023]	-0.5091**	(0.256)
C(Origin_Prov) [British Columbia (BC)]	0.2992*	(0.169)
C(Origin_Prov) [Manitoba (MB)]	0.0560	(0.190)
C(Origin_Prov) [New Brunswick (NB)]	-2.1508***	(0.264)
C(Origin_Prov) [Newfoundland and Labrador (NL)]	0.5896**	(0.281)
C(Origin_Prov) [Northwest Territories (NT)]	2.9151***	(0.498)
C(Origin_Prov) [Nova Scotia (NS)]	1.5961***	(0.342)
C(Origin_Prov) [Ontario (ON)]	-0.8686***	(0.191)
C(Origin_Prov) [Prince Edward Island (PE)]	0.4417	(0.417)
C(Origin_Prov) [Quebec (QC)]	-1.0955***	(0.193)
C(Origin_Prov) [Saskatchewan (SK)]	0.4771**	(0.192)
C(Origin_Prov) [Yukon (YT)]	-22.6068***	(0.309)
C(Dest_Prov) [British Columbia (BC)]	-0.4921**	(0.196)
C(Dest_Prov) [Manitoba (MB)]	-0.6512***	(0.248)
C(Dest_Prov) [New Brunswick (NB)]	-3.0837***	(0.331)
C(Dest_Prov) [Newfoundland and Labrador (NL)]	-0.0517	(0.310)
C(Dest_Prov) [Northwest Territories (NT)]	-2.1489***	(0.378)
C(Dest_Prov) [Nova Scotia (NS)]	0.2031	(0.205)
C(Dest_Prov) [Nunavut (NU)]	-5.9859***	(0.433)
C(Dest_Prov) [Ontario (ON)]	-0.8540***	(0.184)
C(Dest_Prov) [Prince Edward Island (PE)]	-2.2422***	(0.391)
C(Dest_Prov) [Quebec (QC)]	-1.4569***	(0.210)
C(Dest_Prov) [Saskatchewan (SK)]	-0.8736***	(0.175)
C(Dest_Prov) [Yukon (YT)]	-4.5559***	(0.473)
ln_GDP_Origin	1.6394***	(0.072)
ln_GDP_Dest	0.8499***	(0.065)
ln_Air_Distance	0.2787***	(0.065)

Notes: *** $p < 0.01$, ** $p < 0.05$, * $p < 0.10$. N = 28,800. $R^2 = 0.7666$.

Table S 3. Perishables- PPML gravity-model estimates

Variable	Coefficient	Std. err.
Intercept	-86.4788***	(4.343)
C(Year) [2020]	-0.7537	(0.780)
C(Year) [2021]	-1.1015	(0.765)
C(Year) [2022]	-1.1193	(0.770)
C(Year) [2023]	-1.1001	(0.780)
C(Origin_Prov) [British Columbia (BC)]	3.3454***	(0.348)
C(Origin_Prov) [Manitoba (MB)]	-0.1203	(0.478)
C(Origin_Prov) [New Brunswick (NB)]	1.2555**	(0.513)
C(Origin_Prov) [Newfoundland and Labrador (NL)]	2.8458***	(0.589)
C(Origin_Prov) [Northwest Territories (NT)]	4.6659***	(0.983)
C(Origin_Prov) [Nova Scotia (NS)]	6.0069***	(0.420)
C(Origin_Prov) [Ontario (ON)]	1.1456***	(0.373)
C(Origin_Prov) [Prince Edward Island (PE)]	6.9016***	(0.574)
C(Origin_Prov) [Quebec (QC)]	1.1468***	(0.396)
C(Origin_Prov) [Saskatchewan (SK)]	0.4082	(0.432)
C(Origin_Prov) [Yukon (YT)]	-18.3642***	(0.523)
C(Dest_Prov) [British Columbia (BC)]	-0.2961	(0.339)
C(Dest_Prov) [Manitoba (MB)]	-0.7029	(0.481)
C(Dest_Prov) [New Brunswick (NB)]	-3.8465***	(0.797)
C(Dest_Prov) [Newfoundland and Labrador (NL)]	-0.8873	(0.633)
C(Dest_Prov) [Northwest Territories (NT)]	-4.7060***	(1.162)
C(Dest_Prov) [Nova Scotia (NS)]	-0.6821	(0.656)
C(Dest_Prov) [Nunavut (NU)]	-8.5398***	(1.214)
C(Dest_Prov) [Ontario (ON)]	0.3715	(0.487)
C(Dest_Prov) [Prince Edward Island (PE)]	-4.3302***	(1.029)
C(Dest_Prov) [Quebec (QC)]	-0.5735	(0.367)
C(Dest_Prov) [Saskatchewan (SK)]	-0.7892**	(0.372)
C(Dest_Prov) [Yukon (YT)]	-9.0092***	(1.147)
ln_GDP_Origin	2.1019***	(0.123)
ln_GDP_Dest	0.9417***	(0.178)
ln_Air_Distance	1.3618***	(0.190)

Notes: *** $p < 0.01$, ** $p < 0.05$, * $p < 0.10$. N = 28,800. $R^2 = 0.8011$.

Table S 4. High-Value Cargo-PPML gravity-model estimates.

Variable	Coefficient	Std. err.
Intercept	-67.9937***	(5.513)
C(Year) [2020]	-0.3418	(0.447)
C(Year) [2021]	-0.9482**	(0.428)
C(Year) [2022]	-1.2017***	(0.425)
C(Year) [2023]	-1.3164***	(0.499)
C(Origin_Prov) [British Columbia (BC)]	1.1142***	(0.365)
C(Origin_Prov) [Manitoba (MB)]	1.1725**	(0.468)
C(Origin_Prov) [New Brunswick (NB)]	-17.6557***	(0.481)
C(Origin_Prov) [Newfoundland and Labrador (NL)]	0.8668	(0.672)
C(Origin_Prov) [Northwest Territories (NT)]	1.3279	(0.871)
C(Origin_Prov) [Nova Scotia (NS)]	2.3899***	(0.509)
C(Origin_Prov) [Ontario (ON)]	1.1829***	(0.365)
C(Origin_Prov) [Prince Edward Island (PE)]	-17.4689***	(0.569)
C(Origin_Prov) [Quebec (QC)]	0.8688**	(0.421)
C(Origin_Prov) [Saskatchewan (SK)]	0.9884*	(0.506)
C(Origin_Prov) [Yukon (YT)]	-17.0775***	(0.586)
C(Dest_Prov) [British Columbia (BC)]	-0.4906	(0.392)
C(Dest_Prov) [Manitoba (MB)]	0.3793	(0.508)
C(Dest_Prov) [New Brunswick (NB)]	-5.6398***	(0.880)
C(Dest_Prov) [Newfoundland and Labrador (NL)]	-0.8863	(0.690)
C(Dest_Prov) [Northwest Territories (NT)]	-21.2469***	(0.565)
C(Dest_Prov) [Nova Scotia (NS)]	1.5393***	(0.461)
C(Dest_Prov) [Nunavut (NU)]	-21.7769***	(0.547)
C(Dest_Prov) [Ontario (ON)]	0.8396**	(0.371)
C(Dest_Prov) [Prince Edward Island (PE)]	-4.7874***	(1.183)
C(Dest_Prov) [Quebec (QC)]	0.7339*	(0.395)
C(Dest_Prov) [Saskatchewan (SK)]	-0.6497	(0.620)
C(Dest_Prov) [Yukon (YT)]	-21.5064***	(0.565)
ln_GDP_Origin	1.5248***	(0.138)
ln_GDP_Dest	0.9223***	(0.123)
ln_Air_Distance	0.7343***	(0.218)

Notes: *** $p < 0.01$, ** $p < 0.05$, * $p < 0.10$. N = 28,800. $R^2 = 0.6805$.

Table S 5. Pharmaceuticals - PPML gravity-model estimates.

Variable	Coefficient	Std. err.
Intercept	-124.5932***	(8.101)
C(Year) [2020]	4.3423***	(0.705)
C(Year) [2021]	-0.5451	(0.733)
C(Year) [2022]	-0.9015	(0.770)
C(Year) [2023]	-0.0752	(0.771)
C(Origin_Prov) [British Columbia (BC)]	1.5242***	(0.308)
C(Origin_Prov) [Manitoba (MB)]	0.8822*	(0.465)
C(Origin_Prov) [New Brunswick (NB)]	0.3748	(1.027)
C(Origin_Prov) [Newfoundland and Labrador (NL)]	1.3214**	(0.592)
C(Origin_Prov) [Northwest Territories (NT)]	2.5498**	(1.159)
C(Origin_Prov) [Nova Scotia (NS)]	1.4005***	(0.539)
C(Origin_Prov) [Ontario (ON)]	0.7922*	(0.449)
C(Origin_Prov) [Prince Edward Island (PE)]	5.4215***	(1.020)
C(Origin_Prov) [Quebec (QC)]	-0.0535	(0.427)
C(Origin_Prov) [Saskatchewan (SK)]	2.8275***	(0.564)
C(Origin_Prov) [Yukon (YT)]	-11.1982***	(0.849)
C(Dest_Prov) [British Columbia (BC)]	-0.0651	(0.157)
C(Dest_Prov) [Manitoba (MB)]	0.2273	(0.271)
C(Dest_Prov) [New Brunswick (NB)]	-1.7172**	(0.679)
C(Dest_Prov) [Newfoundland and Labrador (NL)]	0.0452	(0.554)
C(Dest_Prov) [Northwest Territories (NT)]	-1.4952	(1.129)
C(Dest_Prov) [Nova Scotia (NS)]	1.0706***	(0.341)
C(Dest_Prov) [Nunavut (NU)]	-3.5676***	(1.123)
C(Dest_Prov) [Ontario (ON)]	-1.1493***	(0.390)
C(Dest_Prov) [Prince Edward Island (PE)]	0.4847	(0.898)
C(Dest_Prov) [Quebec (QC)]	-0.9979***	(0.366)
C(Dest_Prov) [Saskatchewan (SK)]	-1.8516**	(0.768)
C(Dest_Prov) [Yukon (YT)]	-17.3626***	(0.810)
ln_GDP_Origin	2.5247***	(0.158)
ln_GDP_Dest	1.8063***	(0.184)
ln_Air_Distance	1.5054***	(0.211)

Notes: *** $p < 0.01$, ** $p < 0.05$, * $p < 0.10$. N = 28,800. $R^2 = 0.79$.

Table S 6. Dangerous goods - PPML gravity-model estimates.

Variable	Coefficient	Std. err.
Intercept	-101.2876***	(7.362)
C(Year) [2020]	-0.4016	(0.643)
C(Year) [2021]	1.3040**	(0.645)
C(Year) [2022]	1.0910*	(0.624)
C(Year) [2023]	0.9596	(0.608)
C(Origin_Prov) [British Columbia (BC)]	1.3647***	(0.371)
C(Origin_Prov) [Manitoba (MB)]	0.6730	(0.419)
C(Origin_Prov) [New Brunswick (NB)]	-15.3203***	(0.720)
C(Origin_Prov) [Newfoundland and Labrador (NL)]	1.2430*	(0.716)
C(Origin_Prov) [Northwest Territories (NT)]	-13.3164***	(0.983)
C(Origin_Prov) [Nova Scotia (NS)]	1.7576***	(0.580)
C(Origin_Prov) [Ontario (ON)]	0.9070**	(0.429)
C(Origin_Prov) [Prince Edward Island (PE)]	-15.2689***	(0.888)
C(Origin_Prov) [Quebec (QC)]	-0.5931	(0.415)
C(Origin_Prov) [Saskatchewan (SK)]	-1.5917*	(0.854)
C(Origin_Prov) [Yukon (YT)]	-13.6918***	(0.931)
C(Dest_Prov) [British Columbia (BC)]	-0.0770	(0.418)
C(Dest_Prov) [Manitoba (MB)]	-1.9680***	(0.402)
C(Dest_Prov) [New Brunswick (NB)]	-2.8219***	(0.636)
C(Dest_Prov) [Newfoundland and Labrador (NL)]	1.4790*	(0.860)
C(Dest_Prov) [Northwest Territories (NT)]	-2.8714***	(0.844)
C(Dest_Prov) [Nova Scotia (NS)]	-0.5986	(0.618)
C(Dest_Prov) [Nunavut (NU)]	-5.4869***	(1.291)
C(Dest_Prov) [Ontario (ON)]	-1.8068***	(0.498)
C(Dest_Prov) [Prince Edward Island (PE)]	-2.3972***	(0.849)
C(Dest_Prov) [Quebec (QC)]	-2.3827***	(0.496)
C(Dest_Prov) [Saskatchewan (SK)]	-0.7422	(0.660)
C(Dest_Prov) [Yukon (YT)]	-18.7380***	(0.684)
ln_GDP_Origin	2.3425***	(0.243)
ln_GDP_Dest	1.3822***	(0.133)
ln_Air_Distance	0.6906***	(0.167)

Notes: *** $p < 0.01$, ** $p < 0.05$, * $p < 0.10$. N = 28,800. $R^2 = 0.8572$.

Table S 7. Live Animals - PPML gravity-model estimates.

Variable	Coefficient	Std. err.
Intercept	-90.3061***	(4.128)
C(Year) [2020]	-0.1251	(0.421)
C(Year) [2021]	-0.3961	(0.422)
C(Year) [2022]	-0.2338	(0.423)
C(Year) [2023]	0.6159	(0.378)
C(Origin_Prov) [British Columbia (BC)]	0.1784	(0.357)
C(Origin_Prov) [Manitoba (MB)]	1.2694***	(0.296)
C(Origin_Prov) [New Brunswick (NB)]	-0.6132	(0.628)
C(Origin_Prov) [Newfoundland and Labrador (NL)]	1.2626***	(0.480)
C(Origin_Prov) [Northwest Territories (NT)]	2.2924***	(0.772)
C(Origin_Prov) [Nova Scotia (NS)]	1.5487***	(0.358)
C(Origin_Prov) [Ontario (ON)]	-1.3401***	(0.374)
C(Origin_Prov) [Prince Edward Island (PE)]	-14.6281***	(0.396)
C(Origin_Prov) [Quebec (QC)]	-1.0625***	(0.342)
C(Origin_Prov) [Saskatchewan (SK)]	0.7959**	(0.350)
C(Origin_Prov) [Yukon (YT)]	-13.6247***	(0.414)
C(Dest_Prov) [British Columbia (BC)]	0.0544	(0.204)
C(Dest_Prov) [Manitoba (MB)]	-0.3952	(0.270)
C(Dest_Prov) [New Brunswick (NB)]	-1.3249**	(0.547)
C(Dest_Prov) [Newfoundland and Labrador (NL)]	0.4682	(0.312)
C(Dest_Prov) [Northwest Territories (NT)]	-2.5835***	(0.831)
C(Dest_Prov) [Nova Scotia (NS)]	-0.2768	(0.318)
C(Dest_Prov) [Nunavut (NU)]	-22.3941***	(0.501)
C(Dest_Prov) [Ontario (ON)]	-0.9055**	(0.356)
C(Dest_Prov) [Prince Edward Island (PE)]	-0.5882	(0.418)
C(Dest_Prov) [Quebec (QC)]	-0.7049**	(0.301)
C(Dest_Prov) [Saskatchewan (SK)]	-0.2771	(0.286)
C(Dest_Prov) [Yukon (YT)]	-8.0032***	(1.109)
ln_GDP_Origin	2.6144***	(0.114)
ln_GDP_Dest	0.9155***	(0.100)
ln_Air_Distance	0.1841*	(0.105)

Notes: *** $p < 0.01$, ** $p < 0.05$, * $p < 0.10$. N = 28,800. $R^2 = 0.7745$.

Table S 8. Other Special Cargo - PPML gravity-model estimates

Variable	Coefficient	Std. err.
Intercept	-109.6730***	(6.589)
C(Year) [2020]	-0.1704	(0.653)
C(Year) [2021]	-0.0879	(0.656)
C(Year) [2022]	-0.5133	(0.604)
C(Year) [2023]	-0.8188	(0.647)
C(Origin_Prov) [British Columbia (BC)]	0.7852**	(0.342)
C(Origin_Prov) [Manitoba (MB)]	1.6346***	(0.495)
C(Origin_Prov) [New Brunswick (NB)]	-0.4796	(0.607)
C(Origin_Prov) [Newfoundland and Labrador (NL)]	1.9901***	(0.523)
C(Origin_Prov) [Northwest Territories (NT)]	3.9767***	(0.890)
C(Origin_Prov) [Nova Scotia (NS)]	1.8197***	(0.441)
C(Origin_Prov) [Ontario (ON)]	0.0750	(0.311)
C(Origin_Prov) [Prince Edward Island (PE)]	5.3409***	(0.771)
C(Origin_Prov) [Quebec (QC)]	-0.4280	(0.503)
C(Origin_Prov) [Saskatchewan (SK)]	3.2252***	(0.447)
C(Origin_Prov) [Yukon (YT)]	-15.7642***	(0.711)
C(Dest_Prov) [British Columbia (BC)]	-0.2684	(0.421)
C(Dest_Prov) [Manitoba (MB)]	-1.4787	(0.946)
C(Dest_Prov) [New Brunswick (NB)]	-2.7957***	(0.626)
C(Dest_Prov) [Newfoundland and Labrador (NL)]	-1.2099*	(0.622)
C(Dest_Prov) [Northwest Territories (NT)]	-10.0816***	(0.787)
C(Dest_Prov) [Nova Scotia (NS)]	-0.9839	(0.644)
C(Dest_Prov) [Nunavut (NU)]	-3.4495***	(0.547)
C(Dest_Prov) [Ontario (ON)]	0.2197	(0.652)
C(Dest_Prov) [Prince Edward Island (PE)]	-3.3162***	(0.849)
C(Dest_Prov) [Quebec (QC)]	-0.2038	(0.414)
C(Dest_Prov) [Saskatchewan (SK)]	-3.5183***	(0.578)
C(Dest_Prov) [Yukon (YT)]	-7.3450***	(0.702)
ln_GDP_Origin	2.9307***	(0.183)
ln_GDP_Dest	0.8454***	(0.185)
ln_Air_Distance	1.9722***	(0.413)

Notes: *** $p < 0.01$, ** $p < 0.05$, * $p < 0.10$. N = 28,800. $R^2 = 0.7935$.

Table S 9. Commodity Information Pending - PPML gravity-model estimates.

Variable	Coefficient	Std. err.
Intercept	-88.4563***	(6.621)
C(Year) [2020]	-0.5373	(0.371)
C(Year) [2021]	-25.3488***	(0.371)
C(Year) [2022]	-4.5506***	(0.408)
C(Year) [2023]	-1.1480***	(0.370)
C(Origin_Prov) [British Columbia (BC)]	0.1976	(0.370)
C(Origin_Prov) [Manitoba (MB)]	0.7782*	(0.424)
C(Origin_Prov) [New Brunswick (NB)]	6.0629***	(0.789)
C(Origin_Prov) [Newfoundland and Labrador (NL)]	4.2611***	(0.626)
C(Origin_Prov) [Northwest Territories (NT)]	3.1179***	(1.127)
C(Origin_Prov) [Nova Scotia (NS)]	5.1547***	(0.718)
C(Origin_Prov) [Ontario (ON)]	-2.1943***	(0.457)
C(Origin_Prov) [Prince Edward Island (PE)]	3.1733***	(1.025)
C(Origin_Prov) [Quebec (QC)]	-2.1399***	(0.401)
C(Origin_Prov) [Saskatchewan (SK)]	0.8108	(0.509)
C(Origin_Prov) [Yukon (YT)]	-13.3458***	(0.873)
C(Dest_Prov) [British Columbia (BC)]	-0.8397**	(0.362)
C(Dest_Prov) [Manitoba (MB)]	0.2523	(0.348)
C(Dest_Prov) [New Brunswick (NB)]	-0.9671*	(0.569)
C(Dest_Prov) [Newfoundland and Labrador (NL)]	0.5480	(0.418)
C(Dest_Prov) [Northwest Territories (NT)]	-6.0632***	(0.565)
C(Dest_Prov) [Nova Scotia (NS)]	-0.1224	(0.352)
C(Dest_Prov) [Nunavut (NU)]	-7.3920***	(0.523)
C(Dest_Prov) [Ontario (ON)]	0.3003	(0.411)
C(Dest_Prov) [Prince Edward Island (PE)]	-5.9920***	(0.762)
C(Dest_Prov) [Quebec (QC)]	-1.4787***	(0.331)
C(Dest_Prov) [Saskatchewan (SK)]	-0.7181***	(0.270)
C(Dest_Prov) [Yukon (YT)]	-6.0590***	(0.582)
ln_GDP_Origin	2.8388***	(0.222)
ln_GDP_Dest	0.6913***	(0.105)
ln_Air_Distance	0.4146***	(0.125)

Notes: *** $p < 0.01$, ** $p < 0.05$, * $p < 0.10$. N = 28,800. $R^2 = 0.7034$.

Appendix T: Full Service-Level PPML Gravity-Model Estimation Results

This appendix reports the complete Poisson pseudo-maximum-likelihood (PPML) gravity-model estimates for each of the seven cargo service groups. All models share the same specification, log origin GDP, log destination GDP, log air distance, year fixed effects, and origin- and destination-province fixed effects.

Table T 1. Commodity Information Pending-PPML gravity-model estimates.

Variable	Coefficient	Std. err.
Intercept	-99.7555***	(7.619)
C(Year) [2020]	-0.4773	(0.386)
C(Year) [2021]	-0.8793**	(0.377)
C(Year) [2022]	-0.8863**	(0.381)
C(Year) [2023]	-1.1558***	(0.380)
C(Origin_Prov) [British Columbia (BC)]	-0.0795	(0.297)
C(Origin_Prov) [Manitoba (MB)]	0.8671**	(0.349)
C(Origin_Prov) [New Brunswick (NB)]	6.6292***	(0.770)
C(Origin_Prov) [Newfoundland and Labrador (NL)]	4.6520***	(0.598)
C(Origin_Prov) [Northwest Territories (NT)]	3.5192***	(1.204)
C(Origin_Prov) [Nova Scotia (NS)]	5.0861***	(0.544)
C(Origin_Prov) [Ontario (ON)]	-2.6990***	(0.455)
C(Origin_Prov) [Prince Edward Island (PE)]	3.2918***	(1.061)
C(Origin_Prov) [Quebec (QC)]	-2.4915***	(0.359)
C(Origin_Prov) [Saskatchewan (SK)]	0.9192*	(0.484)
C(Origin_Prov) [Yukon (YT)]	0.2641	(1.327)
C(Dest_Prov) [British Columbia (BC)]	-0.5488**	(0.245)
C(Dest_Prov) [Manitoba (MB)]	0.6866**	(0.267)
C(Dest_Prov) [New Brunswick (NB)]	-0.4334	(0.479)
C(Dest_Prov) [Newfoundland and Labrador (NL)]	0.9379**	(0.362)
C(Dest_Prov) [Northwest Territories (NT)]	-5.2654***	(0.626)
C(Dest_Prov) [Nova Scotia (NS)]	0.0132	(0.291)
C(Dest_Prov) [Nunavut (NU)]	-6.9026***	(0.527)
C(Dest_Prov) [Ontario (ON)]	0.1399	(0.316)
C(Dest_Prov) [Prince Edward Island (PE)]	-5.8662***	(0.779)
C(Dest_Prov) [Quebec (QC)]	-1.5072***	(0.230)
C(Dest_Prov) [Saskatchewan (SK)]	-0.5063**	(0.196)
C(Dest_Prov) [Yukon (YT)]	-4.5377***	(0.607)
ln_GDP_Origin	3.0932***	(0.249)
ln_GDP_Dest	0.8855***	(0.112)
ln_Air_Distance	0.4305***	(0.093)

Notes: *** $p < 0.01$, ** $p < 0.05$, * $p < 0.10$. N = 28,800. $R^2 = 0.7453$.

Table T 2. Express and Time-Sensitive Cargo - PPML gravity-model estimates.

Variable	Coefficient	Std. err.
Intercept	-78.0147***	(3.660)
C(Year) [2020]	-0.7328	(0.721)
C(Year) [2021]	-1.0495	(0.707)
C(Year) [2022]	-1.0645	(0.712)
C(Year) [2023]	-0.9996	(0.716)
C(Origin_Prov) [British Columbia (BC)]	2.7938***	(0.269)
C(Origin_Prov) [Manitoba (MB)]	0.6182*	(0.325)
C(Origin_Prov) [New Brunswick (NB)]	1.1349*	(0.604)
C(Origin_Prov) [Newfoundland and Labrador (NL)]	1.9291***	(0.475)
C(Origin_Prov) [Northwest Territories (NT)]	3.1373***	(0.906)
C(Origin_Prov) [Nova Scotia (NS)]	4.9833***	(0.342)
C(Origin_Prov) [Ontario (ON)]	0.8693***	(0.292)
C(Origin_Prov) [Prince Edward Island (PE)]	5.4355***	(0.485)
C(Origin_Prov) [Quebec (QC)]	0.7376**	(0.303)
C(Origin_Prov) [Saskatchewan (SK)]	1.2242***	(0.307)
C(Origin_Prov) [Yukon (YT)]	-19.7976***	(0.439)
C(Dest_Prov) [British Columbia (BC)]	-0.2594	(0.320)
C(Dest_Prov) [Manitoba (MB)]	-0.6530	(0.441)
C(Dest_Prov) [New Brunswick (NB)]	-2.7743***	(0.632)
C(Dest_Prov) [Newfoundland and Labrador (NL)]	-0.7310	(0.554)
C(Dest_Prov) [Northwest Territories (NT)]	-4.3636***	(0.946)
C(Dest_Prov) [Nova Scotia (NS)]	-0.3856	(0.527)
C(Dest_Prov) [Nunavut (NU)]	-7.3403***	(0.757)
C(Dest_Prov) [Ontario (ON)]	0.3771	(0.437)
C(Dest_Prov) [Prince Edward Island (PE)]	-3.3269***	(0.974)
C(Dest_Prov) [Quebec (QC)]	-0.5644*	(0.335)
C(Dest_Prov) [Saskatchewan (SK)]	-0.7141**	(0.314)
C(Dest_Prov) [Yukon (YT)]	-8.4347***	(0.995)
ln_GDP_Origin	1.8670***	(0.112)
ln_GDP_Dest	0.9253***	(0.158)
ln_Air_Distance	1.1868***	(0.160)

Notes: *** $p < 0.01$, ** $p < 0.05$, * $p < 0.10$. N = 28,800. $R^2 = 0.7898$.

Table T 3. General Cargo - PPML gravity-model estimates.

Variable	Coefficient	Std. err.
Intercept	-60.7248***	(2.461)
C(Year) [2020]	-0.6709***	(0.235)
C(Year) [2021]	-0.0196	(0.241)
C(Year) [2022]	-0.2469	(0.234)
C(Year) [2023]	-0.5223**	(0.255)
C(Origin_Prov) [British Columbia (BC)]	0.3030*	(0.169)
C(Origin_Prov) [Manitoba (MB)]	0.0618	(0.191)
C(Origin_Prov) [New Brunswick (NB)]	-2.0903***	(0.262)
C(Origin_Prov) [Newfoundland and Labrador (NL)]	0.5905**	(0.281)
C(Origin_Prov) [Northwest Territories (NT)]	2.9162***	(0.498)
C(Origin_Prov) [Nova Scotia (NS)]	1.6069***	(0.341)
C(Origin_Prov) [Ontario (ON)]	-0.8696***	(0.192)
C(Origin_Prov) [Prince Edward Island (PE)]	0.4442	(0.418)
C(Origin_Prov) [Quebec (QC)]	-1.0944***	(0.194)
C(Origin_Prov) [Saskatchewan (SK)]	0.4784**	(0.193)
C(Origin_Prov) [Yukon (YT)]	-22.6047***	(0.308)
C(Dest_Prov) [British Columbia (BC)]	-0.4958**	(0.197)
C(Dest_Prov) [Manitoba (MB)]	-0.6571***	(0.249)
C(Dest_Prov) [New Brunswick (NB)]	-3.0930***	(0.330)
C(Dest_Prov) [Newfoundland and Labrador (NL)]	-0.0516	(0.309)
C(Dest_Prov) [Northwest Territories (NT)]	-2.1661***	(0.378)
C(Dest_Prov) [Nova Scotia (NS)]	0.2095	(0.205)
C(Dest_Prov) [Nunavut (NU)]	-5.9994***	(0.432)
C(Dest_Prov) [Ontario (ON)]	-0.8503***	(0.184)
C(Dest_Prov) [Prince Edward Island (PE)]	-2.2551***	(0.392)
C(Dest_Prov) [Quebec (QC)]	-1.4574***	(0.210)
C(Dest_Prov) [Saskatchewan (SK)]	-0.8774***	(0.175)
C(Dest_Prov) [Yukon (YT)]	-4.5705***	(0.472)
ln_GDP_Origin	1.6401***	(0.072)
ln_GDP_Dest	0.8466***	(0.065)
ln_Air_Distance	0.2801***	(0.065)

Notes: *** $p < 0.01$, ** $p < 0.05$, * $p < 0.10$. N = 28,800. $R^2 = 0.7657$.

Table T 4. Other Special Cargo (No Service) - PPML gravity-model estimates.

Variable	Coefficient	Std. err.
Intercept	-78.0173***	(4.796)
C(Year) [2020]	-0.1062	(0.429)
C(Year) [2021]	0.1340	(0.476)
C(Year) [2022]	0.0045	(0.451)
C(Year) [2023]	0.3154	(0.408)
C(Origin_Prov) [British Columbia (BC)]	0.7267***	(0.253)
C(Origin_Prov) [Manitoba (MB)]	0.9170***	(0.300)
C(Origin_Prov) [New Brunswick (NB)]	-2.8596***	(0.697)
C(Origin_Prov) [Newfoundland and Labrador (NL)]	0.7880	(0.633)
C(Origin_Prov) [Northwest Territories (NT)]	2.1809**	(0.898)
C(Origin_Prov) [Nova Scotia (NS)]	1.7277***	(0.457)
C(Origin_Prov) [Ontario (ON)]	0.3365	(0.312)
C(Origin_Prov) [Prince Edward Island (PE)]	-19.9369***	(0.535)
C(Origin_Prov) [Quebec (QC)]	-0.3059	(0.275)
C(Origin_Prov) [Saskatchewan (SK)]	0.7551*	(0.442)
C(Origin_Prov) [Yukon (YT)]	-19.4710***	(0.572)
C(Dest_Prov) [British Columbia (BC)]	-0.0917	(0.303)
C(Dest_Prov) [Manitoba (MB)]	-0.5042	(0.333)
C(Dest_Prov) [New Brunswick (NB)]	-1.8622***	(0.571)
C(Dest_Prov) [Newfoundland and Labrador (NL)]	0.6343	(0.535)
C(Dest_Prov) [Northwest Territories (NT)]	-3.0263***	(0.821)
C(Dest_Prov) [Nova Scotia (NS)]	0.2289	(0.319)
C(Dest_Prov) [Nunavut (NU)]	-7.1230***	(1.154)
C(Dest_Prov) [Ontario (ON)]	-0.8295***	(0.276)
C(Dest_Prov) [Prince Edward Island (PE)]	-1.0871**	(0.459)
C(Dest_Prov) [Quebec (QC)]	-0.6989**	(0.353)
C(Dest_Prov) [Saskatchewan (SK)]	-0.5782*	(0.350)
C(Dest_Prov) [Yukon (YT)]	-8.8174***	(1.128)
ln_GDP_Origin	1.9437***	(0.144)
Ln_GDP_Dest	1.0557***	(0.104)
ln_Air_Distance	0.3927***	(0.089)

Notes: *** $p < 0.01$, ** $p < 0.05$, * $p < 0.10$. N = 28,800. $R^2 = 0.7992$.

Table T 5. Oversize and Heavy-Weight Cargo - PPML gravity-model estimates.

Variable	Coefficient	Std. err.
Intercept	-119.3093***	(9.722)
C(Year) [2020]	-0.3723	(0.677)
C(Year) [2021]	-0.5902	(0.699)
C(Year) [2022]	-0.9683	(0.720)
C(Year) [2023]	-1.3913*	(0.711)
C(Origin_Prov) [British Columbia (BC)]	1.5777***	(0.456)
C(Origin_Prov) [Manitoba (MB)]	1.4908**	(0.620)
C(Origin_Prov) [New Brunswick (NB)]	0.4045	(1.279)
C(Origin_Prov) [Newfoundland and Labrador (NL)]	2.5456***	(0.752)
C(Origin_Prov) [Northwest Territories (NT)]	1.5820	(1.638)
C(Origin_Prov) [Nova Scotia (NS)]	2.1716***	(0.604)
C(Origin_Prov) [Ontario (ON)]	-0.3820	(0.674)
C(Origin_Prov) [Prince Edward Island (PE)]	-16.3171***	(1.005)
C(Origin_Prov) [Quebec (QC)]	-0.6161	(0.637)
C(Origin_Prov) [Saskatchewan (SK)]	1.1238*	(0.677)
C(Origin_Prov) [Yukon (YT)]	-14.5942***	(1.222)
C(Dest_Prov) [British Columbia (BC)]	0.1297	(0.356)
C(Dest_Prov) [Manitoba (MB)]	-0.8227	(0.732)
C(Dest_Prov) [New Brunswick (NB)]	-7.7257***	(1.002)
C(Dest_Prov) [Newfoundland and Labrador (NL)]	-2.1834***	(0.688)
C(Dest_Prov) [Northwest Territories (NT)]	-8.0623***	(1.254)
C(Dest_Prov) [Nova Scotia (NS)]	-0.9291*	(0.547)
C(Dest_Prov) [Nunavut (NU)]	-1.5891	(1.271)
C(Dest_Prov) [Ontario (ON)]	0.4682	(0.470)
C(Dest_Prov) [Prince Edward Island (PE)]	-24.5729***	(0.863)
C(Dest_Prov) [Quebec (QC)]	-0.3795	(0.363)
C(Dest_Prov) [Saskatchewan (SK)]	-3.8684***	(0.457)
C(Dest_Prov) [Yukon (YT)]	-10.3320***	(1.318)
ln_GDP_Origin	3.3395***	(0.319)
Ln_GDP_Dest	0.8325***	(0.183)
ln_Air_Distance	1.9184***	(0.229)

Notes: *** $p < 0.01$, ** $p < 0.05$, * $p < 0.10$. N = 28,800. $R^2 = 0.7820$.

Table T 6. Temperature-Sensitive Cargo-PPML gravity-model estimates

Variable	Coefficient	Std. err.
Intercept	-73.2318***	(3.903)
C(Year) [2020]	0.3777	(0.412)
C(Year) [2021]	0.7097*	(0.389)
C(Year) [2022]	0.8137*	(0.416)
C(Year) [2023]	1.3566***	(0.418)
C(Origin_Prov) [British Columbia (BC)]	2.5067***	(0.156)
C(Origin_Prov) [Manitoba (MB)]	0.5449	(0.340)
C(Origin_Prov) [New Brunswick (NB)]	0.9670	(0.714)
C(Origin_Prov) [Newfoundland and Labrador (NL)]	0.5014	(0.378)
C(Origin_Prov) [Northwest Territories (NT)]	-19.7869***	(0.523)
C(Origin_Prov) [Nova Scotia (NS)]	4.4722***	(0.318)
C(Origin_Prov) [Ontario (ON)]	1.0855***	(0.336)
C(Origin_Prov) [Prince Edward Island (PE)]	2.9246***	(0.507)
C(Origin_Prov) [Quebec (QC)]	0.0603	(0.342)
C(Origin_Prov) [Saskatchewan (SK)]	-0.0324	(0.290)
C(Origin_Prov) [Yukon (YT)]	-20.1983***	(0.499)
C(Dest_Prov) [British Columbia (BC)]	1.0291***	(0.234)
C(Dest_Prov) [Manitoba (MB)]	-0.0376	(0.291)
C(Dest_Prov) [New Brunswick (NB)]	-0.9491**	(0.371)
C(Dest_Prov) [Newfoundland and Labrador (NL)]	0.6576**	(0.318)
C(Dest_Prov) [Northwest Territories (NT)]	-3.2831***	(0.717)
C(Dest_Prov) [Nova Scotia (NS)]	0.3067	(0.347)
C(Dest_Prov) [Nunavut (NU)]	-4.1440***	(0.671)
C(Dest_Prov) [Ontario (ON)]	-0.1489	(0.257)
C(Dest_Prov) [Prince Edward Island (PE)]	-0.2530	(0.503)
C(Dest_Prov) [Quebec (QC)]	0.0882	(0.228)
C(Dest_Prov) [Saskatchewan (SK)]	-0.4785*	(0.247)
C(Dest_Prov) [Yukon (YT)]	-5.8402***	(1.099)
ln_GDP_Origin	1.4358***	(0.125)
Ln_GDP_Dest	1.2041***	(0.081)
ln_Air_Distance	0.6675***	(0.082)

Notes: *** $p < 0.01$, ** $p < 0.05$, * $p < 0.10$. $R^2 = 0.8074$.

Table T 7. Vulnerable Cargo - PPML gravity-model estimates

Variable	Coefficient	Std. err.
Intercept	-76.0285***	(6.926)
C(Year) [2020]	0.1612	(0.639)
C(Year) [2021]	-0.9563*	(0.565)
C(Year) [2022]	0.6888	(0.677)
C(Year) [2023]	3.3651***	(0.542)
C(Origin_Prov) [British Columbia (BC)]	0.3992	(0.438)
C(Origin_Prov) [Manitoba (MB)]	-2.0000***	(0.580)
C(Origin_Prov) [New Brunswick (NB)]	-16.9557***	(0.708)
C(Origin_Prov) [Newfoundland and Labrador (NL)]	-1.8375**	(0.824)
C(Origin_Prov) [Northwest Territories (NT)]	-15.5708***	(0.926)
C(Origin_Prov) [Nova Scotia (NS)]	-3.6420***	(0.851)
C(Origin_Prov) [Ontario (ON)]	-1.3232**	(0.558)
C(Origin_Prov) [Prince Edward Island (PE)]	-16.7179***	(0.857)
C(Origin_Prov) [Quebec (QC)]	-2.9770***	(0.731)
C(Origin_Prov) [Saskatchewan (SK)]	1.0358	(1.065)
C(Origin_Prov) [Yukon (YT)]	-15.8901***	(0.892)
C(Dest_Prov) [British Columbia (BC)]	-0.3501	(0.714)
C(Dest_Prov) [Manitoba (MB)]	-0.1610	(1.094)
C(Dest_Prov) [New Brunswick (NB)]	-1.8819**	(0.808)
C(Dest_Prov) [Newfoundland and Labrador (NL)]	0.5090	(0.864)
C(Dest_Prov) [Northwest Territories (NT)]	-15.1757***	(0.889)
C(Dest_Prov) [Nova Scotia (NS)]	-1.1281	(0.886)
C(Dest_Prov) [Nunavut (NU)]	-2.7514**	(1.195)
C(Dest_Prov) [Ontario (ON)]	-0.9907**	(0.496)
C(Dest_Prov) [Prince Edward Island (PE)]	-2.8488**	(1.318)
C(Dest_Prov) [Quebec (QC)]	-4.2356***	(0.672)
C(Dest_Prov) [Saskatchewan (SK)]	-0.5080	(1.066)
C(Dest_Prov) [Yukon (YT)]	-15.4669***	(0.728)
ln_GDP_Origin	1.3587***	(0.200)
Ln_GDP_Dest	1.2684***	(0.194)
ln_Air_Distance	0.5983***	(0.174)

Notes: *** $p < 0.01$, ** $p < 0.05$, * $p < 0.10$. $R^2 = 0.6800$.

Appendix U: Supplementary Modal-Shift Results with Surface Transportation Decarbonization

This appendix presents the commodity-based and service-tag modal-shift results when surface transportation decarbonization is incorporated. In all cases, the quantity of freight shifted from air transportation remains consistent with the modal-shift assumptions described in Section 3.5.2. Truck emissions are adjusted using the fleet-turnover pathway based on the zero-emission heavy-duty vehicle sales targets described in Section 3.5.3.1. The rail emission factors vary according to rail technology scenarios 1, 2, and 3 described in Section 3.5.3.2. The results are reported separately for the nine commodity-based modal shifts and seven service-tag modal shifts. Section 5.3.2 presents rail technology scenario 4 as the representative pathway and therefore does not repeat it in this appendix.

U.1 Rail Technology Scenario 1: Commodity-Based Modal Shifts

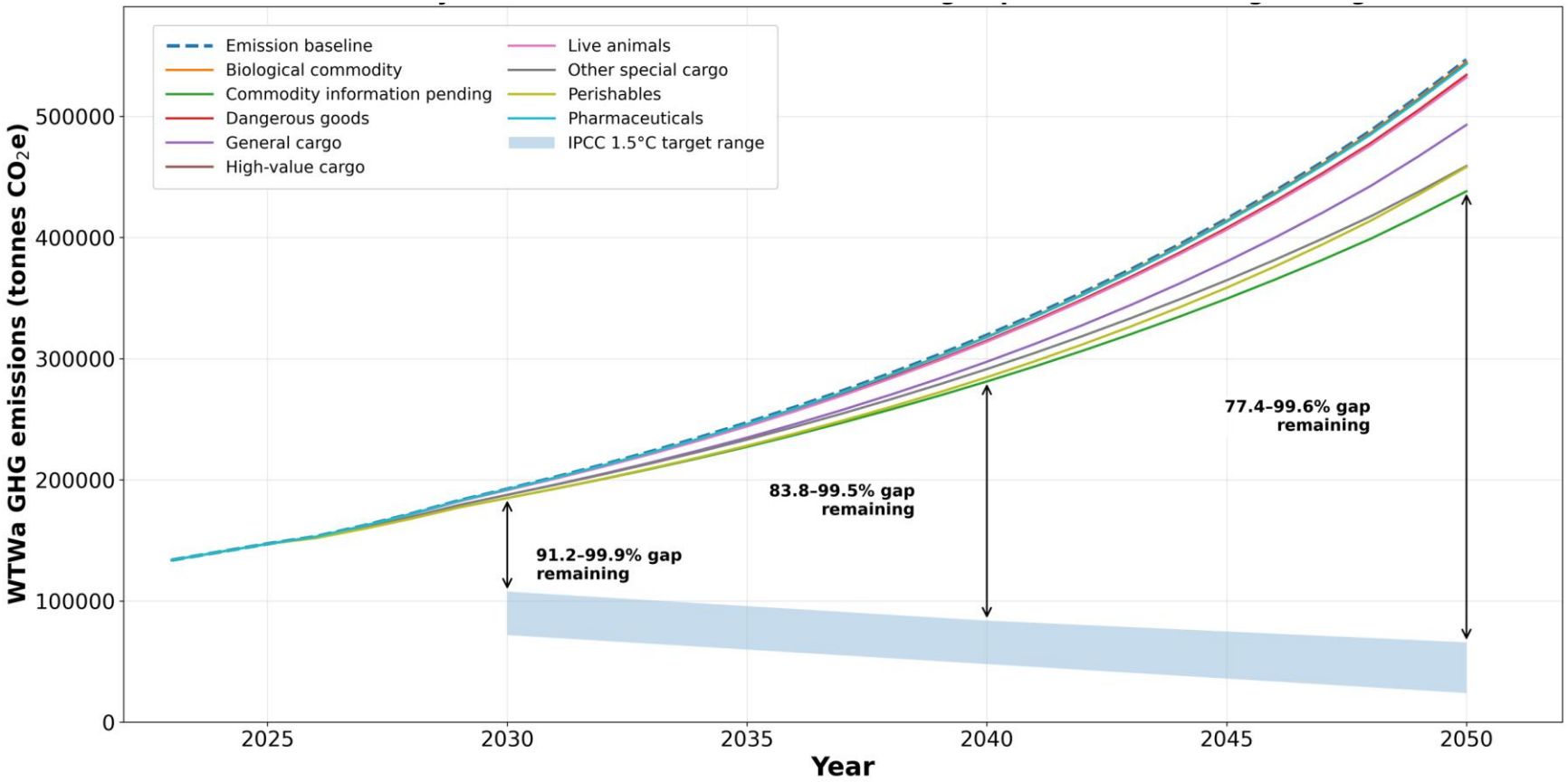


Figure U 1. Commodity-Based Modal-Shift Emissions under Rail Technology Scenario 1 Relative to the IPCC 1.5°C Target Range

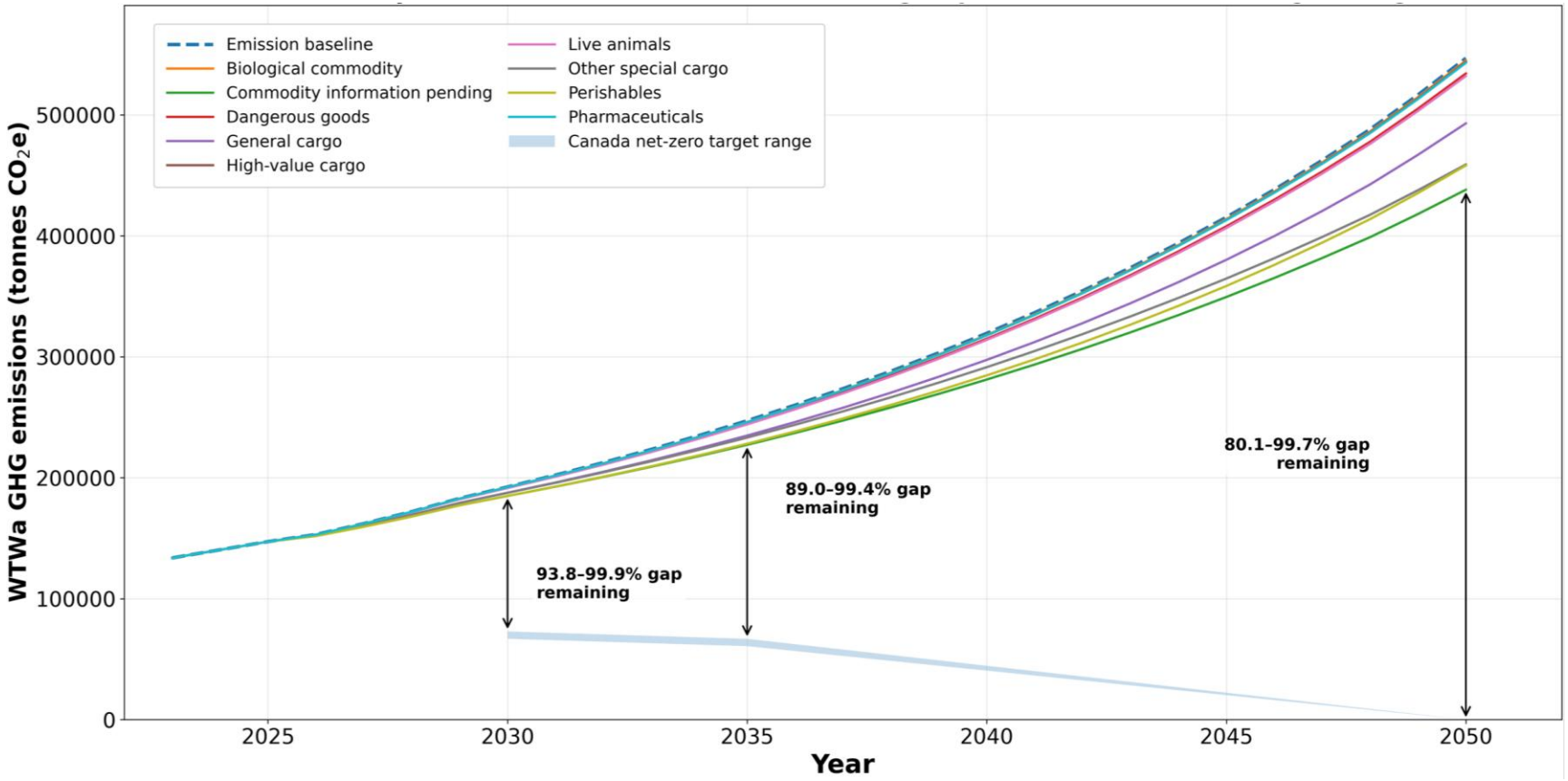


Figure U 2. Commodity-Based Modal-Shift Emissions under Rail Technology Scenario 1 Relative to Canada's Net-Zero Targets

U.2 Rail Technology Scenario 1: Service-Tag Modal Shifts

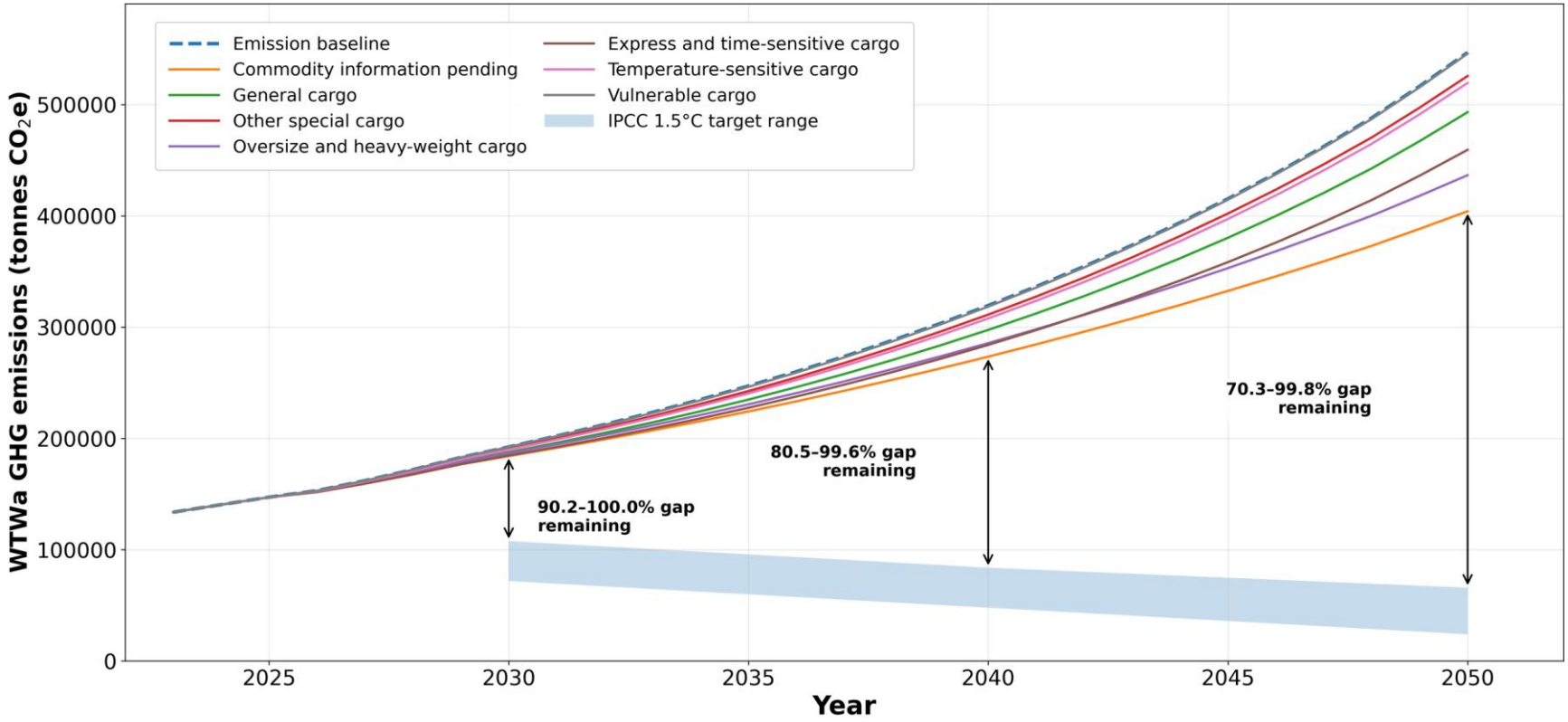


Figure U 3. Service-Tag Modal-Shift Emissions under Rail Technology Scenario 1 Relative to the IPCC 1.5°C Target Range

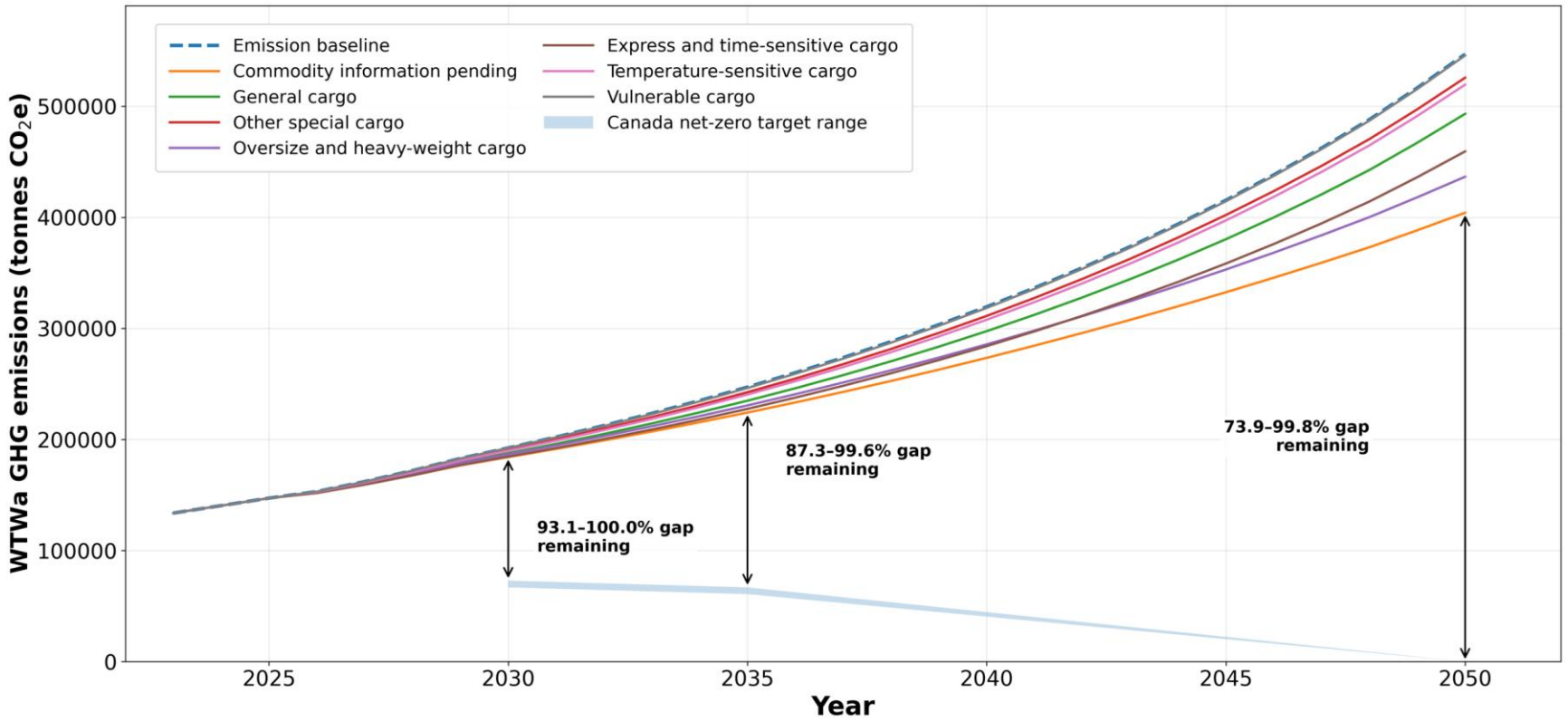


Figure U 4. Service-Tag Modal-Shift Emissions under Rail Technology Scenario 1 Relative to Canada's Net-Zero Targets

U.3 Rail Technology Scenario 2: Commodity-Based Modal Shifts

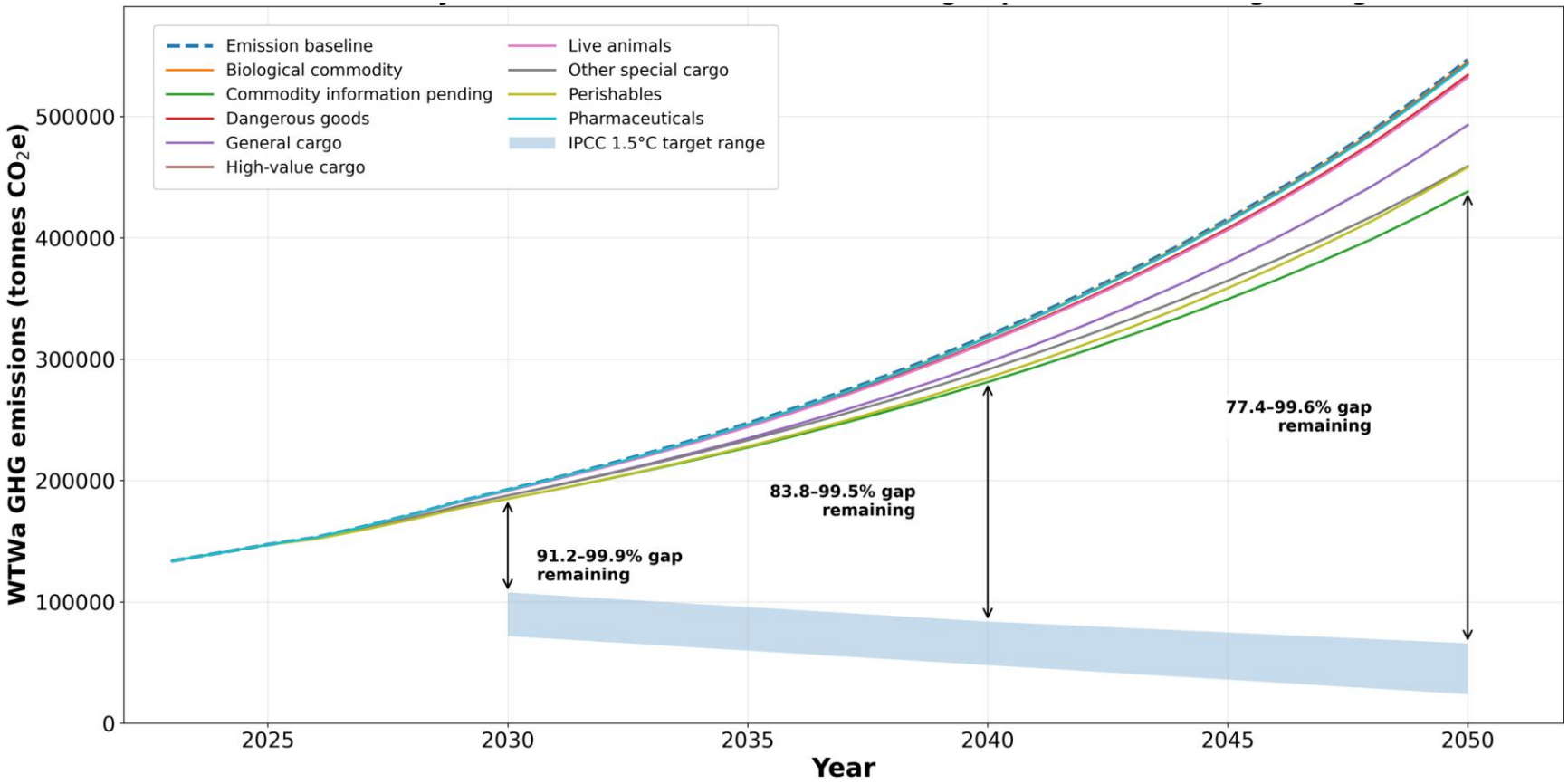


Figure U 5. Commodity-Based Modal-Shift Emissions under Rail Technology Scenario 2 Relative to the IPCC 1.5°C Target Range

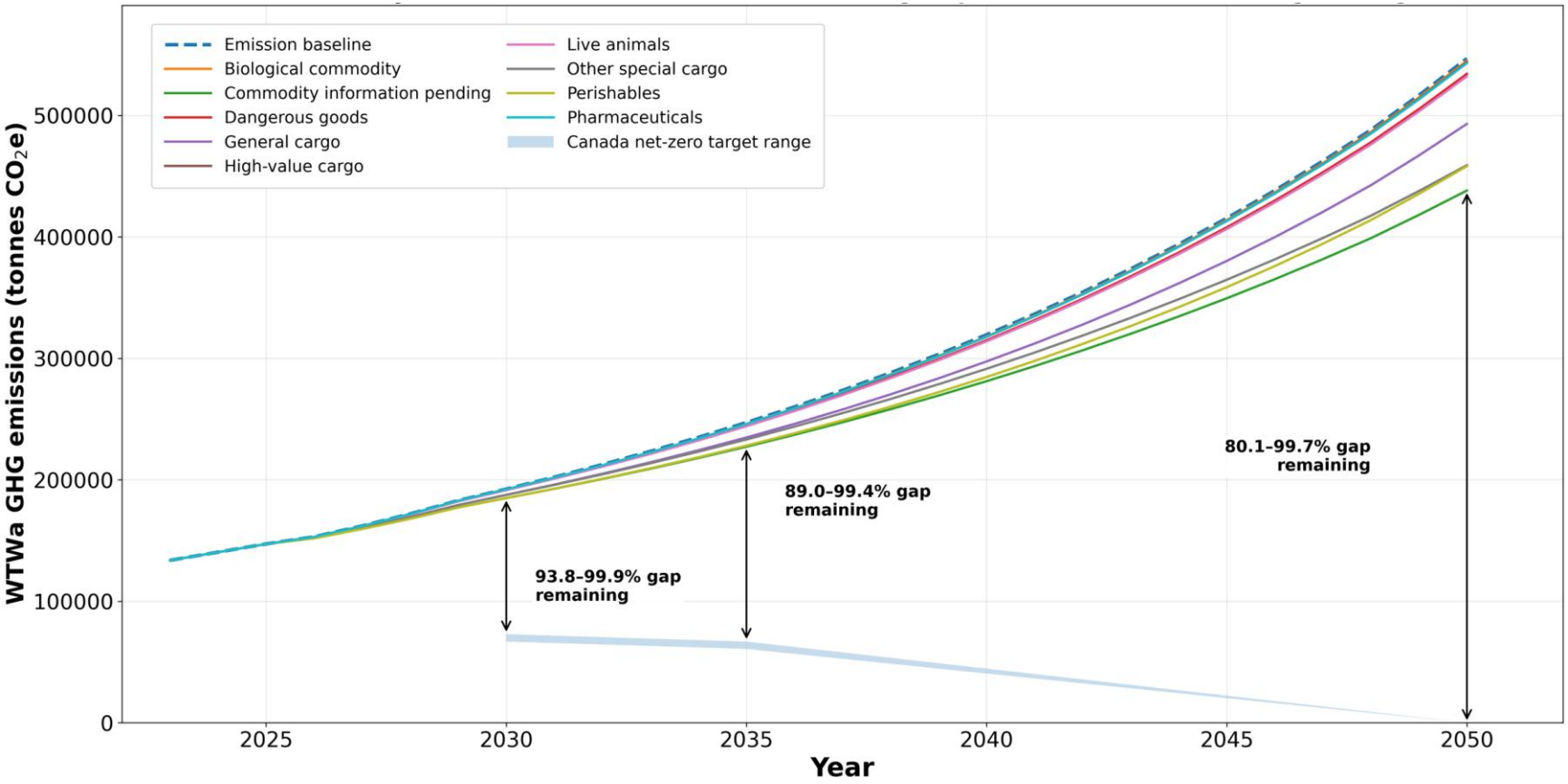


Figure U 6. Commodity-Based Modal-Shift Emissions under Rail Technology Scenario 2 Relative to Canada's Net-Zero Targets

U.4 Rail Technology Scenario 2: Service-Tag Modal Shifts

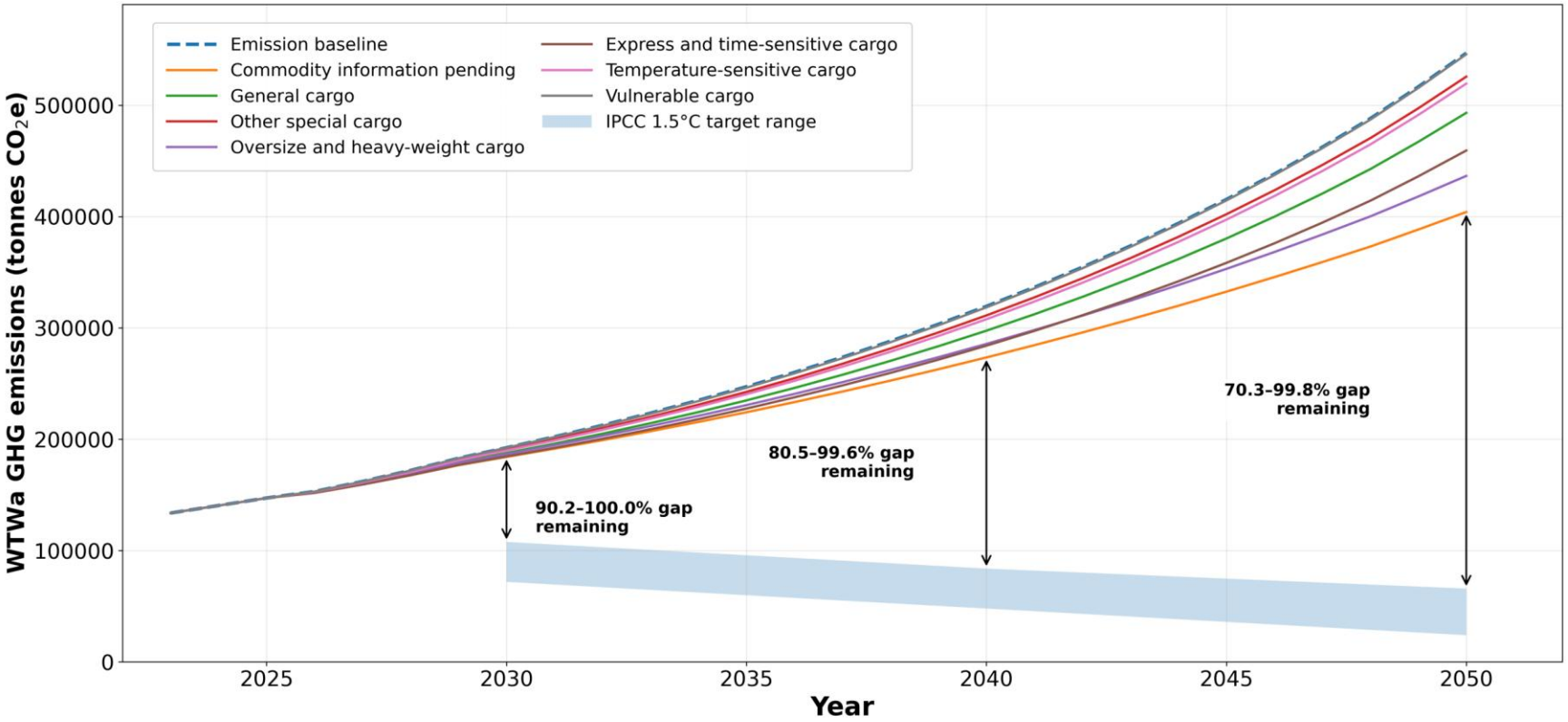


Figure U 7. Service-Tag Modal-Shift Emissions under Rail Technology Scenario 2 Relative to the IPCC 1.5°C Target Range

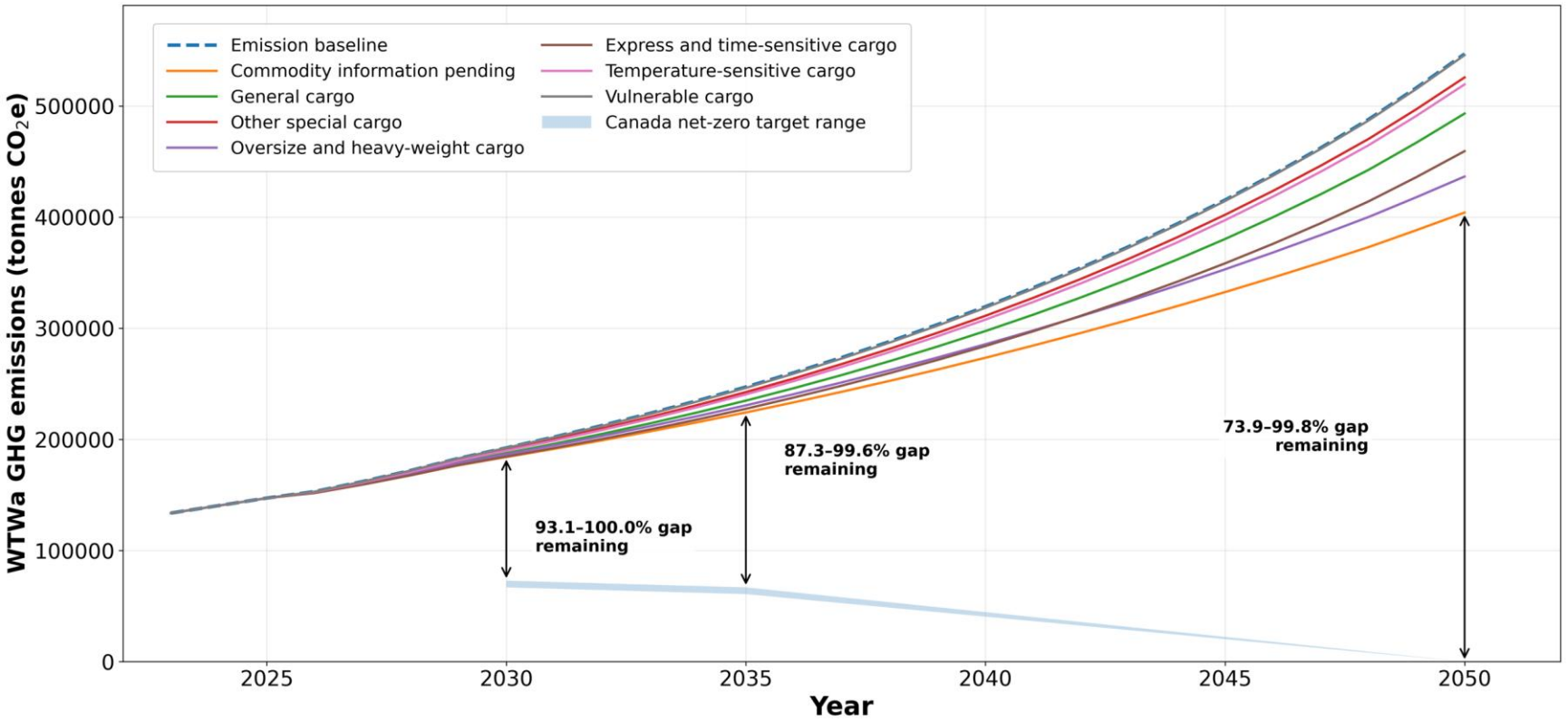


Figure U 8. Service-Tag Modal-Shift Emissions under Rail Technology Scenario 2 Relative to Canada's Net-Zero Targets

U.5 Rail Technology Scenario 3: Commodity-Based Modal Shifts

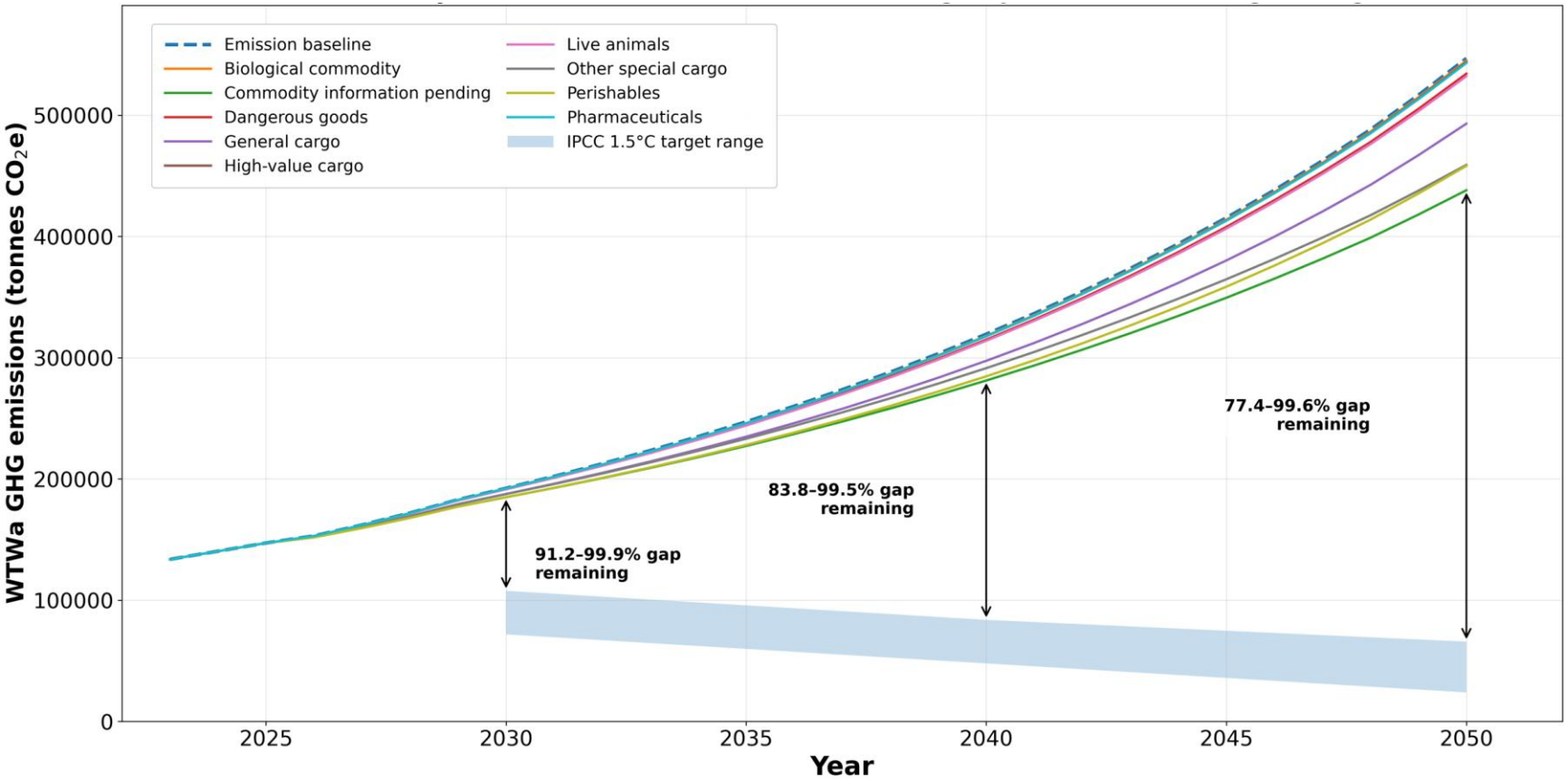


Figure U 9. Commodity-Based Modal-Shift Emissions under Rail Technology Scenario 3 Relative to the IPCC 1.5°C Target Range

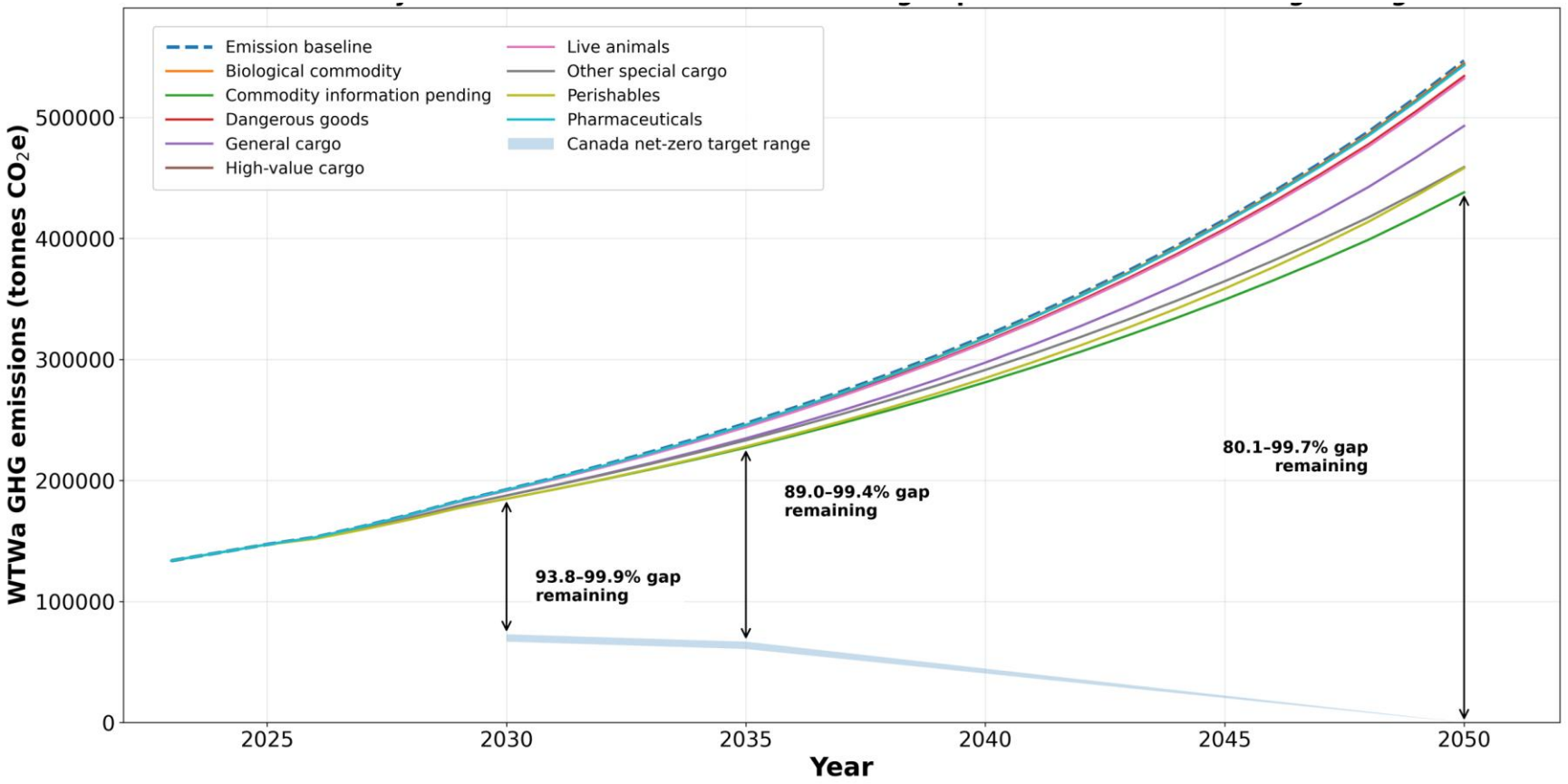


Figure U 10. Commodity-Based Modal-Shift Emissions under Rail Technology Scenario 3 Relative to Canada's Net-Zero Targets

U.6 Rail Technology Scenario 3: Service-Tag Modal Shifts

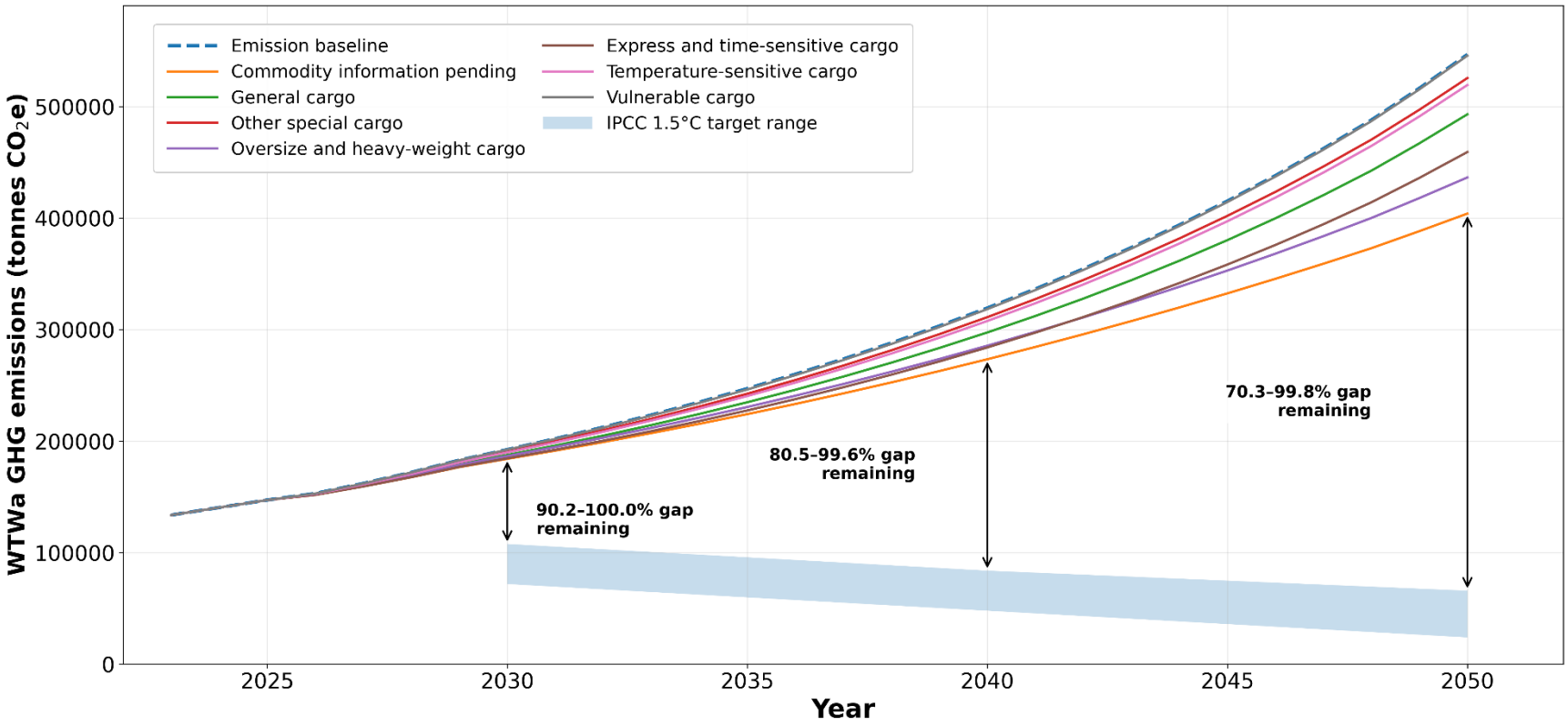


Figure U 11. Service-Tag Modal-Shift Emissions under Rail Technology Scenario 3 Relative to the IPCC 1.5°C Target Range

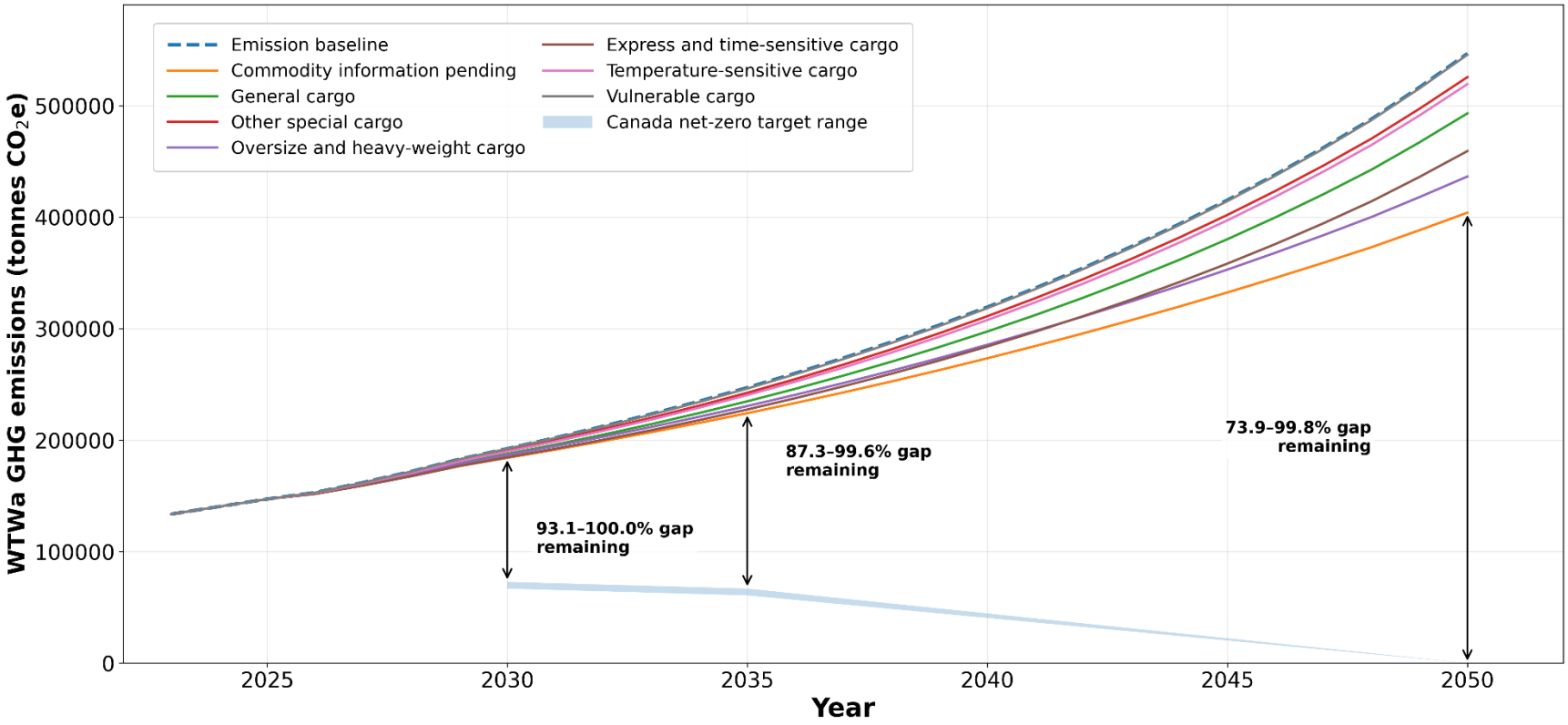


Figure U 12. Service-Tag Modal-Shift Emissions under Rail Technology Scenario 3 Relative to Canada's Net-Zero Targets

Appendix V: Supplementary Results for Alternative Combinations of SAF, Alternative Propulsion, Modal Shift, and Surface-Freight Decarbonization

This appendix presents the intermediate combined mitigation scenarios that are not discussed in detail in Section 5.4. These scenarios evaluate different combinations of sustainable aviation fuel (SAF) adoption, alternative propulsion (AP), modal shift (MS), and surface transportation decarbonization (SD). The appendix reports results for Category 4 (AP + SAF), Category 6 (MS + SAF), Category 7 (MS + AP), Category 8 (MS + AP + SAF), Category 10 (MS + SAF + SD), and Category 11 (MS + AP + SD). Because each category contains many variants, only the minimum- and maximum-emission cases are presented for each category to illustrate the range of possible outcomes.

V.1 Category 4: Alternative Propulsion and Sustainable Aviation Fuel

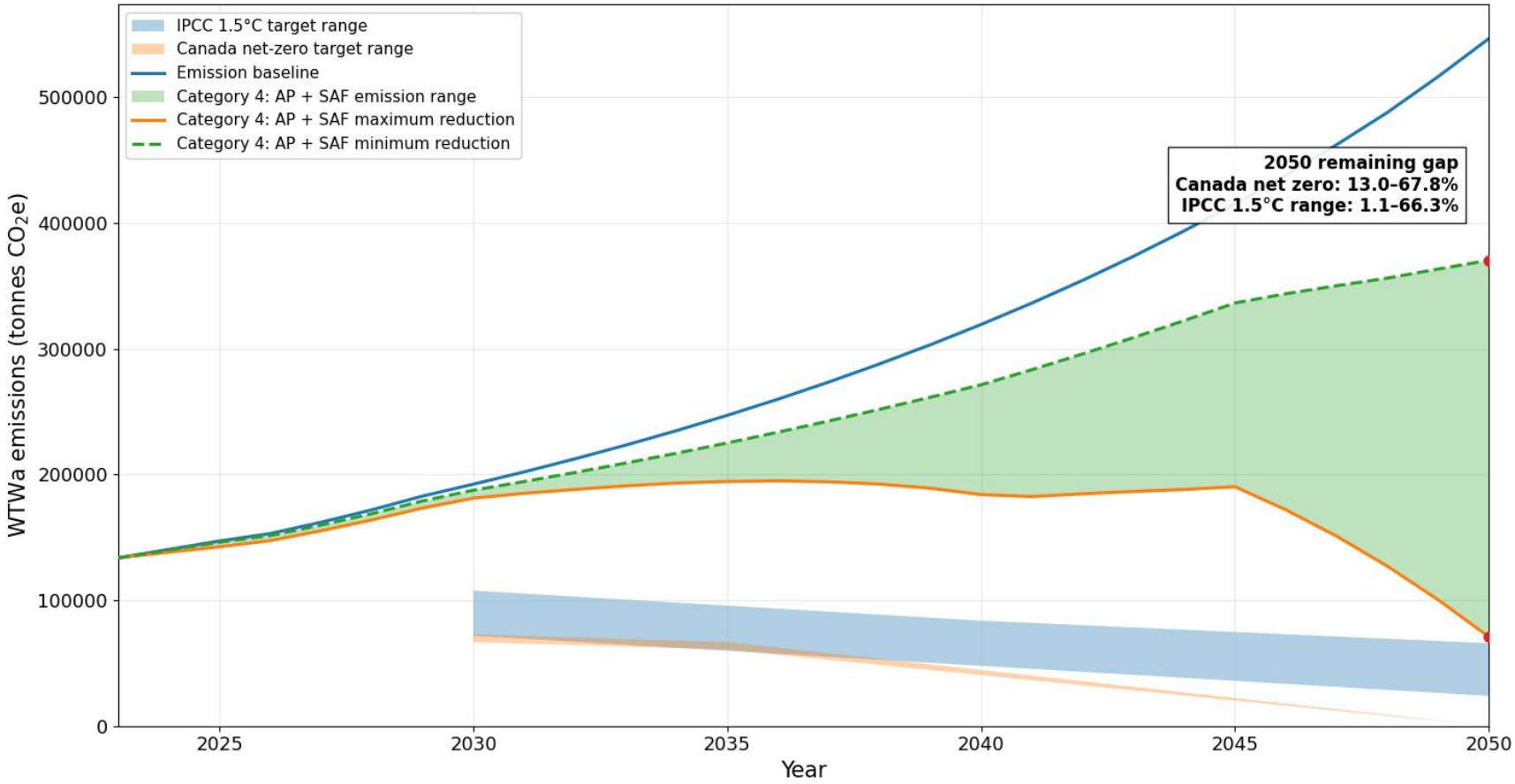


Figure V 1. Category 4 (AP + SAF): Minimum- and Maximum-Emission Cases

V.2 Category 6: Modal Shift and Sustainable Aviation Fuel

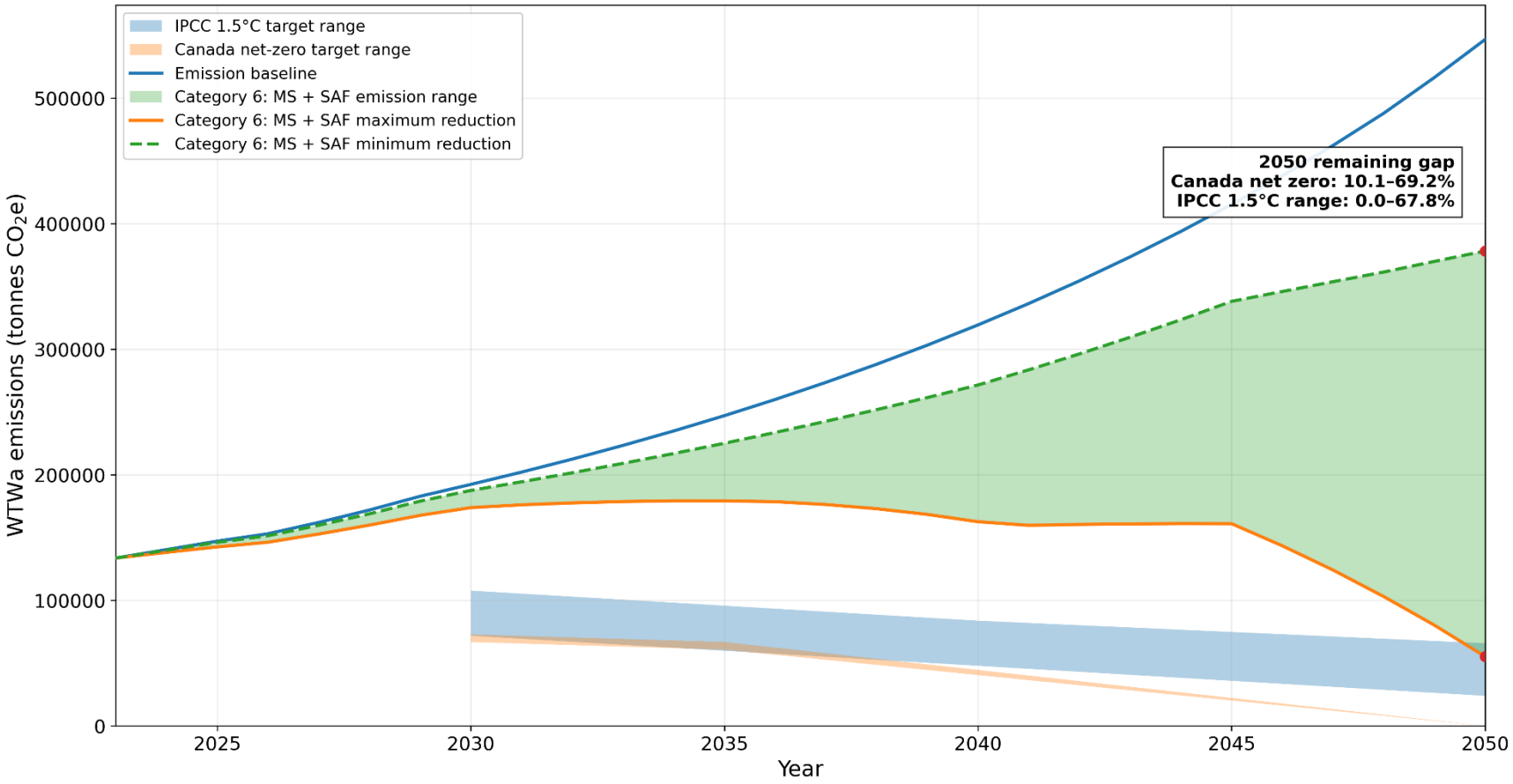


Figure V 2. Category 6 (MS + SAF): Minimum- and Maximum-Emission Cases

V.3 Category 7: Modal Shift and Alternative Propulsion

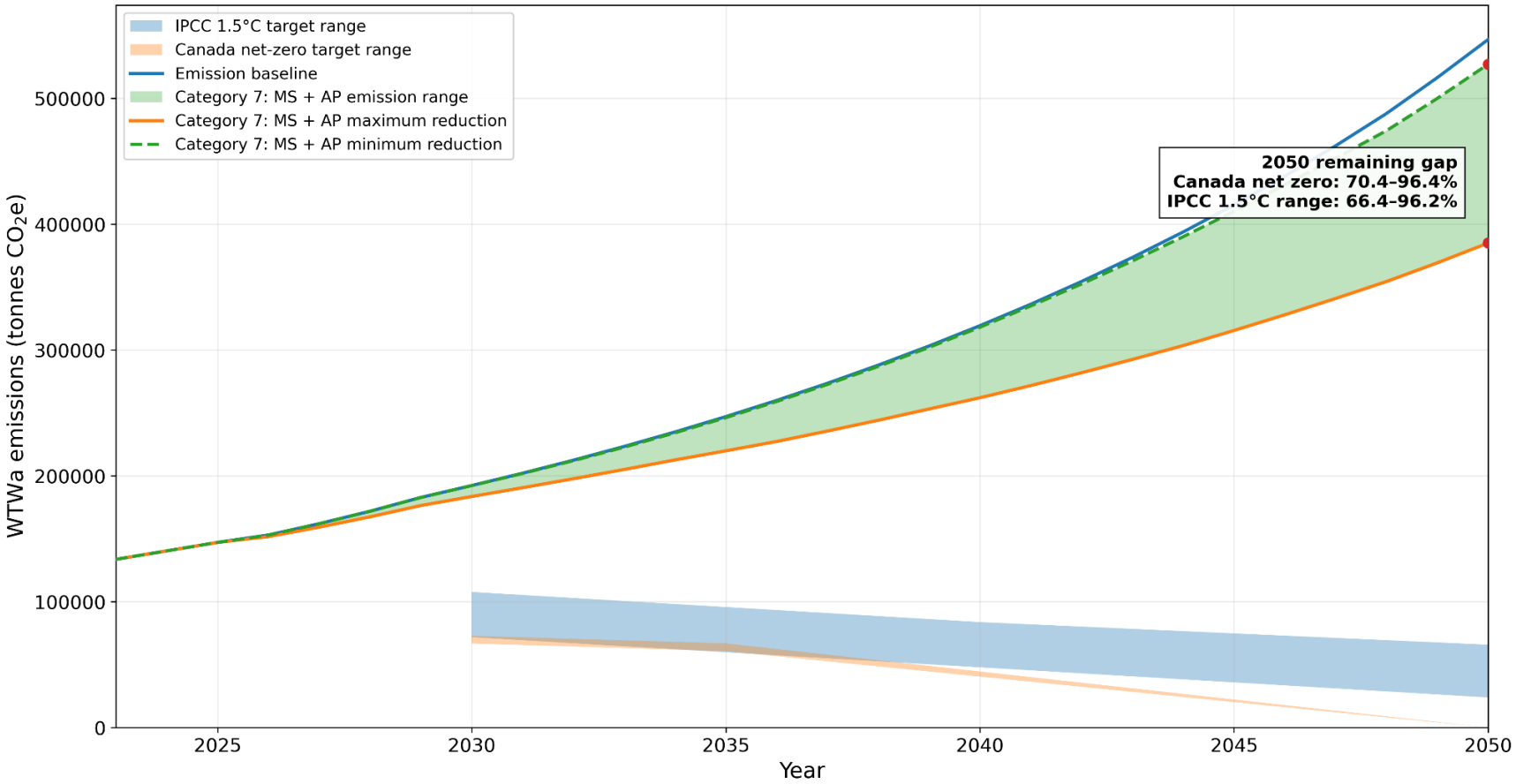


Figure V 3. Category 7 (MS + AP): Minimum- and Maximum-Emission Cases

V.4 Category 8: Modal Shift, Alternative Propulsion, and Sustainable Aviation Fuel

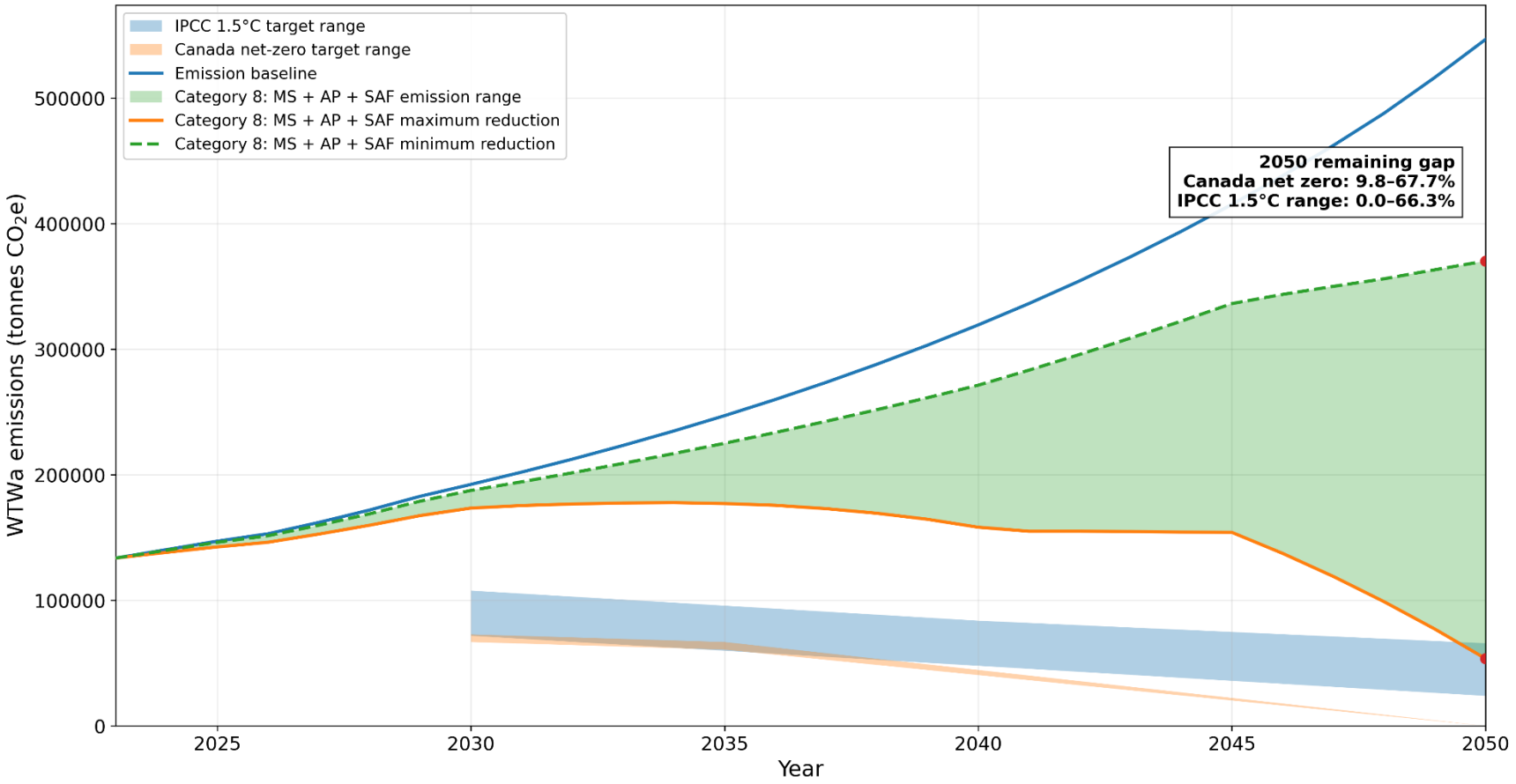


Figure V 4. Category 8 (MS + AP + SAF): Minimum- and Maximum-Emission Cases

V.5 Category 10: Modal Shift, Sustainable Aviation Fuel, and Surface Transportation Decarbonization

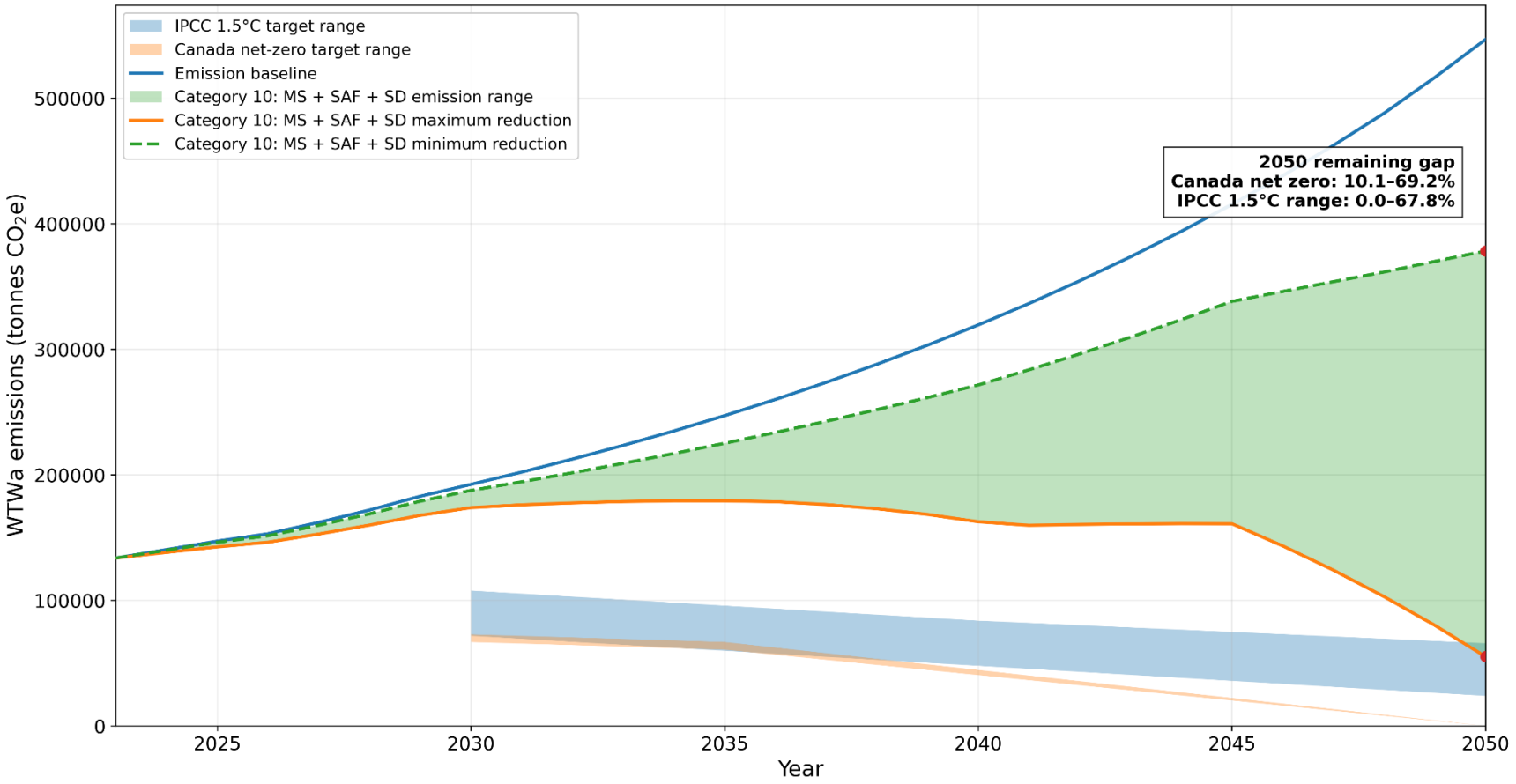


Figure V 5. Category 10 (MS + SAF + SD): Minimum- and Maximum-Emission Cases

V.6 Category 11: Modal Shift, Alternative Propulsion, and Surface Transportation Decarbonization

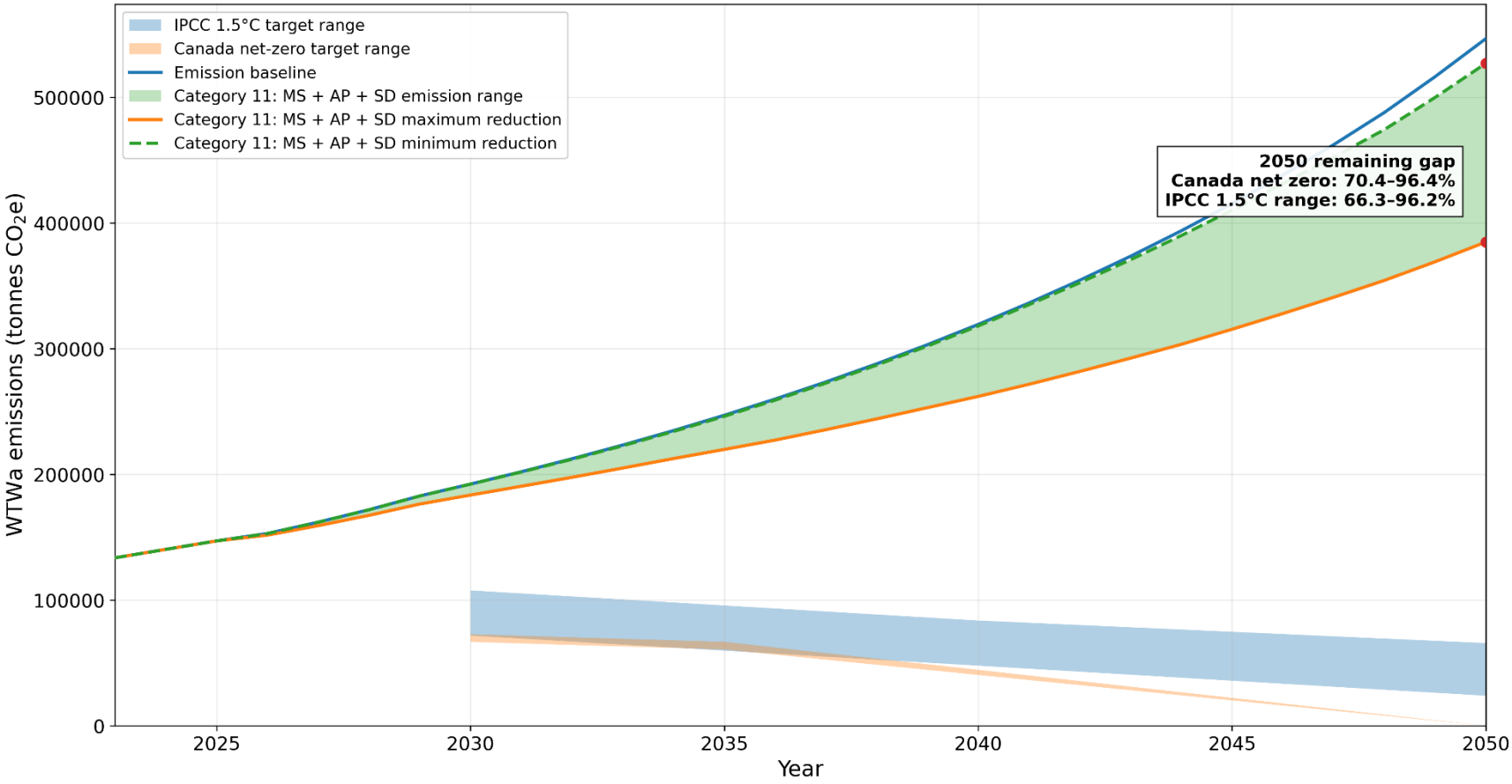


Figure V 6. Category 11 (MS + AP + SD): Minimum- and Maximum-Emission Cases